THE TRIBOLOGICAL EFFECTS OF SOOT CONTAMINATED LUBRICANTS ON ENGINE COMPONENTS

David Green

March 2007

Thesis submitted for the degree of Doctor of Philosophy

Department of Mechanical Engineering
University of Sheffield

ABSTRACT

The work in this thesis investigated the effects of soot contaminated lubricants of engine components. A thorough background review demonstrated that soot related wear is a major issue for the automotive and lubricants industry. A detailed analysis of the physical properties and effects of soot contaminated lubricants highlighted that there are associated effects that will tend to reduce engine performance and efficiency.

The actual wear that was produced is studied for the area of the engine which is most significantly affected by soot contamination, the valve train. A typical elephant's foot to valve tip contact, known to suffer from soot related wear, formed the basis of the specimen ball-on-flat reciprocating wear testing. A standardised wear test rig and method were developed for the testing, which investigated different lubricants (base and formulated oil), increasing levels of soot contamination (using carbon black as a soot surrogate) and different temperatures.

The results demonstrated significant increases in wear with increasing level of carbon black contamination. Furthermore, increased temperature tended to increase the amount of wear produced and using a formulated lubricant reduced the amount of wear measured when compared to tests using base oil.

Significant changes in wear mechanism were visible from surface imaging of the wear scars, showing initially lubricated sliding, which changes to abrasion at higher contamination levels, and then shifting to contact starvation as the contamination significantly reduces the flow of lubricant into the contact at very high contamination levels.

Significantly, the severity of the effects of soot contamination was due to the lubricant film thickness in the contact and therefore ultimately the lubrication regime within which it is operating. Where boundary lubrication is significantly affected by soot contaminated lubricants, but these effects are reduced when the contact operates under elastohydrodynamic (EHD) lubrication conditions.

A region of the engine that is significantly affected by soot contaminated oil is the contact between the piston and the cylinder wall or liner. This is mainly due to the component's proximity to the area where soot in produced. Wear will occur in this highly sensitive region due to the breakdown of the protective oil film, which will occur when the lubricant is contaminated with soot. A method of analysing the effect

of soot is to measure the formation of the lubricating film in that region. This has been has been investigated using an ultrasonic technique to measure the oil film thickness between a piston and a cylinder wall or liner.

The ultrasonic oil film thickness measurement technique (developed at the University of Sheffield) has been used in many static and dynamic applications; therefore an initial trial was performed on a single cylinder engine, demonstrating some success. A motored test engine was then built on which to develop the technique and to provide a platform for future research.

The test engine demonstrated potential for future success, as a variety of ultrasonic transducers were tested. Testing also highlighted that significant future work, regarding reducing electrical interference, improving the data processing electronics and further investigations into the different types of transducer is required to improve the technique.

The Tribological Effects of Soot Contaminated Lubricants on Engine Components

CONTENTS

ACKNOWLEDGEMENTS

The author would really like to thank Dr Roger Lewis and Professor Rob Dwyer-Joyce for their support, guidance and friendship throughout this project.

The author would also like to thank: Dave Butcher for his technical assistance, as well as David Wedlock of Shell Global Solutions, and Tom Mackay, Mahmoud Tarabad and Mehdi Daragheh of Perkins Engines for their help and input.

CHAPTER 1:
INTRODUCTION

1.1. STATEMENT OF THE PROBLEM

Car, engine and lubricant manufacturers are facing increasing pressure to lengthen service intervals and therefore oil life in order to reduce lifetime vehicle costs for the customer and the overall impact the vehicles have on the environment (essentially a reduction in the amount of engine oil discarded). Increasing sump drain intervals, however, means that oil is becoming highly contaminated and increasingly more degraded.

This problem is witnessed most significantly in diesel engines, as the main contaminant of the lubricant, soot, comes directly from diesel fuel combustion. Soot particles are either exhausted to the atmosphere or adsorbed by the lubricant in the engine. Soot particles are extremely small black particles with a diameter of 40nm, but they agglomerate within a lubricant to approximate diameters of 200nm.

Most forms of contaminant in lubricants are known to cause some wear, but because of the quantity of particles present and its material structure it is known to be a major cause of wear in engines and detrimentally affect the service life of the lubricant.

The problem of soot or PM10 (particulate matter less than 10μm in diameter) particulates can be partially solved through further understanding of the formation of soot during fuel combustion and how the amount that is produced can be reduced. This is an area of work that has already attracted a lot of research interest.

The understanding of how soot contaminated lubricants cause wear and effect the operating function of a lubricant is also required to minimise such effects on engine components and increase engine and lubricant service life, as well as improve performance and efficiency.

Three different wear mechanisms due to soot contamination have been proposed. Rounds **[1]**, postulated that chemical adsorption of the anti-wear components in the lubricant by the soot reduced the lubricant's ability to protect the surfaces. Other researchers have suggested that soot wear could occur due to starvation of lubricant in the contact. This is where soot agglomerates to dimensions greater that the oil film

thickness and blocks lubricant entry to the contact [2]. The final mechanism proposed suggests that wear of the surfaces occurs by three body abrasion, where the soot acts as the third body. As agglomerates, soot is reasonably soft, but as individual particles, soot is thought to be hard enough to wear metal surfaces [3]. There is little work, however, where actual component contacts at realistic operating conditions have been used to verify these theories.

Engine lubricants are further contaminated by soot when exhaust gas recirculation is used. The application of exhaust gas recirculation (EGR) in engines is increasing; this is where a portion of the exhaust gases are re-circulated into the inlet manifold. This acts to reduce the peak combustion temperature and therefore reduce NOx emissions. EGR leads to combustion products (including significant amounts of soot) being re-circulated rather than passed out of the engine in the exhaust system. Therefore EGR leads to soot particles re-entering the combustion chamber and a greater likelihood of further lubricant contamination.

1.2. THE WAY AHEAD

In the foreseeable future the issue of elevated soot levels in the engine, will continue to increase as tailpipe emissions are reduced and service periods lengthened, therefore the associated issues of soot contaminated lubricants will escalate. One approach to minimise the effects of soot is to reduce the amount of soot produced directly from combustion, research is ongoing in this area, but the results of this will probably not be seen for many years. A second approach, employed in this project, is to understand the effects that soot contaminated lubricants have on engine contacts, from which a greater understanding can be gain as how to mitigate the effects relating to wear and inefficiencies.

Generic laboratory testing or engine or vehicle testing is often used to evaluate the effects of soot contaminated lubricants. These methods generally provide unhelpful data to gain a real understanding as to the contaminated lubricants effects, as generic laboratory tests apply unrealistic contact conditions which are unrelated to real engine contacts, and engine or vehicle testing, although realistic does not allow for the elimination of other factors which could be affecting the results obtained.

The approach used in this project is to analyse a typical engine contact and relate it to contact that can be reliably reproduced within a laboratory. This provides a cost and time effective testing method, which directly relates to realistic engine operating conditions. Further analysis and understanding of contacts can be gained by increasing the complexity of the contact to a point were testing methods are applied to real engine contacts in controlled laboratory conditions.

1.3. PROJECT OBJECTIVES

The aims of this project are two-fold, firstly to understand the tribological effects of soot contaminated lubricants on typical valve train engine contacts. This has been carried out through lubricant and contact properties analysis and wear testing (using physical measurement and optical analysis). The second aim has been to apply the

knowledge obtained to extend the research to assist the understanding of other critical contacts within the engine, in this case the measurement of the piston to cylinder wall oil film thickness via ultrasonic means.

The findings from this project will ultimately provide information to engine designers and lubricant formulators, which will allow them to minimise the effects of soot contaminated lubricants, to potentially increase service life and efficiency, and reduce costs to their customers.

The key objectives of this project have been to:

- Understand the significant body of previous research that has been carried out and identify general trends in research techniques and findings. From this it is possible to discover areas and methods that have not been investigated, from which a new approach can be formed.

- Devise a testing methodology that is standardised and that can produce reliable and repeatable data, but which tackles the issues relating to soot contaminated lubricants from a realistic, but laboratory based approach.

- Analyse soot contaminated lubricants to understand the effects that the contaminants have on their behaviour and physical properties.

- Assess the differences between different types of lubricant, in this case base oil and a commercial formulated lubricant containing additives which are designed to minimise the effects of contaminants.

- Assess the amount of wear produced under various test conditions and understand the wear mechanisms that are occurring from the worn test surfaces, and therefore any changes in wear mechanism or behaviour that occur due to changes in test conditions.

- Build, develop and assess a test platform for investigating the oil film thickness between a piston and the cylinder wall, to allow for future research on the effects of soot on film thickness.

1.4. BENEFITS OF THE WORK

The benefits of this body of work are outlined below:

- The project will be based on a real engine contact related to a laboratory based specimen test, rather than testing in a generic and unrelated laboratory test.

- The development of a standardised testing and measurement method will provide a cost effective, reliable and repeatable technique to understand the effects of soot contaminated lubricants.

- Analysis of the behaviour and physical properties of the contaminated lubricants will provide an understanding of the relationship between the

contamination level, type of test contact, lubricant film thickness and lubrication regime.

- The wear test data and analysis of the resulting wear scars will provide a quantifiable understanding of the physical impact of contaminated lubricants and the wear mechanisms that occur and change with contamination level.

- The development of a test platform to ultrasonically measure the oil film thickness in a soot affected engine contact (piston to cylinder wall), which will help towards realistically demonstrating the implications and effects of soot contaminated lubricants, and then the impact that new technologies and materials can have on reducing such effects.

- The work from this project will provide opportunities for future research, including tools that could be used within the automotive and lubricants industry to understand the effects of soot contamination on new component or lubricants designs.

1.5. LAYOUT OF THE THESIS

This thesis is divided into two distinct sections. The first section covers the work relating specifically to soot contaminated lubricant analysis and the wear testing and analysis. The second section focuses on the development of an ultrasonic method of measuring oil film thickness in the region of the piston, to ultimately assist the understanding of how soot contamination of a lubricant effects the lubrication of this critical region in the engine. A brief summary of each chapter is given below.

2. *Soot Wear Background.* This chapter reviews previous work that has been performed to investigate the effects of soot contaminated lubricants. It describes what soot is and how it compares to carbon black (used as a soot surrogate in bench testing); it then looks at ways of testing it to examine wear and the wear theories that have suggested to date. Furthermore, the chapter looks at the effects that soot itself has on a lubricant, engine operation and design and finally the associated legislation. Conclusions are drawn highlighting areas in the research that require further investigation.

3. *Wear Testing Procedure.* This chapter outlines the fundamental principle of the wear testing through analysis of an engine contact to be replicated with a ball-on-flat contact. The test rig, specimens, lubricants and procedure are detailed, through to how the wear is measured.

4. *Physical Properties and Effects of Test Lubricants.* A detailed investigation of the associated effects of soot contamination that have implications on the level of wear produced is described in this chapter.

5. *Wear Testing.* The results obtained from the wear testing through a combination of test conditions are presented in this chapter, highlighting the effects of each of the test parameters.

6. *Wear Scar Analysis.* The wear scars produced from the wear testing highlighted in Chapter 5 are examined using optical microscopy and scanning electron microscope (SEM) imaging to highlight wear features and ultimately wear mechanisms.

7. *Soot Wear Discussion.* This chapter combines the results gathered from the previous chapters to form a complete understanding as to how various engine contacts and conditions are affected by soot contamination of engine lubricants.

8. *Oil Film Thickness Measurement of a Piston - Introduction.* This chapter introduces the section of the project to develop a test platform to understand the effects of soot contamination in a realistic engine contact, via the measurement of oil film thickness. Other measurement techniques that have been used to assess the oil film thickness in the piston region are summarised and the theory relating to ultrasonic oil film thickness measurement is presented.

9. *Oil Film Thickness Measurement in a Fired Engine.* The initial test performed to trial this method on an engine is discussed in this chapter. The apparatus, method and results obtained are highlighted.

10. *Development of a Motored Test Engine.* This chapter outlines the test engine built to develop and test the measurement methods and ultrasonic transducers.

11. *Oil Film Thickness Measurement of a Piston - Discussion.* The initial work carried out to develop the method of measure the oil film thickness around a piston is discussed in this chapter, highlighting the key findings that demonstrate future potential success. The future work required to complete the development of the test platform and therefore the possible future research applications are also discussed.

12. *Conclusions and Recommendations.* This final chapter outlines the conclusions drawn from both sections of this body of work. A summary of recommendations of future work and publications arising from this work are also presented.

CHAPTER 2:
SOOT WEAR BACKGROUND

The issue of soot related engine wear has previously been investigated from a lubricant viewpoint, in terms of designing lubricants that will disperse particles within the lubricant and keep them in suspension. Vehicle service intervals are currently dictated by the length of time that lubricants can maintain their physical properties, but also and possibly more importantly by the length of time that they can hold the contaminants in suspension. The soot particles are contained within the lubricant by dispersant additives. Current lubricant technology, however, is nearing a limit on the amount of dispersants that can be added, as too much will result in corrosion problems in the engine due to the free amines associated with the dispersant **[4, 5]**.

A different approach to the above which has already received some research interest is to investigate how engine components and their interfaces are actually affected by soot. This has involved looking at what wear mechanisms occur with soot contaminated engine oil and under what conditions they occur and investigating how much soot the components can tolerate.

This background review firstly looks at what soot is and what problems it creates within the engine, before going on to current wear testing methods and standards. The review continues by investigating all of the previous research that has been carried out, then continues by looking at future implications, including legislation and different fuels.

2.1. WHAT IS SOOT

Soot is a microscopic carbonaceous particle, which is a product of incomplete combustion of hydrocarbons (in this case gasoline or diesel fuel) (see Figure 2.1). It is comprised of carbon, ash and unsaturated (unburned) hydrocarbons. The unsaturated hydrocarbons are essentially acetylene and polycyclic aromatic hydrocarbons (PAH). These components have particularly high levels of acidity and volatility. Measurements have shown that engine soot typically contains 90% carbon, 4% oxygen, 3% hydrogen with the remainder consisting of nitrogen, sulphur and traces of metal **[6]**.

Individual or primary soot particles from diesel combustion have been measured to be approximately 40nm **[6]**. Due to soot's colloidal properties the particles agglomerate up to a maximum of approximately 500nm, with a mean soot agglomerate size of 200nm.

Soot particles tend to be more prevalent in diesel engines than gasoline engines due to the differences in the combustion mechanisms **[7]**. Diesel engines are increasingly being operated at higher air to fuel ratios, which tends to produce greater levels of engine soot.

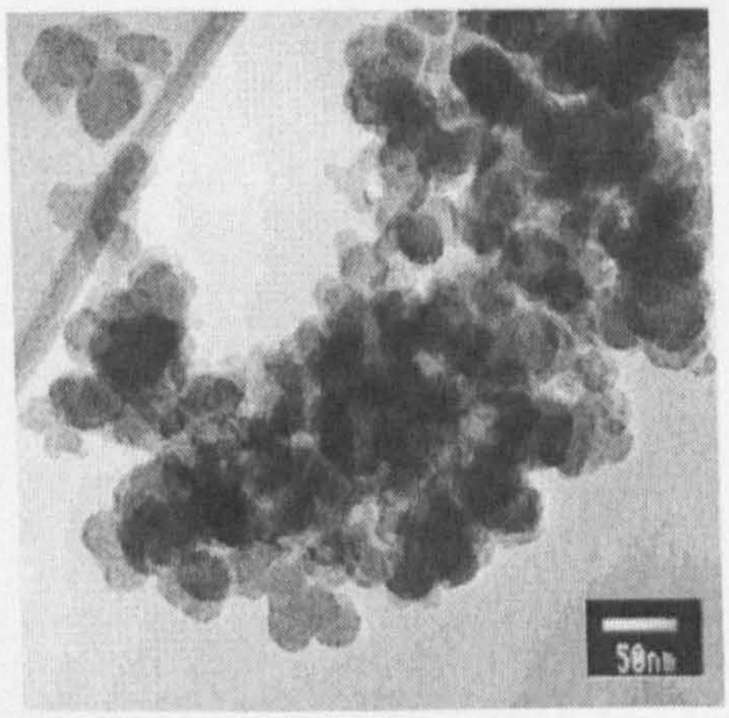

Figure 2.1. Image of a Typical Extracted Engine Soot Agglomeration **[6]**.

The majority of modern diesel engines operate using direct fuel injection and swirl within the combustion chamber to assist fuel/air mixing. Combustion initiates close to the injection point and occurs very rapidly as a diffusion flame. At this point the air and fuel mix well, but the mixture is very fuel rich, causing very high levels of soot to be produced. After diffusion burning, the combustion process progresses through the rest of the combustion chamber by pyrolysis burning which slowly burns the majority of the remaining fuel. This slow burning produces more particulates (soot) and unburned hydrocarbons at the end of the combustion process **[8]**.

Throughout the combustion process soot particles are produced and destroyed; produced by the process explained above, and destroyed by oxidation. Oxidation is a mechanism that occurs when soot or soot precursors come into contact with various oxidising species. When this occurs the hydrocarbons that are trapped inside the soot are burnt out and the particle size reduces. During the diffusion burning stage of the combustion process, the soot particles produced in the initial phase of the combustion process come into contact with a much higher volume of air compared to fuel, and a large proportion of the soot particles are oxidised.

Further oxidation is therefore required to reduce the amount of soot finally exhausted. When the exhaust valve opens the combustion products are emitted to the exhaust system which will contain more oxidising species that will oxidise the soot. Oxidising catalytic converters are used to further reduce the amount of soot emitted from the tailpipe. The majority of the soot formed is oxidised prior to exhaust. This is possibly why a large amount of soot particles are absorbed by the lubricant and relatively little is exhausted **[9, 10]**.

The concentration of the soot particles produced increases with an increasing air to fuel ratio. When the air to fuel ratio nears stoichiometric (14.5 for diesel fuel) [7] the rate of soot production increases dramatically [11]. This is because near stoichiometric there is not enough time and oxygen in the cycle to completely burn all of the diesel fuel, also there will be a low proportion of oxidising species to oxidise the soot. Generally at values of 20% fuel lean of stoichiometric and higher, which are now being used, excessive amounts of soot are produced from the combustion process [9]. Excess air is required to increase diesel cycle efficiency and to reduce hydrocarbon emissions [9, 12].

Investigations have shown that soot contained in the engine lubricant and soot emitted from the tailpipe is quite different [6]. This may be partly due to the oxidation processes the combustion products go through. As mentioned above soot contained in lubricants has a very high content of carbon and low oxygen content. A comparison of approximate content values for engine and exhaust soot can bee seen in Table 2.1.

Table 2.1. Engine and Exhaust Soot Constituents [6].

Soot Constituent	Engine Soot Content	Exhaust Soot Content
Carbon	90%	>50%
Oxygen	4%	<30%
Volatile content	6%	20%

The data in Table 2.1 follows the theory that soot is oxidised as it progresses from the combustion chamber to the exhaust system. It can also be seen that the volatile content dramatically increases in the exhaust soot. The volatile content includes: hydrogen, nitrogen, sulphur, phosphorus, iron, calcium, zinc and traces of other metals.

Work by Lapuerta et al. [13] showed that the fuel used determines the size of the particulates produced. The main factors are the aromatic and sulphur content of the fuel. The aromatic content affects the nucleation of the particles as it is considered to be the main precursors of diesel particulate matter. Aromatics are ring structured hydrocarbons, generally with a distinctive aromatic odour and good solvent properties. The higher the aromatic content in the fuel the greater the concentration of soot particles produced.

Sulphur has been found to increase particulate agglomeration [13], as during combustion the sulphur in the fuel is oxidised and emitted as a gaseous oxide. This oxide will form sulphate drops when in the presence of water in the air, which may deposit onto the surface of the soot particles. These sulphate drops on the surface of the particle will then attach to further soot particles. Finally the viscosity of the fuels has been discovered to affect the amount of soot produced during combustion [13]. It has been shown that a high fuel viscosity hinders the atomization of the fuel and therefore delays the mixing process, leading to higher levels of soot formation [13].

A detailed study of soot formation models by Kennedy [10] demonstrated that complex chemical kinetics play a major role in all stages of soot production, from inception, through surface growth and aging, to surface oxidation. Recent work has also suggested that soot may participate chemically in the reduction of nitric oxide. Oxides of nitrogen are generally formed at very high combustion temperatures

through the process of dissociation [8]. Oxides of nitrogen are highly dangerous pollutants that cannot be emitted from the tailpipe, therefore to reduce the peak burning temperatures engine manufactures generally implement a combination of increased air to fuel ratio and retarded injection timing. Unfortunately both of these approaches tend to increase the production of soot particles.

Soot formation through combustion is mainly a diesel engine issue, due to the quantity and particle dimensions produced. But soot formation is also a minor issue for a spark-ignition petrol (gasoline) engines. Whereas diesel engines produce particles of a minimum of 40nm, a petrol engine is believed to produce much smaller particulates, but there is currently uncertainly as to their dimensions and composition [9]. Diesel engines are more likely to produce soot from the combustion process, firstly due to the chemical composition of the fuel, due to its higher proportion of carbon to hydrogen, and secondly due to the fact that the distribution of petrol and air in the combustion chamber is a homogeneous charge and diesel and air is an heterogeneous charge [7, 8].

Soot particles are generally assumed to be extremely hard individually and much softer when agglomerated. A variety of soots produced from a standard Cummins M-11 engine test had their hardness's measured by Li et al. [5]. The hardness's were determined by carbon plasmon energy methods, obtained from the electron energy loss spectra, which were measured by a high resolution transmission electron microscope. The mean data for each engine operation condition tested are shown in Table 2.2. This shows that soot taken from an engine operating with EGR is slightly harder than soot from an engine without EGR. This increase is hardness is possibly due to the secondary heating and oxidation process the particles experience.

Table 2.2. Soot hardness values [5].

Mode of Operation	Hardness (kg/mm^2) (Vicker's Hardness)
Direct injection, non-EGR, 300hrs	1096
Low injection pressure non-EGR, 300hrs	940
High injection pressure non-EGR, 300hrs	988
Low injection pressure EGR, 300hrs	1235
High injection pressure EGR, 300hrs	1302

2.1.1. Where Does It Go?

It has been shown that of the soot produced within the engine only 29% reaches the atmosphere through the exhaust pipe [14] with the remainder being deposited on the cylinder walls and piston crown. Of the soot that is retained in the engine (mainly in the lubricant), 3% is attributable to blow-by gases, the remainder results from piston rings scraping away soot deposits in the cylinder, which then end up in the sump [4]. It is then transported around the engine where it can be entrained into component contacts.

Within the valve train there are many component interfaces, all of differing geometry and motion, as shown in Figure 2.2. Sliding, rolling/sliding and reciprocating contacts exist, some of which are conformal and some non-conformal. Due to the varying motion and loads at each interface, different regimes of lubrication will be

apparent. This is further complicated by the mechanisms for lubrication application which range from contacts where positive lubrication is used, to those where lubricant reaches the contact in-directly by splash lubrication. In some cases contacts receive little lubrication because of their location and starvation problems can exist **[15]**.

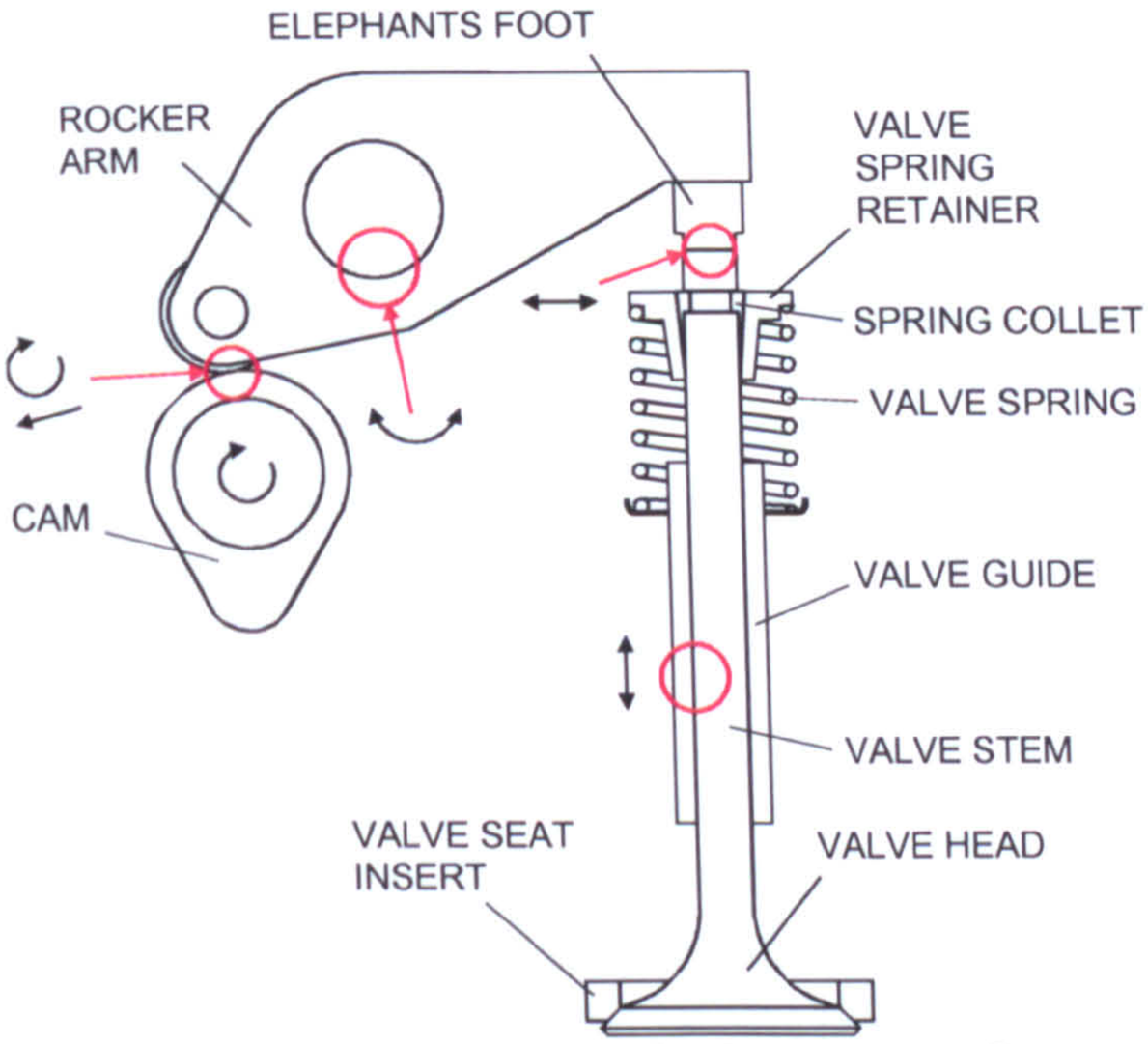

Figure 2.2. Sample Valve train Component Contacts.

A study by Chinas-Castillo & Spikes **[16]** investigated the entrainment of soot particles into a ball-on-flat sliding/rolling contact region, through interferometry and image analysis techniques. Soot particles were found to entrain into an EHD lubricated contact, by adhering to surfaces and accumulating until they formed a non-homogeneous boundary layer, influencing the behaviour in the contact particularly at low speeds or high temperatures when the soot primary particle size will be greater than the oil film thickness. At increased soot concentrations, thicker films were produced and there was a higher probability that soot particles would penetrate the EHD contact.

2.1.2. Where Is It A Problem?

The area in the engine where wear is generally most likely to occur is the valve train. The valve train components require a continuous supply of oil during operation, but as the valve train is generally located near the top of the engine they often operate with inadequate lubrication, particularly during a cold start, where oil pressure will initially be insufficient to pump oil to the top of the engine **[9]**. Also many of the valve train component contacts are not positively lubricated.

Figure 2.3 shows component wear data from engine tests with increasing degrees of EGR (and hence soot). Clearly wear rises in the in-cylinder and valve train components, but is worse in the valve train.

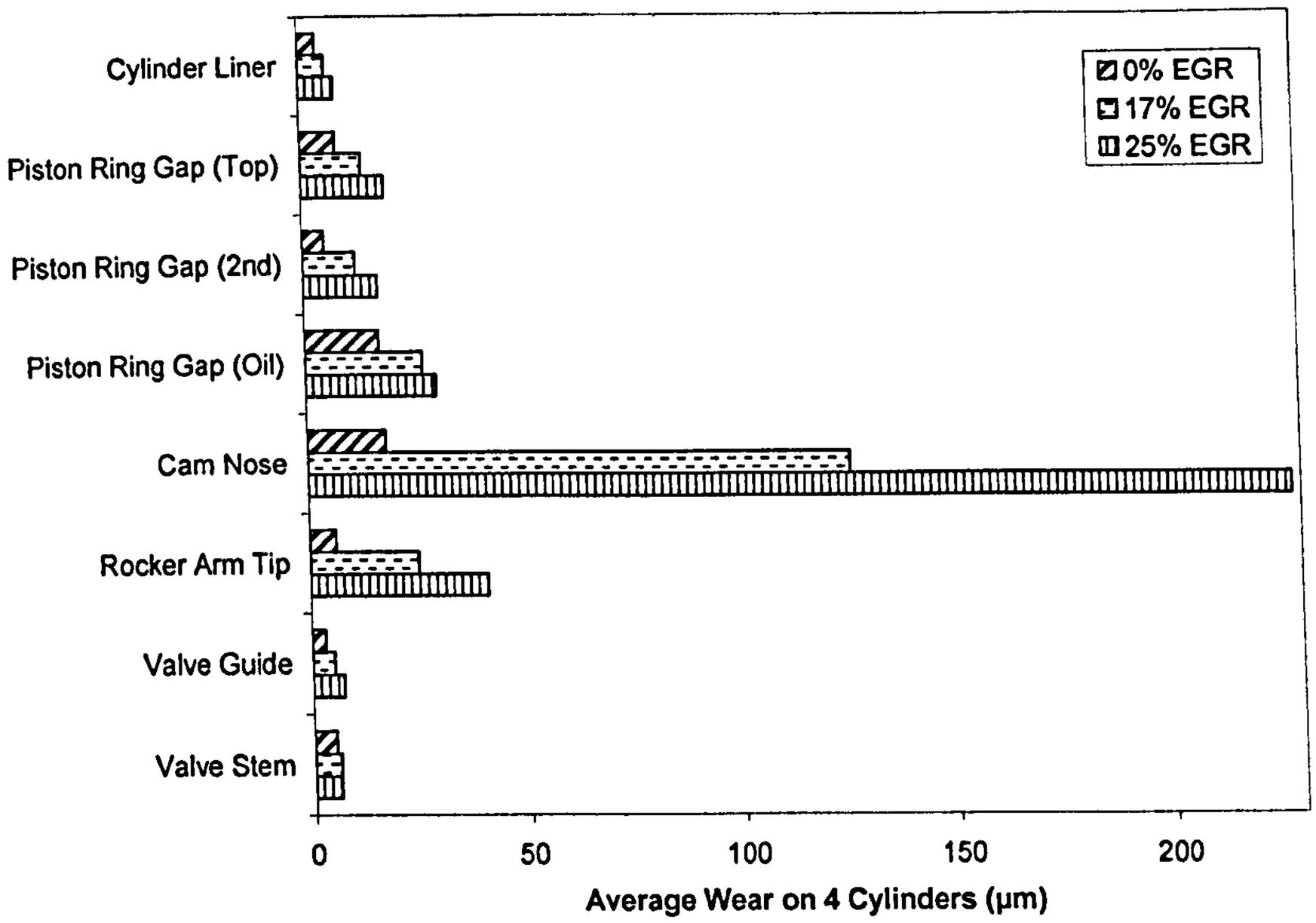

Figure 2.3. A Reproduction of 4D55T/C Engine Wear Data Showing Relative Component Wear Levels [17].

2.2. WEAR TESTING METHODS

Tribological testing can be carried out at a number of different levels. Figure 2.4 illustrates this for engine components. Clearly the complexity decreases with the move down from field testing to specimen tests and greater control can be achieved of the test parameters. The tests are also more repeatable and the statistical significance of the results is greater. However, as the complexity is decreased, exact simulation of the component dynamics and loading conditions is more difficult to achieve. A compromise is needed, usually based on cost and time restrictions that allows generation of results appropriate to the particular application.

With testing involving contaminants it is essential that a good representation of the contact motion, loading and geometry is achieved if bench testing is to be used. Entrainment of the contaminants will be directly affected by these and is key to determining which wear process may occur. This means that the best approach would probably be to use actual components.

Engine tests are always problematical. It is difficult to control many of the test parameters and provide good wear measurements. However, standard engine test cycles designed to promote soot production have been defined, as will be outlined in Section 2.2.2, that allow soot wear studies to be carried out.

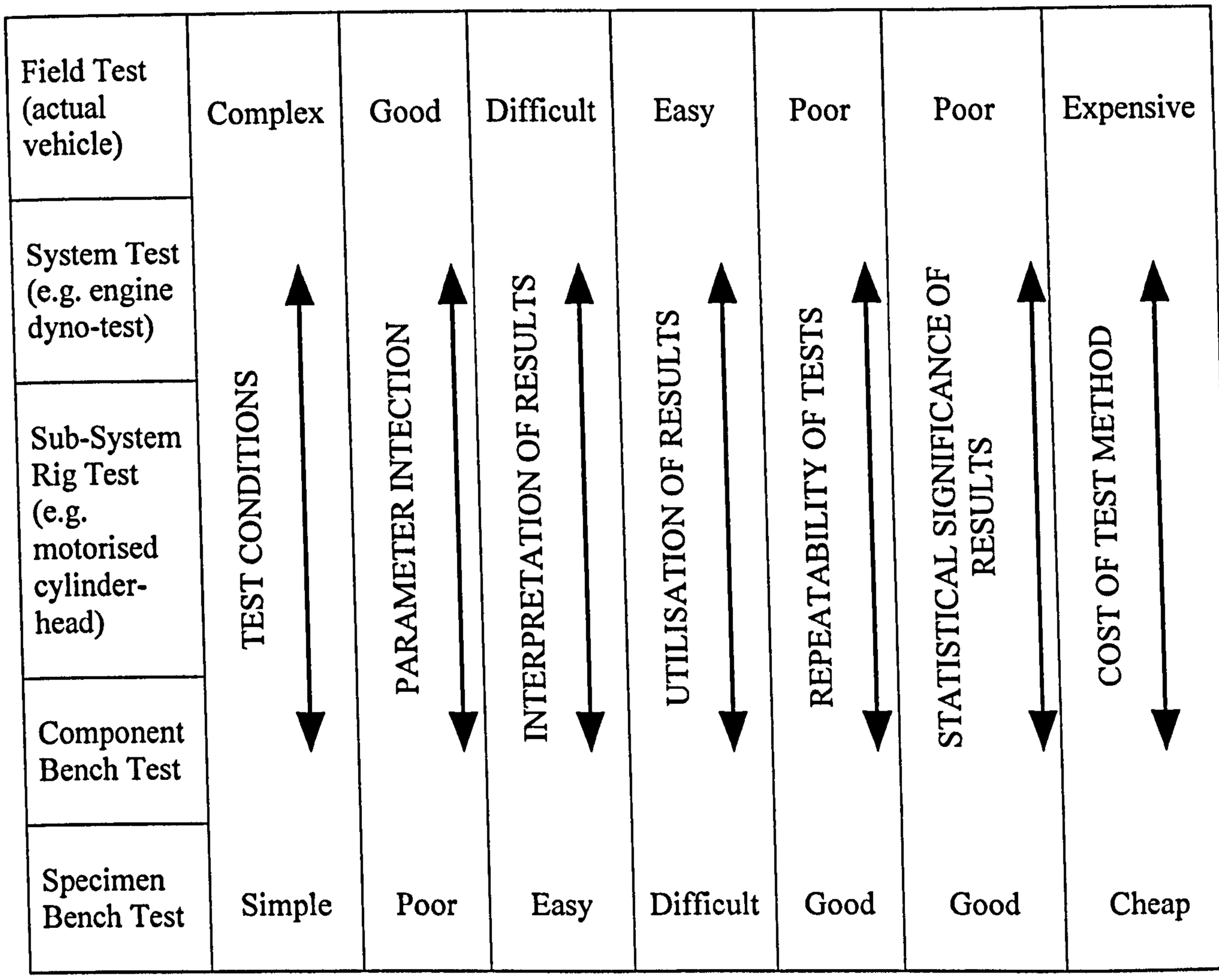

Figure 2.4. Levels of Simulation in Engine Component Tribological Testing.

2.2.1. Test Apparatus

In early work on soot wear the most popular test method was the four-ball approach **[18]** in which various soot contaminated lubricant formulations were tested in a standard 4-ball wear test. High frequency reciprocating rigs, pin-on-disc and ball-on-flat rolling sliding apparatus **[18, 19]** have also been used in more recent times.

These methods have their limitations, as recognised by Bell **[20]**, who realised it was necessary to test the levels of wear using test equipment that was designed to replicate the engine components in question rather than generic wear testers. Engine tests have also been used to study soot related wear usually through industry standard engine tests.

The measurement of wear data to assess the effects of soot contamination is generally carried out through imaging of the wear scar produced after each test. This involves the use of optical microscopes or for a more detailed analysis of the wear surface scanning electron microscopes (SEM) **[21]**.

2.2.2. Testing Standards

Engine testing standards are followed when carrying out engine tests to ensure that the data obtained can be reproduced if necessary in later tests either on the same equipment or elsewhere in the world. It also means that when operating parameters are changed (within the parameters of the testing standard) data from various tests can be compared against each other.

One of the main standard tests used to investigate engine wear under high soot and high load operating conditions is the API CI-4 Cummins M-11 EGR engine test (also known as the Cummins M-11 cross-head wear test). This is done by running the engine fuel rich to create the high load in conjunction with operating retarded injection timing to generate the high levels of soot **[22, 23]**. It determines the effectiveness of lubricating oils in reducing soot related wear of valve train components in engines with EGR, through reduction of filter pressure drop, excessive viscosity increase, sliding valve train wear, bearing corrosion and sludge deposits.

Two tests produced by Mack also investigate the effects of soot build-up. They are the Mack T-8E, where the fuel injection timing is adjusted to achieve a target level of soot in the bulk lubricant (it evaluates an oil's ability to prevent excessive viscosity increase and filter plugging) and the Mack T-9 (ASTM D 6483) an increased soot level in the bulk lubricant is again generated where through adjusted injection timing to investigate piston ring and liner wear in a high-output diesel engine. This evaluates the amount of corrosion due to loss of total base number (TBN) in the oil as it degrades **[22, 23]**.

The Mitsubishi 4D34T4 test increases the soot level within the lubricant to 4.5%, through high speed operation and 10% over fuelling, to analyse the lubricant's protection performance of soot related valve train wear, essentially through a decrease in the cam lobe diameter **[22, 23]**.

The Caterpillar 1R (and 1P – API CH-4) test involves running a Caterpillar 1Y3700 single cylinder oil test engine for 504 hours at fully rated speed and load to evaluate the performance of lubricants for direct injection high speed engines operating low sulphur fuels. Analysis of the piston deposits and oil consumption, pistons, piston rings and cylinder liner is carried out to evaluate performance **[22, 23]**.

The roller follower wear test (ASTM D-5966) used by GM is a useful method for directly understanding an oil's ability to prevent valve train wear with aging oil. Analysis is carried out via the valve lifters, which are replaced between each test **[22, 23]**.

Of the above tests the Cummins M-11 EGR test appears to provide the most useful standard soot induced wear engine test as it focuses on many areas of potential wear and therefore many opportunities for analysis and understanding. This is also the test that appears to be the most commonly used in industry.

Standard tests are also available for specimen testing. One of the most common specimen tests is the reciprocating ball-on-flat test as detailed in ASTM standard G133-05 **[24]**. ASTM standard G133-05 is essentially only applied to fresh oil, but

work is in progress to create ASTM standards that account for contaminants in the test lubricant, focusing on testing between a piston ring and cylinder liner **[25]**.

2.3. CARBON BLACK

To investigate soot wear there are essentially three options to choose from regarding the test particles. These are:

- used engine oil
- extracted engine soot mixed with fresh engine oil
- carbon black mixed with fresh engine oil

Used engine oil is the most realistic option, but adds complications as the oil will contain other contaminants and wear debris, all of which will affect wear results dramatically. An extra complication of testing with used oils is that they are naturally degraded, but this is extremely dependant on use. Test oils would each need to be produced in an identical manner in an attempt to consistently degrade the lubricant the same amount each time, as used engine oils will be mixed together to produce the required soot content for testing purposes. However, even this will not allow full control over the final amount of soot produced, which will vary from batch to batch. Laboratory techniques exist for aging engine oils outside of an engine (without producing soot) **[26]**. This is quite an unpredictable process, however, and would add further complications to the process. The process of producing used engine oils is expensive and time consuming.

The second method of extracting engine soot alone from a used lubricant, allows for the assessment of the affect of soot alone on wear without any other contaminants or lubricant degradation issues. Using this method the extracted soot is simply mixed in with the desired test lubricant. This method is less time consuming and expensive than the first method and reasonably practical for experimental purposes.

The final method of using carbon black has for many years been the standard method assessing the wear level due to soot contamination. This method is quick and inexpensive. The major drawbacks of this method are that carbon black, though very similar to engine soot, is not engine soot, producing results that industry has argued may be relative to tests with soot from used engine oil, but not directly comparable.

A particularly time consuming process was described by Rounds **[27]**, using a method of heat treating carbon black particles in oil and air. Heating at different temperatures produced soots that had different pro-wear properties relating to real engine soots experiencing low or high engine loading.

Investigations by Clague et al. **[6]**, however, have shown that carbon black particles do have the capability of mimicking the behaviour of soot from engine oils. Findings showed that when looking at primary soot particles (30 to 50nm) using electron microscopy techniques, there is very little difference between engine soot and carbon black. There was a great deal of similarity in particle size and structure, confirming that the two are essentially the same at the nanometre scale.

When investigating agglomerated soot and carbon black particles (up to 500nm), carbon black was again found to be similar to engine soot, although a slight difference was discovered **[6]**. The carbon black particles disperse in a similar fashion, but create a larger agglomerate diameter than extracted engine soot, greater by approximately 50nm. Chemical analysis of soot and carbon black particles showed that carbon black particles display higher carbon contents and lower ash and volatile contents. Oxygen and hydrogen were shown to concentrate on the surface of the carbon black particles, creating a relatively polar surface, meaning it will tend to have a greater tendency to interact with other polar species, i.e. other carbon black particles. Prior to extraction from its lubricant the engine soot displays a higher polar surface than carbon black, but once the soot has been extracted from the lubricant it becomes less polar than carbon black. This explains why (as mentioned above) carbon black particles created a larger diameter agglomerate than extracted engine soot. This is one of the main areas of soot chemistry where a major difference occurs between soot and carbon black particles.

Investigations by Wedlock et al. **[28]** into soot particle aggregation demonstrated that when carbon black particles are mixed in a lubricant, particularly by ultrasonic means, the particle structures formed are essentially similar to those formed by engine soot. This work demonstrated that soot aggregate structures are fractal bodies, meaning they create chaotic complex formations when they agglomerate. This was investigated through Transmission Electron Microscopy (TEM) analysis and was shown to be reproduced in various engine soot and carbon black lubricant mixtures.

2.4. WEAR THEORIES

Initial investigations (circa 1970's) were carried out from a purely chemistry point of view, as the soot was known to be one of the contributing factors to long term oil degradation **[1]**. Observations showed that as the oil degraded the amount of engine component wear increased. As very little was known at the time about engine soot, lubricant scientists assumed that the soot must have been degrading the lubricant's anti-wear additives. As further investigations were carried out it was found that even after the soot had degraded various elements of the anti-wear additives, the elements required to produce the anti-wear function of the lubricant remained. The function of the anti-wear additives are mainly to prevent against various forms of engine component wear e.g. corrosion etc., therefore the wear seen in many engines with soot contaminated lubricants must have been due to more fundamental mechanisms, such as abrasion.

Research has developed in more recent years to investigate the physical and mechanical actions of particles in lubricants. Various studies have individually highlighted polishing on a macroscopic level, microscopic abrasion and lubricant contact starvation due to the soot contained within the lubricating oil. Consensus of agreement appears to be difficult to achieve, but in recent years (2000 onwards) many studies are obtaining similar findings, leading to considerable agreement between researchers and acceptance of the theories by lubricant and engine manufacturers. Greater understanding and acceptance of the research is due to an increasingly broad scope of investigations involving different lubricants, soot (and soot surrogate) types,

other contaminant particles, and specimen, component and engine testing methods. This is all discussed in greater detail below.

2.4.1. Breakdown Of Anti-Wear Layers

The earliest investigations into soot wear were performed by Rounds **[1, 27]**, in which tests were performed with a 4-ball wear test machine, using base oils with various additives mixed with carbon black and centrifuged engine soot. The wear tests demonstrated an increase in specimen wear with increasing contamination level. Rounds proposed that increasing wear was due to the carbon black and soot particles preferentially adsorbing anti-wear species within the lubricant e.g. ZDDP (zinc dialkyldithiophosphate).

A study by Hosonuma et al. **[29]** using a Japanese valve train wear test showed that during engine tests ZDDP decomposes quickly initially, but the lubricants still retained their anti-wear properties. Analysis of diesel soot showed that it adsorbs compounds containing zinc, but very few compounds containing phosphorus, with the phosphorus compounds being retained within the lubricating oil, maintaining the oils performance. This study agrees with Rounds's theory that soot adsorbs some of the ZDDP compounds, but dismisses the suggestion that the performance of the lubricant is degraded due to this.

Nagai **[17]** suggests that the soot acts to strip off the anti-wear film on the surface of the metal surface, leaving it exposed, resulting in increased wear. This study proposes that the anti-wear film is removed through abrasion and not adsorption as analysis of the centrifuged oils show very little sign of zinc and phosphorus depletion, as would be expected if the ZDDP had been adsorbed.

Recent work carried out by Torrance **[30]** investigated the wear resulting from a reciprocating test contact with a variety of lubricant combinations of carbon black level and type and with or without the anti-wear additive ZDDP. Investigations are centred on the properties of the lubricant in the contact region, rather than that of the bulk of the lubricant. The results from this work suggested that the addition of ZDDP to a lubricant containing carbon black can aggravate wear, with corrosion being the most likely wear mechanism. It is suggested that the carbon black abrades the anti-wear reaction film, therefore continuously exposing a fresh reaction surface.

2.4.2. Abrasion

During the 1980's research into soot wear of engine components increased. The general trend of the findings tended to disprove the early work by Rounds where it was suggested that the soot adsorbed the anti-wear additives in the lubricant and favoured abrasion being the major factor in soot induced wear (Kawamutra et al. **[31]**, Berbezier et al. **[32]**).

Early research into the abrasion of surfaces due to soot suggested that polishing mechanisms prevailed. Berbezier et al. **[32]** discovered that the size of the carbon black particles was very important. Berbezier found that carbon black particles with a

20nm diameter produced a lower wear rate than particles of 300nm by a factor of approximately 60%. The term polishing wear was used at the time as wear scars from tests with carbon black and other similar abrasive particles including silica and aluminium produced apparently featureless surfaces at micrometre scale, but with apparently minor wear features in the range of tens to a few hundreds of nanometres as discovered by Ryason **[33]**.

Gautam **[3, 34, 35]**, using data from a three-body pin-on-disc wear tester, showed that soot contaminated lubricants (using collected engine soot) produced higher wear than uncontaminated oils. It was also suggested that the wear increase was due to an abrasive wear mechanism. Sato et al. **[36]** studied the resulting wear of various used engine oils in a four-ball wear tester. The results showed wear increasing relatively proportionally with soot concentration. SEM imaging showed fine streaks on the surface of the material, thought to be primary soot particles, therefore again highlighting abrasion as one of the main contributing factors to wear.

Mainwaring **[37]** performed Mack T-8E and Cummins M11 engine tests and discovered that the primary particle dimension has a significant effect on the amount of wear produced, due to the particles disrupting the lubricant flow, especially if the soot particle diameter is greater than the prevailing oil film thickness. It was also shown that good soot dispersant control can promote lower wear levels, but it does not guarantee satisfactory wear control. Good wear control with soot present was found top be dependent on viscous and oil film forming compounds in the lubricant. Further work by Chinas-Castillo & Spikes **[16]** using carbon black, lamp black colloid and engine sooted oils in an EHD test rig, confirmed the abrasive action of soot particles in creating wear, and also showed it was affected by primary particle size as well its concentration and its dispersed stability.

Using a mini traction machine (MTM) Yamaguchi et al. **[19]** performed ball-on-disc sliding wear tests to determine ball wear and obtain a Stribeck curve for the test conditions. Results obtained correlated with results from Cummins M-11 engine tests with high soot concentrations (in the region of 9%).

2.4.3. Link Between Laboratory And Engine Testing

A study by Kuo et al. **[21]** used the Cummins M-11 engine test to investigate engine wear under various operating conditions, where the soot level reached 5% content by mass. After 200 hours of testing the crosshead components of the engine valve train were examined using SEM (Scanning Electron Microscope) imaging. The components were shown to have heavily worn surfaces. The wearing process was shown to progress from lubricated wear, where the oil film thickness is greater than the primary soot particles present due to oil thickening, to abrasive 3-body wear. In addition to the abrasive wear seen fatigue cracking and mico-spalling of the component surface were visible. Li et al. carried out M-11 EGR engine tests **[5]**, cylinder liners, valve train crossheads and top ring faces were shown to be key areas where wear occurred, due to soot abrasion.

Cam on follower test rig experiments were performed by Soejima et al. **[38]**, with a fresh engine lubricant and another identical lubricant that had been used. Findings

showed that the soot dispersed in the oil caused the wear rate to increase over that of the fresh lubricant. Engine tests were performed by Kim et al. on a 6.2litre GM diesel engine [39]. These showed that a correlation was evident between engine testing and four-ball wear testing. Wear in both cases increased with increasing soot concentration.

2.4.4. Starvation

Starvation wear is caused by a blockage of the lubrication inlet to a contact. In the case of diesel engines it is thought that soot agglomeration at critical zones could cause a blockage capable of restricting the flow of lubrication enough to starve the contact zone, therefore causing unlubricated sliding wear.

Work carried out by Sato et al. [36] who, after carrying out four-ball tests, suggested that when soot particles aggregate within the lubricant starvation may occur as the diameter of soot agglomerates is much larger than the oil film thickness. In an actual engine some contacts receive little lubricant, because they are not lubricated positively and rely on splash from other lubricant supplies [15], so starvation is even more likely to occur with soot present.

2.4.5. In-Cylinder Wear Mechanisms

The main focus of soot related wear of engine components has been on the valve train, but some research has shown that the in-cylinder region around the piston rings to cylinder wall contact suffer from soot related wear.

Investigations by Devlin et al. [40] demonstrated that carbonaceous materials, aromatic species and oxygenated carbon, all of which are combustion products, were deposited on piston land regions. Testing using a single cylinder diesel engine by Ishike et al. [41] demonstrated that with the application of EGR top piston ring wear increased. They also suggested that that the wear was due to abrasion from the soot particles. Similar engine testing by Dennis et al. [4] showed again that with the application of EGR piston ring and cylinder wall/liner wear increased, but only under high load conditions. It was also suggested that corrosion induced wear could possibly occur within the in-cylinder region of the engine, depending on the composition of fuel and lubricant used. It is understood that sulphur used in fuels and lubricants is a corrosion inhibitor, therefore current legislation to reduce the amount of sulphur in fuels and lubricants could lead to corrosion occurring, especially as such a region in the engine contains high levels of acid products post combustion. Lubricants therefore need to have a sufficient neutralising ability in that region to prevent corrosion occurring. Yahagi [42] demonstrated that corrosion wear of the cylinder bore in diesel engines is aggravated by changes to the combustion conditions, mainly through the use of EGR. Under such conditions high levels of sulphuric acid and soot are produced. The presence of sulphuric acid leads to corrosive wear.

Engine testing on an Cummins M-11/EGR test engine by Li et al. [5] with soot contamination levels of 6% and 9% produced very high wear levels on both piston ring faces and cylinder wall/liner. As previously demonstrated, high levels of wear

were due to abrasion due to the soot particles acting as a third body within the contact, but also significant signs of corrosion. The corrosive wear was detected through SEM micrographs and elemental analysis **[5]**.

Tests carried out by Masuko et al. **[43]** to understand the anti-wear performance of simulated used engine oil, using base oil, ZDDP (an anti-wear additive) and carbon black in a four ball wear tester. The test lubricants were degraded and the results showed corrosive wear on the test balls, due to the compounds present in the degraded oils.

2.5. THE EFFECTS OF SOOT ON LUBRICANTS

2.5.1. Friction

Through cylinder-on-disc reciprocating testing Liu et al. **[44]** measured the variation of friction coefficient with different types of diesel lubricant with various soot contamination levels, using soot produced in a fired engine. A high degree of variability in the results was found as is generally common with soot testing, but results showed that the friction coefficient decreased with soot present in the lubricant. It is suggested that the soot particles acted as friction modifiers.

EHD oil film thickness measurement by Chinas-Castillo and Spikes **[16]** indicated that soot contamination of a lubricant affected the oil film produced, and therefore influenced the frictional characteristics of the contact, especially when the primary soot particle diameter was greater than the film thickness. Pin-on-disc measurements by Ramkumar et al. **[18]** demonstrated that with diesel engine soot mixed with a model diesel lubricant at different contamination levels the wear increased as did the friction coefficient.

Measurements by Devlin et al. **[45]** of oil aged in vehicle and engine fuel economy tests showed changes in the molecular weight distribution of the dispersant, which led to an increase in the high temperature high shear viscosity. Further testing by Devlin et al. **[46]** showed that the aging of engine oils caused an increase in the boundary friction coefficients measured. This work concluded that the fuel economy performance of aged oils (particularly at low temperatures) is dependent on the lubricants high temperature high shear viscosity.

2.5.2. Viscosity

Various studies have been carried out to attempt to understand the properties of soot contaminated lubricants. Early work carried out by Ryason **[47]** investigated the shear rate rheometry of used oils. The study showed that soot contamination of oil has the effect of increasing the viscosity and therefore reducing its ability to perform its function, particularly at lower operating temperatures. Further investigations showed that, below 1% (by weight) soot concentration in the lubricant, the viscosity increase is linear. However, above 1% the viscosity rose rapidly. The work also suggests that soot suspended in oil is thixotropic, meaning a contaminated lubricant's properties are dependant on its shear histories **[47]**.

Investigations by Batko et al. **[48]** looked at the increase in viscosity of oils from the field, specifically passenger cars equipped with 2.7litre DOHC V6 engines operating under "taxi-cab" conditions including "stop and go" and idling situations (which would promote soot production). Oil sampling and testing was performed at 4000 kilometre operating periods, up to 16000 kilometres. At the end of the tests, kinematic viscosities had risen up to between 300 and 350cS (mm^2/s) from an initial viscosity of approximately 60cS. Unfortunately no data is available from the study by Batko regarding the soot contamination levels of the test lubricants. An investigation by Zeidan et al. **[49]** into the simulation of aggregation of soot laden lubricants demonstrated that a strong relationship was found between the soot level and the aggregate morphology. This demonstrated that higher soot loading rates lead to a much lower fractal dimension and a higher degree of aggregate dispersion, producing an increased lubricant viscosity.

Investigations into the real effects of lubricant viscosity increase have shown that in hydrodynamically lubricated engine contacts, friction is roughly proportional to the square root of the lubricant's dynamic viscosity **[50]**. This clearly demonstrates that increasing levels of soot contamination have a detrimental effect on fuel consumption and tailpipe emissions.

2.5.3. Lubricant Degradation

The degradation of engine oil is an irreversible chemical deterioration of the lubricant, essentially a significant reduction of its total base number (TBN). The TBN is essentially a measure of a lubricant's alkaline content and therefore its ability to neutralise acids created during combustion. The lubricant degrades as the TBN reduces as it will reach a point where it can no longer neutralise acids, increasing the likelihood of corrosion, fouling of engine contacts and the failure of lubricating films. This indicates that soot will tend to degrade a lubricant, by reducing the TBN, as soot particles are highly acidic.

Lubricant degradation factors that lead to component wear are summarized in work by Kawamura **[31]**. There are many by-products of the diesel combustion process, these include: soot, carbon monoxide, carbon dioxide, oxides of nitrogen, unburnt hydrocarbons **[9]**. Most combustion by-products have high acidic levels, certain inhibitor lubricant additives are known to neutralise these acidic materials, but will ultimately become depleted after exposure to a significant amount of such products. Further aging effects on a lubricant are decreases in the function of the additives. Such additives include: detergents, anti-wear, viscosity improvers, anti-oxidants, friction modifiers and dispersants **[7]**. Dispersants retain soot and wear particles within the lubricant to assist with the general reduction of engine wear. Dispersants are increasingly depleted as they retain rising levels of soot and wear debris. On completed depletion the lubricant cannot efficiently retain anymore particles. Many of the other additives are degraded by exposure to acid combustion products and lubricant shearing. All of these effects lead to lubricant degradation and the inability to perform its function.

2.6. EFFECT OF ENGINE OPERATION & DESIGN ON SOOT PRODUCTION

Engine operating conditions significantly affect the amount of soot produced by an engine. Increasing engine speed has the effect of increasing the amount of soot produced. This is due to a reduction in the amount of residence time of the soot particles in the cylinder, therefore reducing the amount of oxidation that can occur **[14]**. The amount of soot produced has been shown to dramatically increase at critical engine speeds, seemingly determined by piston stroke length. A second engine operating condition that significantly affects soot production is engine load, relating to the measurement of how hard it is working (generally termed as a percentage). At high load (100%) soot production is very high due to the high flow rate of fuel injected into the cylinder. High load conditions are generally associated with an increase in engine speed, therefore a decrease in the amount of time available during the combustion cycle for soot oxidation. Essentially as discussed by Lapuerta et al. **[13]** when an engine's brake mean effective pressure (BMEP) is increased, the amount of soot particles produced increases considerably.

As explained earlier, in terms of the soot formation process and testing methods, an increased air to fuel ratio significantly increases soot production, when combined with high engine speed. Soot production is further increased with retarded injection timing. These have the affect of reducing the amount of time available in the combustion chamber for the soot particles to oxidise and reduce in volume. Increasing engine size has the effect of reducing the amount of soot produced as an increased amount of time is available for soot oxidation to occur. Soot formation is known to take place between approximately 1000K and 2800K, but due to the difficulty of analysing and controlling the combustion temperature, it is not known whether combustion temperature has a more important effect.

There are essentially two types of diesel engine design – indirect injection and direct injection. Indirect injection engines pre-mix the diesel fuel and air in a small pre-chamber to increase combustion speed via increase air turbulence, this process has traditionally been used on small capacity engine, typically less than 1 litre per cylinder. Typically large volume engines (over 1 litre per cylinder) have used direct fuel injection. These inject the fuel directly into the combustion chamber to provide excellent control of air and fuel mixing and increased injection pressures to reduce the specific fuel consumption. Development of the direct injection process has seen it introduced on smaller capacity engines, this has improved small diesel engine fuel consumption and with the development of more detailed fuel spray characteristics engine speed and power output has also been increased. Typically indirect injection engines produce more soot than direct injection engines, due to increased amount of fuel that they consume and reduced oxidation that occurs, due to the increased engine speeds and lack of control over fuel and air mixing. In the future indirect injection methods may be re-introduced as demands increase for higher engine speeds, this will further increase soot production within such engines.

Gasoline engines do not produce anything near the level of soot particulates that diesel engines do, but there is a possibility that soot production levels will increase with the introduction of direct injection gasoline engines. Direct injection gasoline engines operate in a similar fashion to diesel direct injection engines, but there is a

chance that with varying air-to-fuel ratios within the combustion chamber that soot particulates may form. These particulates would be smaller that those produced by diesel fuel, due to the differences in the fuel's composition and idiosyncratic combustion process.

One final effect on engine operation that can lead to an increase in soot production is oil consumption. A great deal of work is being carried out to optimise the lubricant films produced around the piston to therefore reduce the amount of oil entering the combustion chamber, as engine lubricants burn slowly and inefficiently leading to increased levels of soot and unburnt hydrocarbons **[51]**.

2.7. LEGISLATION

Currently typical levels of soot contamination are in the region of 3 to 5% by mass; such levels are already displaying signs of significant engine wear. Current oil change intervals are up to almost 50,000km for a passenger car or 120,000km for trucks. The automotive and lubricants industries are expecting to see soot contamination levels of up to 10% by 2010, the lubricants industry is designing engine oils to cope with such levels, without significant increases in viscosity and the engine companies are designing engines to minimise the effects of highly contaminated lubricants **[50]**.

Another impact on the quality and ability of the oil to perform its function is the level of stress it is under, increasing the degradation of the lubricant through shearing and heating. Oil stress has been increasing for the last 50 years and is expected to rise at an increasingly faster rate in the future **[51]**, as shown in Figure 2.5. Therefore significant further development is required to help maintain lubricant performance under these expected conditions.

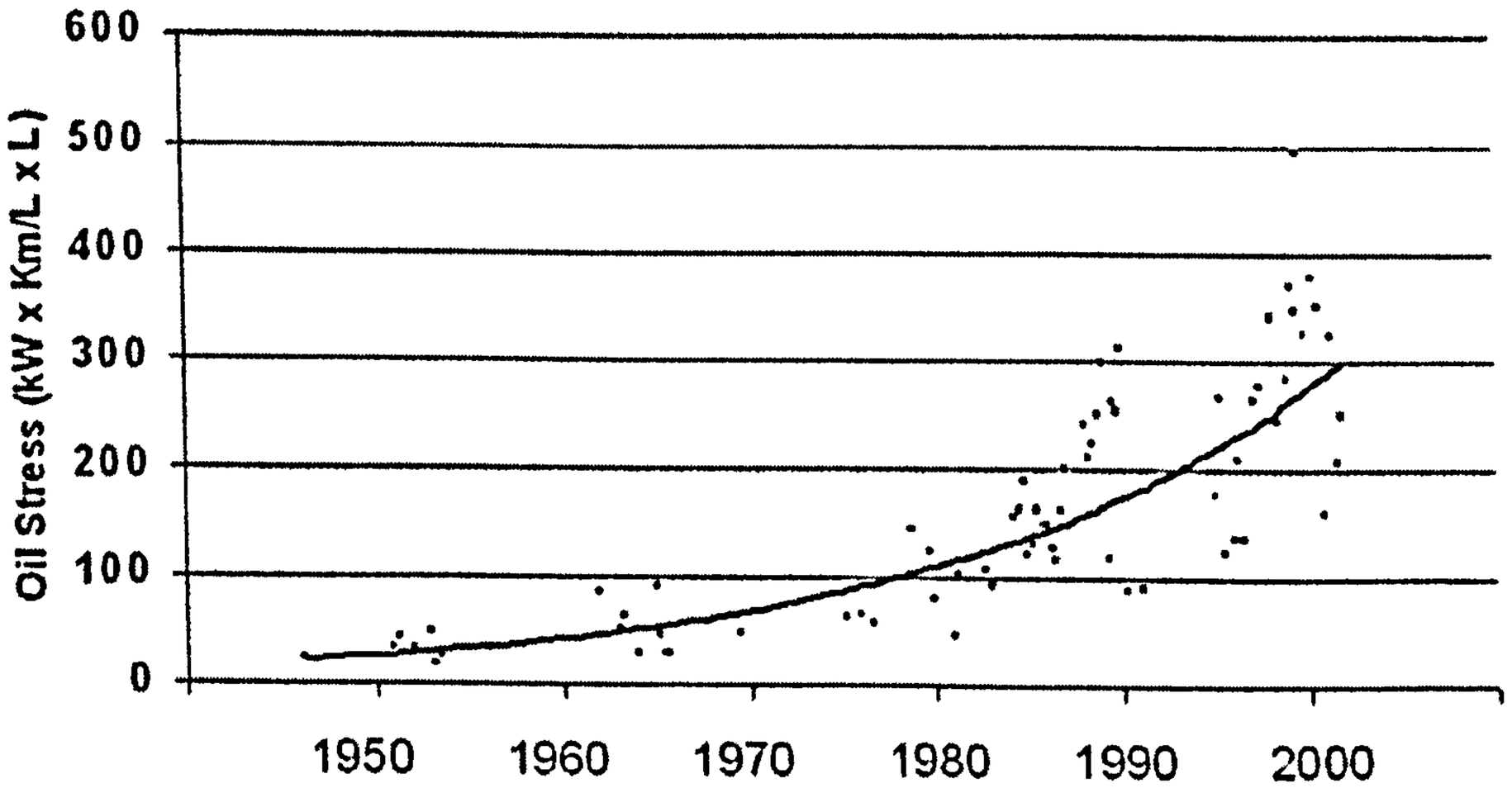

Figure 2.5. Graph of Oil Stress with Time **[51]**.

The current and future level of soot contamination of engine lubricants is partially due to the legislation for tailpipe emissions. The European vehicle emissions legislation

for heavy duty diesel vehicles relating to NOx (oxides of nitrogen) and particulates is shown in Figure 2.6. It can be seen that both types of vehicle emission have been vastly reduced in recent years with the forthcoming Euro 5 target for 2008 and will continue to do so **[50]**.

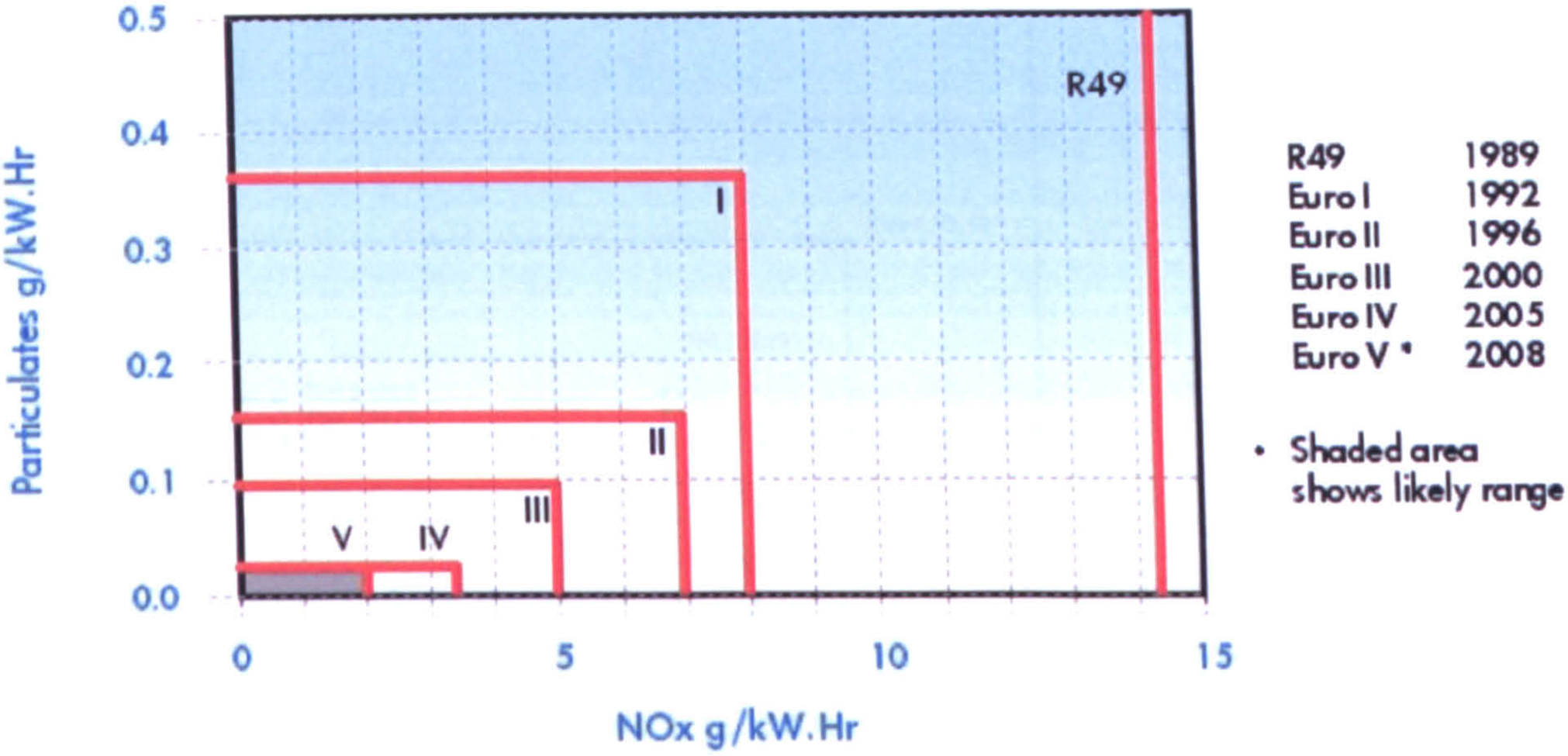

Figure 2.6. European Heavy Duty Vehicle Emissions **[50]**.

The NOx target (as shown in Figure 2.6) requires the use of EGR which causes an increase in the amount of soot returned into the engine. The restriction on the amount of particulates emitted, introduces the need for exhaust particulate filters to be fitted, resulting in soot particles being contained onboard the vehicle. Particulate filters may though have an effect on the efficiency of the engine, as they gradually trap increasing amounts of exhaust soot, and the engine's back pressure will be detrimentally affected **[51]**. The results of such targets may lead towards an increased level of servicing, but technological advances are required to overcome such issues and continue the trend of reduced vehicle servicing.

Some of the most stringent tailpipe emissions targets are produced by the Environmental Protection Agency (EPA) in the United States with their latest Tier 2 legislation, where reductions in carbon dioxide, carbon monoxide, unburnt hydrocarbons, oxides of nitrogen (NOx) and particulate matter are required **[52]**. The US tailpipe legislation for NOx and particulate matter are shown in Figure 2.7 **[53]**.

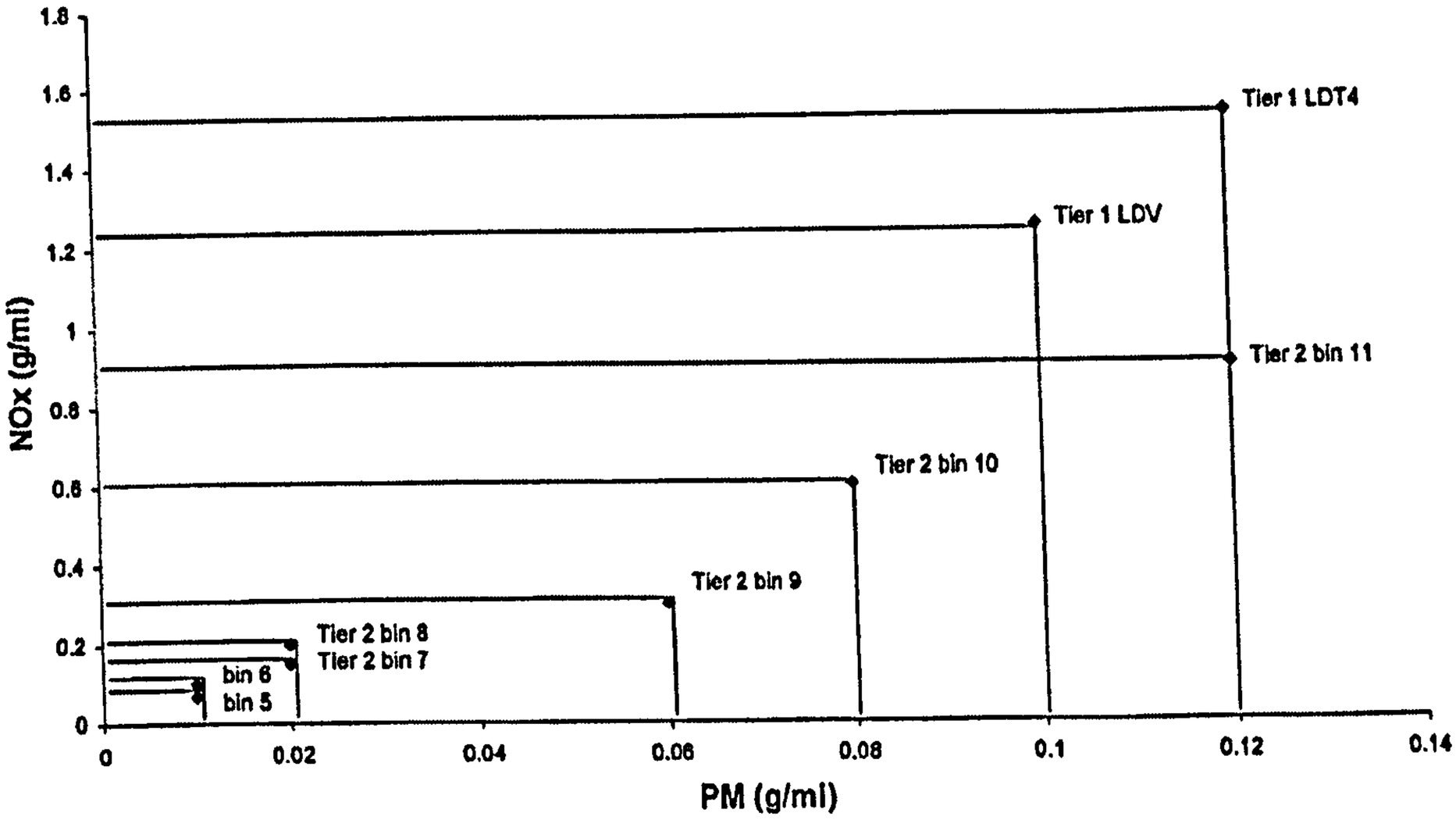

Figure 2.7. US Tier 1 Light-Duty Diesel and Tier 2 Full Useful Life Exhaust **[53]**.

2.7.1. Other Fuels

With an aim to reduce the amount of carbon dioxide emitted into the atmosphere by internal combustion engines due to the global concern that increased levels of greenhouse gases in the atmosphere accelerates the rate of global warming new fuels are being investigated. These fuels include modified diesel i.e. water-diesel fuel emulsions, synthetic fuels produced through advanced gas to liquid conversion technologies, biofuels and hydrogen technology to name but a few.

Additive modified diesel fuels and water-diesel fuel emulsions have been tested and shown to be potential substitutes to current diesel fuels **[54, 55]**, as have synthetic diesel fuels produced through the Fischer-Tropsch gas to liquid fuel production method **[56, 57]**. There have though been findings from various authors demonstrating reductions in particulate matter emitted during engine test using biofuels, in particular rape seed oil **[58, 59]**, palm oil **[60, 61]** and soybean oil **[62, 63]**.

2.8. DISCUSSION

2.8.1. Testing

Although full scale engine testing is preferred, due to the more realistic results achieved results from bench specimen testing are displaying significant similarities, allowing cost effective and reliable testing to be carried out to gain an understanding of an extremely difficult issue that has many influencing factors. A large variety of test rigs have been used to try to understand the wear created by soot contaminated lubricants. This approach generally appears to confuse many issues and does not allow for different tests to be compared against each other. In order to allow for comparisons standards need to be established to provide consistency.

The main issues to be considered when creating a test standard for investigating soot wear include: contaminated oil mixture method, test specimen preparation, test method and procedure and wear analysis. When considering the contaminated oil mixture itself, the elements used are important. The lubricant should be selected depending on the aims of the testing, base oil should be used to demonstrate wear that occurs when there are no anti-wear additives present (with base oil a dispersant is required to suspend the test particles), formulated oil should be used to test the wear resistance of new lubricants and for comparison between different finished lubricants. Ideally extracted engine soot mixed into a fresh test lubricant is the best soot simulant for testing, but there are variability issues with such particles, to avoid such variability carbon black particles are next best option. A variety of mixing methods have been applied, but heating and ultrasonic agitation of the mixture has been proven by many to be the most appropriate method.

Test contacts should replicate the real engine conditions, and ideally the specimens should be similar in terms of material composition and dimension to real engine contacts, experiencing a realistic contact pressure. The duration for the tests should be long enough to produce wear data that is unaffected by a running-in period, but is short enough to be a practical laboratory test (in terms of minutes, not hours). Current analysis techniques use wear scar imaging (using microscopes and SEMs) and surface profilometry are providing extremely useful information. The latest advanced techniques such as scanning interferometry may provide much more detailed information on the wear features produced.

Standard techniques are being investigated and used, such as the ASTM standard G133-05 for a reciprocating ball-on-flat, but specific standards are required to incorporate all of the issues above for soot contaminated oil wear testing. Such a standard is currently being developed for piston ring on cylinder liner specimens with contaminated oil **[25]**.

Testing with contaminated lubricants provides many complex and contentious issues. One main issue relates to the real dispersion of particles within the test lubricant. Practically it is known that in any mixture of contaminated oil there is a significant amount of residue in the bottom of the receptacle containing the mixture. In many cases further analysis is required to assess the contamination level in the sample rather than bulk test mixture.

2.8.2. Wear And Friction

It has been clearly shown that significant majority of research does not demonstrate that soot particles reduce the performance of the anti-wear additives in lubricants; but that abrasion is the major wear mechanism that occurs with soot related engine wear. Various authors have referred to such wear as either abrasion or polishing, as does the automotive industry. Abrasive wear scars are generally only clearly visible under a microscope, but when viewed with the naked eye or under low magnification (macroscale) as some previous investigations have found, they appear to be polished (not abraded).

As the levels of contamination used in various investigations have increased, the amount of wear produced has also increased and the wear mechanisms witnessed have also changed to that of contact starvation of lubricant. As lubricants are expected to retain up to 10% soot by 2010, further investigations are required to investigate the wear levels produced with modern lubricants containing this level of contamination.

One main area of testing that has had very little attention is that of visualisation of soot entrainment into a contact. Visualisation techniques vastly improve the understanding as to how soot enters the contact (if it does) and how it forms around the contact to starve it of lubricant. Such research would complement wear and friction testing and assist with the understanding of the motion of soot around contacts.

Engine valve trains have been shown to be the most susceptible to soot related wear due to type of motion (generally reciprocating) not creating uninterrupted oil films, low lubricant flow rates and related design issues. But the effect of soot contamination around the piston has also proven to create significant wear. Abrasive wear occurs to a lesser degree as the reciprocating motion in that region of the engine is more effecting in creating oil films, but due to the extreme temperatures, volatile gasses and presence of oxygen corrosive wear is highly likely to occur.

2.8.3. Wear Modelling

Currently no modelling of soot related wear has been performed, but it has been attempted though on the related issues of soot production through combustion and soot adsorption and agglomeration within lubricants. Similar models are required to complement the above models and to make significant use of the testing that has been performed and the wear mechanisms that have been proposed to simulate wear due to soot in a variety of engine contacts in various operating conditions.

2.8.4. Soot Removal

Current flow-through filtering is expected to be used in the near future as there is alternative available with the ability the match it in terms of both performance and cost. By-pass filters with increasingly finer grade filers and deep-bed filters are expected to continue to perform this function.

Possible future lubricant filtering techniques can draw inspiration from various other industries; such techniques may include magnetic **[64, 65]**, ultrasonic **[66, 67, 68, 69]** and electrostatic **[67, 70, 71, 72]** means. Chemical and biological treatment of the contaminated lubricant may also be a possibility in the future **[73, 74]**.

Another approach to take in relation to the problem of lubricant contamination is possibly not to retain the contaminant in the lubricant at all. With this process the particles would be flushed through the engine and into the sump. This process would be extremely dependent on detailed engine design to ensure that all of the particles travel through the engine to the sump and are not retained within the main body of the engine and therefore entering any critical contacts to cause wear. In the sump, the

particles could be filtered through a deep-bed filter, to ensure good retention of particles, to avoid re-contamination of the lubricant. This method would be extremely dependent on engine design as in certain circumstances (particularly for industrial machinery applications) engines experience significant angles of disturbance and rotation when in use. If this method were to be applied, the life of a lubricant would not be determined by its particulate contamination level, but by its natural degradation through use, possibly leading to extended engine oil drain periods.

The detection of soot in a contact or in the lubricant alone is also important as it increases the understanding of the transportation of soot around the engine and also the amount of soot in the lubricant at that point or as a bulk quantity. It is thought that this may be possible with various removal techniques.

2.8.5. Other Fuels and Lubricants

Alternative fuels such as modified diesel, synthetic diesel and biofuels in tests have been known to reduce the amount of particulate matter produced **[54-63]**. Certain biofuels have also been shown not to produce anymore wear than conventional diesel fuel **[60]**. Such testing needs to be continued as these fuels will reduce both the amount of carbon dioxide emitted and the level of soot related wear in engines, whilst allowing the trend of increasing service interval to continue.

Increasingly synthetic lubricants are being used in engines and are a requirement for high performance engines. The use of synthetic lubricants over mineral based lubricants are that their can be very carefully controlled to provide the properties required. They also have a very high viscosity index, meaning their viscosity is not highly dependent on temperature changes. This is important in the role of controlling the oil film thickness produced at high engine operating temperatures to reduce the wear effects of soot related wear issues.

2.9. CONCLUSIONS

This review has brought together a significant amount of information and research in the field of soot contaminated lubricants and the associated engine wear problem. It has been shown essentially that in fuel rich and high load engine operating conditions soot production increases dramatically, the primary soot particles of approximately 40nm diameter are either transported to the exhaust system or absorbed by the lubricant. When absorbed by the lubricant the soot particles tend to agglomerate into clumps of an approximate mean diameter of 200nm. If exhaust gas recirculation (a technique used to reduce NOx emissions) is fitted to the engine then some of the exhausted air is reintroduced in to the engine, increasing the soot loading in the lubricant.

Soot contaminated lubricants have been shown to dramatically increase wear of many engine components. An engine's valve train has proven to be the most seriously affected due to the thin oil film thicknesses experienced in many of its reciprocating contacts. The film thicknesses produced in such contacts are believed to be less than the diameter of the soot particles contained within the lubricant.

To understand the degree to which soot in a lubricant increases component wear and more importantly the wear mechanisms that cause the wear and variety of testing has been performed. The tests have included laboratory bench tests all the way through to full engine tests. Each type of test provides more information to add to the increasing knowledge on the subject. The dominant wear mechanism that has been discovered is that of abrasion, but recent research suggests that a starvation wear mechanism may also occur.

Soot contamination has also shown to adversely affect the properties of lubricants, particularly increasing the viscosity, which in turn increase contact friction, which lead to a reduction in engine efficiency. Such a reduction in efficiency will increase fuel consumption and therefore tailpipe carbon dioxide emission.

Many future research opportunities are possible in this area as it adversely affects operating costs to the customer, wear of the engine and exhaust emissions. Further testing to thoroughly determine the wear mechanism theories is required, especially with various materials and possibly contact conditions. From such testing wear prediction models can be produced to predict how wear will occur in new engine contact designs and how to minimise the wear effects of soot contaminants. Investigations are required into the actual removal of the particles from the lubricant, to attempt to reduce the potential of wear occurring.

A reduction in the amount of soot produced through the combustion process can be achieved through development of current diesel fuels and through the introduction of synthetic diesel fuels where tighter component control is possible due to the nature of the production process. Biofuels are also showing promise as they naturally tend to produce less combustion soot than current diesel fuels. Finally improvements in lubricant technology can assist in the retention of soot particles and anti-wear performance through additive improvements. Also increased wear protection can be achieved through the very high viscosity indexes possible with modern synthetic lubricants.

CHAPTER 3:
WEAR TESTING PROCEDURE

The wear testing method was developed from the understanding of a typical valve train contact. The contact used as the model for the wear testing exhibited reciprocating motion, under a relatively high load. The model contact has been analysed to understand its operating conditions in terms of speed, load and temperature, but also its predicted oil film thickness. From the analysis, test parameters and conditions have been calculated for a ball-on-flat reciprocating specimen wear test. The analysis is presented in this chapter.

The test lubricants and the methodology for mixing with carbon black (acting as a soot surrogate) are also detailed. Finally the test procedure and conditions for specimen and component wear testing is presented.

3.1. FORD ELEPHANT'S FOOT TO VALVE TIP CONTACT – CASE STUDY

An example of a rocker arm reciprocating contact is that of the elephant's foot to valve tip contact, which has been known to be susceptible to wear due to soot contaminated lubricants. Previous work **[17]** has also shown that the valve train is the area most prone to soot related wear, see Figure 2.4. A schematic diagram of the contact's reciprocating movement is shown in Figure 3.1. This component has previously been shown to be susceptible to wear as shown by wear scar images in Figure 3.2, comparing a new elephant's foot against a used one from a 2.4 litre, 16 valve diesel engine.

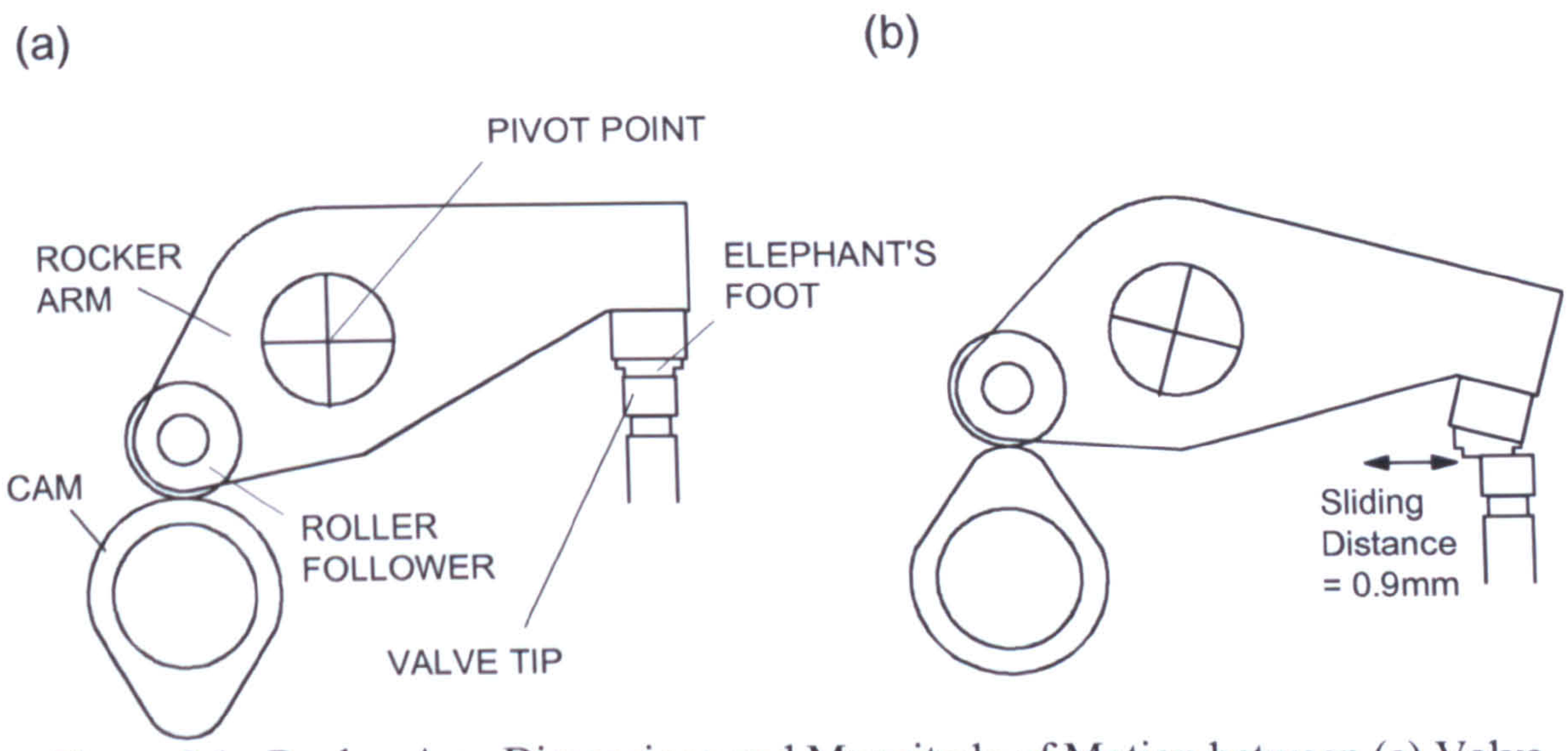

Figure 3.1. Rocker Arm Dimensions and Magnitude of Motion between (a) Valve Closed Position and (b) Valve Closed Position.

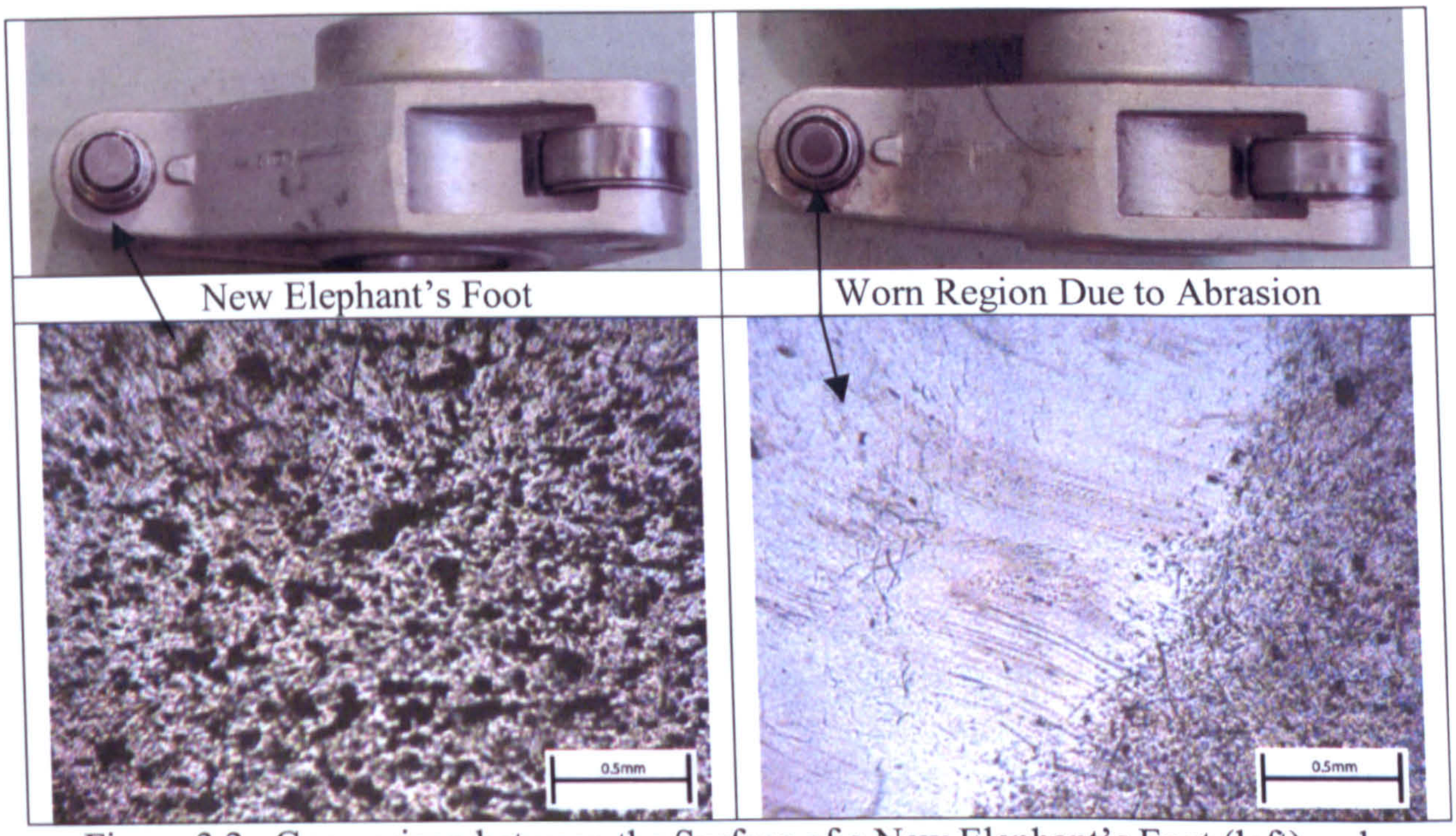

Figure 3.2. Comparison between the Surface of a New Elephant's Foot (left) and a Used Elephant's Foot (right).

Figure 3.2 clearly shows that considerable wear is visible on the surface of the elephant's foot that has been used in normal engine running conditions. The wear appears to be abrasive wear due to scratch marks in the direction of sliding on the surface of the component. Analysis reveals that through the wear process the rough surface becomes polished. Figure 3.2 also reveals that wear occurs only in the centre of the elephant's foot, this is because it is slightly radiused, probably to allow lubricating oil to be entrained into the contact. The effects of this wear could lead to changes in valve timing and lift.

The elephant's foot contact consists of two hard steel surfaces experiencing relatively high loads of up to 660N (approximately 100MPa), reciprocating in a sinusoidal motion at an average speed of 0.0594m/s. The roughness of the surfaces of the

elephant's foot (0.45μm) and the valve tip (0.175μm), combined with the experienced loads mean that the contact operates within the boundary lubrication regime.

To understand the levels of wear and the mechanisms that occur during use with soot contaminated lubricants a fundamental study is required. A simple approximation of the above contact is a ball-on-flat specimen test.

3.2. ANALYSIS OF CONTACT

The elephant's foot to valve tip contact conditions required to simulate the ball-on-flat contact were calculated using Hertzian contact equations (see for example **[75]**). Contact parameters were calculated assuming that the contact would be between a 5mm diameter steel ball against a flat steel counterface, with hardness's similar to the values of the elephant's feet and valve tips. The test contact conditions were chosen to simulate engine operating conditions, applicable to a range of component contacts to gain a fundamental understanding, rather than perform a direct comparison.

As the maximum contact pressure, p_0 of the actual contact is known, contact load required, P, was obtained from:

$$P = \frac{2p_0\pi a^2}{3} \tag{3.1}$$

where the contact radius, a is:

$$a = \sqrt[3]{\frac{3PR}{4E^*}} \tag{3.2}$$

The contact conditions and oil film thicknesses were calculated using Hertzian and EHD theory (see for example **[75]** and **[76]** respectively). The oil film thicknesses for the tests were selected to be as close as possible to the actual elephant's foot contact conditions. The load required for the ball-on-flat contact was calculated to be 0.64kg (or 6.3N). The EHD oil film thicknesses, H is determined in terms of four dimensional parameters **[76]**:

Load, W

$$W = \frac{F}{2E^* R_x^2} \tag{3.3}$$

Speed, U

$$U = \frac{\eta_0 u}{2E^* R_x} \tag{3.4}$$

Materials, G

$$G = 2\alpha E^* \tag{3.5}$$

Ellipticity, k

$$k = 1.03\left(\frac{R_y}{R_x}\right)^{0.64} \tag{3.6}$$

Where:

F=total normal load

R_x=reduced radius in the x-direction, the direction of motion

R_y=reduced radius in the y-direction

u=mean surface speed

η_0=viscosity of oil as it enters the contact

α=pressure viscosity coefficient

E^*=reduced modulus

The film thickness parameter can be calculated according to:

Central film thickness, H_c:

$$H_c = 2.69U^{0.67}G^{0.53}W^{-0.067}\left(1-\left(0.61e^{-0..73k}\right)\right) \tag{3.7}$$

Minimum film thickness, H_{min}:

$$H_{\min} = 3.63U^{0.68}G^{0.49}W^{-0.073}\left(1-e^{-0.68k}\right) \tag{3.8}$$

It was decided to run tests at a sinusoidal mean sliding speed of 0.36m/s, and a lower speed of 0.18m/s to see if similar trends were obtained (only for base oil tests). These test sliding speeds are higher than those in the case study, to accelerate wear and to produce the required oil film thickness. The tested conditions are best compared through the theoretical film thicknesses; these are shown in Table 3.1, where they are compared to typical engine soot diameters as discussed in Chapter 2, from reference [6]. The film thicknesses are taken from the theoretical modelling detailed above, for uncontaminated oil. Table 3.1 highlights that increasing temperature and decreasing sliding speed have the combined effect of reducing oil film thickness. It is important to note that the conditions stated in Table 3.1 are all within the boundary lubrication regime.

Table 3.1. Comparison of Theoretical Film Thickness for Tested Conditions **[6]**.

		Oil used	Mean Soot Particle size (μm)	Soot Agglomerate size (μm)	Mean initial sample roughness (μm)	Minimum Film Thickness (μm)
25°C	Ball on Flat (Full Speed)	Base Oil	0.2	0.5	0.42	0.05
25°C	Ball on Flat (Half Speed)	Base Oil	0.2	0.5	0.42	0.03
100°C	Ball on Flat (Full Speed)	Base Oil	0.2	0.5	0.42	0.02
100°C	Ball on Flat (Half Speed)	Base Oil	0.2	0.5	0.42	0.01
25°C	Ball on Flat (Full Speed)	Formulated Oil	0.2	0.5	0.42	0.12
100°C	Ball on Flat (Half Speed)	Formulated Oil	0.2	0.5	0.42	0.03

3.3. RECIPROCATING TEST RIG

A universal high frequency reciprocating wear tester was used to carry out all of the wear tests. Figure 3.3 shows a simplified schematic diagram and Figure 3.4 shows a photograph of the wear tester. The tester holds the specimen balls in a clamp on the reciprocating arm and flat disc specimens in the heated base unit via another clamp. Prepared oil specimens (of approximately 2ml) are contained in the recessed zone with the flat disc specimens. The heated base is controlled by a programmable PID temperature controller. The reciprocator (LDS V201 vibrator) is controlled by a function generator. Friction measurements can be taken via a load cell located on the rig.

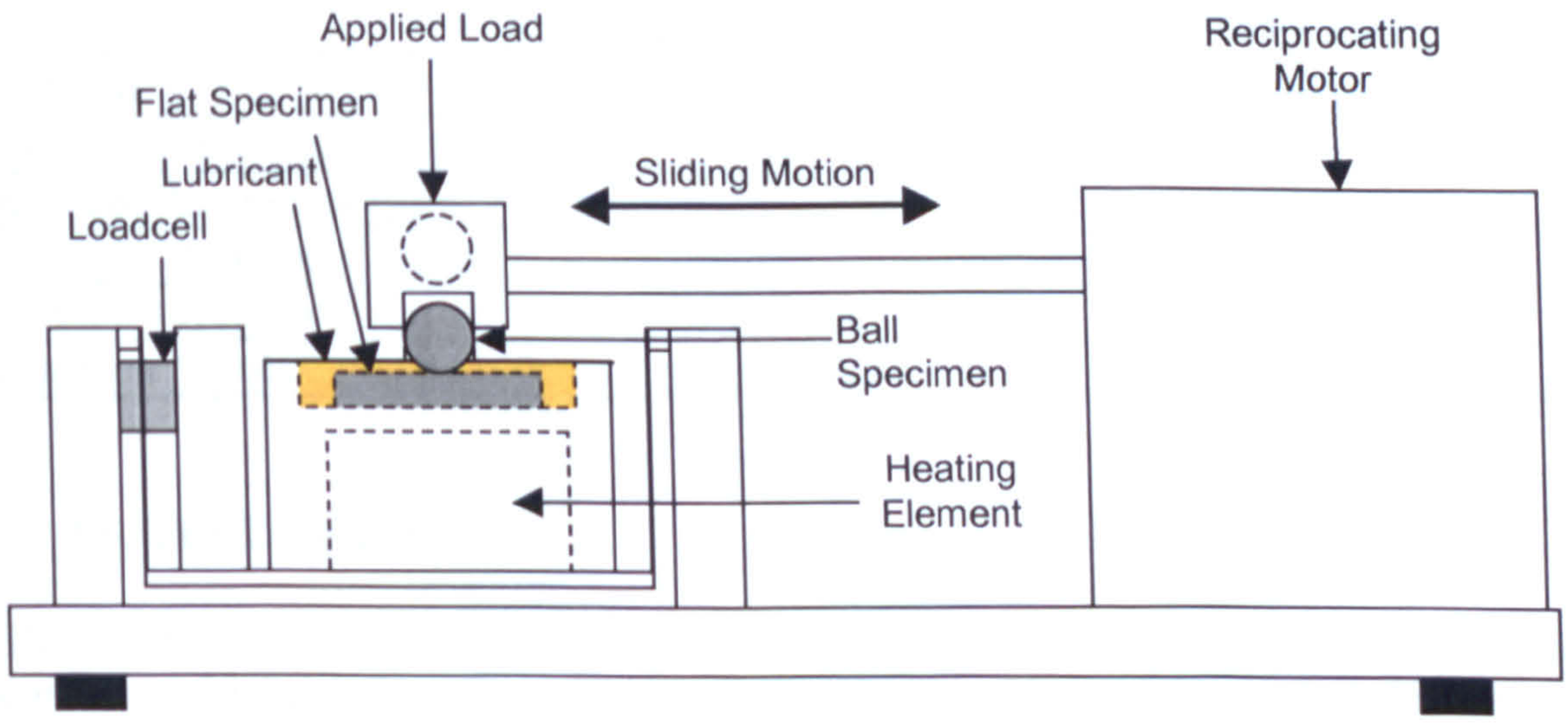

Figure 3.3. A Simplified Schematic Diagram of the Reciprocating Wear Tester.

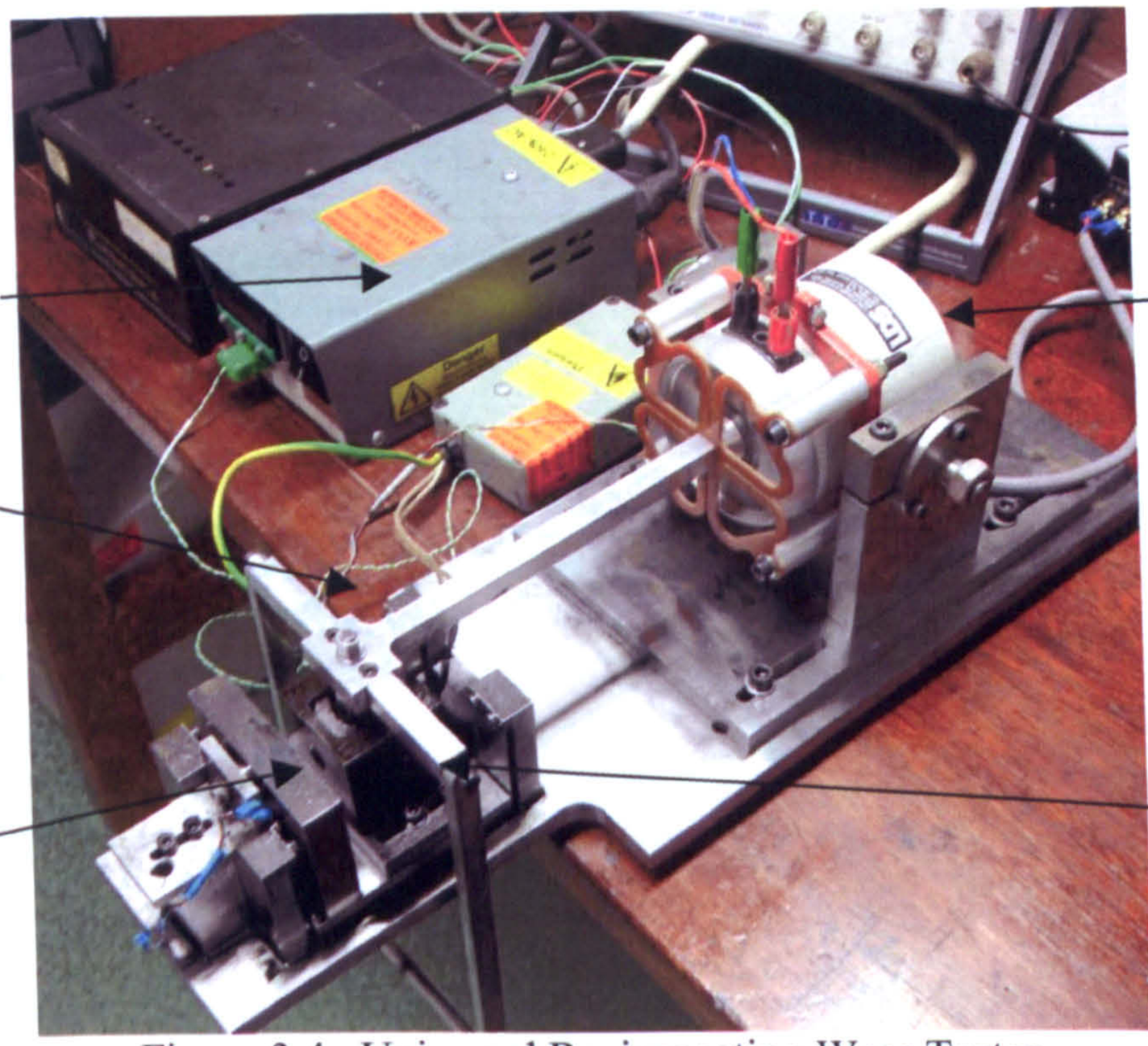

Figure 3.4. Universal Reciprocating Wear Tester.

3.4. TESTS SPECIMENS

Details of the ball-on-flat specimens are shown in Table 3.2. The ball and flat test specimens were cleaned of any residue oxide layer or machining lubricant before the tests by washing in ethanol in an ultrasonic bath.

Table 3.2. Details of ball on flat specimens.

	Ball Specimen	Flat Specimen
Material	Chrome Steel EN31	EN24 Hardened & Tempered
Average Hardness (Hv)	600	400
Average Roughness (μm)	0.05	0.5
Young's Modulus, E (GPa)	210	210
Poisson's Ratio, ν	0.3	0.3
Diameter (mm)	5	18 (3mm thick)

3.5. TEST LUBRICANTS

The wear tests were performed with an automotive base oil and a fully formulated commercial lubricant as the test oils. Each lubricant was used in tests on its own and mixed with varying amounts of carbon black. Ashless dispersant was added to the base oil to retain the particles in the lubricant (details of all components are shown in Table 3.3). No anti-wear additives were added to the base oil mixtures as this would affect the amount of wear measured, reduce the chemical independence of the testing and make the results specific to just one type of anti-wear additive. The mixing of ashless dispersant with the base oil is thought to have a negligible effect on the viscosity of the oil due to its low total weight content in the mixture and it will not

appreciably add any anti-wear properties. The dispersant was purely mixed in to suspend the carbon black within the base oil, as would occur in the formulated lubricant.

The mixed oils were prepared in 100g samples using a precision digital balance, which has a resolution of 0.01mg. The base oil mixtures contained a 4% (by weight) addition of ashless dispersant (this is the same treat rate as in the formulated oil). The percentage of carbon black (by weight) required for the mixture was added (1 to 5% for the base oil mixtures and 1 to 7% for the formulated oil mixtures), to produce a 100g sample.

The test lubricants were mixed using an ultrasonic bath for 20 minutes at 60°C (the blending temperature of the dispersant with base oil is approximately 60°C). An ultrasonic bath was used as the mixing device so as to reduce the chances of oil aeration; a spatula was used during the mixing process to ensure carbon black particles were being transported through the oil and did not reside on the bottom of the beaker.

Table 3.3. Test Lubricants and Components

Substance	Title	Description
Base oil	Shell HVI 60 (Typical automotive base oil)	Kinematic viscosity @ 40°C = 29.38 cSt Dynamic viscosity (η_o) @ 40°C = 0.022 Ns/m^2 Kinematic viscosity @ 100°C = 6.8 cSt Dynamic viscosity (η_o) @ 100°C = 0.005 Ns/m^2 Density (approx.) = 750 kg/m^3
Formulated oil	Shell Helix Plus 10W-40 (semi-synthetic)	Kinematic viscosity @ 40°C = 113.3 cSt Dynamic viscosity (η_o) @ 40°C = 0.091 Ns/m^2 Kinematic viscosity @ 100°C = 22.2 cSt Dynamic viscosity (η_o) @ 100°C = 0.018 Ns/m^2 Density (approx.) = 870 kg/m^3
Ashless Dispersant	SAP 285	Lubricant dispersant for dispersing ash/soot. (Added to base oil at the same treat rate as appears in the formulated oil)
Carbon Black	N/A	Acetylene black (AB) 50% compressed, 99.9+% (metals basis), mean particle diameter = 42nm. The datasheet is available in Appendix 1.

3.6. TEST PROCEDURE

The test equipment as described in Section 3.2 was used for each test. All tests were performed for 20 minutes. All full speed tests were performed at least three times, to ensure repeatability of results.

The oil temperature (apart from carbon black content) was the main parameter that was varied during the testing programme. The lubricant mixtures were tested at three different temperatures: room temperature (approximately 25°C); engine working temperature (100°C) and a ramped temperature profile (base oil tests only) of controlled linear heating from room temperature to 100°C in 10 minutes and then held

at 100°C for the final 10 minutes. The test temperatures were to represent: cold working, normal engine working temperature and start-up conditions respectively. All constant test parameters are detailed in Table 3.4.

Table 3.4. Constant Test Parameters.

Reciprocating distance (mm)	2 (amplitude)
Test duration (minutes)	20
Load (kg)	0.64 (including mass of arm)
Mean Contact Pressure (MPa)	Approximately 500
Herzian contact diameter (microns)	47

Further tests were performed at half sliding speed with the base oil samples to ensure the trends measured were consistent under various conditions. An outline of the tests performed is shown in Table 3.5, where 'B' relates to tests carried out with base oil and 'F' relates to tests carried out with formulated oil.

Table 3.5. An Outline of the Wear Tests Performed.

Carbon Black Content	Temperature			Sliding Speed	
	25°C	25-100°C	100°C	0.18m/s	0.36m/s
0%	B & F	B	B & F	B	B & F
1%	B & F	B	B & F	B	B & F
2%	B & F	B	B & F	B	B & F
3%	B & F	B	B & F	B	B & F
4%	B & F	B	B & F	B	B & F
5%	B & F	B	B & F	B	B & F
7%	F	-	F	-	F

To analyse how the wear varied with time, further tests were performed for 40 minutes with measurements taken every 10 minutes to measure how the wear scars developed, with an initial measurement taken after 3 minutes (to aid understanding of the early wear development). The tests were carried out at 25°C and 100°C with a 3% carbon black mixture.

3.7. WEAR MEASUREMENT

The wear tests produced wear scars on the flat steel specimens and steel balls. The wear on the balls was negligible compared with that on the flat specimens and therefore not measured. The wear tests produced measurable grooves on the flat specimens. The length, l and width, w of a groove was measured using a digital camera and analysis software for accurate dimensioning. The wear depth of each groove was measured using a Mitutoyo Surftest Profilometer. As the depth varied along the length of the groove a number of depth measurements (transverse to the length of the groove) were taken. The experimental average depth, d was taken from these measurements. From this information the volume of a 'perfect groove' could be calculated, shown graphically in Figure 3.5.

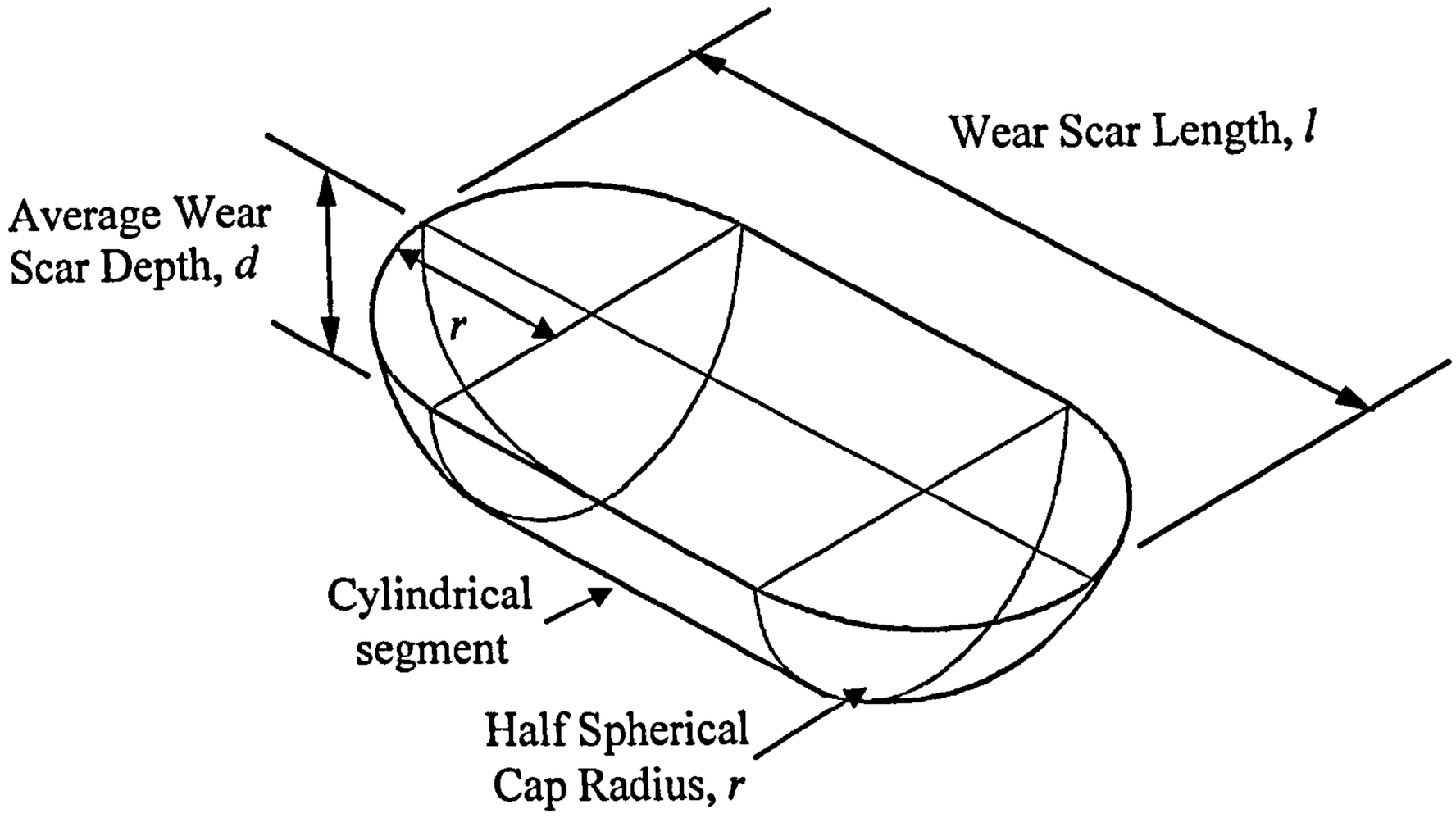

Figure 3.5. A 'Perfect Groove' Wear Scar

The 'perfect groove' consisted of a cylindrical segment and two half spherical caps at each end. Calculated using the following method, using a ball of 5mm diameter, D or 2.5mm radius, R:

Cylindrical Segment:

$$\text{Volume} = \left(R^2 \cos^{-1}\left(\frac{R-d}{R}\right) - (R-d)\sqrt{2Rd-d^2} \right)(l-2r) \tag{3.9}$$

Spherical Cap (whole cap):

$$\text{Volume} = \frac{1}{3}\pi d^2(3R-d) \tag{3.10}$$

The total wear scar volume is the sum of the cylindrical segment and the spherical cap (whole cap).

3.8. COMPONENT TESTING

Further wear tests were performed using the model valve train components in the reciprocating test rig for comparison with the ball-on-flat tests. Tests were carried out using the same method, only some of the test conditions were changed. The test conditions for the component wear testing are detailed in Table 3.6.

Table 3.6. Test Conditions for Component Wear Testing.

Carbon Black Content	Test Lubricant	Applied Load	Temperature	Sliding Speed	Test Duration
0%	Base Oil	3.1kg	100°C	0.24m/s	20mins
3%					
5%					

The test components used for the wear testing are shown in Figure 3.6, the valve tip had to modified to suit the reciprocating test rig. A schematic diagram of the reciprocating test rig contact is shown in Figure 3.7.

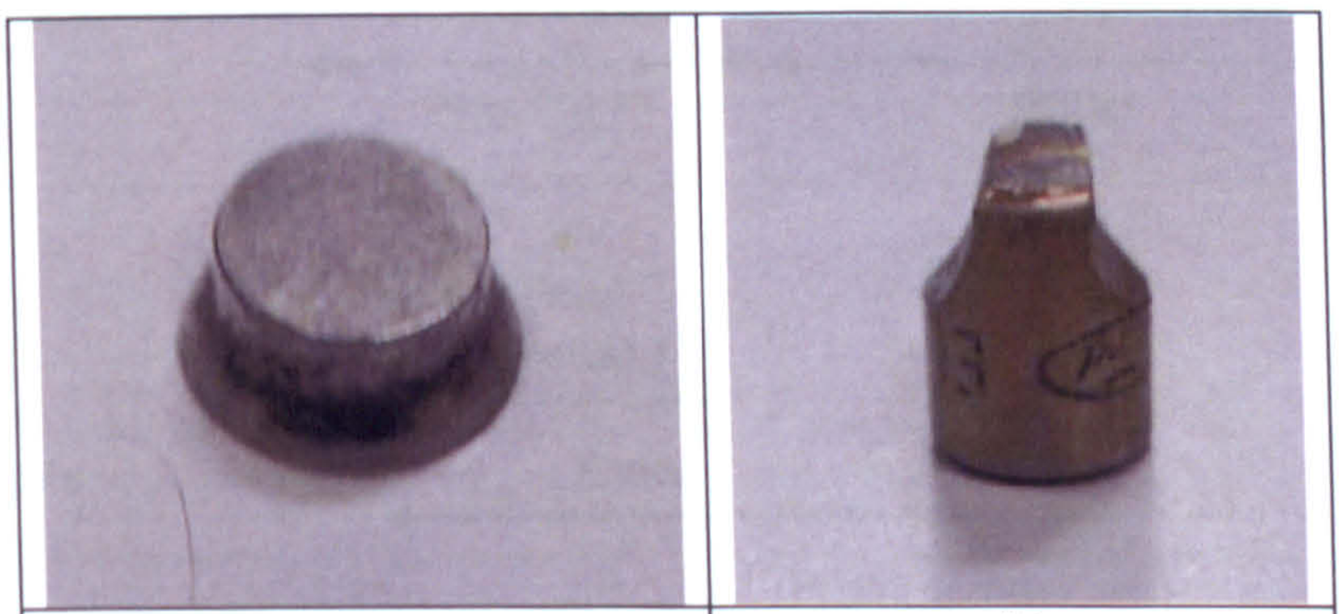

Figure 3.6. Test Components: (a) Elephant's Foot and (b) Modified Valve Tip.

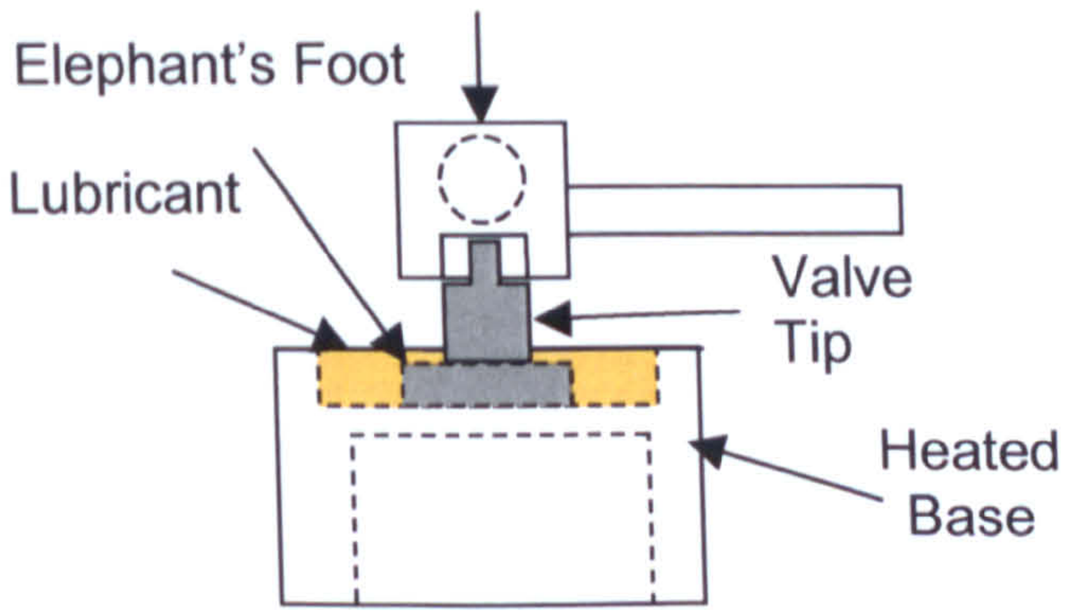

Figure 3.7. A Simplified Schematic Diagram of the Reciprocating Wear Test Rig, with the Test Components.

3.9. SUMMARY OF TESTING METHODOLOGY

The testing methods described in this chapter and chapter 6 are designed to operate in boundary and EHD lubrication regimes. These test conditions related directly to real engine contacts. The testing methods and engines contact lubrication regimes are described schematically in Figure 3.8, related through □, the minimum oil film thickness divided by the root mean square of the roughness of the two contacting surfaces, or expressed as:

$$\lambda = \frac{h_{min}}{\sqrt{(Ra,1)^2 + (Ra,2)^2}} \tag{3.11}$$

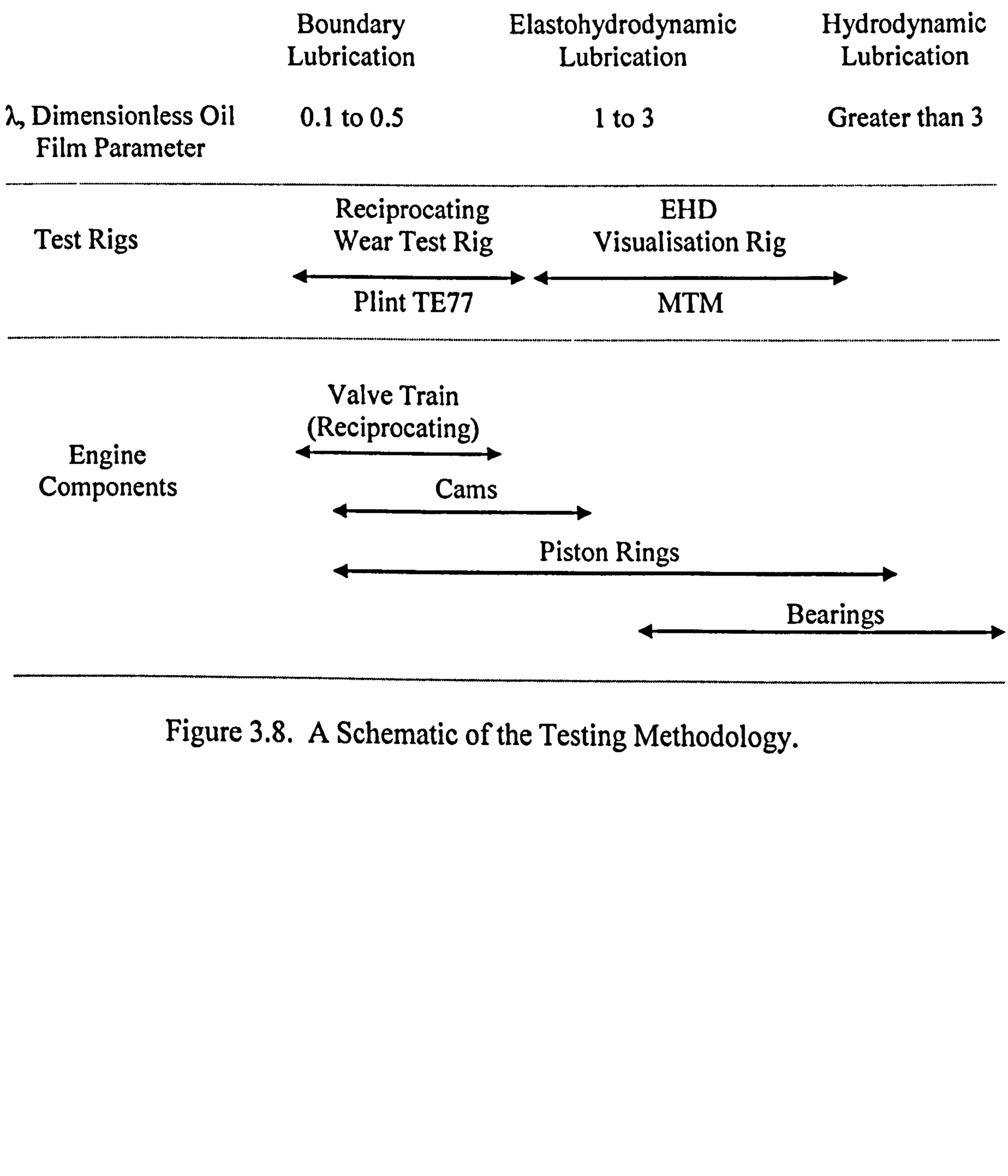

Figure 3.8. A Schematic of the Testing Methodology.

CHAPTER 4:
WEAR TESTING

This chapter details the amount of wear calculated from the physically measurable wear scars produced by the ball-on-flat specimen wear testing, using both base oil and formulated oil mixed with increasing levels of carbon black. An analysis of the wear scar formation rate is performed to assess the effect of the different test parameters, in particular the test duration.

4.1. BASE OIL RESULTS

The results of the base oil tests to evaluate the amount of wear produced from increasing levels of carbon black contamination are shown in Figure 4.1. The amount of wear is represented as a percentage increase over the amount of wear produced by an identical wear test where the test lubricant is neat base oil with no contamination. These tests were performed at a sliding speed of 0.36m/s with a contact load of 6.2N (approximately 500MPa). Figure 4.1 presents results for the tests performed at 25°C, with ramped heating (25-100°C ramp for 10 minutes, then held at 100°C for a further 10 minutes), and at 100°C, with increasing levels of carbon black contamination.

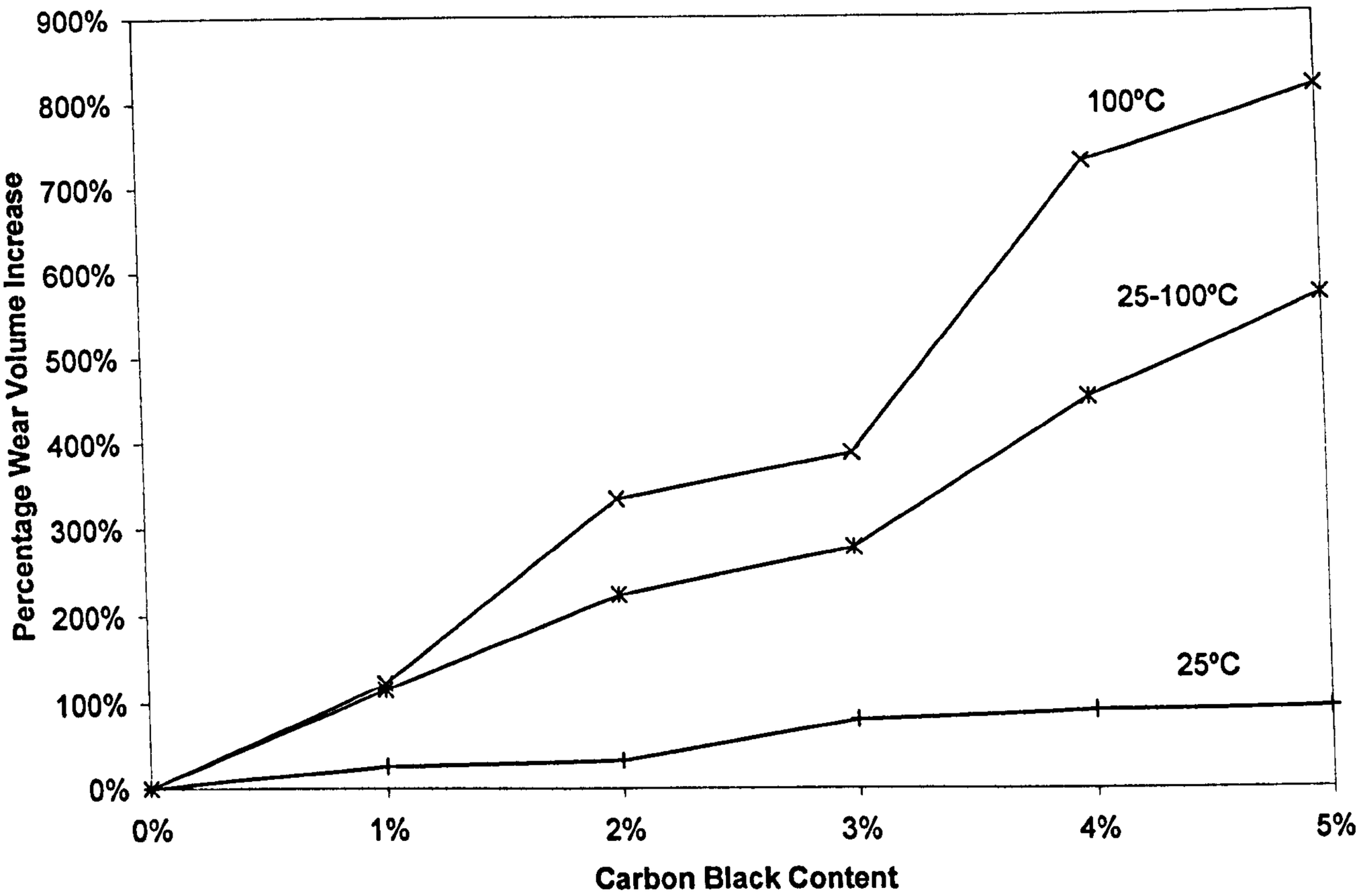

Figure 4.1. Results from Ball-on-Flat Testing Relative to 0% Carbon Black Content Tested at 25°C, Ramped Heating and 100°C (base oil at 0.36m/s sliding speed).

The results in Figure 4.1 follow the expected trend of increased carbon black content and high test temperatures (due to their thinner oil films) producing more wear. The wear levels measured for the ramped heating test are clearly between those of the 25°C and 100°C, as the ramped test involves conditions experienced in both the 25°C and 100°C tests.

The data from the testing presented in Figure 4.1 has been analysed for its statistical variation. The average standard deviation of the wear volume measurements is 0.00025mm^3, this alone gives very little understanding of the accuracy of the results obtained. Further analysis shows that all measured data lies within ±1.2 standard deviations. The measure of dispersion of the data obtained can be calculated with the coefficient of variation (standard deviation divided by the mean), giving a value of 47%, a relatively good result for wear data. The accuracy of the data in the distribution can also be measured using the following rule where the standard deviation should be roughly equal to the range of the data divided by the square root of the number of samples obtained (this applies for datasets of less than 12) [77]. Using this method the standard deviation and the test agree very well, with less than 2.5% variation. All of the data taken and the calculated wear volumes are available in Appendix 2.

To ascertain whether the results and most importantly the trends measured in Figure 4.1 were maintained for a variety of contact conditions, further tests were performed at a sliding speed of 0.18m/s (Figure 4.2). The results are again represented as a percentage increase over the amount of wear produced in a test using neat base oil.

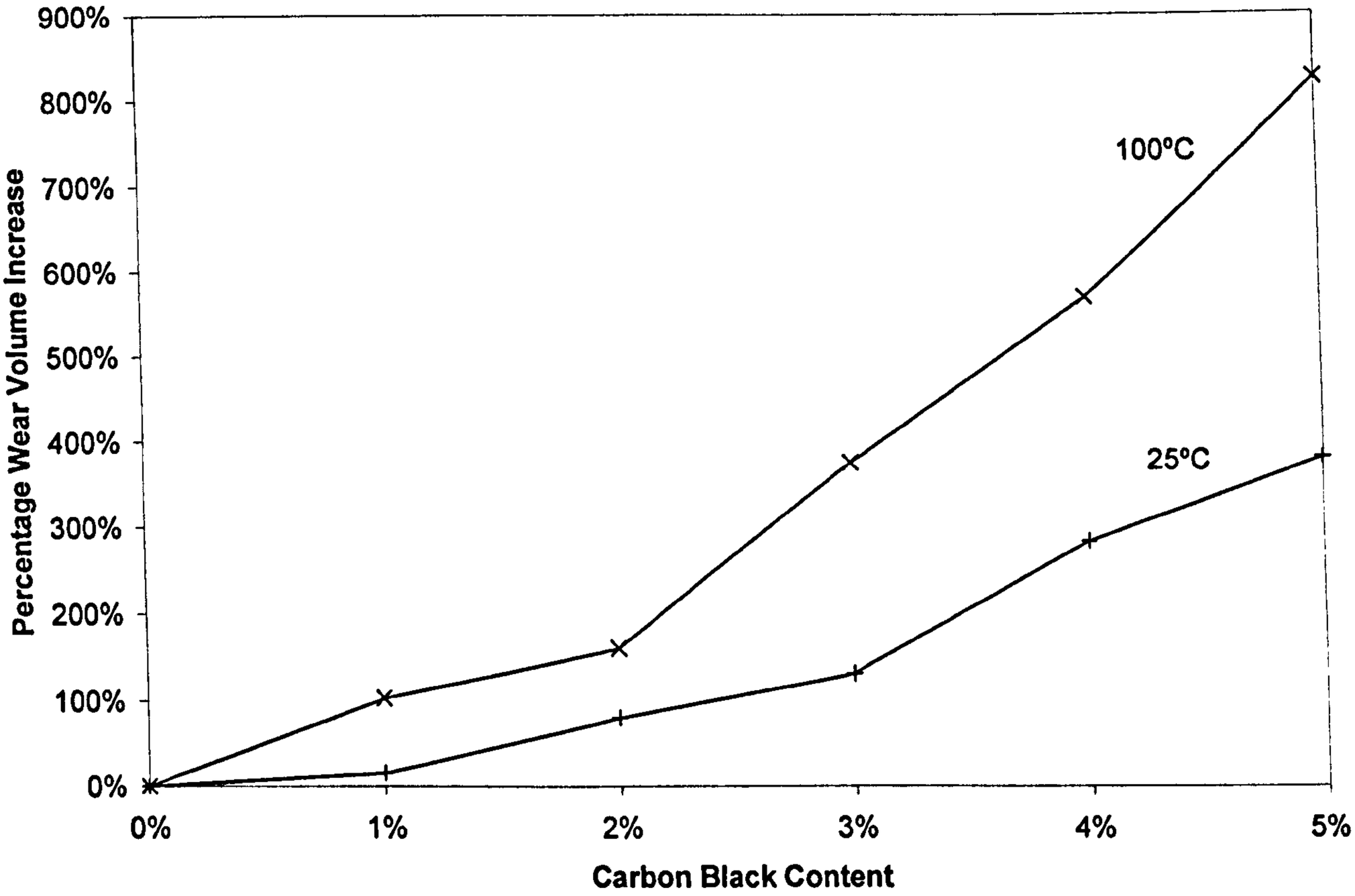

Figure 4.2. Results from Ball-on-Flat Testing Relative to 0% Carbon Black Content Tested at 25°C and 100°C (base oil at 0.18m/s sliding speed).

All of the results follow a pretty much linear trend in wear volume with carbon black content up to 2% to 3% contamination level, at which point the gradient decreases (particularly so on the 0.36m/s results, shown in Figure 4.1), indicating a possible wear mechanism change. The gradient again changes at 3% to 4% contamination (for high temperature tests) indicating another possible wear mechanism change.

4.2. FORMULATED OIL RESULTS

The wear data from the reciprocating tests using formulated oil are shown in Figure 4.3. The tests were performed under identical test conditions to those previously using base oil (Section 4.1). Due to the formulated lubricant's improved dispersant additive properties, wear tests containing up to 7% carbon black contamination were performed. The data is presented again as a percentage increase in wear over an identical test where the test lubricant is neat formulated oil with no carbon black contamination. Wear tests were only performed at a sliding speed of 0.36m/s and a contact load of 6.2N (approximately 500MPa) for this test lubricant, as testing with base oil demonstrated that trends maintained for a different sliding speed, but due to differences in the lubricant oil film thickness, different wear volumes were produced.

Figure 4.3 demonstrates that the wear performance of the formulated lubricant at 25°C was essentially the same as the performance of the base oil tested at 25°C (see Figure 4.1 for comparison). This is because at low temperatures a lubricant is designed so that the properties of the base oil dominate. Lubricant additives significantly modify the performance of the lubricant at elevated temperatures, when

the viscosity of the base oil reduces. At these elevated temperatures the viscosity improver additives (long chain polymers) are designed to retain some of the viscosity of the lubricant seen at low temperatures, therefore increasing the viscosity index. This effect is evident in the results for formulated lubricant testing at 100°C, where the wear is only slightly higher than the 25°C results.

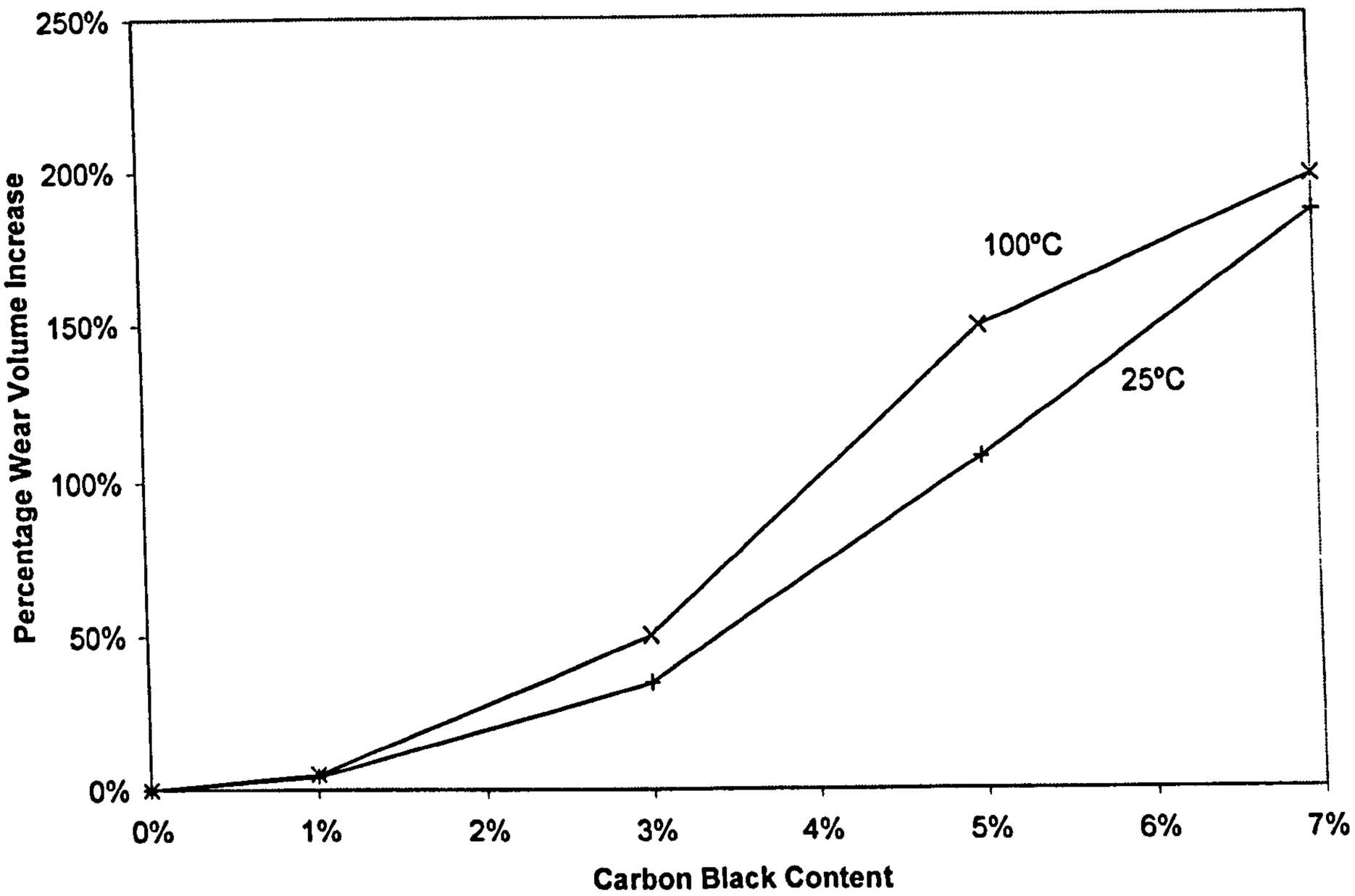

Figure 4.3. Results from Ball-on-Flat Testing Relative to 0% Carbon Black Content Tested at 25°C and 100°C (formulated oil at 0.36m/s sliding speed).

These results demonstrate firstly that additive packages in formulated lubricants help to considerably reduce the effects of soot related wear. Secondly the results demonstrate that carbon black (acting as a soot simulant) does not preferentially adsorb the antiwear additives in formulated lubricants, resulting in increased component wear. This can be demonstrated from the data in Figures 4.1 and 4.3. The data from both (base oil and formulated oil) sets of tests would be expected to produce roughly similar levels of wear if soot was preferentially adsorbed by the antiwear additives. The witnessed reduction in relative wear is predominantly due to the combination of antiwear additives and viscosity improvers. The separation of effects of the antiwear additives and viscosity improvers can be inferred from the data relating to the viscosity of the neat formulated lubricant (Section 6.2) and that of the base oil. The viscosity of the formulated lubricant at 25°C is higher than that of the base oil, due to the additives it contains. This increased low temperature viscosity provides protection under high load, low temperature conditions. The viscosity of the formulated oil reduces at an increased temperature (100°C), producing a kinematic viscosity, which is approximately three times higher than that of the base oil (at the same temperature). Therefore if viscosity was the dominant factor relating to wear, the level of wear from base oil to formulated oil would reduce accordingly, but the reduction in wear level is significantly greater, by a factor of 5.3, rather than just 3. Therefore it is assumed that this further reduction in wear level must relate to the

antiwear additives present in the formulated oil, consequently meaning that carbon black (soot) particles do not preferentially adsorb antiwear additives. This argument though can only be truly justified by comparative testing of neat base oil (without additives) and neat base oil with only the antiwear additives.

Using the same statistical methods used in Section 4.1, to understand the spread of the data, the results for the formulated wear tests have been analysed. Prior to testing it was predicted that formulated lubricants would produce more consistent wear than identical tests with base oil, but this was not the case, therefore repeat tests were performed to improve the reliability of the data. The increased variability produced with formulated lubricants is probably due to two factors, firstly compared to base oil alone there are going to be many more chemical interactions occurring within the contact due to the various additives present. Secondly as formulated oil reduces the overall amount of wear, this leaves the results more vulnerable to relatively minor variations in wear appearing magnified due to the very small scale of the actual wear scars. The standard deviation of all of the wear volume measurements is $0.00031mm^3$, and all of the data lies within ±1.8 standard deviations. The coefficient of variation (standard deviation divided by the mean), which measures the dispersion of the data obtained, gives a value of 49%, which is similar to the analysis with base oil, and is thought to be relatively good for wear data. Finally using the rule where standard deviation should be roughly equal to the range of the data divided by the square root of the number of samples obtained, they agree very well, with a variation of less than 6.5%. Each of these statistical measures are slightly higher for the formulated oil tests than the base oil tests, but this is due to the increased spread of wear measurements. All of the data taken and the calculated wear volumes are available in Appendix 3.

4.3. WEAR RATE

The rate at which wear occurs during the tests is important as it can aid the understanding of the wear mechanisms. Wear rate tests using a sample of base oil mixed with 3% carbon black are shown in Figure 4.4, the results are presented as increases in actual wear volume. The results show reasonably high wear rates during the first 5 to 10 minutes and by 10 minutes the majority of the wear has occurred. The results for the wear volume produced after 20 minutes of testing with neat base oil are displayed in Figure 4.4 for comparison. It shows that carbon black contamination produces a greater wear volume, significantly so when the test temperature is 100°C.

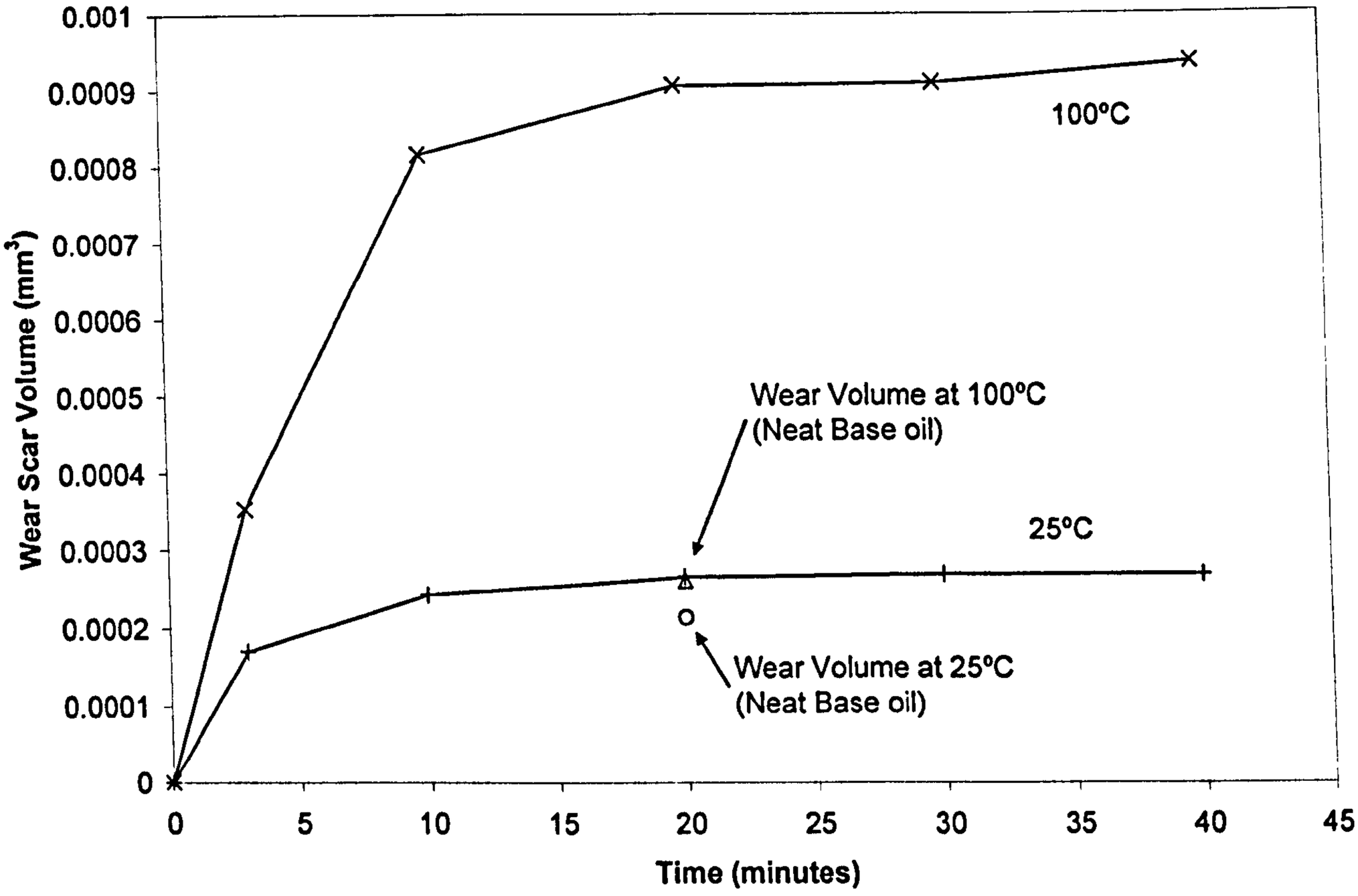

Figure 4.4. Results from Ball-on-Flat Wear Rate Testing with 3% Carbon Black Content Tested at 25°C and 100°C (base oil at 0.36m/s sliding speed).

CHAPTER 5:
WEAR SCAR ANALYSIS

The wear data alone in Chapter 4 is not sufficient to demonstrate the effects of soot contaminated lubricants on specimen and engine component wear. The effects of the wear are demonstrated visually in this chapter through various microscope and scanning electron microscope (SEM) images.

5.1. TEST SPECIMENS

To assist the understanding of the wear mechanisms, images of unlubricated and lubricated (but with no carbon black contamination) are shown in Figure 5.1. They demonstrate the two extremes of the wear observed. The unlubricated specimen (Figure 5.1a) has significant levels of plastic deformation (signs of plastic material flow) and galling from adhesive wear. This is typical of the wear that is seen in acutely starved contacts. The lubricated specimen (Figure 5.1b) displays typical running-in wear, as asperities and light machining marks have been worn away to produce a smooth surface finish. The high magnification image shows that some of the heavier machining marks still remain on the wear surface in such a case.

In some cases the low magnification wear scar is not easily visible, therefore in many of the following images the perimeter of the wear scar is highlighted by a dashed line.

Low Magnification	High Magnification
	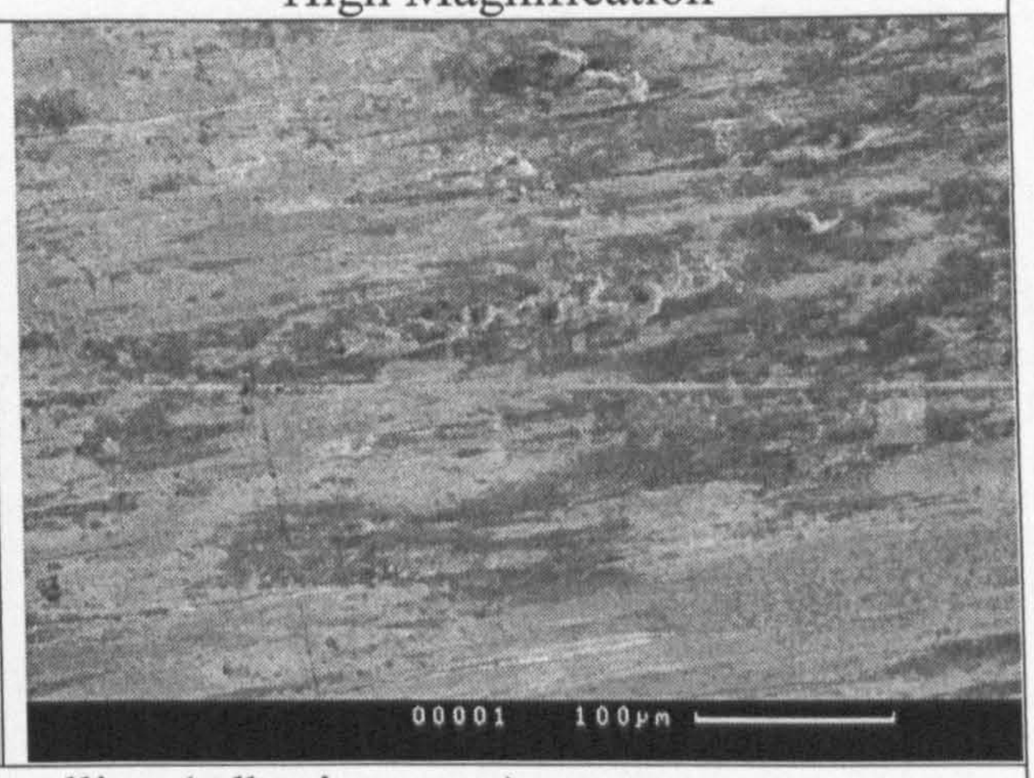
Plastic deformation and galling (adhesive wear)	
(a) Unlubricated	
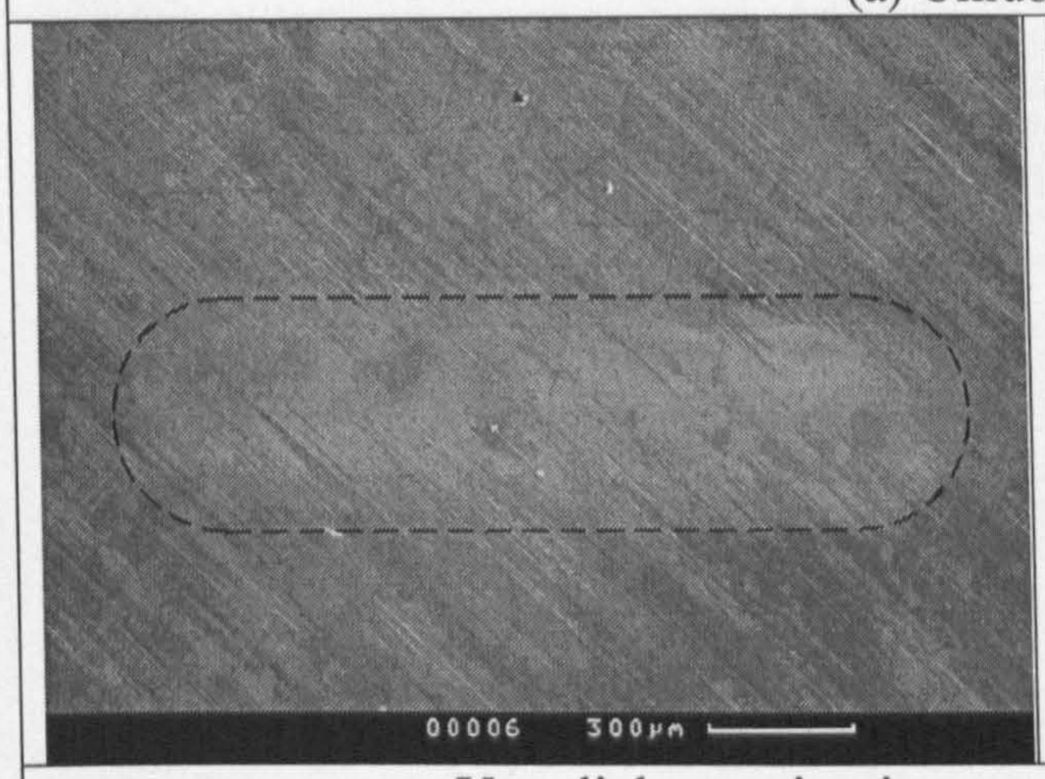	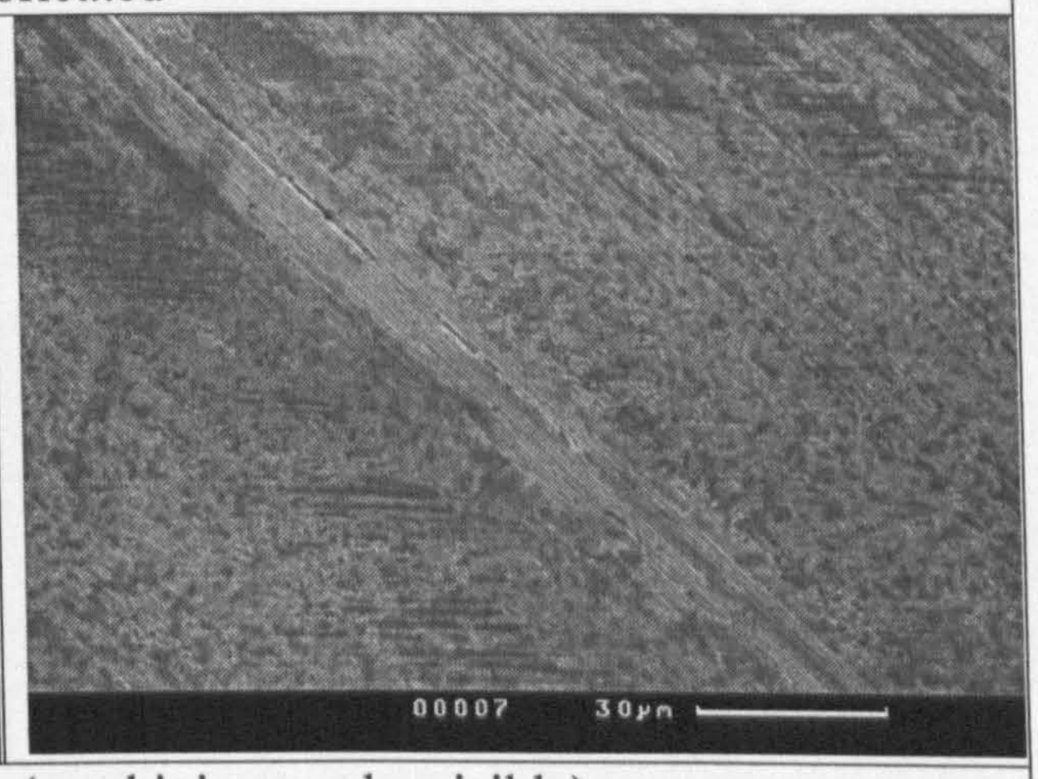
Very light running-in wear (machining marks visible)	
(b) Lubricated (0% Carbon Black)	

Figure 5.1. SEM Imaging of (a) Unlubricated and (b) Lubricated Test Specimens (No Carbon Black).

5.1.1. Base Oil Results

5.1.1.1. Optical Microscope Images

The wear scars presented in Figure 5.2 demonstrate how the characteristics of the wear produced varied with increasing carbon black content and change in temperature. The change in wear scar characteristics indicates possible changes in wear mechanisms.

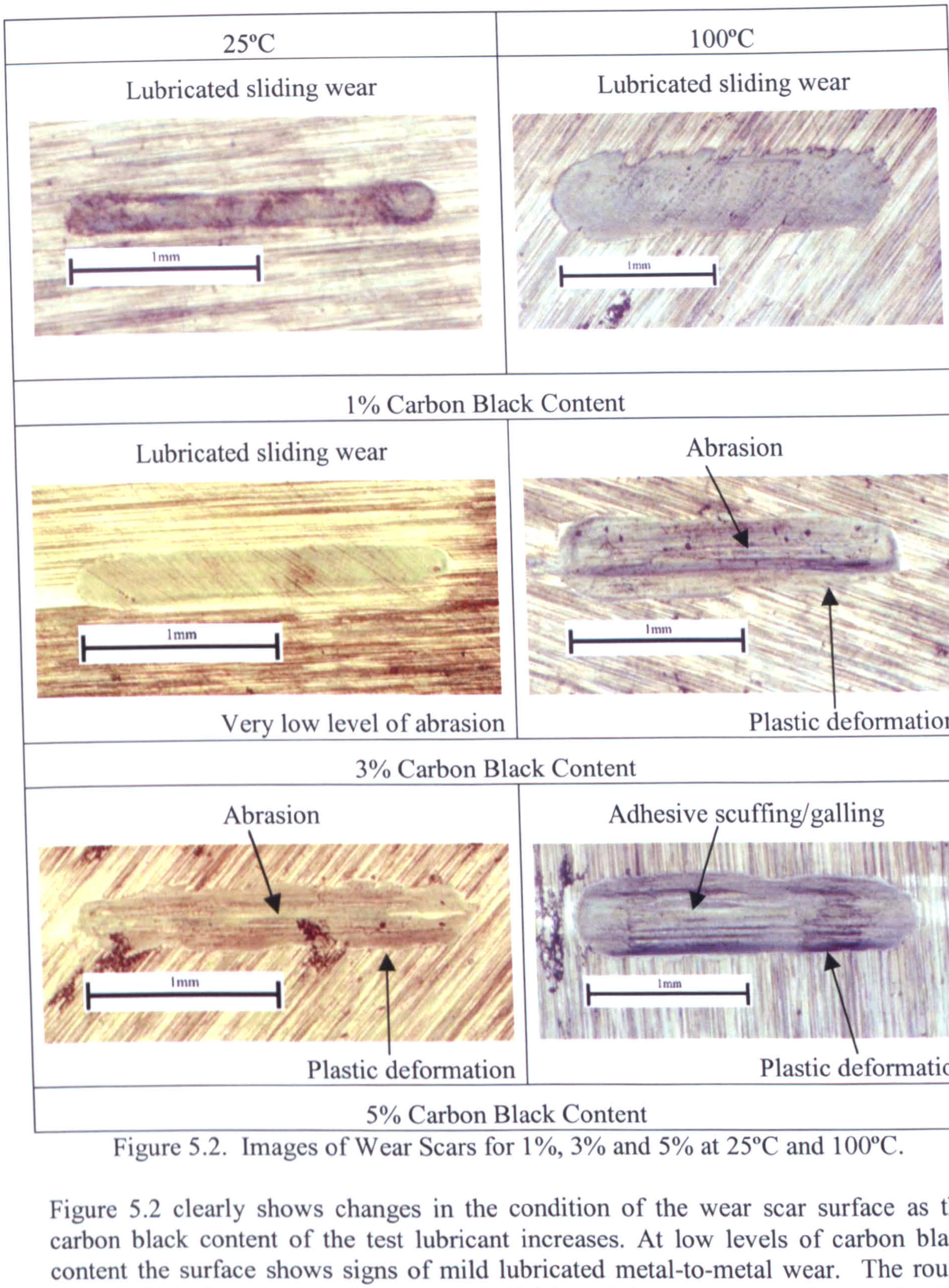

Figure 5.2. Images of Wear Scars for 1%, 3% and 5% at 25ºC and 100ºC.

Figure 5.2 clearly shows changes in the condition of the wear scar surface as the carbon black content of the test lubricant increases. At low levels of carbon black content the surface shows signs of mild lubricated metal-to-metal wear. The rough surfaces have been polished to a smooth finish and there are no scoring or abrasion marks. Evidence of machining marks still remain on the surfaces where low-level wear has occurred. As the carbon black content increases, signs of abrasion in the direction of sliding and plastic deformation are evident from scoring marks and an uneven wear pattern around the circumference of the wear scar. The highest levels of carbon black content show increased levels of abrasion (as adhesive scuffing/galling wear) and plastic deformation indicating metal-to-metal contact, due to possible starvation of lubricant from the contact. The visible evidence for lubricant starvation

are the regions within the stroke showing signs of heavy metal-to-metal contact and some polishing wear.

Essentially the optical microscope images displaying the wear relating to 1% carbon black contamination show running-in wear with some of the deeper machining marks still present. The wear scar images from the 3% carbon black tests show signs of abrasive wear. Finally the wear scars from tests with 5% carbon black contamination indicate starvation of the contact, as some galling from adhesive wear is visible as is some plastic deformation of the surface.

5.1.1.2. SEM Images

Further analysis of these specimens has been performed with an SEM, the higher magnification images, shown in Figure 5.3 clearly indicate the differences in the wear features visible on the surface of the test specimens, which progress from running-in wear through abrasion to significant levels of abrasion and contact starvation at high carbon black contamination levels.

Low Magnification	High Magnification
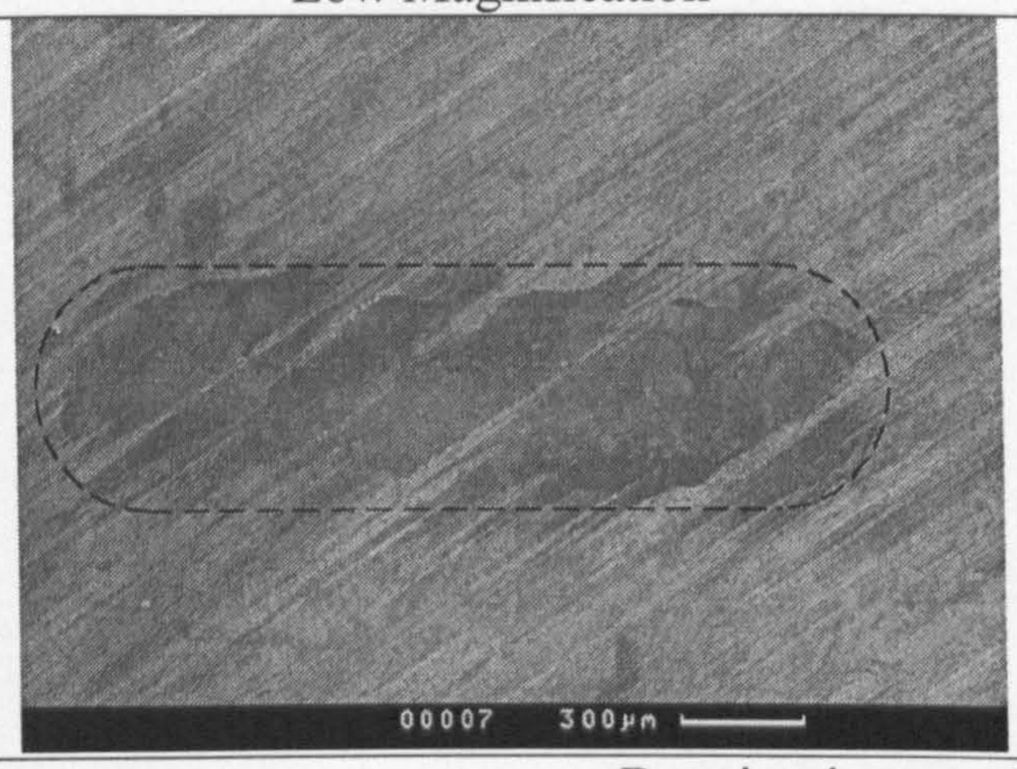	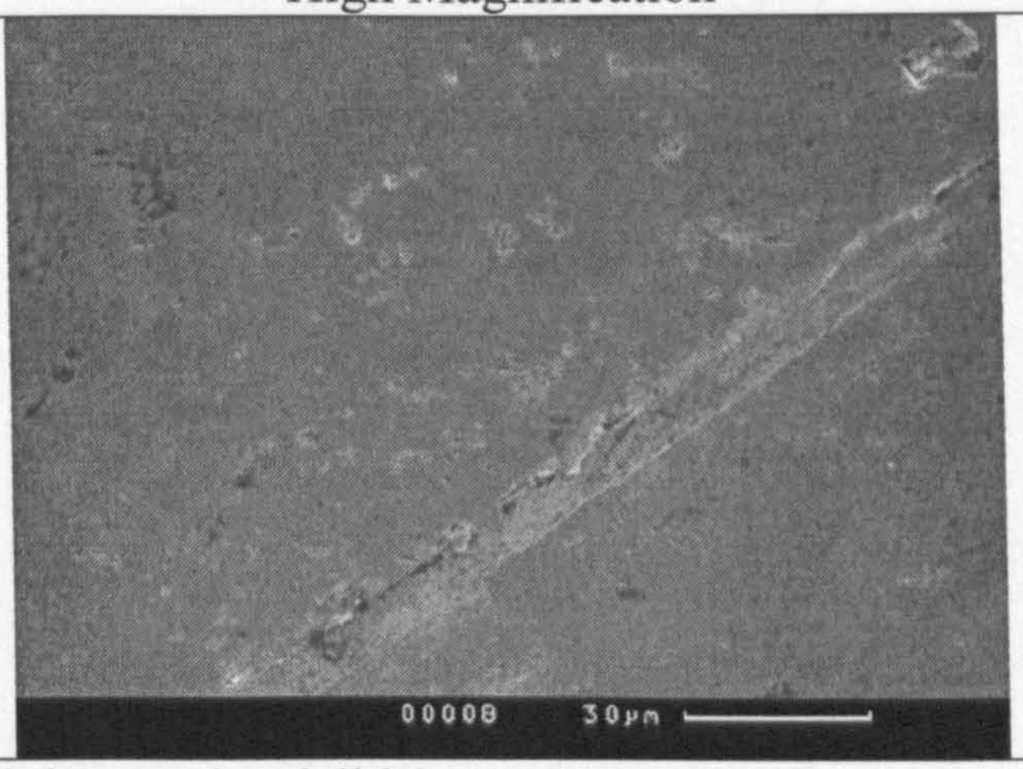
Running-in wear (machining marks visible)	
1% Carbon Black	
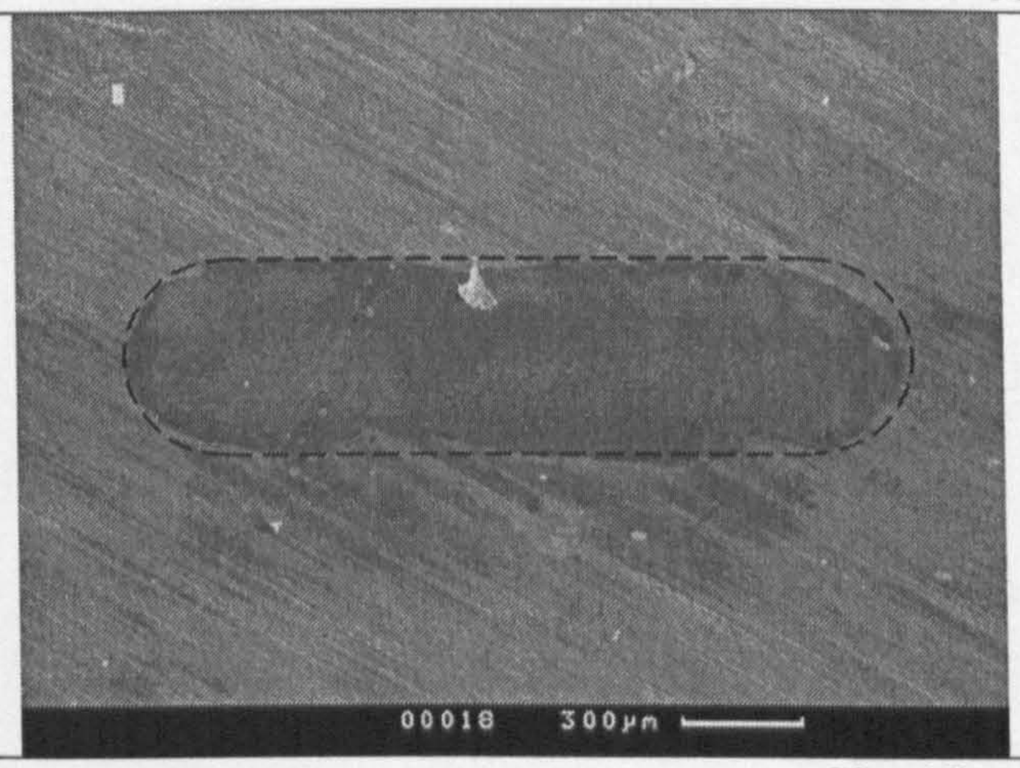	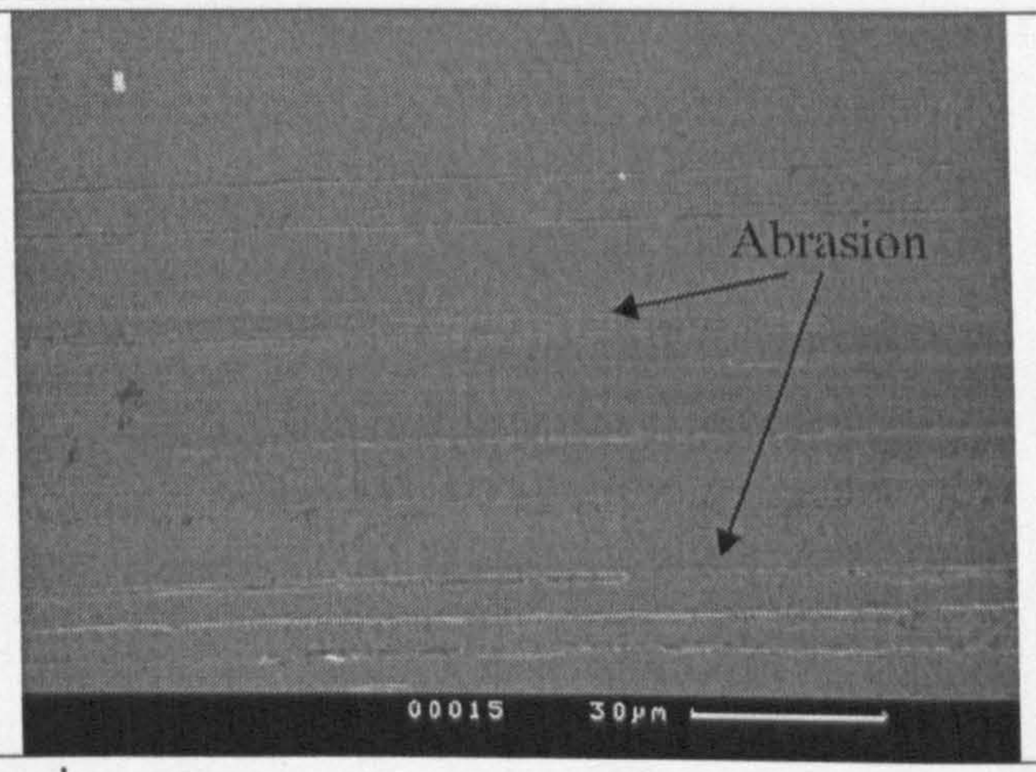
Significant abrasive wear	
3% Carbon Black	
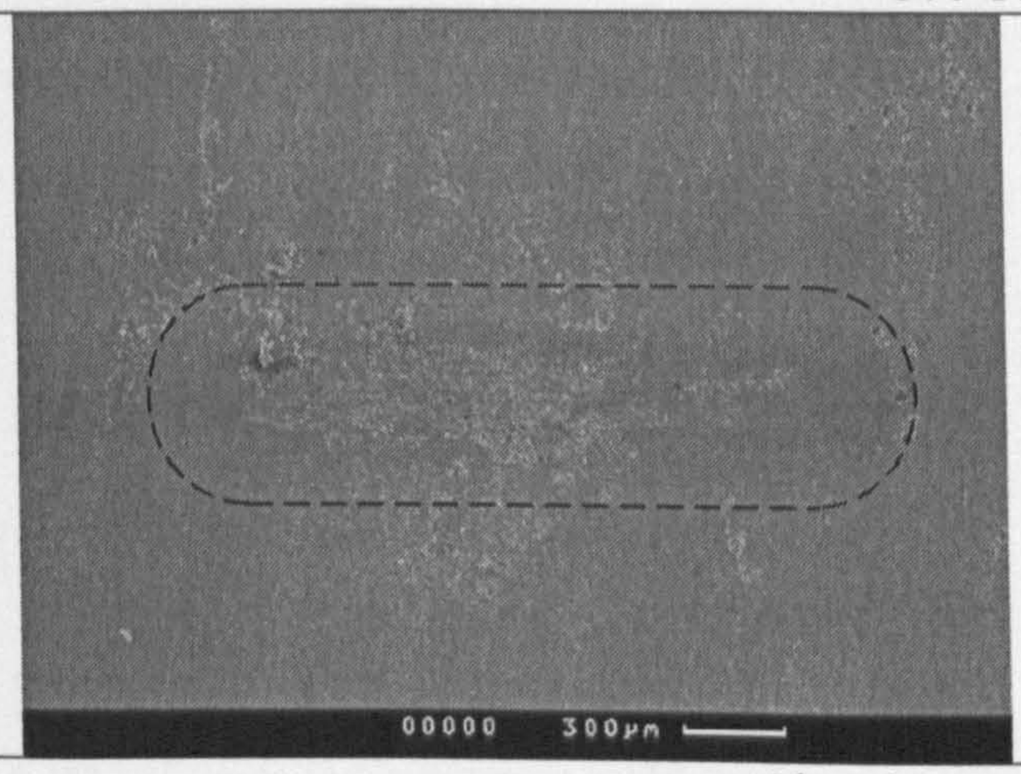	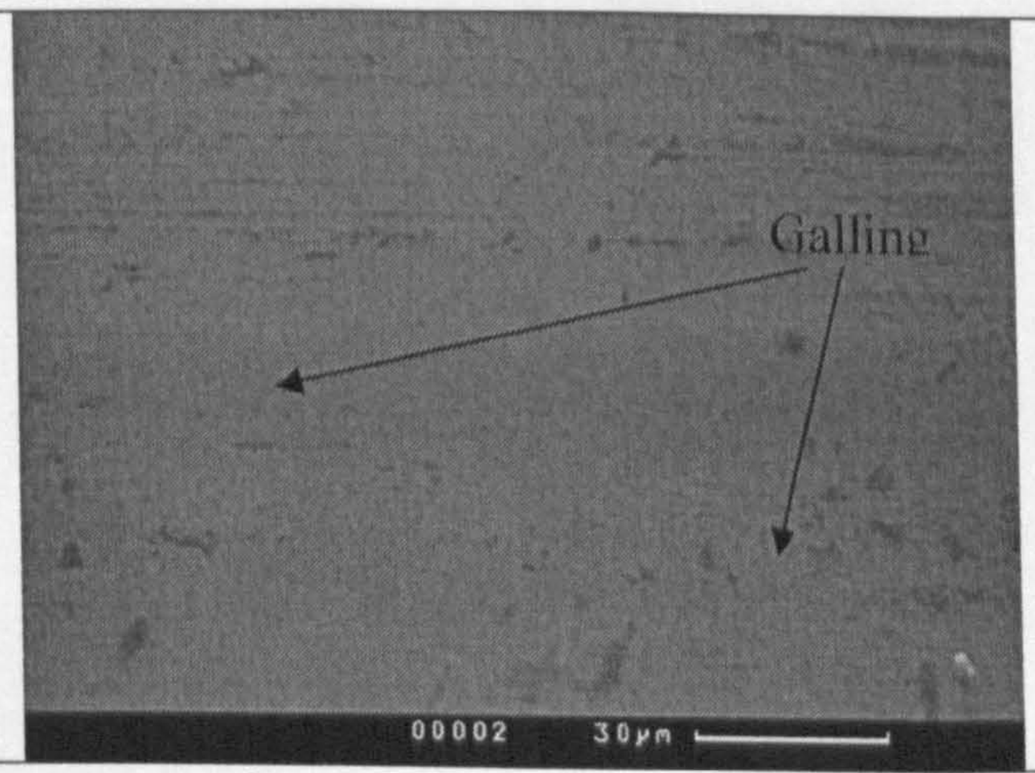
Abrasion and contact starvation	
5% Carbon Black	

Figure 5.3. SEM Imaging of Base Oil Tests Specimen Wear Scars (100°C Tests).

5.1.2. Formulated Oil Results

The most useful images for analysing the wear features and therefore mechanisms that are occurring, are those taken using the SEM. Also for the case of formulated test oil as the data shows very little wear occurs, and the results follow essentially the same trend as the base oil tests. Only SEM images from the 100°C tests demonstrate the changes in wear mechanisms sufficiently (and are presented), the images from the 25°C tests provide the reader no extra information, only demonstrating some abrasive wear mechanisms at the highest carbon black contamination levels.

Figure 5.1 demonstrates that low levels of wear are witnessed with uncontaminated oil as the test lubricant. At higher carbon black contamination levels the three key wear mechanisms discussed earlier (relating to base oil testing) should also appear. Figure 5.4 demonstrates that this theory is true, but the properties of the formulated oil provide greater protection to the specimen and the mechanisms occur at slightly higher carbon black contamination levels.

The progression of the development of wear features (shown in Figure 5.4) witnessed from testing with increasing levels of carbon black in formulated lubricants shows that at 1% and 3% contamination levels the visible wear scars appear to be similar. The images for 1% and 3% demonstrate running-in wear, but with some signs of light abrasion (only visible in the high magnification images). The images relating to 5% carbon black contamination demonstrate significant levels of abrasive wear, but no indication that starvation may have occurred (as visible for 5% carbon black contamination with base oil). The images for 7% carbon black contamination indicate that some starvation of the contact has occurred. The low magnification image of the wear scar is slightly hidden by post-test surface corrosion around the area of the wear scar, which formed when the specimen was in storage. The wear scar though is still visible, showing signs of abrasion and starvation similar to wear features seen in the unlubricated image in Figure 5.1. The high magnification of the 7% test sample clearly shows wear scars indicating contact starvation, again similar to wear features seen in the unlubricated image in Figure 5.1.

	Low Magnification	High Magnification
1% Carbon Black	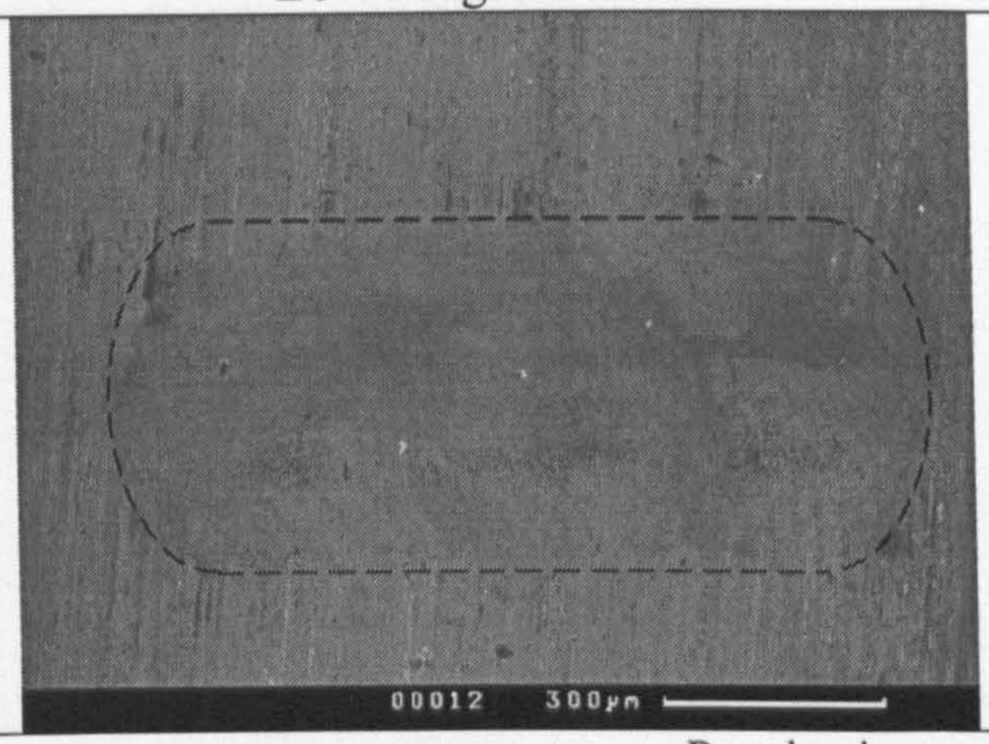	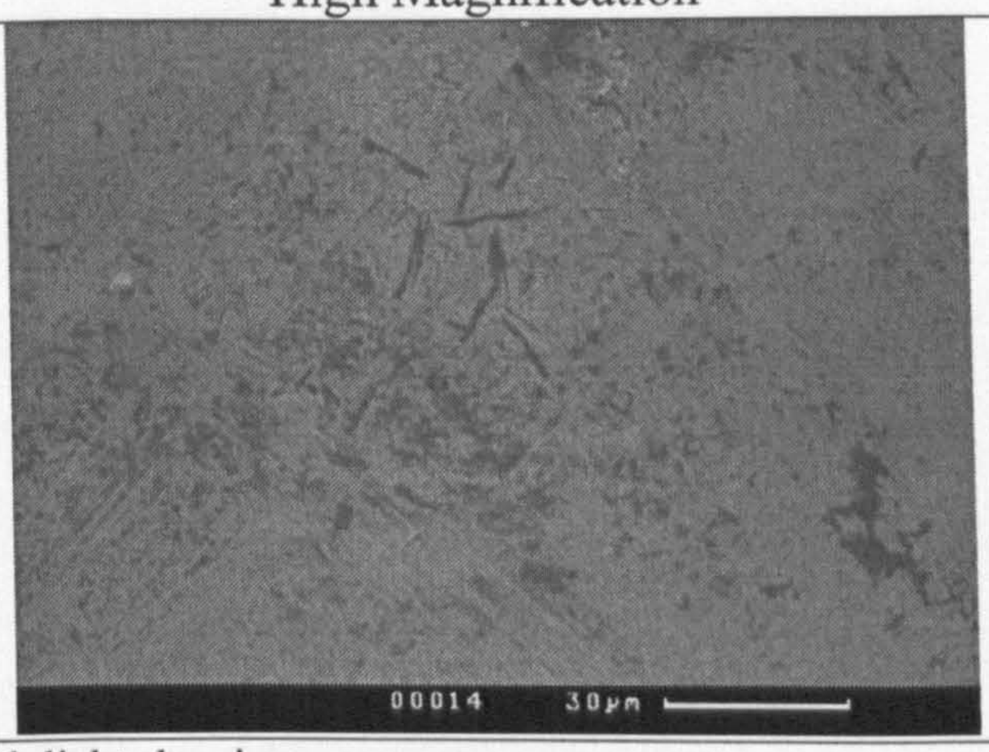
	Running-in wear with light abrasion	
3% Carbon Black	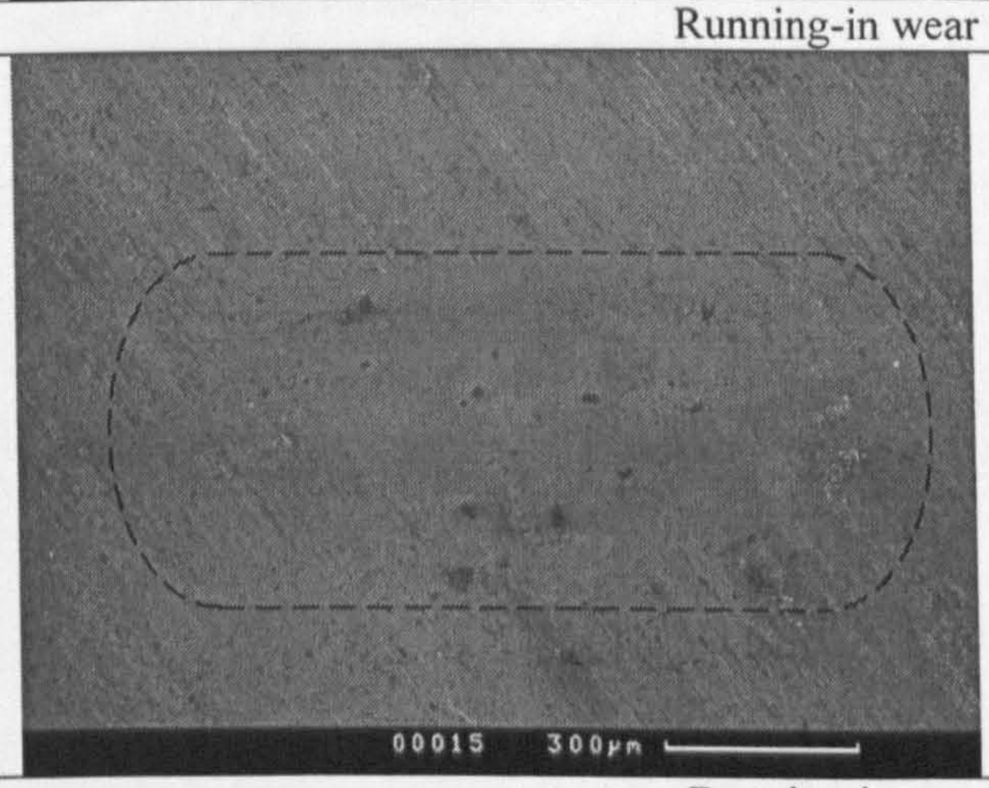	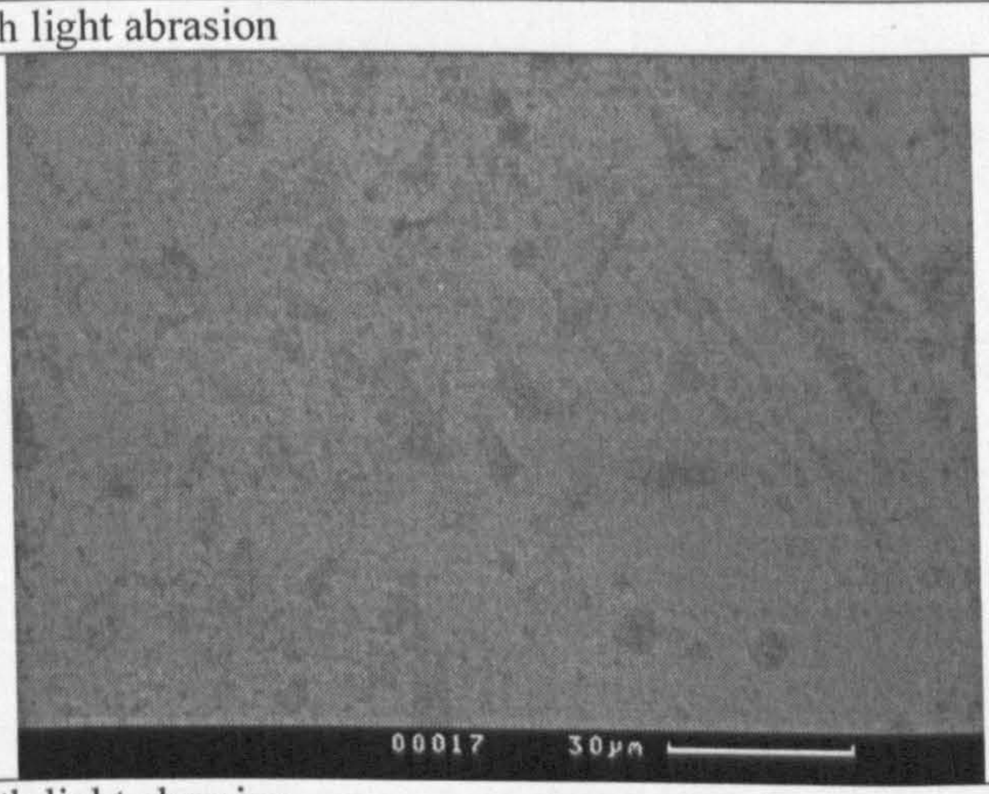
	Running-in wear with light abrasion	
5% Carbon Black	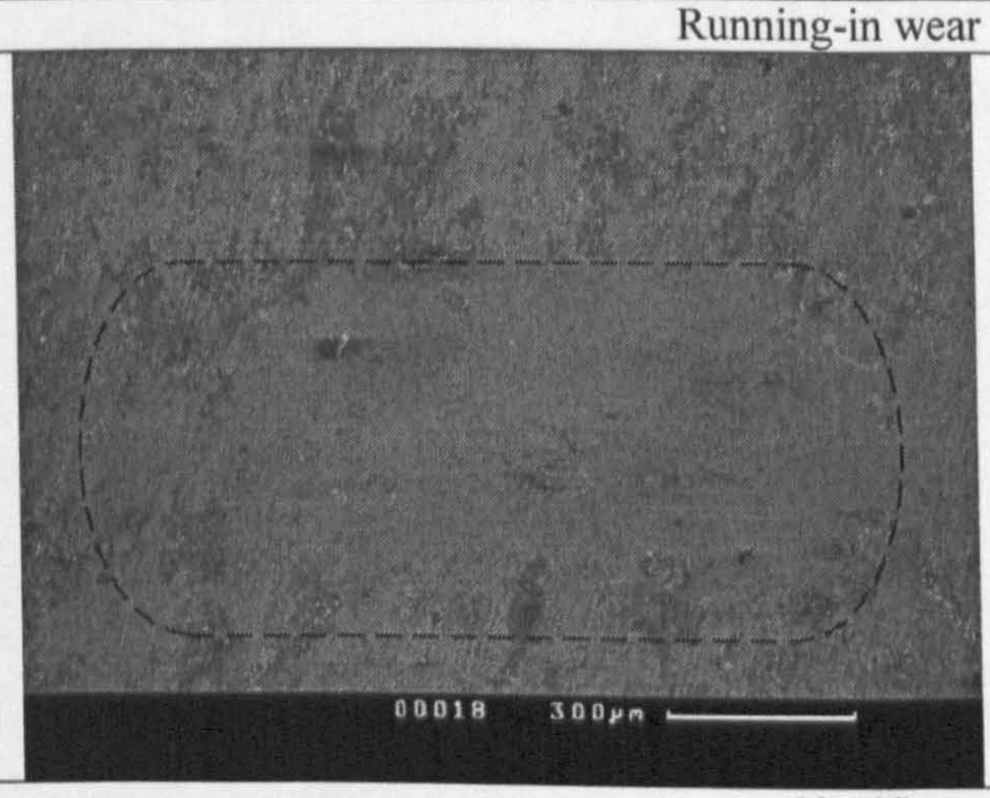	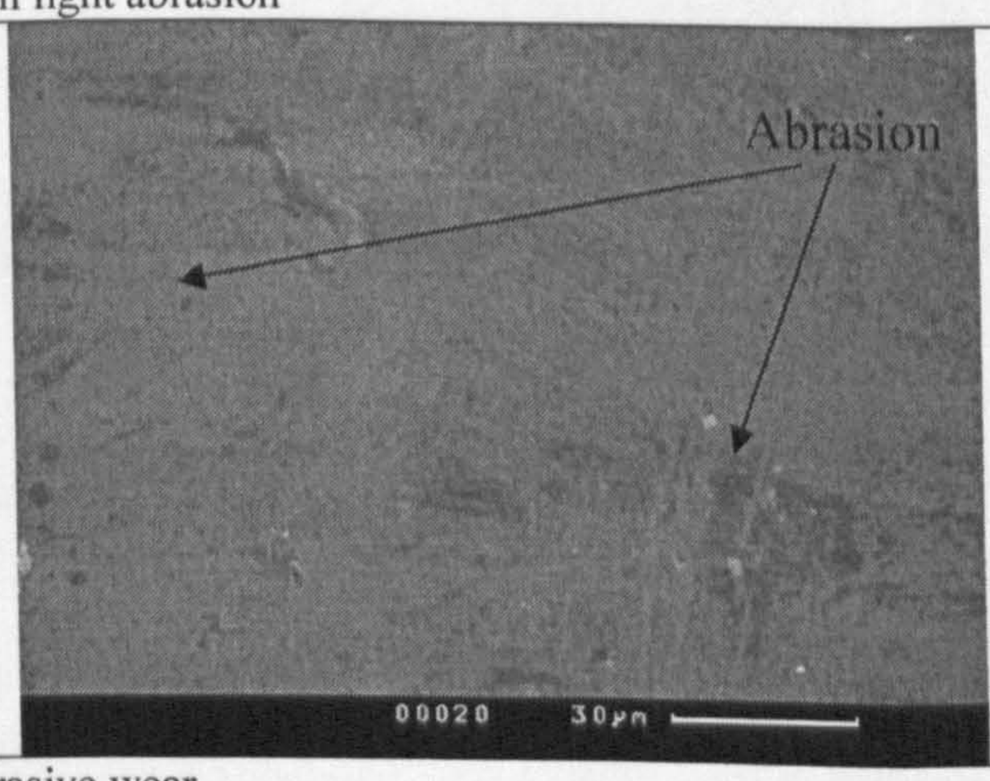
	Significant abrasive wear	
7% Carbon Black	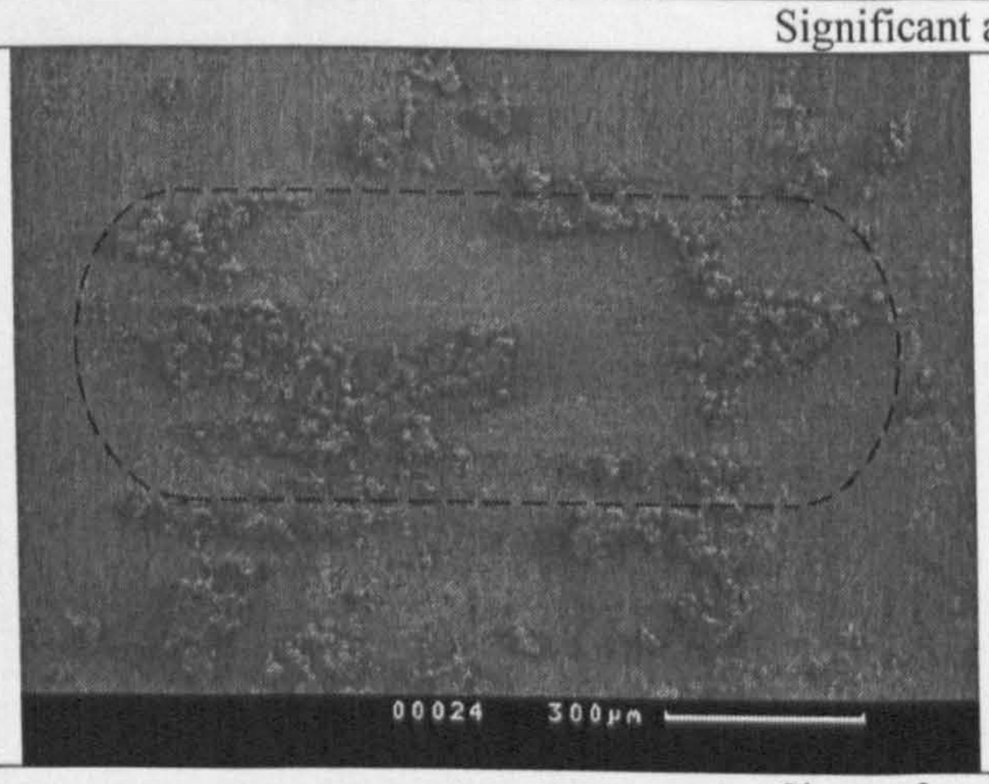	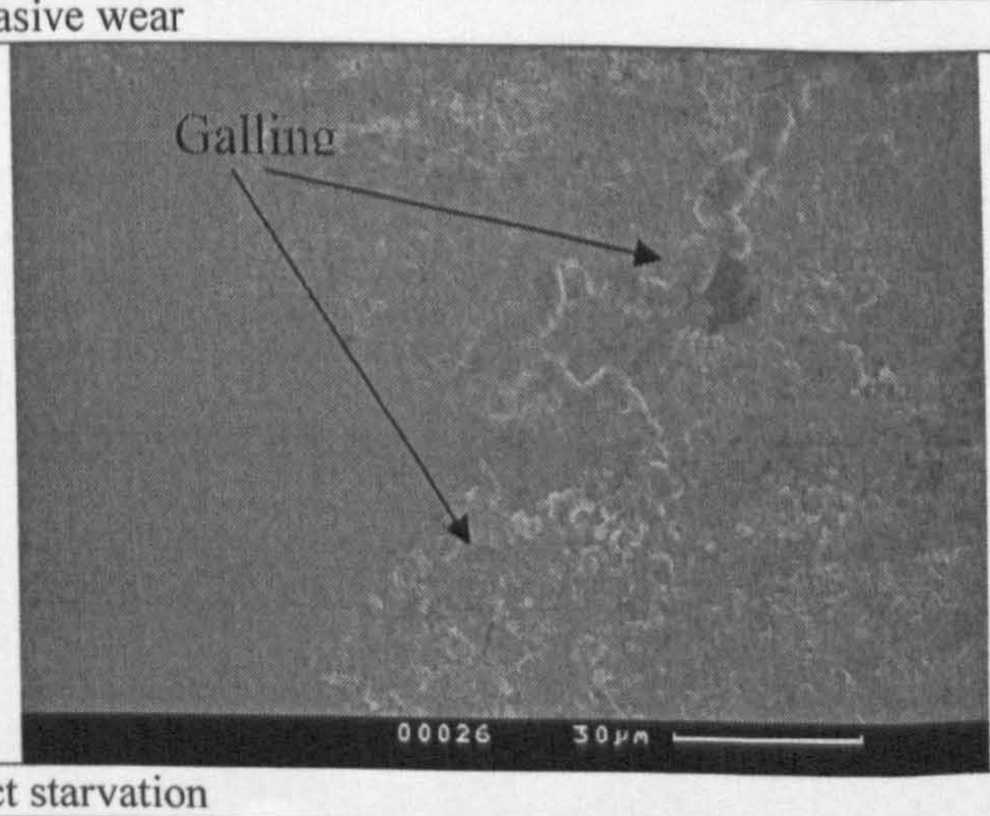
	Signs of contact starvation	

Figure 5.4. SEM Imaging of Formulated Oil Tests Specimen Wear Scars (100°C Tests).

5.2. COMPONENT TESTING

The fundamental study of the ball-on-flat specimens test can be verified through the analysis of a valve train contact that has similar fundamental features as the ball-on-flat contact. The contact chosen for testing is the elephant's foot to valve tip interface in a 2.4l, 16 valve diesel engine. The elephant's foot is part of the overhead valve train rocker arm. A schematic diagram of the arrangement is shown in Chapter 3, Figure 3.1.

Wear scar images similar to those in Figure 5.2 have been observed on used elephant's feet and valve tips from the engine, indicating that the wear scars from ball-on-flat testing and the mechanisms proposed strongly agree with wear experienced in the actual engine. Tests have been performed on the same reciprocating rig used for the ball-on-flat wear testing. Some of the test conditions were slightly modified to relate more directly with real engine operating conditions. Full details of the test conditions are detailed in Section 3.8.

The wear scar images recorded from elephant's foot to valve tip reciprocating testing are shown in Figure 5.5, for carbon black contamination levels of 0%, 3% and 5%.

Figure 5.5 demonstrates that as carbon black content increases, levels of visible wear on the surface of the components increase too. The elephant's foot results display wear over the majority of the image, but with some machining marks still visible. The valve tip images have more machining marks remaining visible on the surfaces, along with regions of wear. Such a variation in visible wear for the valve tips is due to the point made earlier regarding the high points on the surface; this has lead to increased wear, but this has not affected the order in which the visible wear mechanism characteristics occur. At 0% carbon black content both surfaces appear to be having mild wear, typical of normally lubricated contact. The test performed at 3% carbon black content indicates signs of abrasion, particularly on the surface of the valve tip. At 5% carbon black content the images show extremely high levels of abrasion and scoring on the surface the elephant's foot, and high levels of plastic deformation on the surface of the valve tip. The wear mechanisms observed in Figure 5.5 correlate extremely well with those proposed from the base oil ball-on-flat reciprocating tests in Section 5.1.

	Elephant's Foot	Valve Tip
0% Carbon Black Content	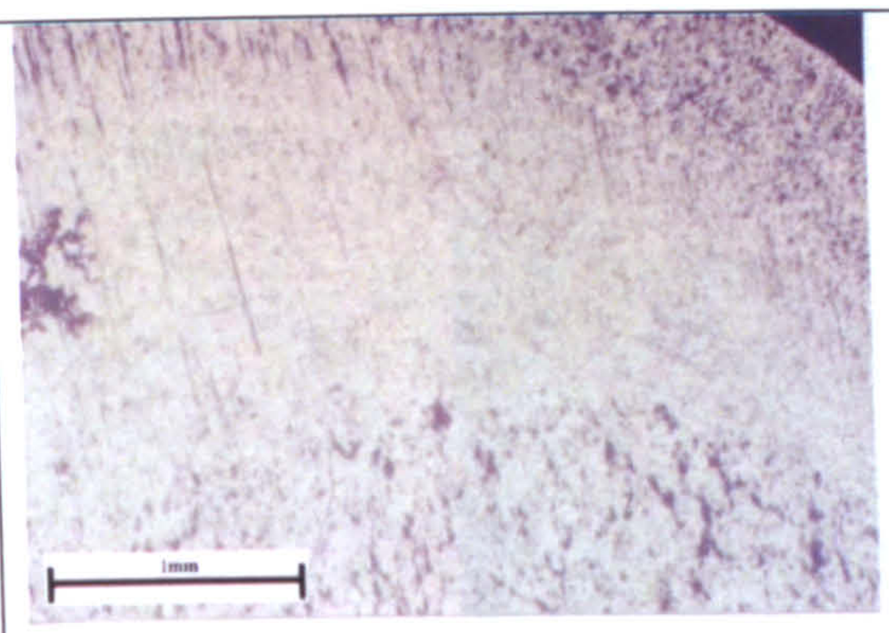	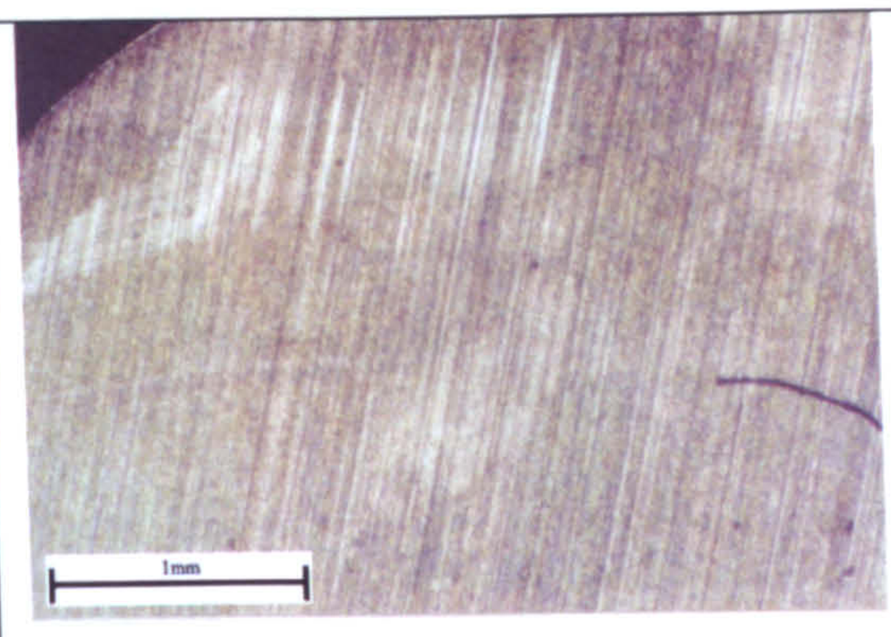
3% Carbon Black Content	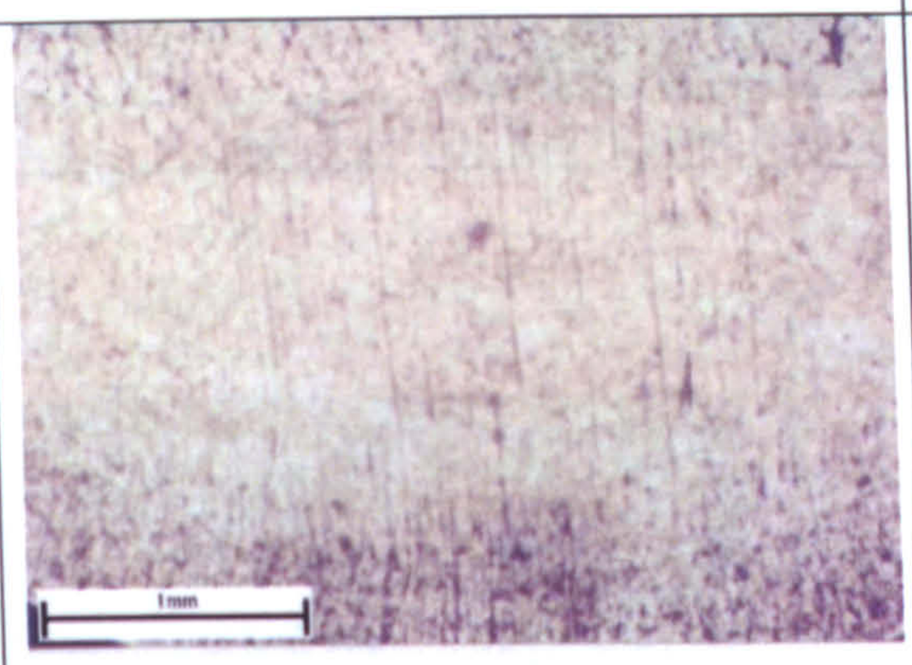	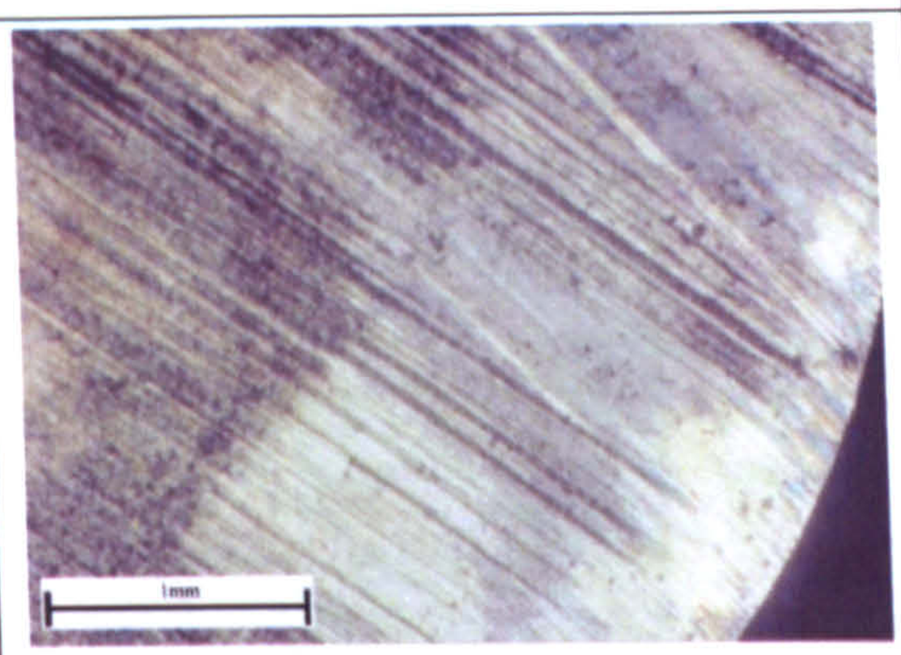
5% Carbon Black Content	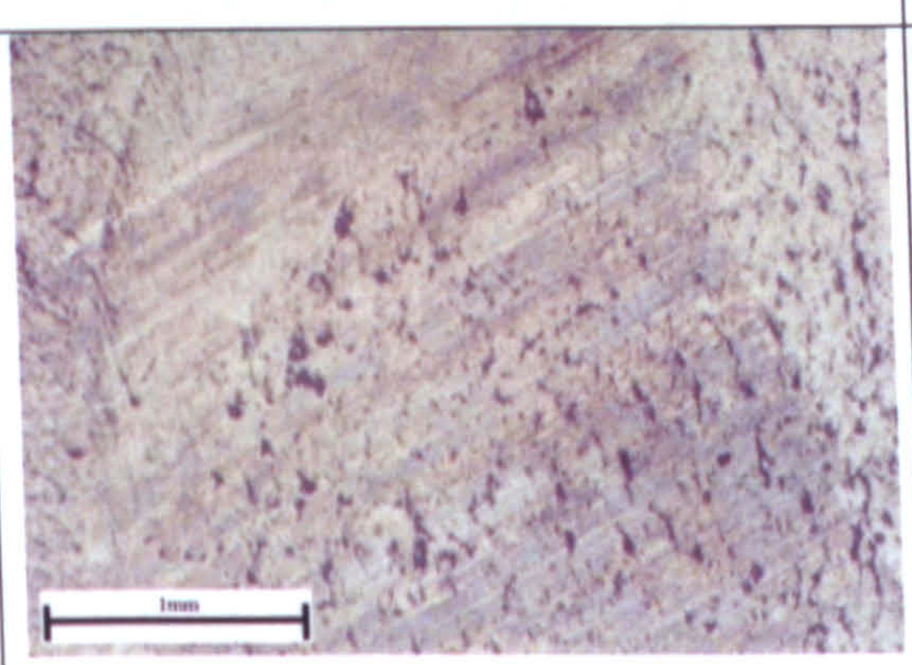	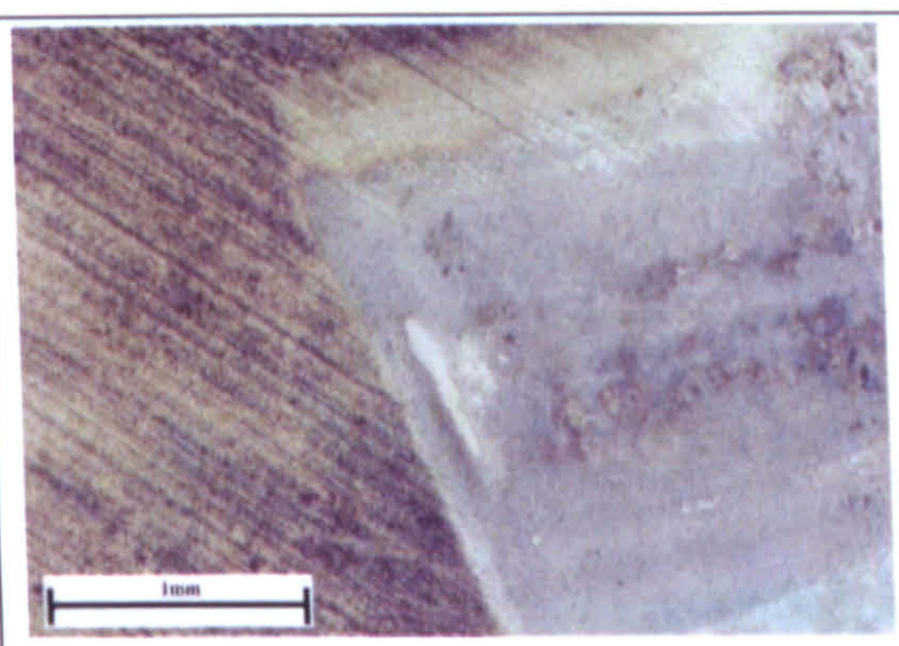

Figure 5.5. Images of component reciprocating tests performed at 100°C.

5.3. WORN ENGINE COMPONENTS

To provide a system level test (as discussed in Section 2.2) and to compare with specimen and component bench test wear features, components were analysed using an optical microscope and an SEM. The components were from a general variable-speed heavy duty durability test (including running at rated-speed and peak torque speed) performed on a development Perkins 1100 series engine, lasting for 2,000 hours. The lubricant was changed every 500 hours throughout the test, at which point the soot content test lubricant was approximately 2 to 3% (by mass) as is typical for a heavy duty diesel engine of this type. The test cycle performed is accelerated duty and is equivalent to a full 'in the field' engine lifetime of approximately 8000hours.

The main components of interest are tips of the valves and the rocker pads with which they make contact. The valve train components are shown in Figure 5.6.

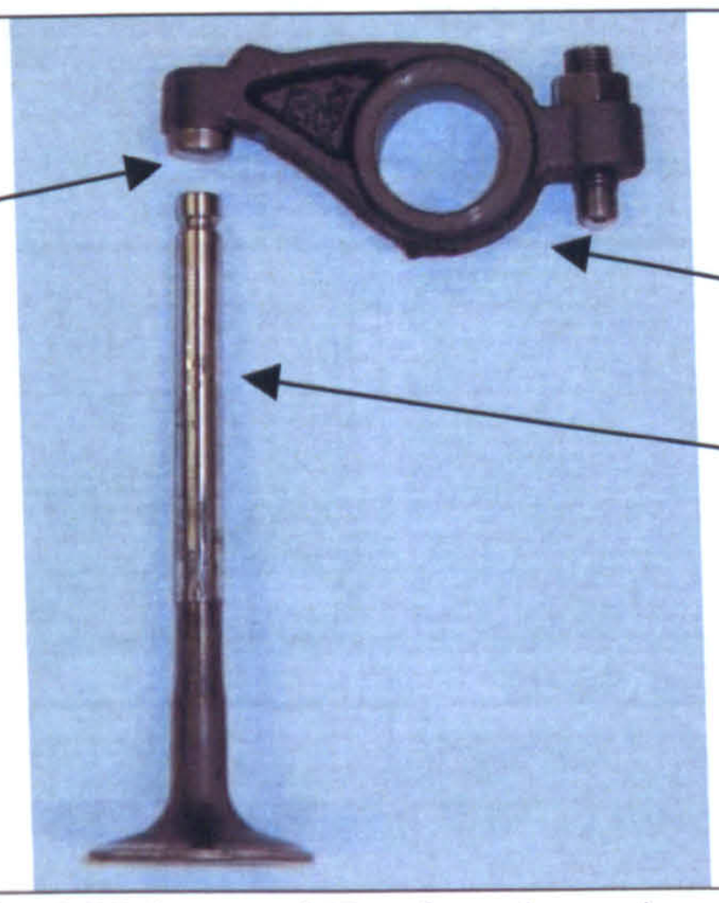

(a) Typical Valve and Rocker Arm Arrangement

(b) Worn Rocker Pad

(c) Worn Valve Tip

Figure 5.6. Perkins 1100 Series Engine Valve Train Components.

Typical wear scars on the surface of a valve train rocker pad are shown in Figure 5.7. These images were taken using an optical microscope. The images indicate high levels of surface abrasion as would be expected with the soot content in the test lubricant. The pattern of the abrasion marks is irregular, probably due to the lubricant flow and valve rotation. Under the naked eye, such surfaces appear to be 'polished', but in reality the surface has a high level of microscopic abrasion marks, produced by soot and/or possibly wear debris contained in the lubricant. Significantly higher levels of abrasion and/or starvation of the contact (possibly due to higher levels of soot contamination) would tend to considerably reduce the 'polishing' of the surface, producing a duller finish. It is more likely that soot is the cause of this abrasion rather than debris, as due to modern machining techniques surfaces are finished to a very high tolerance, producing very little asperity wear and therefore debris. The debris that is present after running-in would most likely produce a few significant surface marks, whereas soot, which is well dispersed in the lubricant and abundant, would produce numerous abrasion marks.

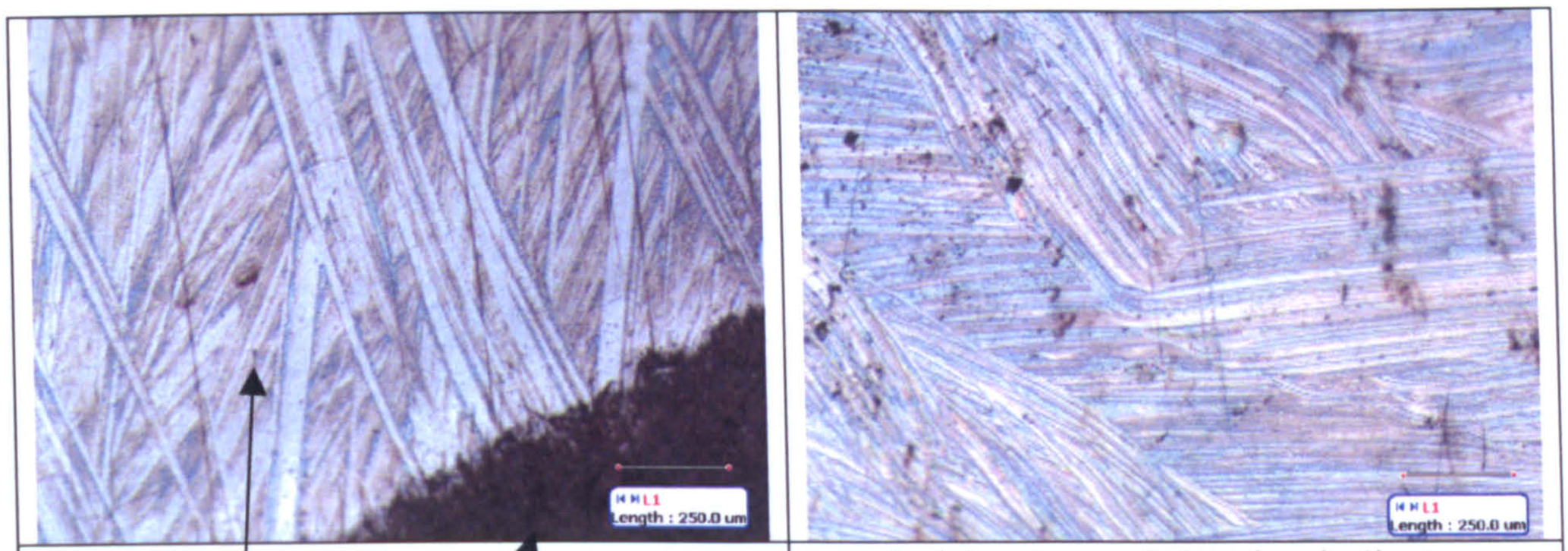

Abrasion and an unworn region.	Swirl pattern of abrasion indicates irregular lubricant flow and valve rotation.

Figure 5.7. Optical Microscope Images of a Worn Rocker Pad from an Engine Test.

The wear scars in Figure 5.7 were further magnified using an SEM as shown in Figure 5.8. The low magnification image shows numerous pitting marks and fine grooves in the surface of the specimen. There is also one large wear groove, this may either be due to piece of wear debris or it may be a region in the contact where large amounts of soot tend to form, leading to increased wear. The high magnification image shows a large number of irregular grooves. These very fine grooves (most probably due to soot) will form the large grooves shown in Figure 5.7.

Low Magnification	High Magnification

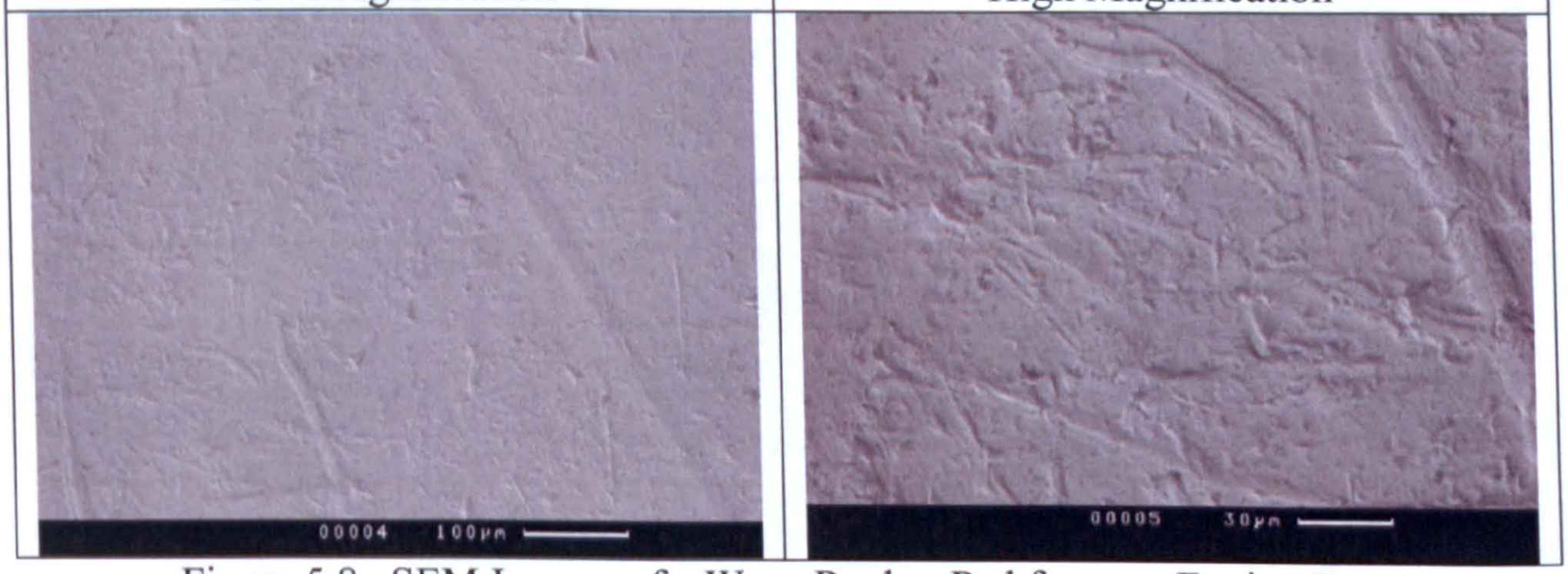

Figure 5.8. SEM Images of a Worn Rocker Pad from an Engine Test.

Typical wear scars on the surface of a valve tip are shown in Figure 5.9; these images have been taken with an optical microscope. The images clearly show abrasion marks in multiple directions, due to soot and possibly wear debris as explained earlier. The abrasion marks are in multiple directions first due to the irregular flow of the soot contaminated lubricant around the contact region and secondly due to valve rotation. As the valve rotates a new preferential direction relative to the motion of the rocker pad produces a new direction for wear to occur. Valve rotation also tends to even out the wear over the surface of the valve tip, therefore reducing the overall depth of wear that occurs; this is visible when Figure 5.7 and Figure 5.9 are compared.

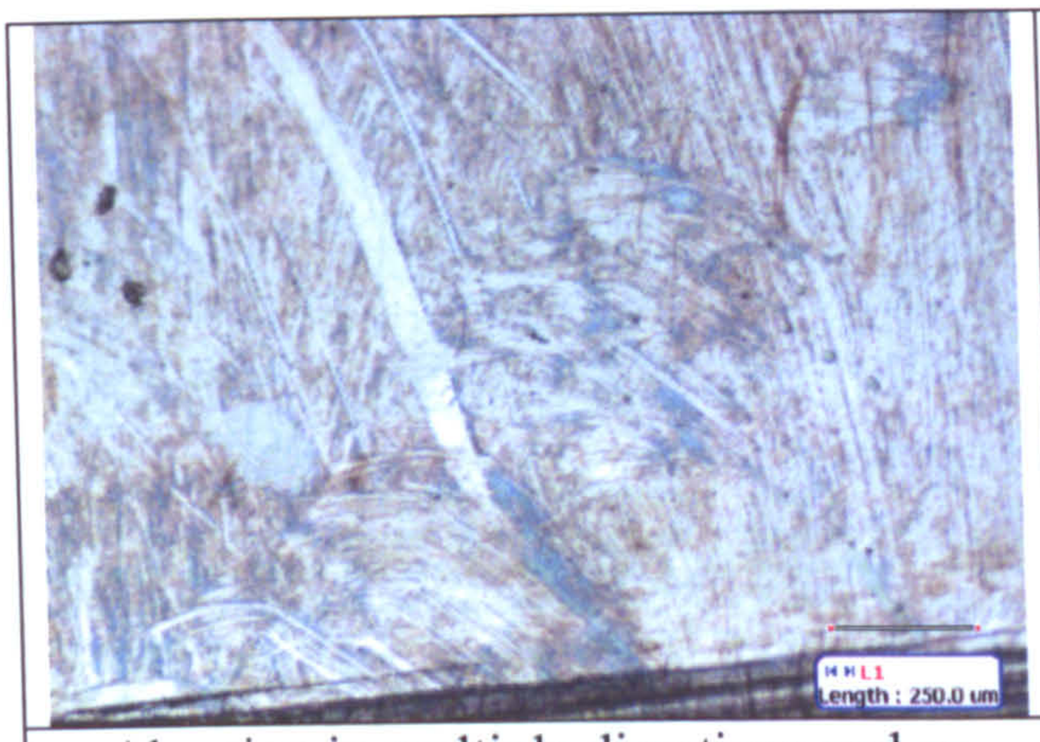

Abrasion in multiple directions and an unworn Region.

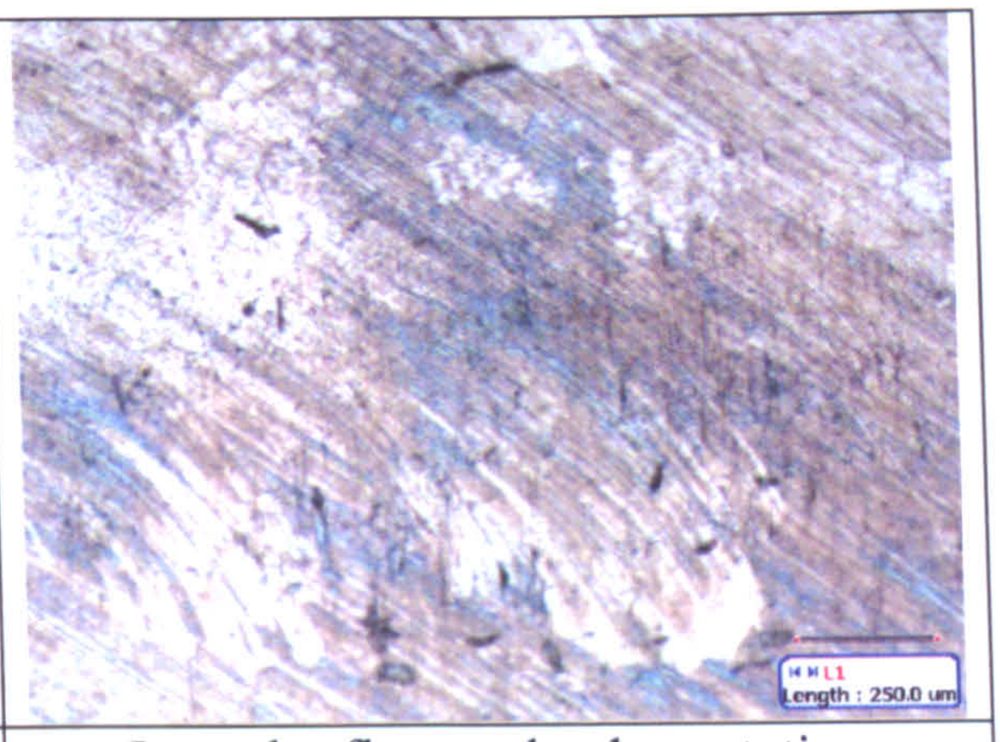

Irregular flow and valve rotation indicated by swirling pattern.

Figure 5.9. Optical Microscope Images of a Worn Valve Tip from an Engine Test.

The wear scars in Figure 5.9 are further magnified using an SEM as shown in Figure 5.10. The lower magnification image clearly shows very fine abrasive grooves from the soot particles in different directions (due to valve rotation). The high magnification image shows the fine grooves in more detail, showing that the grooves are not perfectly straight, but irregular which is most probably due to the flow of the soot contaminated lubricant in the contact.

Low Magnification	High Magnification

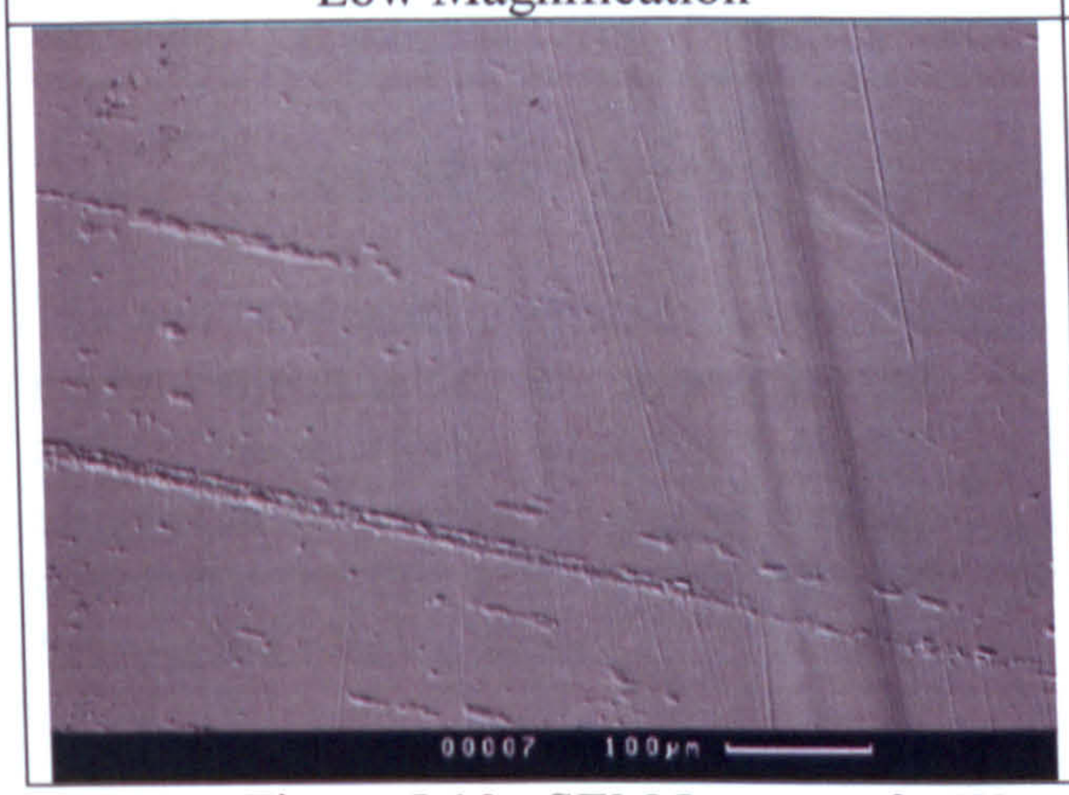

Figure 5.10. SEM Images of a Worn Valve Tip from an Engine Test.

The images obtained from the engine test components, clearly demonstrate a strong correlation in wear features with the specimen test images. The final soot content of the test lubricant was approximately 3% (measured using standard oil analysis techniques) and all specimen surfaces showed surface abrasion. Abrasion was also the dominant wear mechanism to occur at that contamination level in the specimen tests too. Although high levels of surface abrasion are visible, such wear is typical of that found in many engine valve train systems and 3% soot contamination is not usually detrimental to engine performance due to the increased protection offered by modern lubricants.

CHAPTER 6:
PHYSICAL PROPERTIES AND EFFECTS OF TEST LUBRICANTS

To fully investigate the effects of soot contamination and why it causes wear, an understanding of how a lubricant's properties and behaviour changes when mixed with increasing levels of soot is required; this chapter uses various techniques to develop such an understanding.

6.1. ASSESSMENT OF SOOT/CARBON BLACK CONTENT

The test lubricants prepared for all the testing carried out were produced using the method which is detailed in Section 3.5. Practically, it is believed that not all of the carbon black mixed with the base oil (and dispersant) or formulated lubricant is retained in suspension or mixed evenly. To assess the accuracy of the mixing method developed for this testing, the test lubricant mixtures were analysed to measure the true carbon black content.

6.1.1. Test Equipment

A schematic of the equipment used to assess the actual quantity of carbon black in a sample of test lubricant mixture is shown in Figure 6.1. Evaporation was used to reduce the lubricant mixture to solid components alone. Using a hot plate in a fume cupboard to extract the evaporated lubricant, a beaker containing a sample of the test oil is heated.

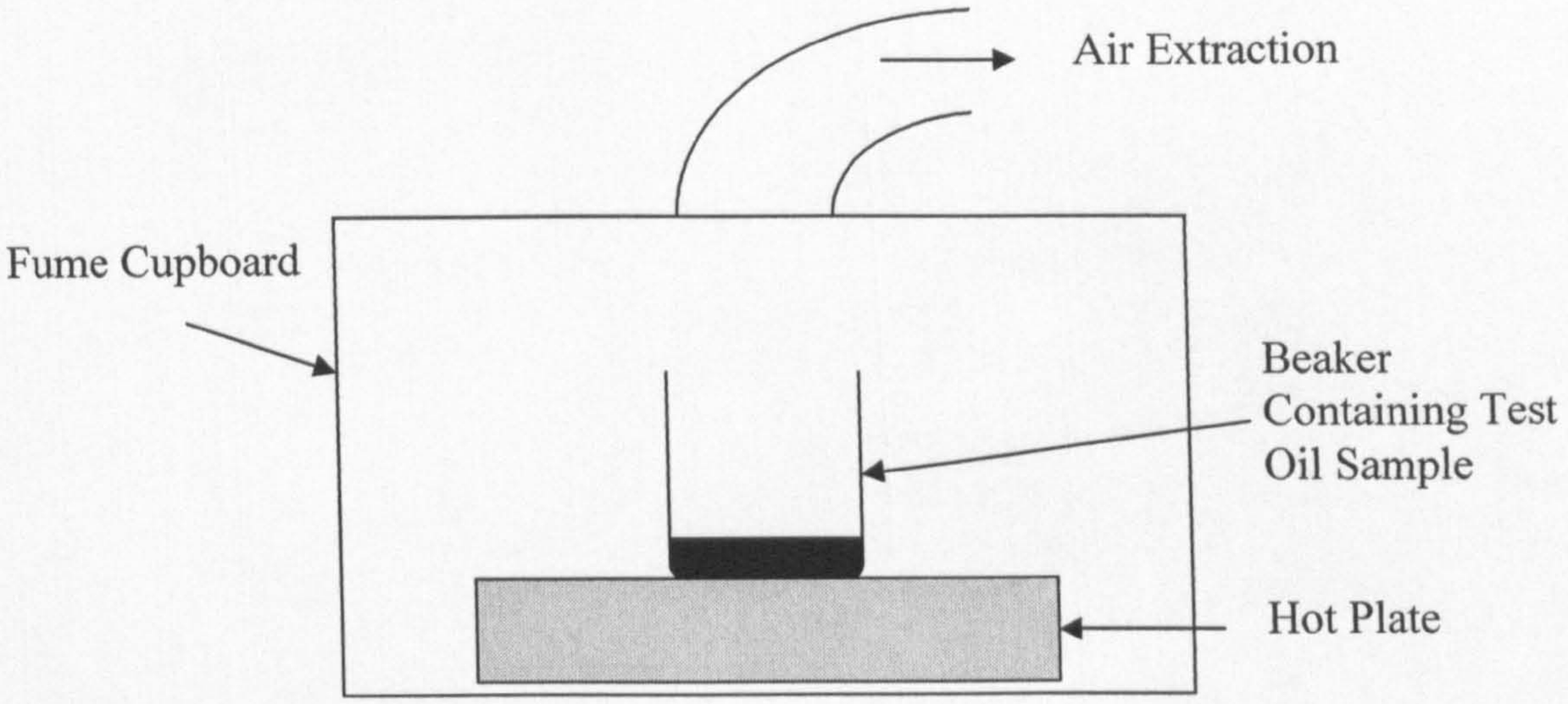

Figure 6.1. Schematic of the fume cupboard used for carbon black content analysis.

6.1.2. Method

All measurements to assess the actual carbon black content were performed by weight. An uncontaminated lubricant contains components that reduce to solid substances and these will always be present in any lubricant test sample. This value was calculated as a percentage of the total mass of a lubricant. The remaining percentage mass of solid components from test oils containing carbon black, require the percentage mass remaining from the uncontaminated lubricant to be subtracted, to produce the actual mass of carbon black present in the test oil.

Initially the beaker to be used in the evaporation test was weighed, using a bench-top balance. A small quantity of test oil was added to it and weighed, in this case approximately 5 grams was added. Only a small quantity of test oil was used to maximise the surface to volume ratio to increase the speed and efficiency of the evaporation process. 5 grams of test oil was an acceptable quantity to analyse as it was similar to, and in many cases greater than the quantity used for other tests in this research study.

The glass beaker containing the oil to be evaporated was placed on the hot plate, with the air extraction system operating, to prevent the evaporated oil from condensing inside the fume cupboard. The hot plate was heated until the test lubricant was evaporating but the surface temperature was kept below the oil flash point, to avoid any chance of ignition. The lubricant surface temperature was measured using an infrared non-contact thermometer. The samples were left evaporating for approximately 5 hours, after which time all liquid was evaporated and only solid (and solidified) components remain. At this point the beaker was removed from the hot plate and allowed to thoroughly cool to the temperature that the initial measurements were taken (room temperature). When cooled the beaker and its contents were weighed.

The actual carbon black content of the test oil mixture is calculated using the following method:

$$\text{Mixture mass before test (oil \& carbon black)} = \text{Total mass before test (oil mixture \& beaker)} - \text{Mass of beaker} \quad (6.1)$$

$$\text{Mass of solid components after test (oil \& carbon black)} = \text{Total mass after test (oil mixture remains \& beaker)} - \text{Mass of beaker} \quad (6.2)$$

$$\text{Percentage mass of solid dry components} = \frac{\text{Mass of solid components after test (oil \& carbon black)}}{\text{Mixture mass before test (oil \& carbon black)}} \quad (6.3)$$

$$\text{Percentage mass of carbon black in mixture} = \text{Percentage mass of solid dry components} - \text{Percentage mass of solid dry components from uncontaminated oil test} \quad (6.4)$$

6.1.3. Results

These carbon black content assessment tests were only carried out with base oil, mixed with dispersant and carbon black. It was considered unnecessary to perform the tests on formulated oil mixtures as a base oil and dispersant mixture should have similar (if not better) carbon black retention properties.

Tests were performed with neat base oil (mixed with dispersant) and 1, 2, 3, 4 and 5% carbon black contamination levels. Tests were performed twice and averaged. The analysis results are shown in Table 6.1.

Table 6.1. Assessment of Carbon Black Content in Test Oil Mixtures.

Carbon Black Content	Average Percentage mass of solid dry components	Measured Percentage Mass of Carbon Black Content
0%	6.05%	0%
1%	6.95%	0.90%
2%	7.82%	1.77%
3%	8.80%	2.75%
4%	9.63%	3.58%
5%	11.37%	5.32%

Practically, with any laboratory based mixing technique or even when a lubricant is contaminated with real engine soot through use in an engine, soot particles and soot sludge is present in the bottom of the mixing beaker or engine sump respectively. This unmixed soot/carbon black will obviously not play a role in the test oil mixture, leading to a reduction in the percentage mass content measured. Finally when soot/carbon black is mixed in the lubricant the final mixture is not homogeneous, producing regions within the test mixture that maybe below or even above the average mass percentage content. This mixing issue is most noticeable at the highest soot/carbon black contents, as seen in Table 6.1 where 4% and 5% carbon black

soot/carbon black contents, as seen in Table 6.1 where 4% and 5% carbon black content samples (which are visually particularly lumpy) produce a greater range of measurements, highlighting sampling issues specifically for highly contaminated samples.

6.2. VISCOSITY MEASUREMENTS

To fully understand how soot contaminated lubricants cause wear, the effects of soot on the properties of the test lubricant are required. One fundamental property of the lubricant that will change with soot concentration, is the viscosity.

6.2.1. Test Equipment

Viscosity measurements were performed on a Bohlin rheometer-viscometer (CVO120), at 40°C and 100°C, and a shear rate of $500s^{-1}$. This shear rate was selected to reduce any viscous drag effects that may occur. A photograph of the viscometer is shown in Figure 6.2. The viscometer is a cone-on-plate type, a photograph of the test contact is shown in Figure 6.3.

Figure 6.2. Bohlin Rheometer-Viscometer (CVO120).

Figure 6.3. The Test Contact of the Bohlin Rheometer-Viscometer (CVO120).

6.2.2. Method

Measurements were taken of base oil (with a dispersant) and formulated oil samples contaminated with increasing levels of carbon black. These viscosity measurements were taken from unused oil samples (i.e. samples not previously used for wear testing) and could therefore demonstrate the direct viscosity effects of carbon black contamination.

To carry out the tests only a small quantity of lubricant was required on the test surface, approximately 0.5ml. A test programme profile was created in the computer controlling the viscometer, the test plates were brought together (leaving a gap of 100μm, they were then heated to 40°C, the top plate was rotated and measurements taken, then it was heated again to 100°C, the plate was rotated and the second set of measurements were taken.

6.2.3. Results

The results from the viscosity measurements are shown in Figure 6.4. It is clear to see that carbon black contamination of both base oil and formulated lubricant increases the viscosity.

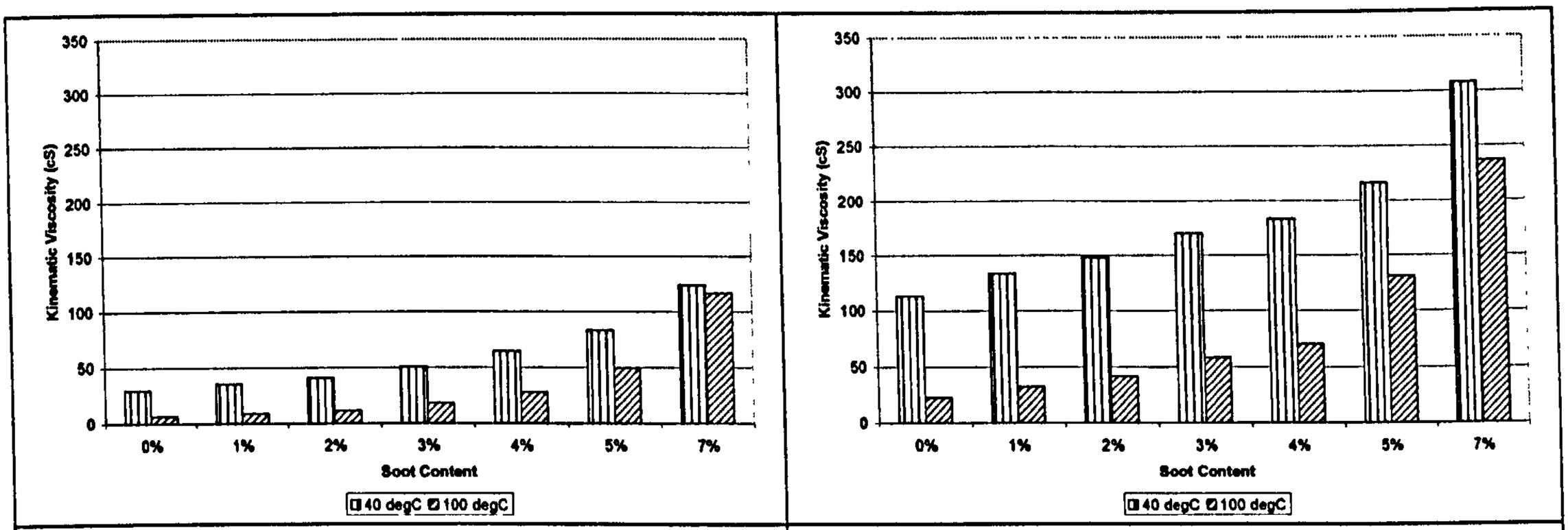

(a) Base Oil Viscosity Measurements | (b) Formulated Oil Viscosity Measurements

Figure 6.4. Viscosity measurement data at 40°C and 100°C for test lubricants with increasing levels of carbon black (a) base oil (b) formulated oil.

Using the viscosity measurements in Figure 6.4, the kinematic viscosities relating to 25°C and 100°C for both base oil and formulated oil were determined and are summarised in Table 6.2. The viscosity was calculated using an ASTM standard technique **[78]**.

Table 6.2. Kinematic Viscosities for the Tested Lubricants.

	Base Oil		Formulated Oil	
	Kinematic Viscosity (cS)			
Carbon Black Content	25°C	100°C	25°C	100°C
0%	55	6.8	210	22.2
1%	60	8.5	225	31.9
2%	66	11.1	235	41.6
3%	74	17.8	254.5	58.1
4%	80	27.4	260	70
5%	102	49.3	265	131.3
7%	129	116.8	340	236.3

It is possible to predict the minimum oil film thicknesses produced for the ball-on-flat wear tests (see Chapter 4 – Wear Testing) from the data in Table 6.2, using Hertzian and EHD theory **[75, 76]** (as calculated in Section 3.2). The calculated oil film thicknesses are displayed in Figure 6.5 (calculated for 0.36m/s sliding speed).

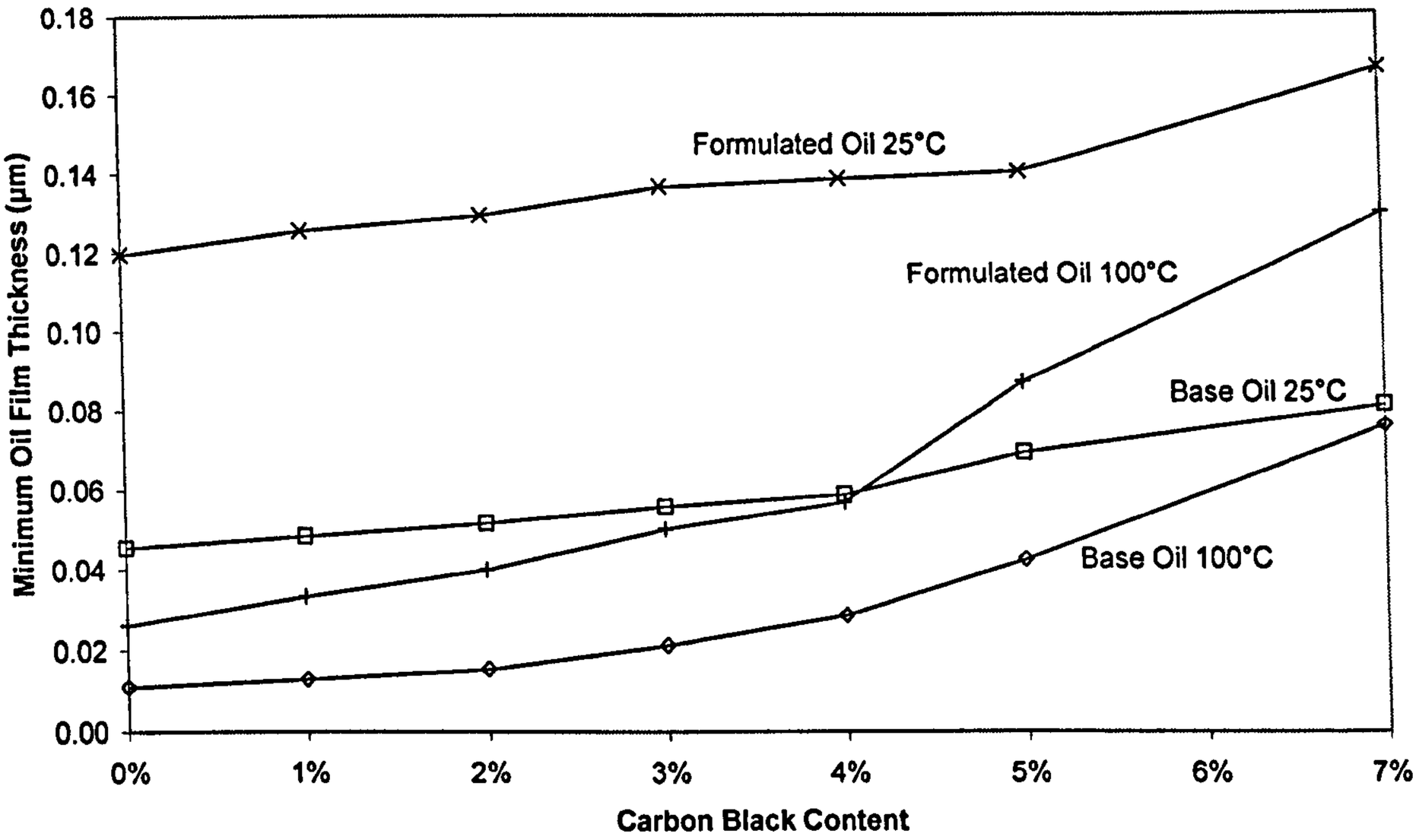

Figure 6.5. Calculated Oil Film Thicknesses for Tested Lubricants and Carbon Black Contamination Levels used in Wear Testing (0.36m/s sliding speed).

The viscosity measurements and calculated oil film thicknesses both demonstrate that the effects of soot in the contact are most significant at high soot concentration levels essentially above 4% contamination. Above 4% contamination the data in Figures 6.4 and 6.5 rise sharply.

It is well understood that the minimum diameter of individual soot particles is approximately 40nm (the same size as the carbon black particles used in this investigation), the mean soot particle size is 0.2µm and the soot aggregation size is 0.5µm. Clearly the oil film thicknesses predicted in Figure 6.5 for these tests are lower than many of these soot particle sizes, meaning that the carbon black contamination will significantly affect the amount of wear produced. Formulated oil produces a higher predicted minimum oil film thickness than base oil, offering greater protection. The increased oil film thickness is due a higher viscosity partially due the additives contained in the formulated oil.

6.3. TRACTION MEASUREMENT

6.3.1. Test Equipment

To gain further understanding of soot contaminated contacts, tests were performed in a Mini Traction Machine (MTM). A schematic of the MTM test rig is shown in Figure 6.6. This rig has a motorised steel ball as the upper contact and a motorised steel disc as the lower contact, immersed in a bath of test oil. The load is applied mechanically within the MTM unit. This test rig is designed to test contacts and lubricants under EHD lubrication conditions.

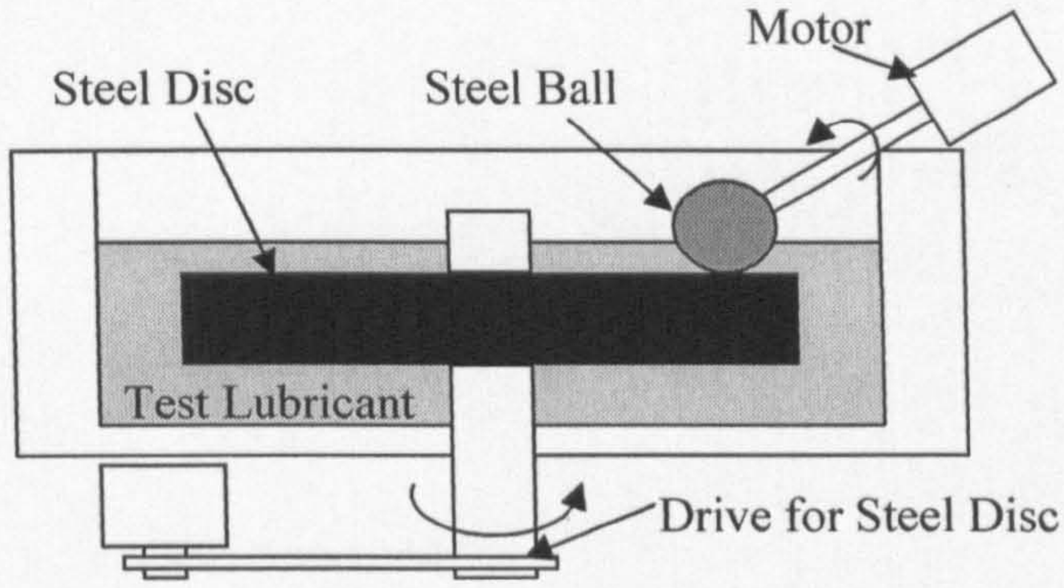

Figure 6.6. A Schematic of the MTM test rig.

6.3.2. Method

Three types of test were performed in this rig with base and formulated oil samples containing various carbon black contamination levels ranging from 0% to 7%. The types of test performed were: increasing ball load (from 0 to 40N) at a mean sliding speed of 1m/s and 10% relative slip; increasing levels of slip between the upper and lower specimens (from 1% to 10%) at 40N contact load and a mean sliding speed of 1m/s, and increasing mean sliding speed (from 0 to 2000mm/s or 2m/s) at 40N contact load and 10% relative slip.

6.3.3. Results

Figures 6.7a and c clearly demonstrate that presence of carbon black in the base oil has a significant effect on the traction coefficient with both increasing ball load and mean sliding speed. This effect is visible, but much less pronounced on Figure 6.7b, where the relative slip is increased. These results clearly demonstrate that carbon black is entrained into the contact, which has been questioned previously. The spike witnessed in Figure 6.7c relates to the start-up condition of the test where there is very little oil in the contact, producing boundary lubrication conditions and therefore a high traction coefficient. This high traction coefficient is visible again towards the end of the test where similar boundary lubrication conditions were produced.

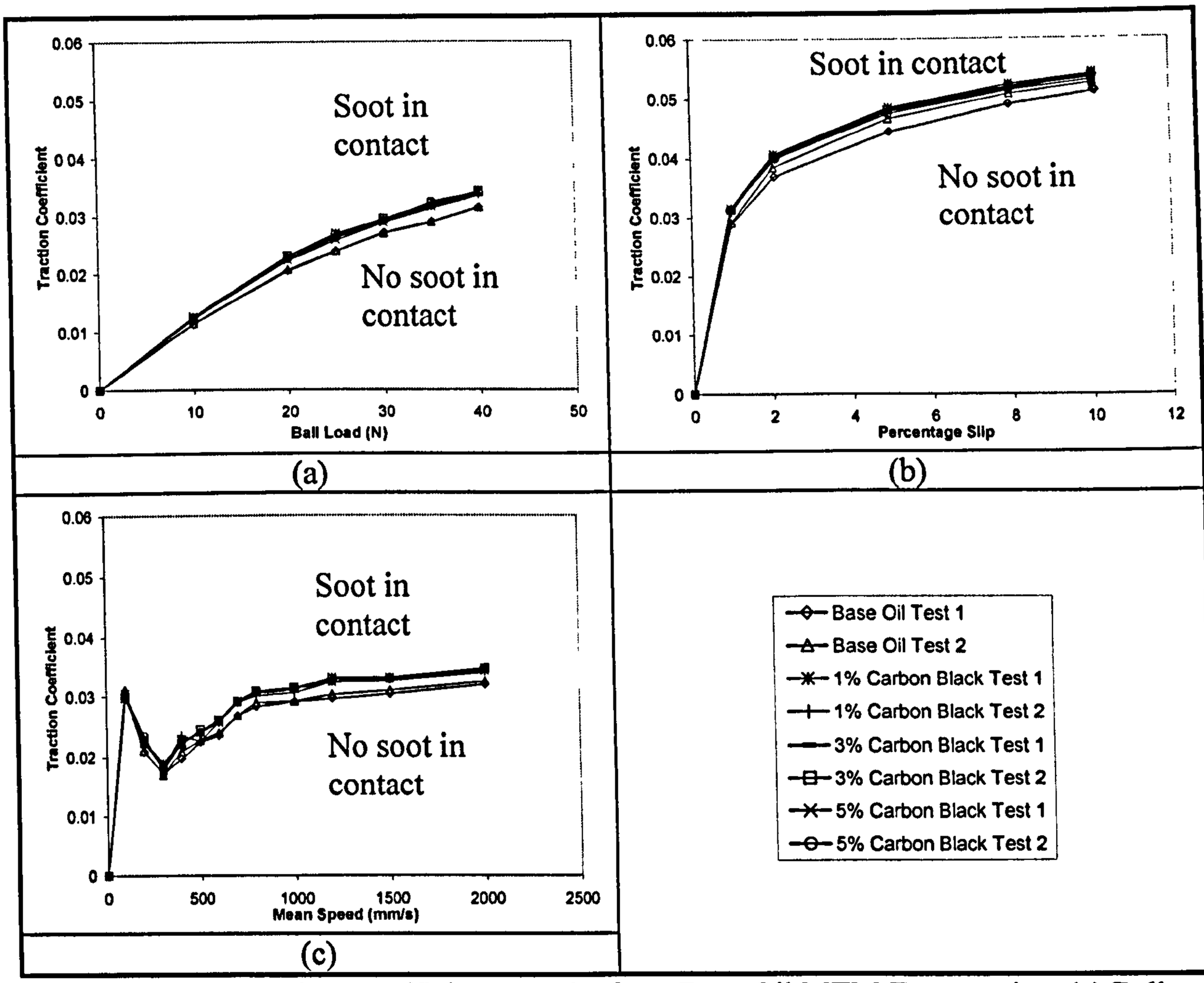

Figure 6.7. Traction Coefficient Results from Base Oil MTM Tests against (a) Ball Load (Speed:1m/s & Slip: 10%); (b) Percentage Slip (Speed: 1m/s & Load: 40N); (c) Mean Sliding Speed (Load: 40N & Slip: 10%).

The tests that were performed using formulated oil were mixed with carbon black at contamination levels of 1%, 3%, 5% and 7%. The results of these tests are shown in Figure 6.8. All of the tests demonstrate that formulated lubricants tend to reduce the measured traction coefficient (when compared to base oil), significantly so in the case of increasing ball load and mean speed.

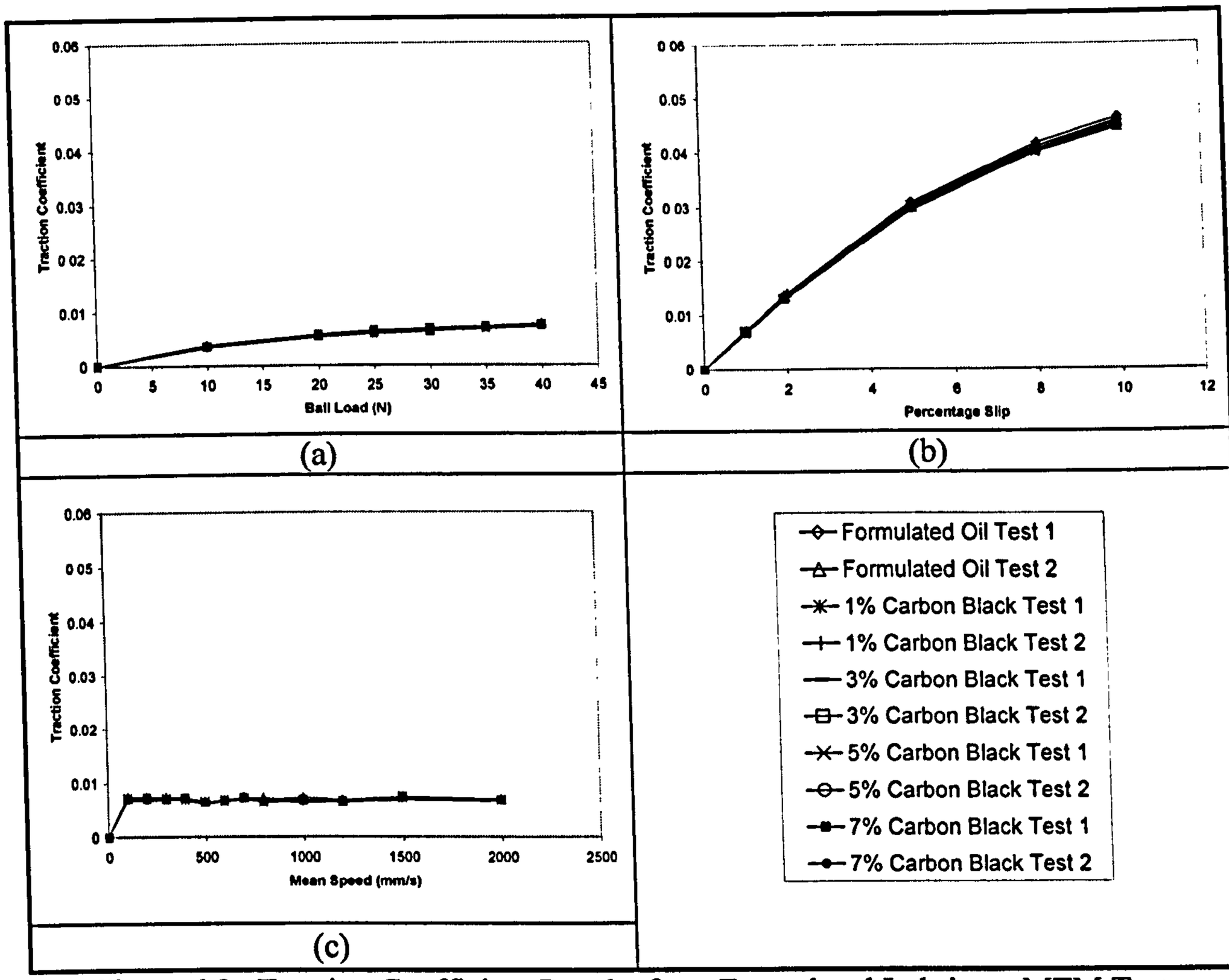

Figure 6.8. Traction Coefficient Results from Formulated Lubricant MTM Tests against (a) Ball Load (Speed:1m/s & Slip: 10%); (b) Percentage Slip (Speed: 1m/s & Load: 40N); (c) Mean Sliding Speed (Load: 40N & Slip: 10%).

The contact in an MTM machine is still essentially a ball-on-flat as with the friction testing (see Section 6.4) and wear testing (see Chapter 4), but instead of reciprocating it is continuously sliding. This test contact produces a predicted minimum oil film thickness of 0.28μm, assuming the oil is base or formulated oil alone and maximum applied ball load and mean speed. A continuously sliding contact is predicted to produce a partially lubricated or elastohydrodynamic lubricant oil film. A fully formulated oil film is likely to occur due to the fact that it continuously entrains the lubricant in one direction, as opposed to two with a reciprocating contact. Results from such a contact will not produce significant wear, but will demonstrate whether contaminants significantly affect a fully formed oil film. Such significant effects are demonstrated in Figure 6.7, where an increase in traction coefficient occurs when carbon black is present in a base oil, but has very little effect thereafter (i.e. further increased carbon black content). These results are essentially the inverse of the viscosity measurements (see Section 3.1) where low levels of carbon black contamination produced a low increase in viscosity, but at high levels of carbon black the viscosity increased significantly. All the tests using formulated oil (Figure 6.8), demonstrate that the presence of soot has practically no effect when mixed into formulated oil, demonstrating that under EHD conditions contaminants have a minimal effect and any effect is reduced when in a formulated lubricant, due to the additives contained within them.

6.4. FRICTION MEASUREMENT

Previous investigations into lubricant formulation have shown that the friction experienced in a contact is roughly proportional to the square root of lubricant viscosity **[51]**. As has been demonstrated (Section 6.2), increasing levels of carbon black lead to an increase in lubricant viscosity, therefore contact friction should also increase.

6.4.1. Test Equipment

To investigate this hypothesis testing was carried out on a Cameron-Plint TE77 low frequency - long displacement reciprocating sliding wear tester. This wear tester has the ability to measure instantaneous friction force measurements via a piezoelectric force transducer. A photograph of the Cameron-Plint TE77 is shown in Figure 6.9 and a typical contact is shown in Figure 6.10.

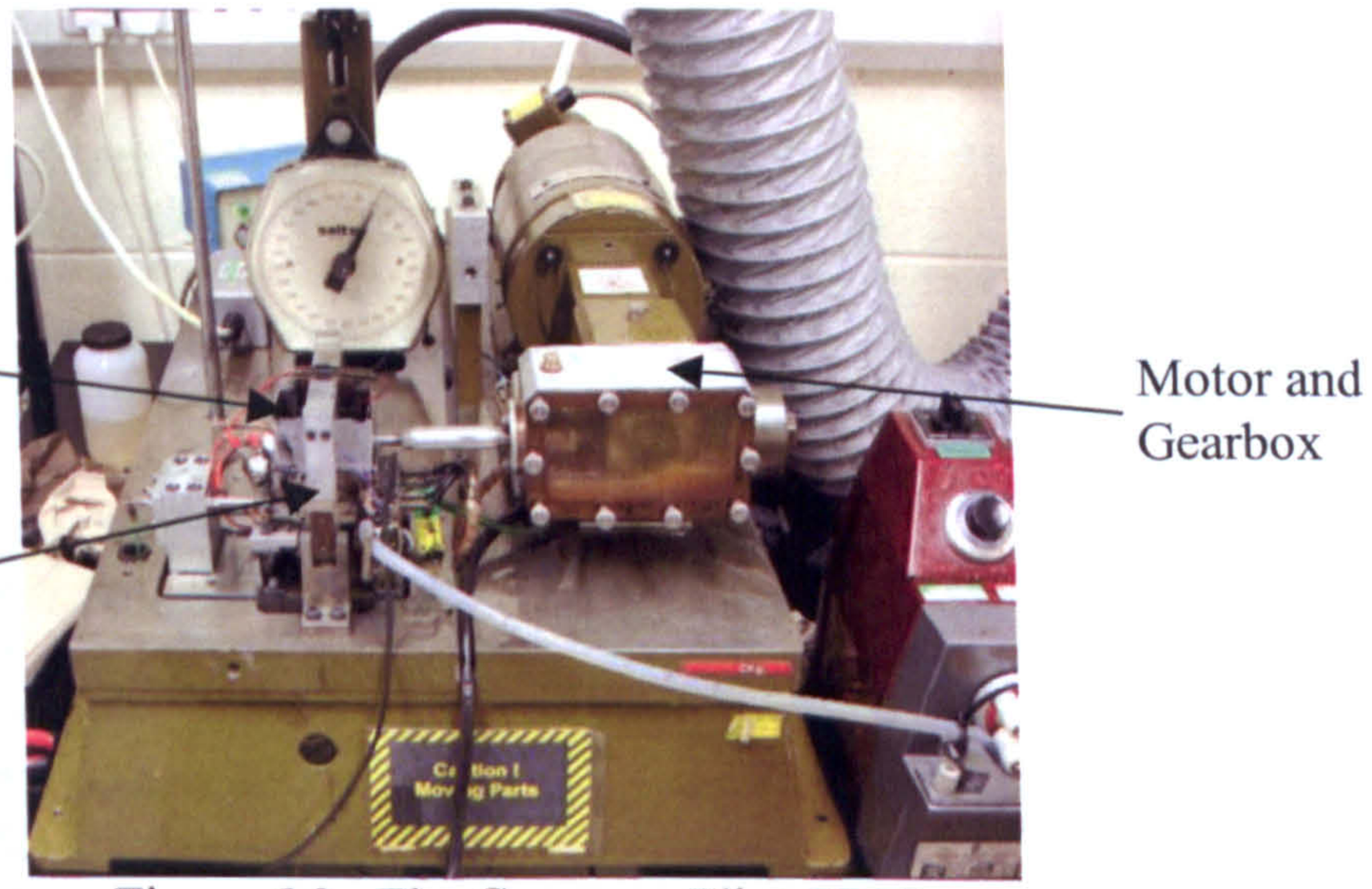

Figure 6.9. The Cameron-Plint TE77.

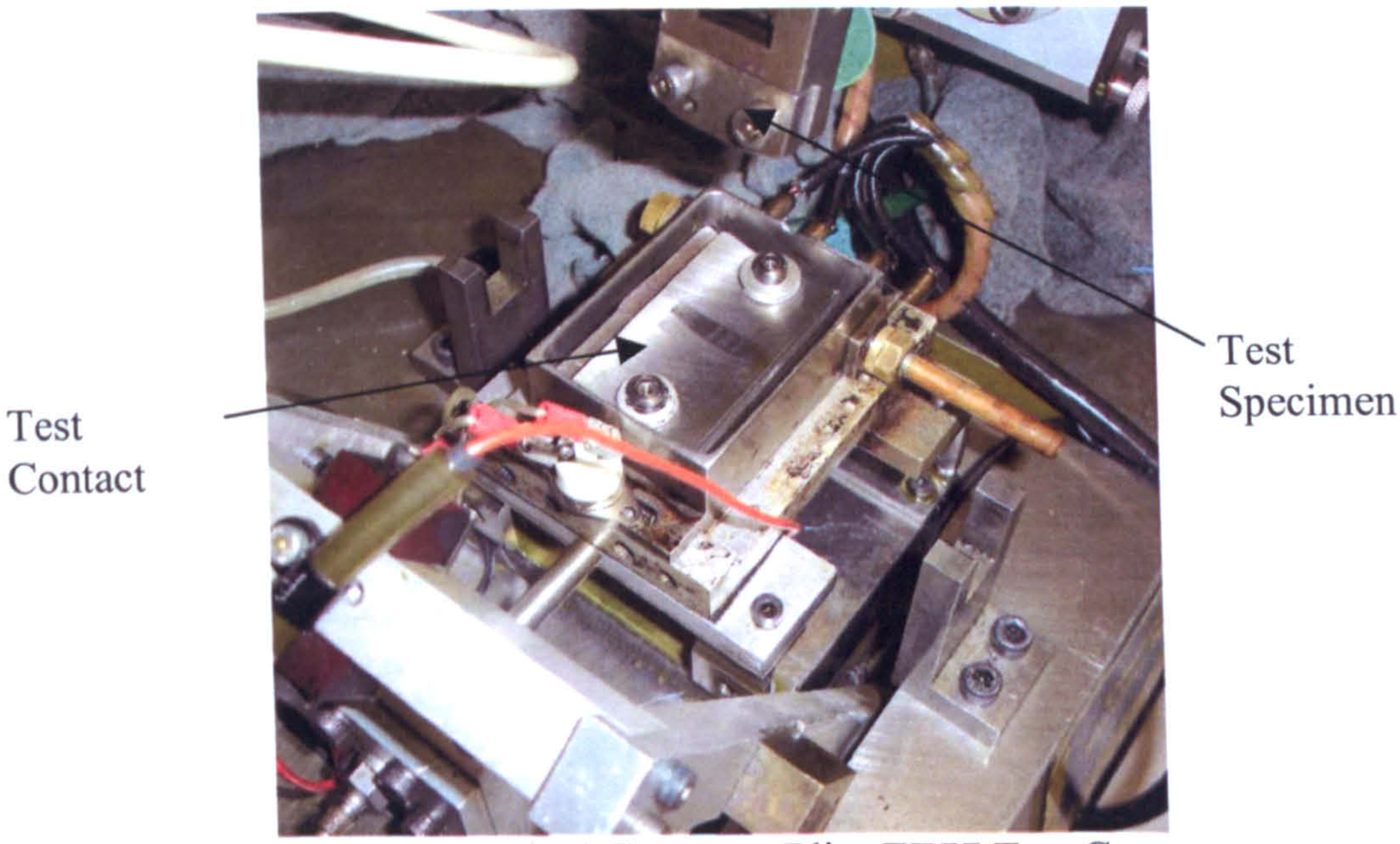

Figure 6.10. Typical Cameron-Plint TE77 Test Contact.

6.4.2. Test Method

The friction tests were performed with an 8mm EN31 chrome steel ball reciprocating against an EN24T steel flat counterface. The steel balls and counterfaces were replaced for each test. The chrome steel balls had an average surface hardness of 600Hv and a surface roughness (Ra) of 0.05μm. The EN24T steel counterfaces had an average surface hardness of 290Hv and a surface roughness (Ra) of 0.23μm.

Tests were carried out with a 250N contact load; this load was selected as it produces oil film thicknesses comparable with the wear testing (Chapter 4) and typical engine valve train contacts via calculations used in Section 3.2. This ball on flat contact produces a mean contact pressure of 2GPa over a Herzian contact diameter of 190micrometres (this contact pressure is high, but it was selected to produce a suitable oil film thickness for testing on the particular test rig used). The test temperature of 100°C was selected to replicate normal engine operating conditions. The motor for the reciprocating arm was operated at 2000rpm, this speed translates to a contact frequency of 33□Hz and mean sliding speed of 0.21m/s. To reduce the effects of running-in, test were carried out for a period of 20 minutes and friction measurements were taken at 5 minute intervals. Twenty minutes proved to be sufficient for these tests as the resulting friction measurements stabilised after approximately 10 to 15 minutes. Tests were carried out with base oil and formulated oil contaminated with increasing levels of carbon black.

Using the viscosity data (Figure 6.4), the oil film thicknesses produced in friction tests under the conditions for the friction testing were calculated and are presented in Figure 6.11, applying the same procedure as discussed in Section 3.2. Further analysis also demonstrated that each of these friction tests operated within the boundary lubrication regime.

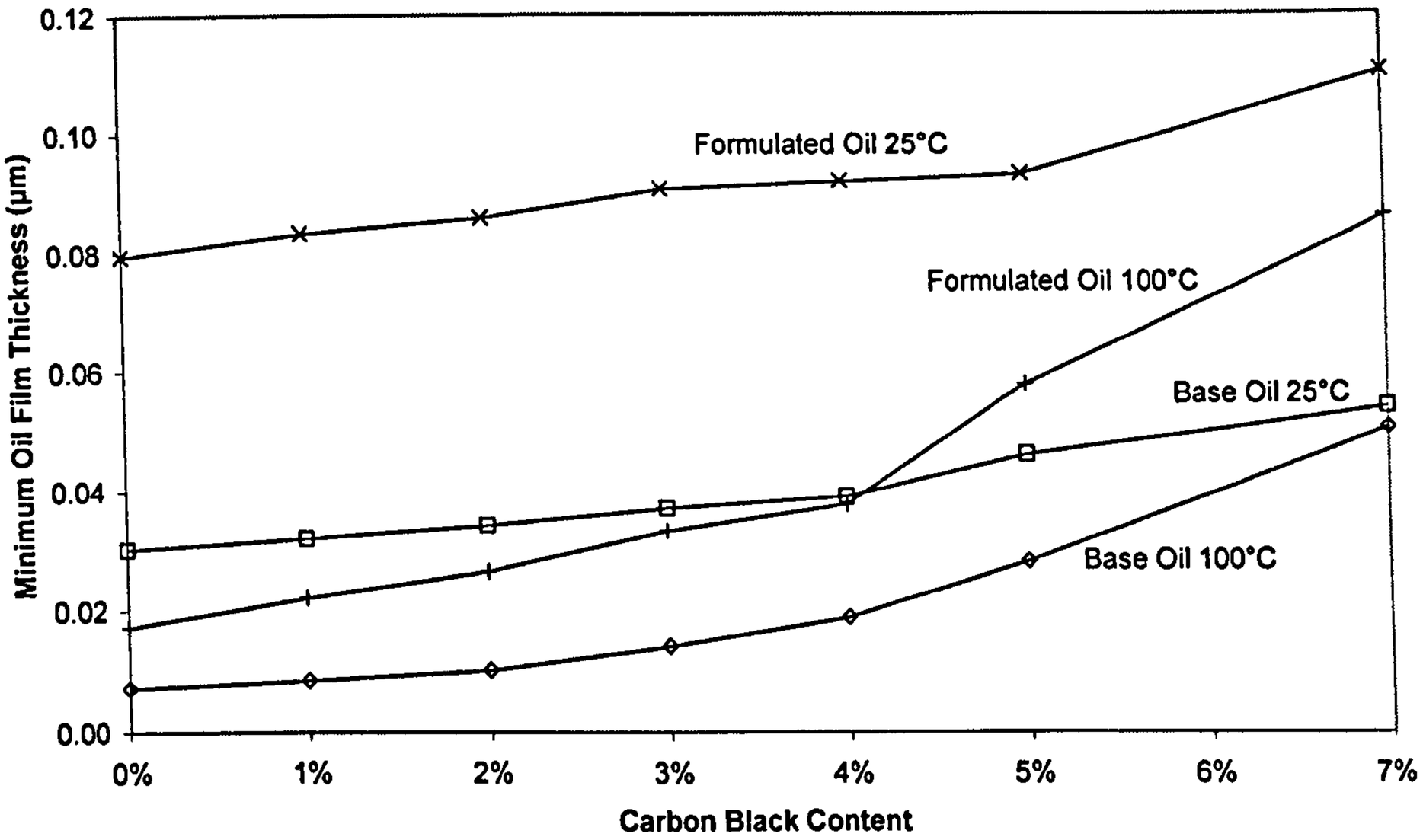

Figure 6.11. Calculated Oil Film Thicknesses for Tested Lubricants and Carbon Black Contamination Levels used in Friction Testing.

As with the calculations for the wear test contact (Figure 6.5), oil film thicknesses are predicted to be lower than the soot dimensions. Again under these conditions the carbon black particles will play a significant role in the friction data measured as they become entrained and potentially starve the contact of lubrication.

6.4.3. Results

The friction data presented in Figure 6.12 relates to measurements taken after 20 minutes of running.

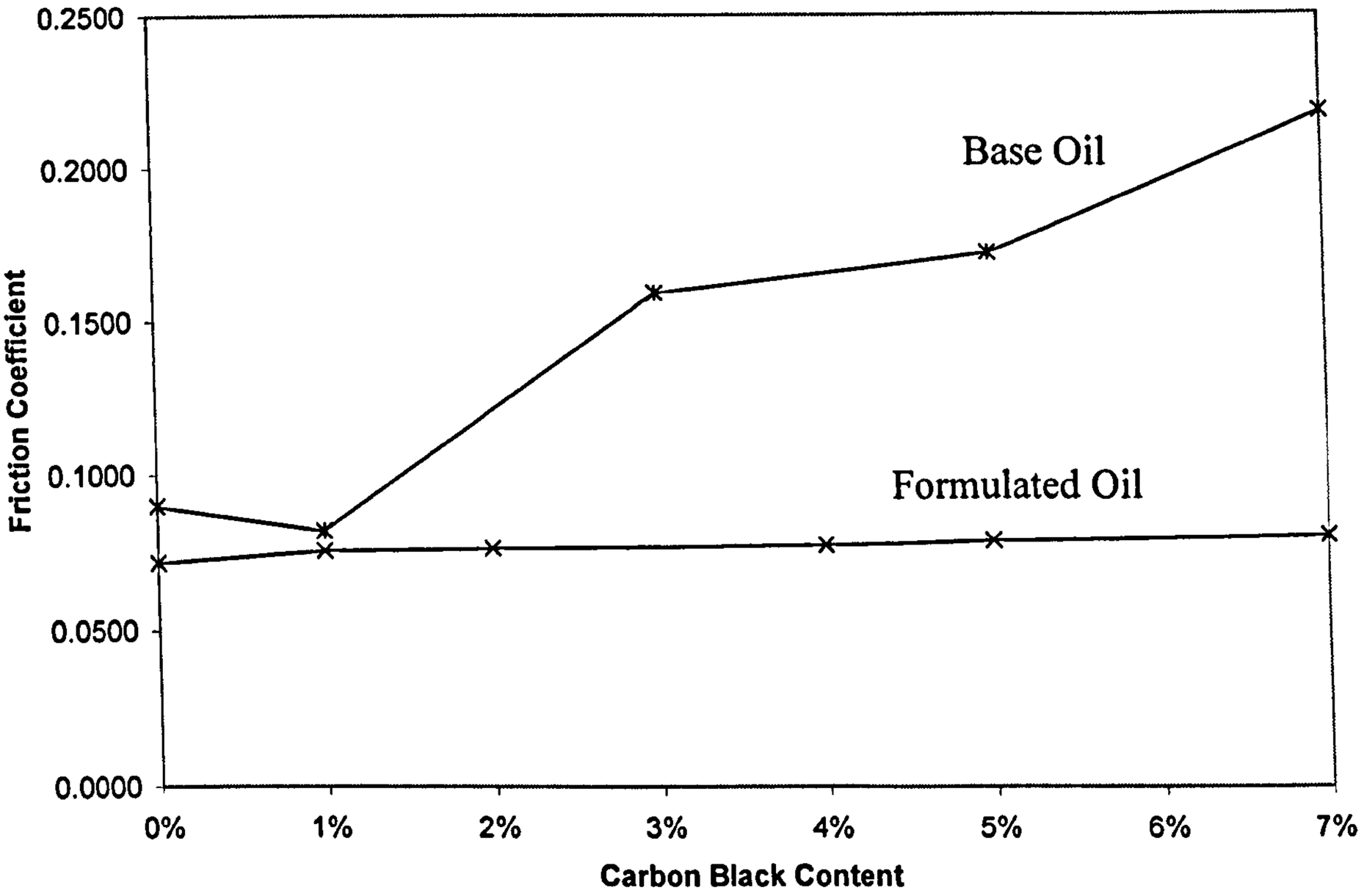

Figure 6.12. Reciprocating Friction Measurements with Base Oil and Formulated Oil Contaminated with Increasing levels of Carbon Black.

Figure 6.12 demonstrates that base oil contaminated with carbon black significantly affects the resulting contact friction. When the base oil results are compared to the formulated oil results, it is clear that the contact friction with formulated oil is less affected by the carbon black contamination and it produces a lower friction measurement overall too. The friction measurements taken in tests using base oil show the friction coefficient rising to approximately 0.22, this is very close to published friction coefficients for a dry steel contact **[75]**, indicating that starvation is beginning to occur in the contact. Formulated oil produces lower overall friction coefficients than base oil because of the additives in the lubricant to reduce friction whilst retaining other lubricant properties. Figure 6.12 clearly demonstrates that carbon black contamination has the effect of increasing friction.

6.5. VISUALISATION SOOT MOTION

To understand how contamination particles affect a lubricated contact it is useful to observe the contact as well as measure physical properties of the lubricant and the variation of forces transmitted through it. Two previous investigations have investigated the effects of soot particles in an elastohydrodynamic contact, firstly reference **[16]** reported that primary soot particles were entrained into EHD contacts at slow sliding speeds and influenced the friction and wear characteristics of the lubricant. Secondly reference **[79]** demonstrated that with a lubricant containing 6% soot that differences were observed in the contact region, depending on sliding speed and slide-to-roll ratio (slip). A similar type of investigation was performed within this body of work, but compares an uncontaminated lubricant to a lubricant containing a very low content of carbon black.

6.5.1. Test Equipment

For this work, an optical EHD rig was used, it consists of a steel ball (19mm diameter), partially submerged in a bath of oil, which is loaded against a glass disc. Both disc and ball can be rotated to create relative slip, but in this case only the glass disc was rotated. The rotational speed of the disc is changed via an external speed controller. The ball is loaded against the disc via an internal hydraulic jacking system.

As the glass disc rotates, oil is entrained into the ball/disc contact, and due to their relative geometries, a thin EHD film is formed. The contact produced is then viewed from above via a microscope or in this case, the eyepiece was replaced with digital video camera and recorded onto a PC. An external cold light source was fed into the optical system, at the bottom of the focusing above, above the final lens via a beamsplitter. A photograph of the EHD test rig is shown in Figure 6.13 and Figure 6.14 shows the glass disc and steel ball below the focusing tube.

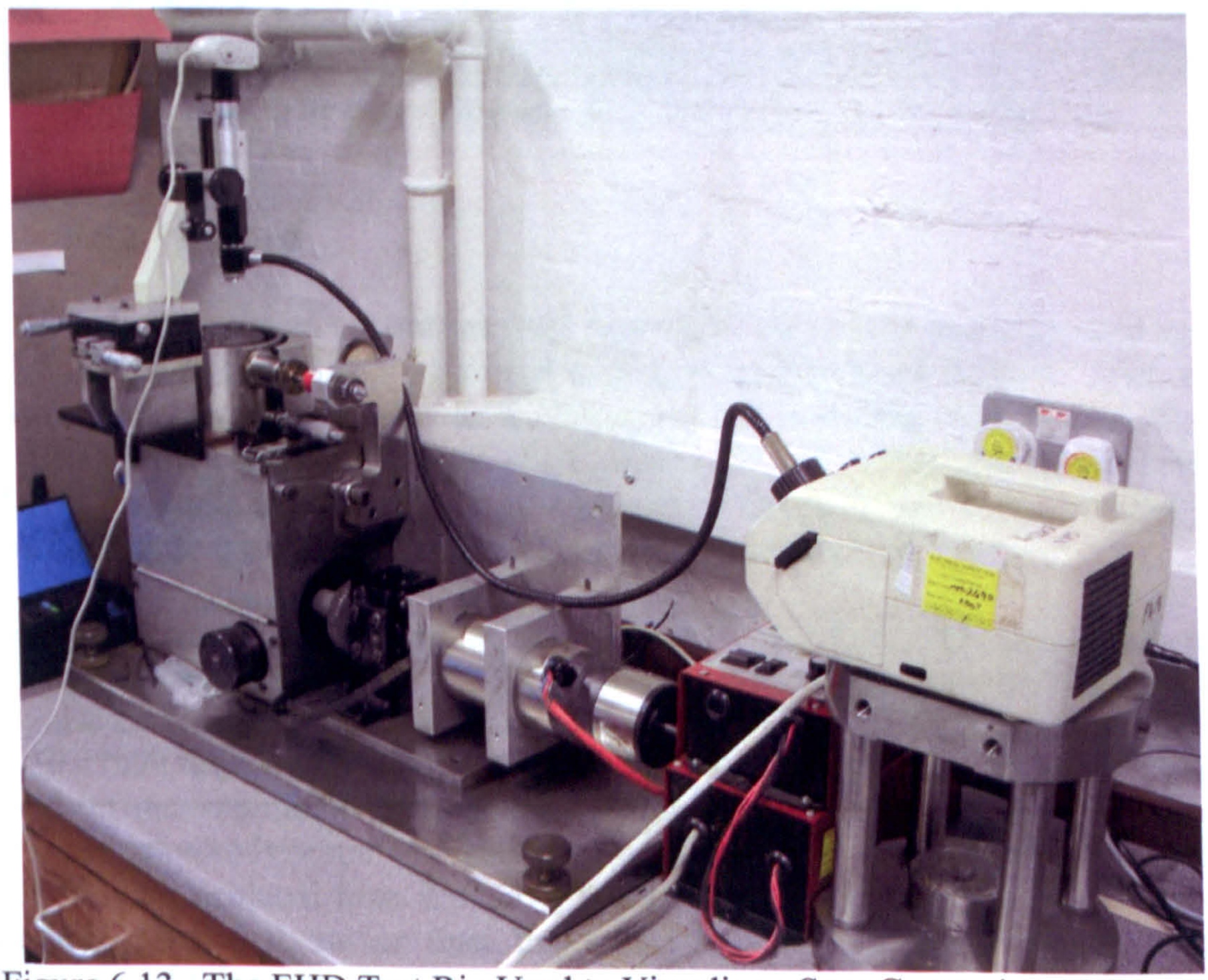

Figure 6.13. The EHD Test Rig Used to Visualise a Soot Contaminated Contact.

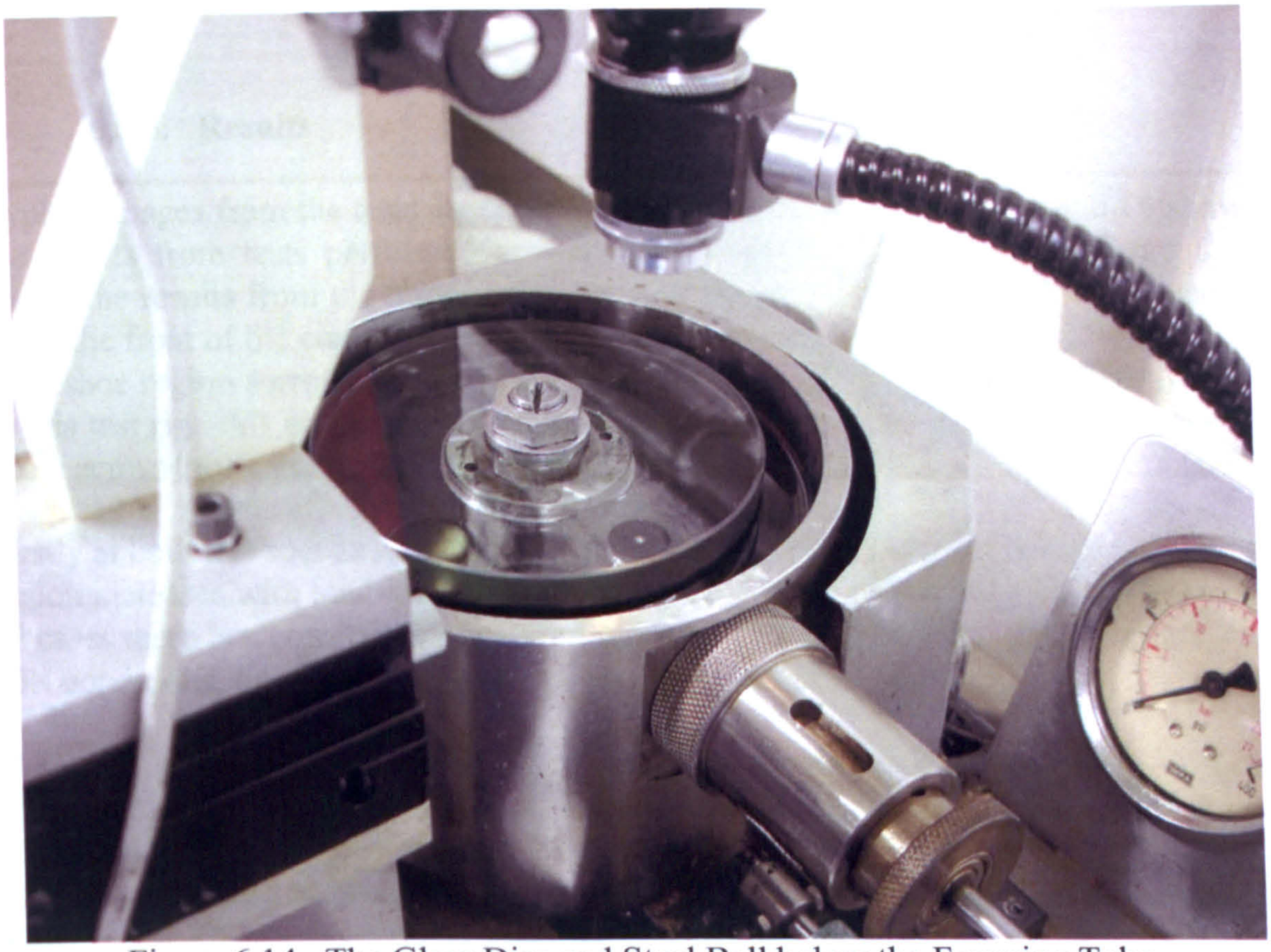

Figure 6.14. The Glass Disc and Steel Ball below the Focusing Tube.

6.5.2. Method

For this investigation an uncontaminated formulated oil sample was compared against the same type of formulated oil, mixed with 0.5% carbon black content. Such a low mass content of carbon black was used because MTM testing (Section 6.3) showed that EHD films containing carbon black produced very similar test results between different contamination levels. A second reason for using this contamination level was practical, to ensure the test contact could be clearly viewed.

Four loads were used in the testing, they were: 20, 40, 60 and 80N, equating to mean Hertzian contact pressures of: 0.37, 0.47, 0.54 and 0.59GPa respectively. The tests were also performed at two rotational speeds: 500rpm and 1000rpm, equal to: 5.24m/s and 10.47m/s respectively at the test contact point. The predicted oil film thicknesses (based on uncontaminated formulated oil) are shown in Table 6.3 and all operate under elastohydrodynamic lubrication conditions. The actual oil film thicknesses could not be calculated from the EHD rig measurements as the whole contact region was being analysed, rather than the minimum oil film thickness region. The importance of this testing was to investigate how lubricant contamination effects flow in the contact.

Table 6.3. Predicted Minimum Oil Film Thicknesses for all Test Conditions.

		Test Loads			
		20N	40N	60N	80N
Test Speeds	500rpm	0.5μm	0.48μm	0.47μm	0.46μm
	1000rpm	0.8μm	0.76μm	0.74μm	0.73μm

6.5.3. Results

Typical images from the tests are shown in Figures 6.15 and 6.16. Figure 6.15 shows the results from tests performed at a rotational speed of 500rpm and Figure 6.16 shows the results from the tests performed at 1000rpm. The images are orientated to show the front of the contact at the bottom of each of the images. All results show the horseshoe region surrounding the minimum oil film thickness region which is formed in this test rig. All images are compared via internal diameter (width) measurements taken across the centre of the contact.

Firstly at both test speeds it is clear to see that (as expected) that the horseshoe shaped region increases with load under all speed and lubrication conditions. Interestingly, in all cases there is a considerable increase between 20N and 40N and between 60N and 80N conditions, but not so between the 40N and 60N load conditions.

The most significant difference is between the uncontaminated and carbon black contaminated test lubricants, as the test with the contaminated lubricant produces horseshoe shaped regions that are noticeable smaller than those produced in tests using uncontaminated lubricant. Table 6.4 indicates the relative size of each region in terms of percentage decrease in diameter from uncontaminated tests to contaminated tests.

Table 6.4. Percentage Decrease in Horseshoe Shaped Region Diameter from Uncontaminated Tests to Contaminated Tests.

Test Conditions		Percentage Decrease in Diameter
Load	Speed (rpm)	
20	500	47.1%
40	500	29.7%
60	500	29.5%
80	500	30.3%
20	1000	43.3%
40	1000	47.5%
60	1000	47.5%
80	1000	54.4%

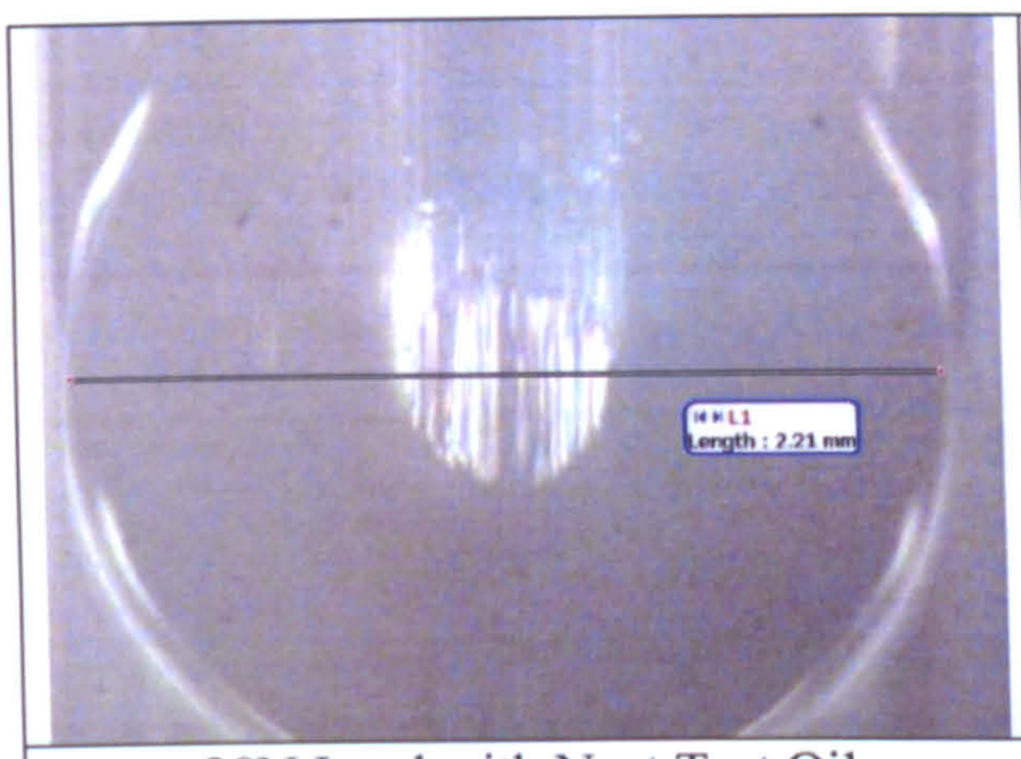

20N Load with Neat Test Oil

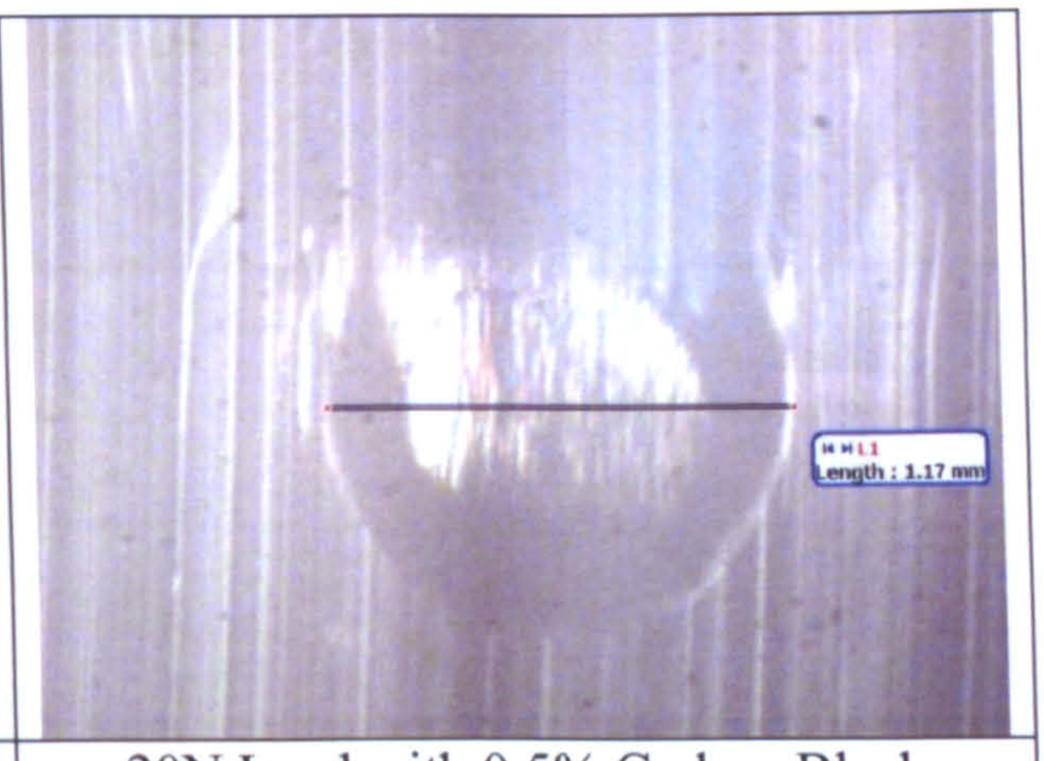

20N Load with 0.5% Carbon Black

40N Load with Neat Test Oil

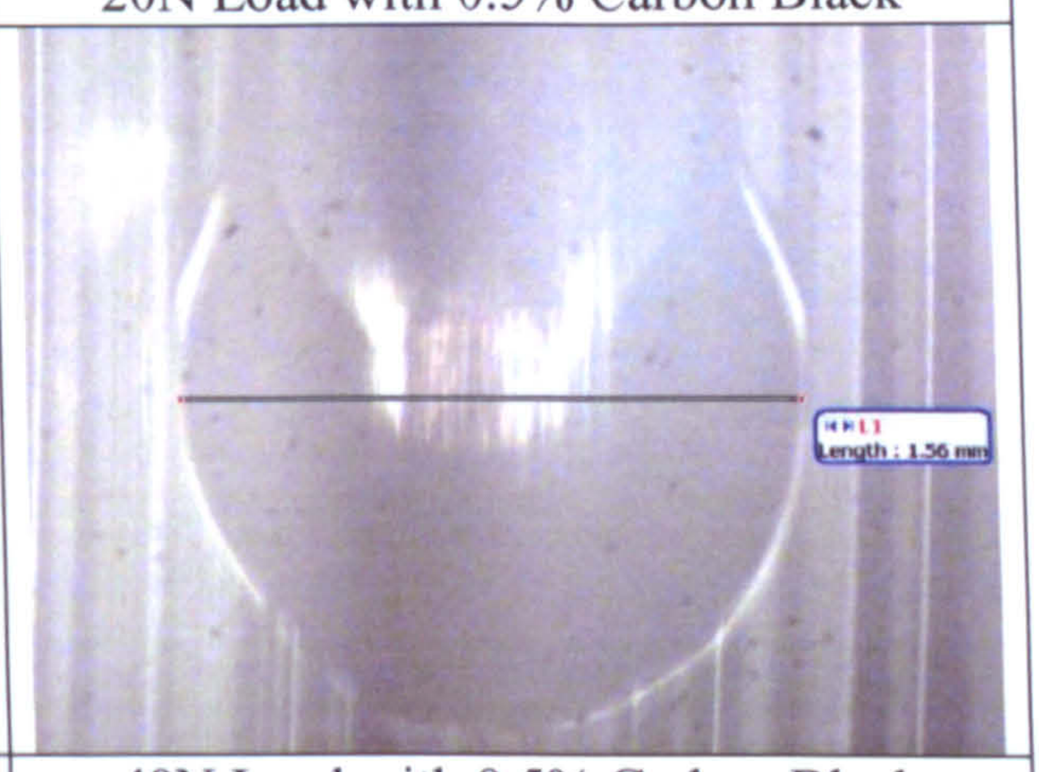

40N Load with 0.5% Carbon Black

60N Load with Neat Test Oil

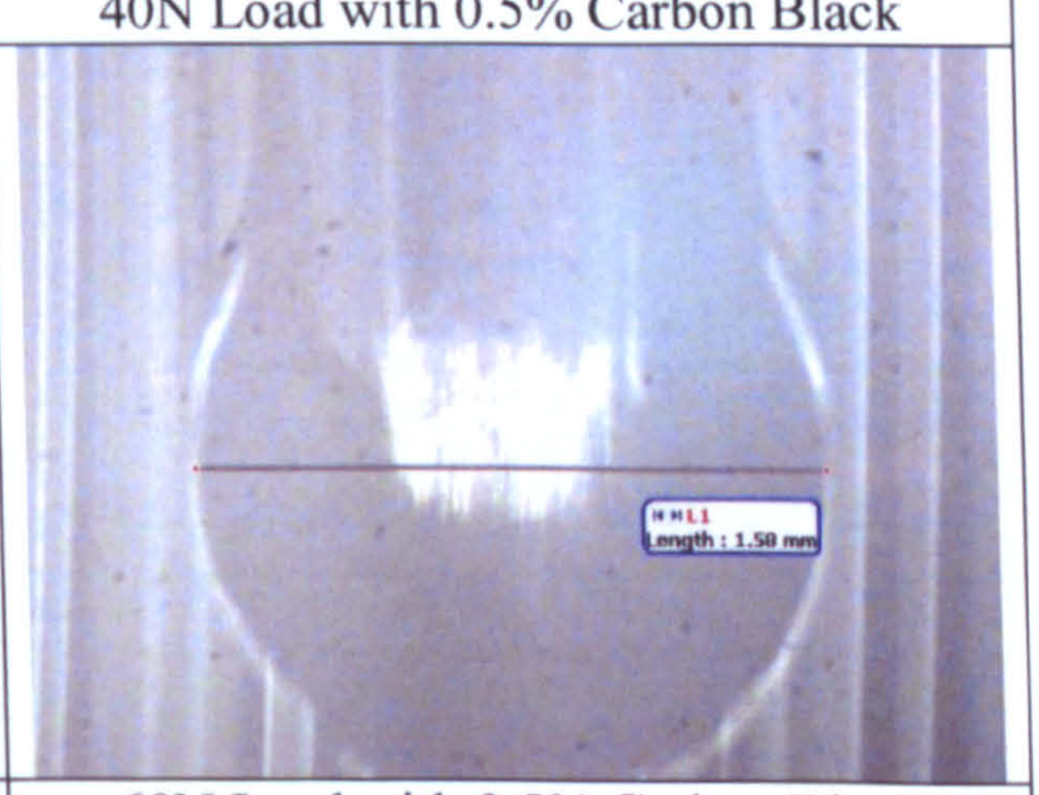

60N Load with 0.5% Carbon Black

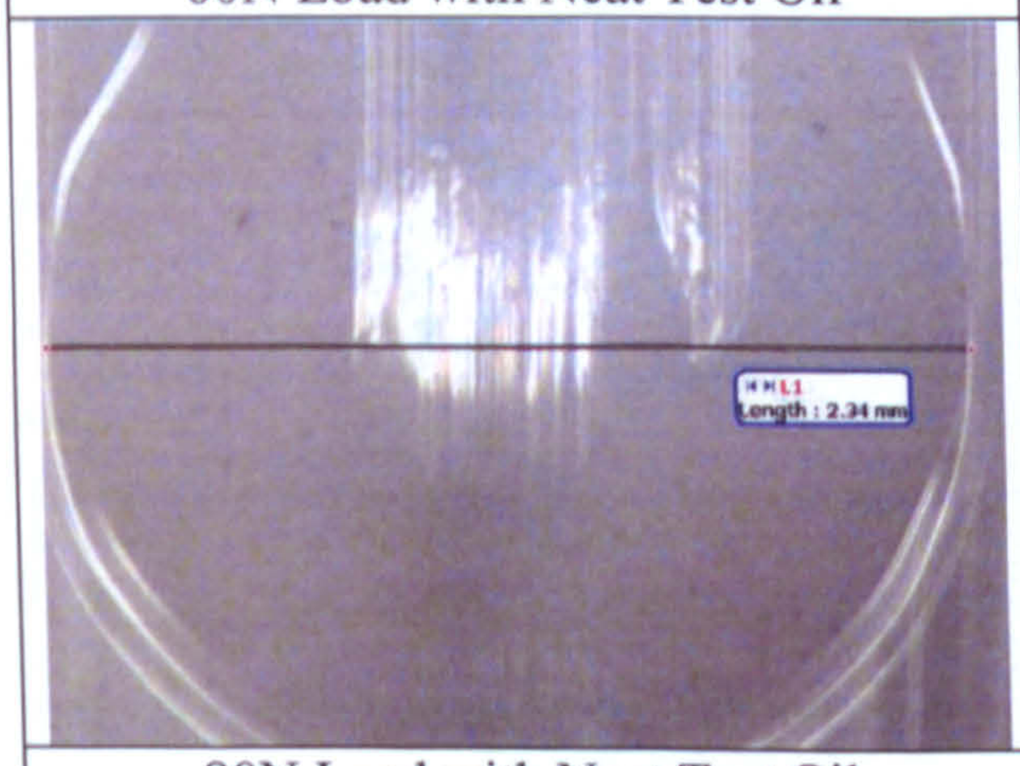

80N Load with Neat Test Oil

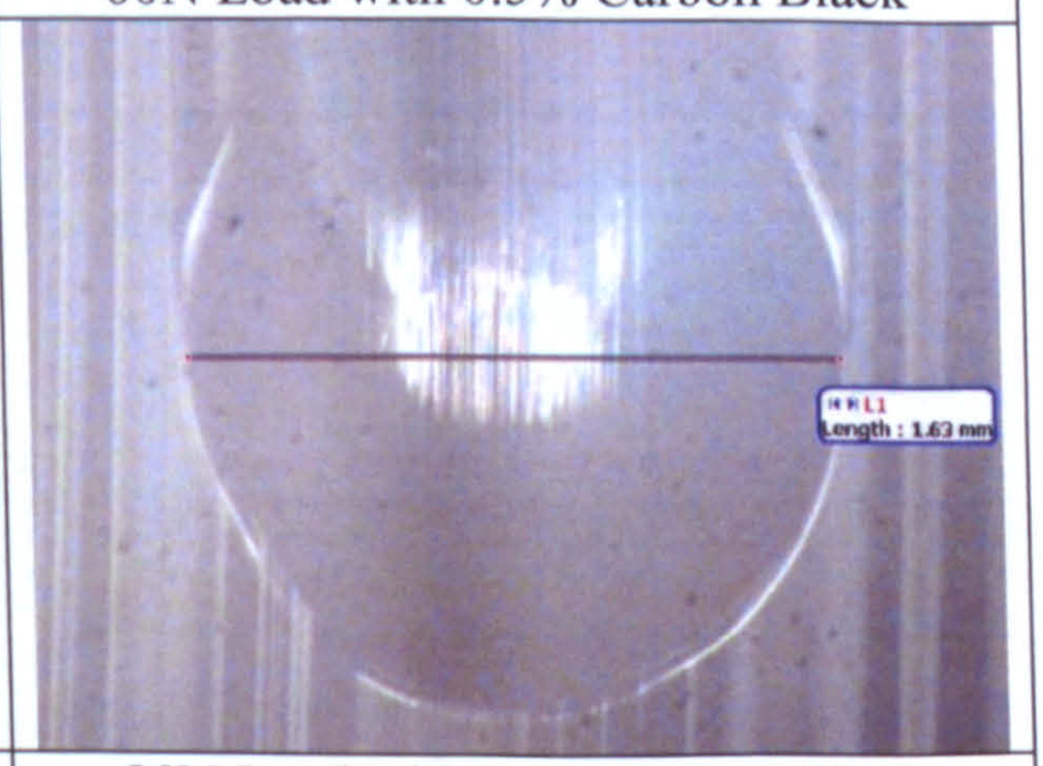

80N Load with 0.5% Carbon Black

Figure 6.15. Typical Images from EHD Visualisation Tests at 500rpm & 25°C.

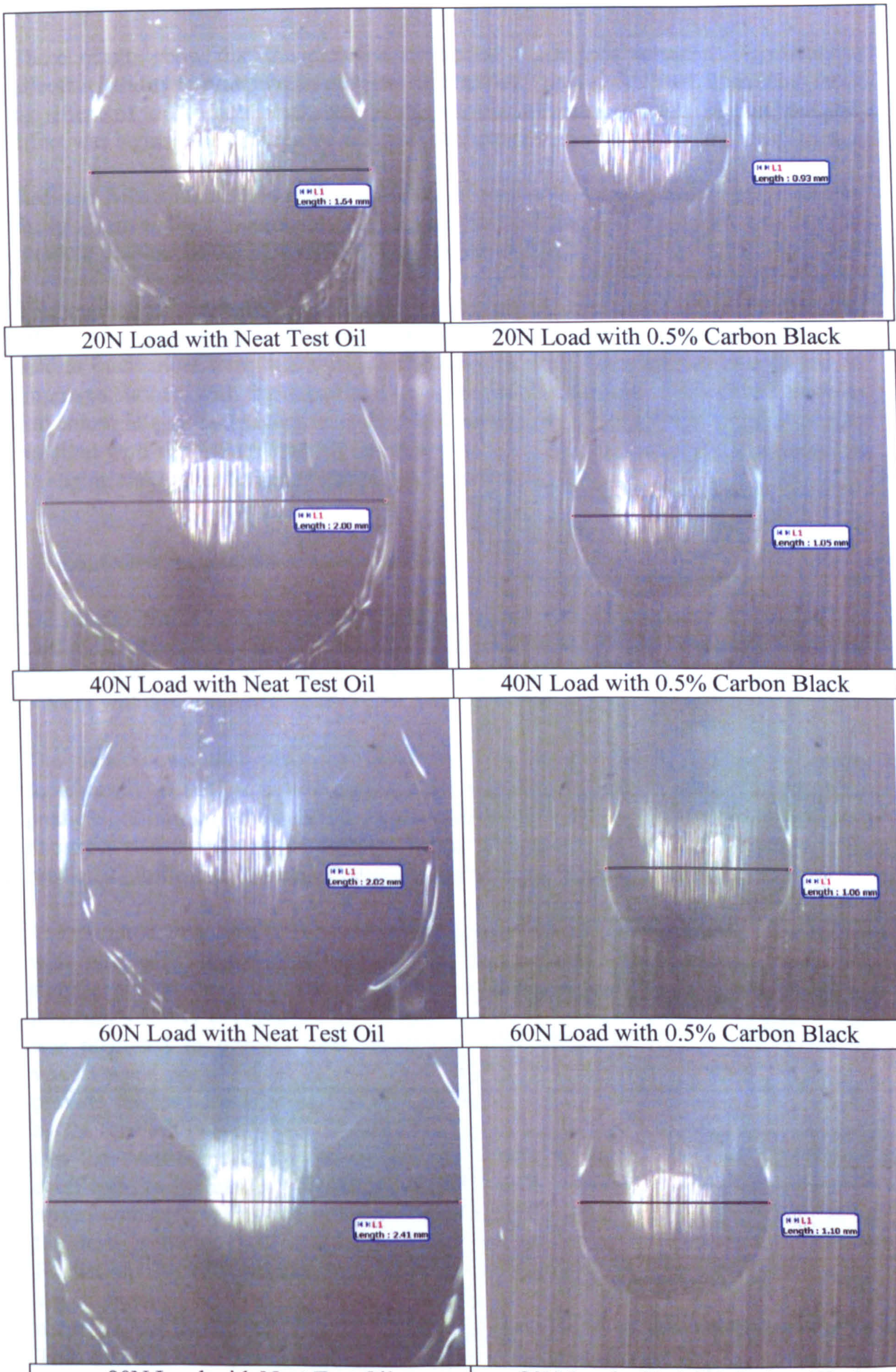

20N Load with Neat Test Oil | 20N Load with 0.5% Carbon Black

40N Load with Neat Test Oil | 40N Load with 0.5% Carbon Black

60N Load with Neat Test Oil | 60N Load with 0.5% Carbon Black

80N Load with Neat Test Oil | 80N Load with 0.5% Carbon Black

Figure 6.16. Typical Images from EHD Visualisation Tests at 1000rpm & 25°C.

These results show that the presence of carbon black in a lubricant significantly affects its ability to maintain an oil film. The testing showed that with increasing load the effect of the carbon black was to disturb the minimum oil film region, but the effect was significantly increased with a higher contact speed.

Reduced horseshoe shaped region diameter occurs when contamination is present in the lubricant as the contaminants will disrupt the flow into the region, by reducing the pressure gradient of the lubricant into the contact region.

This method of analysis has proved very successful in visually demonstrating the effects of carbon black in a contact and most probably why contaminated lubricants tend to cause more wear than uncontaminated lubricants. This method though can be improved further, with the use of a more advanced digital camera, which can achieve full colour images at a higher resolution and capture rate. Further investigation is also required with slip induced which are related to real EHD contact conditions found in an engine and higher levels of carbon black contamination.

6.6. CONCLUSIONS

The results in this lubricant analysis chapter produce strong evidence of the fact that carbon black contamination of oil significantly affects its properties and behaviour. Some of these results are initially conflicting as to whether an increased carbon black content will produce more wear.

The data shows that viscosity increases with carbon black content, but more significantly at higher concentrations, this therefore has the effect of causing the predicted minimum oil film thickness to increase accordingly. This increased oil film thickness will create greater wear protection as surfaces are separated, although the predicted oil film thicknesses are still operating under boundary lubrication.

The reciprocating friction measurements demonstrated higher friction coefficients with increasing levels of carbon black contamination. The increase was most significant with base oil at high carbon black contents; this is mainly due to the lubricant's ability to retain the particles and an oil film. The reciprocating test contact was predicted to operate under boundary lubrication conditions. The increased viscosity and predicted oil film thickness of the test lubricants would be expected to provide surface separation and therefore a lower friction coefficient (as demonstrated by the Stribeck curve **[75]**). Therefore under such conditions it can only be assumed that the carbon black particles were the significant factor in causing the friction coefficient to increase. The friction measurements carried out using formulated oil mixed with carbon black demonstrated the lubricant's ability to retain the particles, as the tests show a less significant effect on the measured friction coefficient. Predictions for this contact show that the oil film thickness should increase again, which should lead to a reduction in contact friction. The contact friction does not decrease, but the increase in friction is less significant than the tests using base oil. This demonstrates that the carbon black particles are still affecting the contact, but that the formulated oil is reducing that effect.

The MTM testing demonstrated that the presence of carbon black alone in base oil caused the traction coefficient to increase, most significantly in the tests where load and speed were varied. The test that changed slip produced a less significant increase in traction coefficient. The tests with carbon black mixed in formulated oil demonstrated no significant change in traction coefficient with the addition of carbon black; this demonstrates the performance of the formulated lubricants additives to maintain the required viscosity and oil film thickness even with contamination. The contacts in the MTM tests typically operated within the partially lubricated or elastohydrodynamic lubrication regimes. Therefore during the MTM tests the viscosity of the test lubricant alone would have effected the traction coefficient measurements, though the measured traction coefficient in the MTM contact is not directly proportional to test lubricant viscosity. This is probably why changes in traction coefficient for the test lubricants were in reality very low. The increased viscosity and predicted oil film thickness of the lubricants when operating within the partially lubricated or elastohydrodynamic lubrication regimes will tend to increase contact friction (as demonstrated by the Stribeck curve **[75]**).

The measured differences between the friction testing and MTM testing, combined with viscosity measurement and predicted oil film thicknesses demonstrate that the carbon black particles have the most significant effect on contact friction (traction) when a contact is operating under boundary lubrication and very minimal effects under EHD lubrication conditions.

The visualisation analysis tests demonstrated that even with a small quantity of carbon black contained within a lubricant, the lubrication film in a contact is significantly disturbed. This therefore means that the predicted oil film thicknesses calculated from viscosity measurements are possibly incorrect, leading to different contact than would be expected when any soot/carbon black contamination is present in a lubricant.

CHAPTER 7:
SOOT WEAR - DISCUSSION

The results from Chapters 4, 5 and 6 have highlighted various key findings relating soot contamination of engine lubricants to changes in the lubricant's properties, friction and traction coefficient, flow and most significantly wear. The findings are discussed in this chapter.

7.1. RECIPROCATING WEAR TESTS

The comparison of dimensions for the tested specimens show that higher sliding speeds produce thicker oil films and that higher temperatures produce thinner oil films. An understanding of these main points and how these dimensions compare to the various soot particle sizes can explain why various test conditions produce more wear than others.

In Chapter 4 the results for the base oil wear tests demonstrated that at both low and high temperatures, wear increases with increasing carbon black content. The 25°C wear tests showed a very low increase in wear compared to the 100°C tests. The 25°C tests showed that at 5% carbon black content the increase in wear volume is roughly 90% of the neat base oil tests. The 100°C tests demonstrated that at 5% carbon black content the increase in wear volume is roughly 800% of the neat base oil tests. This dramatic increase in wear between the 25°C and 100°C tests is due to the oil film thickness decreasing by approximately a quarter, taking the film thickness much thinner than the mean soot particle size.

The 25°C results demonstrate a noticeable increase in wear between 2% and 3% contamination, and the 100°C results demonstrate a noticeable increase in wear between 3% and 4% contamination; these increases may indicate a possible change in wear mechanism.

The ramped heating tests show increases in wear volume of a similar profile as the 100°C tests. The increase in wear volume is less than the 100°C tests, with an increase of just less than 600% of the neat base oil tests. This is because for the first 10 minutes of the tests the oil is operating in temperature regions where its thickness is relatively high compared to when it is operating at 100°C, wear levels are then

increased during the final 10 minutes of the tests when they are held at 100°C. The wear levels for the ramped heating tests all appear to be approximately 70% of the 100°C test results. Again there is an increase in wear between 3% and 4% contamination; indicating a possible change in wear mechanism.

The tests performed at half sliding speed followed similar trends to those in of the full sliding speed base oil wear tests. The wear measured was higher, particularly so for the 25°C tests, this is due to the oil film thickness reducing with the reduction in sliding speed. The wear for the 25°C tests have increased dramatically because film thickness in this case is within the range of the carbon black agglomerates. For these test conditions the 25°C tests show that at 5% carbon black content the increase in wear volume is nearly 400% of the neat base oil tests. The 100°C tests showed that at 5% carbon black content the increase in wear volume is over 800% of the neat base oil tests. Again there is an increase in wear between 2% and 4% contamination; indicating a possible change in wear mechanism.

The wear volumes data from the formulated oil wear tests follow a similar profile to those carried out with base oil. The 25°C tests produce extremely similar wear volume results as the base oil testing at 25°C, each producing an increase in wear between 100% and 150% at 5% carbon black contamination levels. The range of wear produced (between 100% and 150% increase in wear volume) is most probably due to the experimental variability experienced when performing wear testing with particles suspended in a fluid. The similarities in the formulated and base oil testing at 25°C are because at low temperatures a lubricant is designed so that the properties of the base oil dominate. Lubricant additives significantly modify the performance of the lubricant at elevated temperatures, when essentially the viscosity of the base oil (alone) reduces significantly. This effect is evident in the results (Section 4.2) for formulated lubricant testing at 100°C, where the wear results are only slightly higher than the 25°C results.

7.2. WEAR RATE TESTS

The tests to measure the rate at which the wear occurs during tests showed that the majority of the wear occured in the first 10 minutes – approximately 90%, shown in Section 4.3. This follows the expected profile of a component experiencing 'running-in' and subsequent steady state wear, which is showing much higher levels of wear than would be seen with clean oil. The 100°C tests exhibit approximately 4 times as much wear as the 25°C tests – similar to the levels measured in Section 4.1. These results demonstrate that for such tests 20 minutes is a practical running time.

Section 4.3 displays typical running-in of a component where lubricated metal-to-metal wear and abrasive wear normally dominates, producing a polished surface. After 20 minutes the results reach a threshold value where the two surfaces have become separated by the oil film. This threshold value will be a function of several factors, including: contact geometry, lubricant, temperature and contamination level. It is thought that carbon black contamination enhances this process, by performing a similar function to a say a grinding paste and increasing the wear level and therefore the component surface separation until a threshold (dependant on the contact conditions) has been reached.

7.3. MORPHOLOGY OF WEAR SCARS

With respect to Chapter 5 it can be concluded that at both 25°C and 100°C in the base oil tests that the wear scars show typical lubricated metal-to-metal contact for the 0% carbon black content tests, but with the 100°C case having greater wear. For the 3% carbon black content tests the 25°C case again shows signs of metal-to-metal contact, but with a very low level of abrasion; the 100°C case due to its thinner film thickness shows signs of abrasion and some plastic deformation. The 5% carbon black content test shows at 25°C signs of abrasion and some plastic deformation, the 100°C tests show a great deal of abrasion and plastic deformation, and possible starvation of the lubricant from the contact.

The specimen testing using formulated lubricants produces exactly the same wear scar trends, but the transitions occur at slightly higher levels of carbon black contamination, due to the additive protection present in the formulated lubricant. Typically abrasion will dominate above approximately 4% contamination and then a combination of abrasion and plastic deformation at approximately 7% contamination.

Further proof of the wear scars discussed above appearing on the test surfaces was demonstrated in both the component and system level reciprocating wear tests.

7.4. WEAR MECHANISMS

From the above discussion, possible wear mechanisms can be proposed. These wear mechanisms are dependant on temperature (therefore oil film thickness) and carbon black content. For both low and high temperature (25°C and 100°C respectively) and low carbon black content (2% and below) there appears to be low levels of wear dominated by boundary lubricated metal to metal contact. This type of wear generally remains the case for higher carbon black contents (approximately 3%) and low temperatures, but with signs of low levels of abrasion. At 3% carbon black content and high temperatures wear is possibly occurring due to abrasion from entrained carbon black particles producing significant scratch marks, also showing signs of some plastic deformation. For the highest levels of carbon black content tested (5%) and low temperatures the wear mechanism appears to be similar to that of 3% carbon black and high temperatures, but at high temperatures another wear mechanism seems to be dominating. At both high carbon black content levels and temperature wear is possibly occurring due to high levels of abrasion and starvation due to particles blocking the contact region, dramatically reducing the flow of lubricant; again showing a large amount of plastic deformation. Component wear at such high contamination levels appears to be due to adhesive scuffing/galling wear.

The wear scar images from the formulated oil tests indicate the progression of the same wear mechanisms with increasing levels of carbon black contamination, but the changeover between mechanisms occurs at higher carbon black levels. The change to abrasive wear appears to occur at approximately 4% contamination and contact starvation occurs at approximately 7% contamination. The reason for this change is due to the properties of the formulated oil as demonstrated in Chapter 6. Viscosity

measurements and the associated oil film thickness calculations demonstrate that a formulated lubricant will produce a thicker oil film than base oil, providing greater surface separation and therefore a lower probability that soot particles will affect the contact. The carbon black particles do still cause an increase in wear, as the agglomerated particles are greater in size than the predicated oil films. This leads to the possibility of oil films being disrupted, causing metal-to-metal contact with carbon black particles in the contact. Anti-wear additives will also help to reduce the total level of wear as they are deposited onto the surface, producing a protective chemical layer. Reciprocating friction measurements also demonstrate the benefits of formulated lubricants with lower overall friction coefficients, and a less significant rise in friction with increasing carbon black content.

Finally the analysis of the worn engine components from the system test demonstrates that abrasive wear is occurring as would be expected at such soot contamination levels. Further engine testing has also shown that these levels of abrasion do not pose a threat to engine reliability. Unlike the wear witnessed in the specimen testing, the wear on the used engine components is more evenly distributed (shown clearly on the SEM images) showing much more consistent abrasive markings.

The wear scars from the tests with the most heavily contaminated lubricant mixtures, shows signs of all three wear mechanisms, where their formation is essentially dependant on the sliding speed within the stroke, see Figure 7.1. At low sliding speeds (start of stroke), wear appears due to lubricated metal-to-metal contact as carbon black particles are not built-up around the contact (see point 1). At increasing sliding speeds the carbon black particles start to build-up around the contact, where the contaminant particles cause abrasive wear (see point 2). At the highest sliding speeds (mid stroke) carbon black particles have built-up enough before the contact to reduce lubricant flow into the contact zone and cause starvation and the associated metal-to-metal wear, shown by heavy scoring marks (see point 3) from adhesive scuffing/galling wear. The above process occurs in reverse order during the second half of the stroke as the sliding speed decreases.

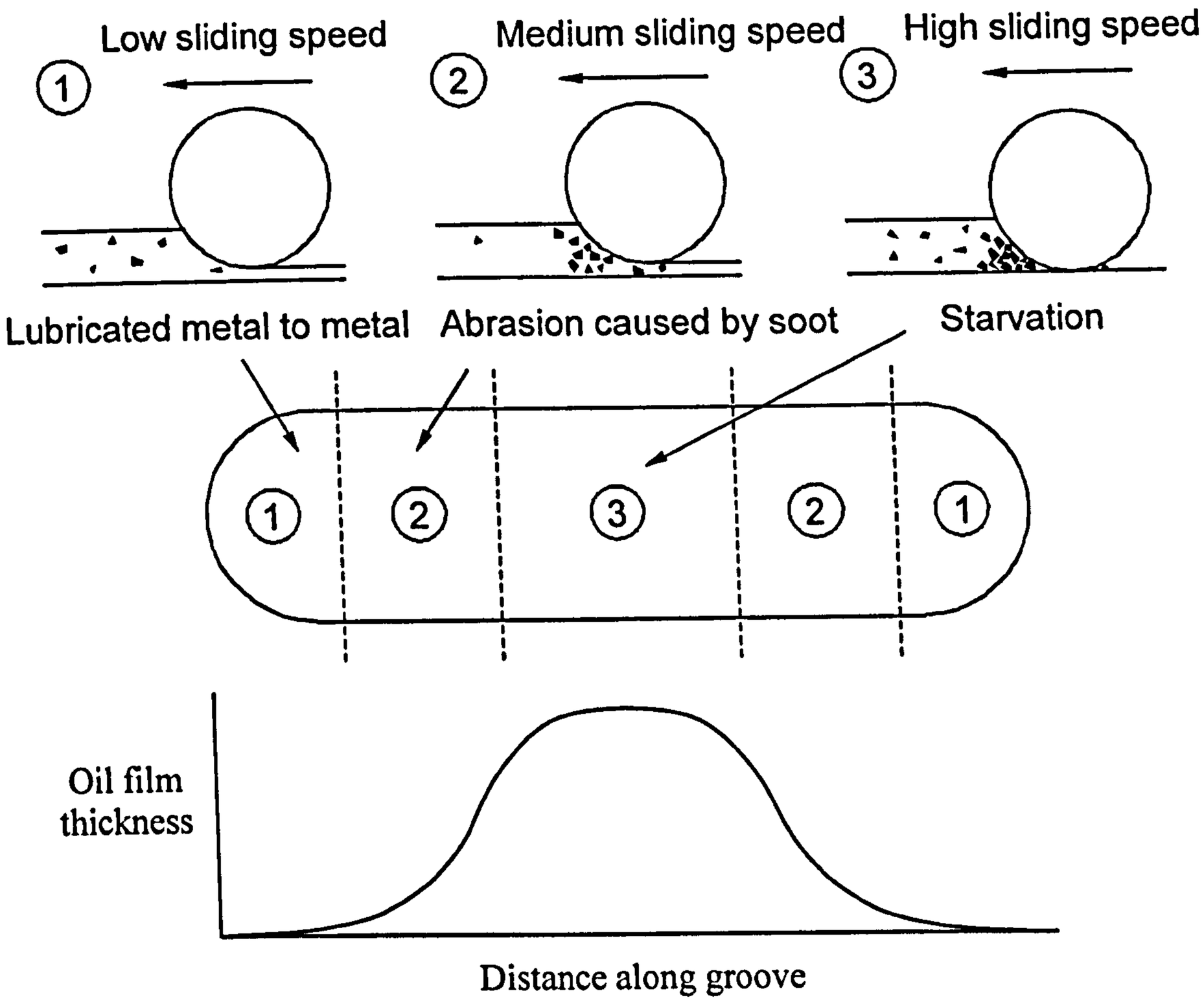

Figure 7.1. A Schematic of the Wear Mechanisms at a High Carbon Black Contamination Level.

The combination of all of the data presented in Chapters 4, 5, 6 and the above discussion provide an understanding of why soot contamination significantly increases wear in certain engine contacts and will cause a decrease in engine efficiency due to increased friction.

The viscosity, friction and traction coefficient measurements combine to demonstrate the significance of the contact type and the lubrication regime within which the contact is operating. The results show that reciprocating contacts operate under the boundary lubrication regime, where an increase in viscosity should cause a decrease in friction, but due to the interaction of the carbon black particles the friction increases, probably due to a breakdown in the lubricant film. This breakdown of the oil film was seen clearly in the visualisation tests (Section 6.5), where just 0.5% of carbon black present in a lubricant significantly disturbed the lubricant flow into the contact region. In continuously sliding contacts, where lubricant is entrained into the contact to produce a partially lubricated or elastohydrodynamic lubricant oil film, the carbon black particles should not affect the contact, as the main factor should be the lubricant's viscosity. Under these lubrication conditions an increase in viscosity should cause an increase in friction (traction), depending on its location on the Stribeck curve. This increase in friction does occur as predicted, but the increase is minimal when compared to the reciprocating contact results.

These results demonstrate the importance of the type of contacts used in engines to minimise the effects of soot contamination of engine lubricants. Contacts operating in

the boundary lubrication region of the Stribeck curve suffer significantly from contaminated lubricants, whereas contacts that operate in the partially lubricated or elastohydrodynamic lubrication region of the Stribeck curve are less prone to the effects of contaminated lubricants. This is shown on a schematic of the Stribeck curve in Figure 7.2, where zone A, the boundary lubrication region, indicates the region in which contacts are significantly affected by soot/carbon black contaminated lubricants. Zone B is the mixed or EHD lubrication region where, due to the increased oil film thickness, contacts show much less susceptibility to lubricant contamination. Finally, there is zone C relating to hydrodynamic lubrication, where although no testing has been performed in this lubrication regime for this body of work, it is commonly accepted that in this region, the lubricant oil film thicknesses are relatively very thick, and the viscosity of the lubricant dominates, therefore such contacts will suffer significantly from reduced efficiency due to the increased viscosity of soot contaminated lubricants. These effects also relate to the wear of the components operating under the different lubrication regimes. An investigation by Nagai **[17]** shows that certain reciprocating valve train components (rocker arm tip) suffer greater wear than contacts relating to components with a much longer reciprocating stroke such as the cylinder liner or valve stems and guides, these are more likely to operate within the mixed lubrication regime. The MTM testing demonstrated that continuously sliding contacts improve the lubrication conditions in the contact (compared to a reciprocating contact), reducing the effect of contaminants, therefore in an engine journal bearings on camshafts and crankshafts should be less prone to soot related wear and increases in friction.

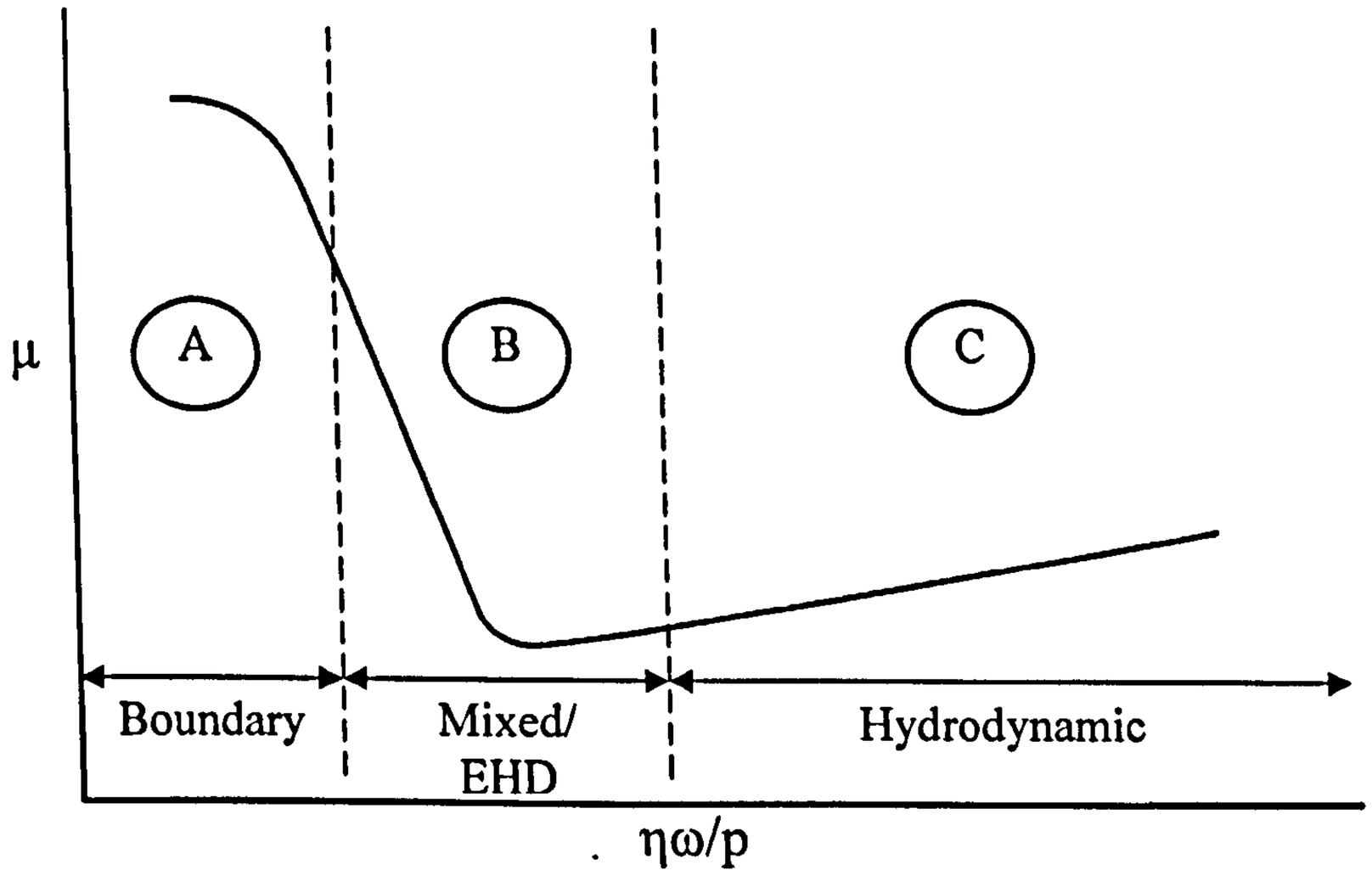

Figure 7.2. Schematic Diagram Demonstrating the Different Lubrication Regions of the Stribeck Curve and How They are affected by Soot Contamination.

The combined effect of all of the results discussed relating to soot contaminated contacts will have the effect of reducing total engine efficiency due to increased contact friction and the breakdown of lubricant films by the soot particles, having a negative impact on the lubrication regime within which the contact is operating.

7.5. WEAR MODEL

Wear models are extremely useful for engine designers as measured wear data in various specimen testing conditions can be related to another geometrical condition to understand impact of different designs.

Using the Archard wear equation **[80]**, wear coefficients can be calculated for each of the test conditions with the ball on flat testing, with base and formulated oils, using the following dimensionless equation:

$$K = \frac{VH}{PL} \tag{7.1}$$

where K is the dimensionless wear coefficient, V is the wear volume, H is the surface hardness, P is the applied load and L is the total sliding distance.

The wear coefficients are shown graphically in Figure 7.3 for the base oil wear testing and in Figure 7.4 for the formulated oil wear testing. Wear coefficients are an extremely useful method of categorising wear for a particular situation into a standard format. Such wear coefficients can be applied to current wear models to increase the accuracy of wear predictions.

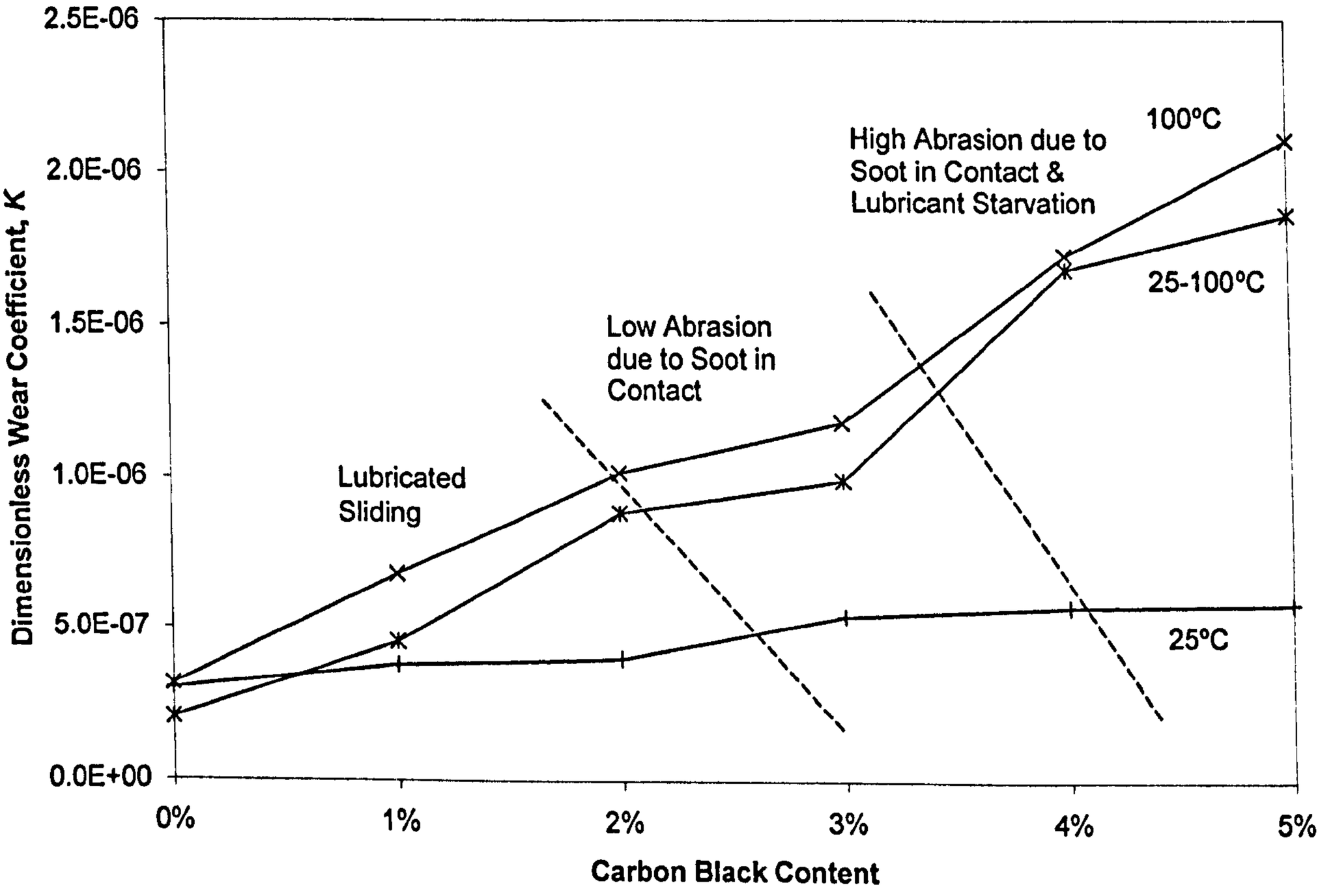

Figure 7.3. Wear Levels Plotted as Wear Coefficient against Carbon Black Content for Base Oil Tests. (Wear Mechanism Regimes are Indicated)

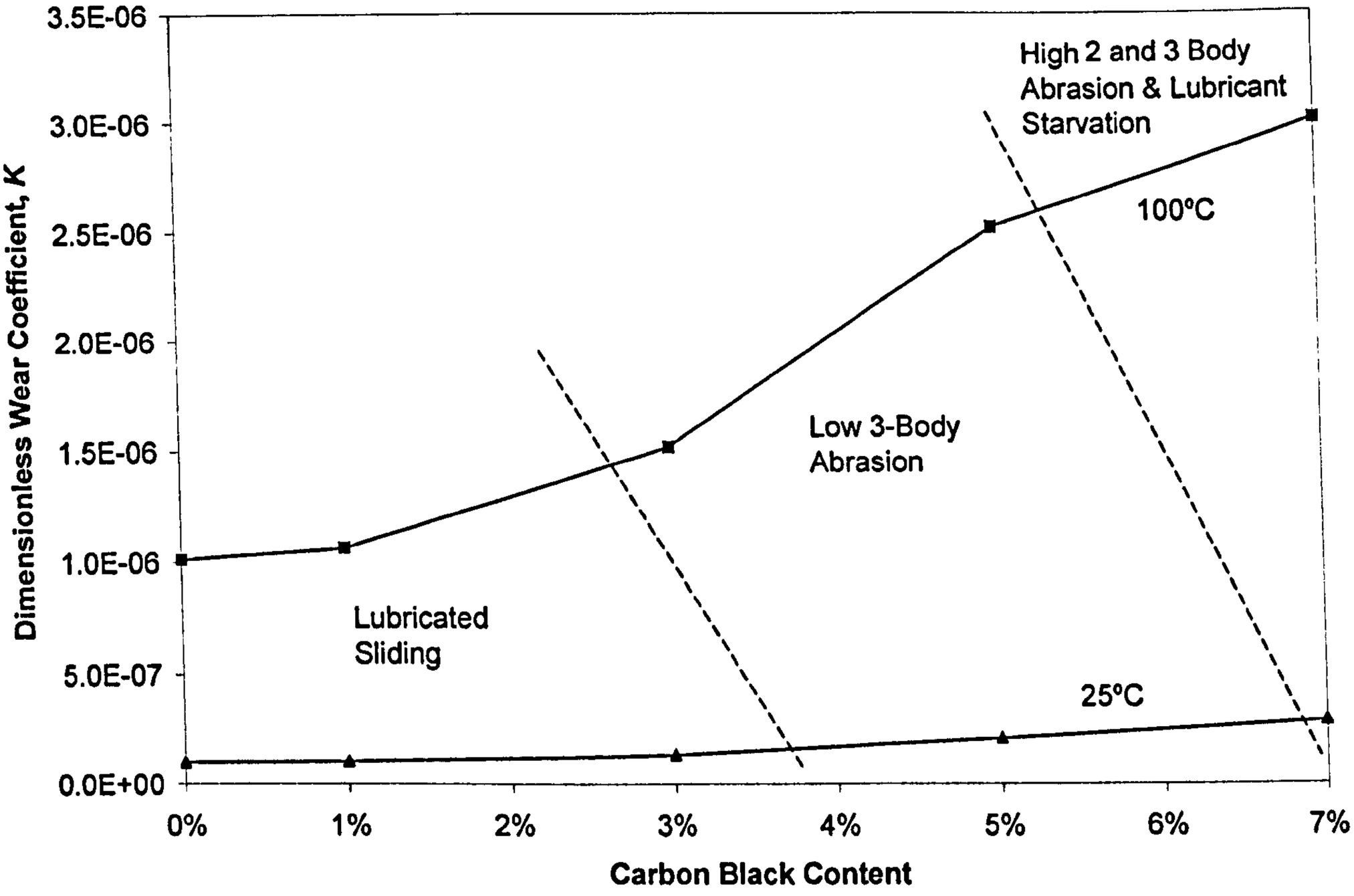

Figure 7.4. Wear Levels Plotted as Wear Coefficient against Carbon Black Content for Formulated Oil Tests. (Wear Mechanism Regimes are Indicated)

The coefficients detailed in Figures 7.3 and 7.4 compare favourably with previously measured wear coefficients by Rabinowicz [80]. The results are within the region of excellent lubrication for identical metals and 2 and 3 body abrasive wear. The distinct regions of the wear mechanisms highlighted earlier are highlighted as three regions in Figures 7.3 and 7.4, giving an indication of wear regimes.

To make such wear coefficient data useful, further testing is required to understand the effects of different contact and lubrication conditions, as well as differences in material too. Once enough data is available a detailed wear model can be developed.

7.6. FUTURE WORK

The work from this study has highlighted many areas of interest and situations where soot contamination of lubricants affects the normal operation of the lubricant and the related contact. Future possible areas of research are discussed below.

7.6.1. Types Of Carbon Black And Soot

Various types of carbon black are available (as discussed in Chapter 2), but it is believed that between the different types commercially available with similar chemical contents as actual engine soot, very little difference would be noticed through testing of bulk lubricant properties and wear. The majority of industries interested in the problem of soot wear understand that carbon black is a practical and

reliable alternative to actual engine soot, but to influence others, testing with actual engine soot may be required.

7.6.2. Lubricants And Additives

The wear testing carried out in this body of work has set a baseline for the amount of wear produced with base oils and formulated lubricants, further developments in lubricant technology to minimise the effects of soot related wear could be tested using the same approach.

Further testing using base oil mixed with various additives, especially Zinc dialkyl dithio phosphate (ZDDP) with this testing method would increase knowledge even further. Other future lubricants and additives that would need to be tested include fully synthetic lubricants (including lubricants produced from biomass), as well as new organic additives (developed to reduce the environmental impact of additives, which is currently quite significant).

7.6.3. Standardise Testing Method

The high frequency reciprocating rig designed and built for this work as well as the testing method that was devised, have proven to be reliable and produce repeatable data. It would therefore be ideal as an international testing standard to allow ranking and further wear testing of new lubricants. As it is well understood that excessive component wear in engines leads to inefficiencies, increased fuel consumption, increased emissions and ultimately failure, such a test would place further limits on lubricant standards and help to reduce total engine wear and minimise it effects.

7.6.4. Relation To Fuels

The first impact of fuel on this issue is fuel dilution lubricants, which is quite significant in the region of the combustion chamber. When a lubricant is diluted with some fuel, one of the most significant effects is that the viscosity will be decreased, leading to a thinner oil film, which will in turn lead to increased component wear.

The second fuel related effect is that of new fuels to come on the market in near future, most significantly of all being biofuels (specifically biodiesel). As mentioned in Chapter 2, such fuels have been shown to produce soot in similar quantities as current diesel fuels. This may mean that the effect of it may be the same as with current diesel fuels, but further analysis is required as to whether the composition and structure of the soot produced by new fuels, to see if this is true.

7.6.5. Test Materials

The work in this study has focused on steel contacts as it is currently the main material used in engine valve trains. There is increasingly a trend of using lighter weight materials, such as aluminium and plastic, some of these materials also provide

a significant cost saving. Another material that is seeing an increased use is PTFE as a seal around shafts, or on various low load contacting components to reduce friction.

These materials are also known to be susceptible wear, due to high ductility and low strength. Plastics and PTFE are also prone to degradation when in contact with oil and some PTFE shaft seals have failed due to excessive levels of soot content in the lubricant. Therefore specimen testing with such materials would add significantly to this body of knowledge.

7.6.6. Test Contacts

Although all of the wear testing has centred on short stroke reciprocating wear testing (operating under boundary lubrication), some of the analysis in Chapter 4 demonstrated that contacts with EHD lubrication would provide very different results. Therefore to carry this out longer stroke reciprocating test could be carried out, as well as wear testing with a continuously formed EHD oil film, this would be possible in an MTM testing machine. Further testing could also be performed with hydrodynamic oil films to investigate if viscosity is the only effect on the efficiency of such a contact and if contaminants have any effect on wear

7.6.7. Component And System Testing

Along with a full understanding of the wear that occurs with various lubricants and additives, relationships to various fuels and test materials and contacts, this knowledge needs to be expanded through testing of more engine components under similar test conditions to the specimen tests, to provide a realistic comparison.

The next step after specimen and component testing to provide increased understanding, would be system testing, with possibly a valve train system to measure the differences in efficiency due to different levels of soot contamination. Through such testing a relationship between soot contamination and differences in engine BMEP could be measured. From this improvements in efficiency could be gained through advances in engine design.

7.6.8. In-Cylinder Testing

One final area of the engine which suffers significantly from soot related wear is the in-cylinder region. This area suffers high wear due to the high concentration of soot present; it is also the region where soot and lubricant mix in the first place. Analysis of this area is possible through a long stroke reciprocating rig, which can test a piston to cylinder wall arrangement to analyse wear. Analysis of the flow of lubricant and soot in this contact can be measured with the cylinder wall replaced with a transparent material, such as Perspex or glass.

CHAPTER 8:

OIL FILM THICKNESS MEASUREMNT OF A PISTON - INTRODUCTION

The chapter presents a novel method for the measurement of lubricant film thickness in the piston – liner/cylinder wall contact. Direct measurement of the film in this conjunction has always posed a problem, particularly under fired conditions. The principle is based on capturing and analysing the reflection of an ultrasonic pulse at the oil film. The proportion of the wave amplitude reflected can be related to the thickness of the oil film.

8.1. INTRODUCTION

In-cylinder frictional characteristics are directly related to the regime of lubrication. This is governed by operating conditions and rheological properties of the lubricant. Sufficient separation of piston skirt and ring-pack from the cylinder wall reduces the frictional losses in an IC engine. It is reported that this accounts for nearly 40-50% of all such losses **[82]**.

Clearly, it is important to optimise the lubricant film formation to minimise friction and limit emissions. Therefore, design of piston skirt and rings to encourage lubricant entrainment into the contact are important criteria. Their axial profiles include chamfered edges or relief radii to create the necessary wedge effect for entraining of the lubricant with relative motion of surfaces. The material composition of the contiguous surfaces is also important, particularly encouraging localised deformation under load, enhancing the separation and inducing formation of a thicker coherent film **[83]**. Finally, cylinder bores or liners may be treated to provide lubricant retaining features. This promotes film by entrapment with cessation of entraining motion at dead centres, where there is no relative motion of surfaces.

With these considerations, numerical predictions indicate an improved regime of lubrication. However, it is necessary to ascertain the validity of these predictions through measurement of film thickness **[84, 85]**. This has proven to be difficult, owing to the inaccessible nature of the contact, as well as the inhospitable environment, particularly under fired conditions, especially at high speeds.

This section describes a new technique using ultrasonic pulses transmitted and collected via the use of an ultrasonic sensor, bonded to a wet cylinder liner to measure the transient variation in lubricant film thickness between the liner and the piston skirt in a fired engine. Further work is discussed which describes the building of a motored test engine and some preliminary tests to develop the measurement technique.

Film thickness measurement by ultrasonic reflection has previously been applied to steady-state operations in power station thrust bearings **[86]**, hydrodynamic journal bearings **[87]**, a rolling element bearing **[88]**, and a hydraulic motor piston ring/liner **[89]**.

The investigations, results and conclusions discussed earlier (Chapters 2 to 7); demonstrate that the condition of the lubricating oil significantly affects its behaviour. One area in the engine that is critical to engine efficiency and is responsible for highest proportion of mechanical power losses is the piston assembly **[90]**. Investigations by Nagai et al. **[17]** demonstrate that after the valve train, the piston rings and cylinder liner suffer the greatest level of soot related wear.

Several investigations have demonstrated that lubricant types and grades vary the piston ring to liner friction coefficient, therefore significantly affecting engine efficiency **[91, 92, 93]**. However these tests have been developed and extended to investigate lubricant condition **[94]**, demonstrating that used lubricants (produced by standard test procedures) compared with unused lubricants display a significant variation of friction coefficients. Neither the variation of soot content nor viscosity of the lubricants tested display any correlation to the resulting friction coefficient.

The previous investigations discussed above demonstrate that lubricant condition, properties and soot content affect lubricating film formation in the region of the piston rings. It is also considered a significant area to study as a detailed tribological understanding of the contact is required to minimise this component's effect on mechanical power losses and therefore increase total engine efficiency.

8.2. BACKGROUND

Understanding the lubrication conditions around the piston of an internal combustion engine has long been of interest as it significantly affects wear, friction and ultimately total engine efficiency. The measurement of the oil film thickness produced around the piston can assist the understanding. Oil films are thin compared with the geometry of the lubricated components, and frequently of a transient nature, this makes them hard to measure. The two main areas of interest are the piston ring pack region and the piston skirt area. The thinnest film thicknesses will be found where the piston rings contact the cylinder wall, but only over a small contact area. This area is designed to have a thin oil film thickness to minimise the amount of oil that passes into the combustion chamber, to reduce the level of hydrocarbon emissions. Secondly the piston rings against the cylinder wall should produce low friction, to increase engine efficiency. The piston skirt is designed to maintain piston stability and reduce the effects of piston secondary motion (manifesting itself as rapid lateral motion) and

piston tilt about the gudgeon pin. Piston secondary motion is due to combustion loading and connecting rod dynamics **[95]**.

Oil in the region of the piston provides two functions. Firstly the oil is required to act as a heat carrier to transfer heat away from the piston and the ring-liner contact to the oil sump/oil supply system. The second function is to provide mixed to hydrodynamic lubrication at the piston ring-liner contact zone contact. If an insufficient lubricating film is produced at the contact, excessive wear and friction will occur and potentially engine seizure.

Theoretically, a thicker oil film is produced by increasing engine speed or oil viscosity, or by reducing the temperature or piston ring to cylinder wall load (via cylinder pressure). The relative influence of each of these factors is currently not understood, as are the interacting effects of a fired engine. Some work has been published in this area, but with inconsistent results **[96, 97, 98, 99]**.

Various techniques have been used to attempt to measure the oil film thickness in the region of the piston, via electrical and optical methods.

One of the earliest electrical methods attempted was inductance **[100]**, but in recent years eddy current and capacitance methods have been developed. The eddy current techniques using eddy current displacement sensors has shown measurable differences of piston ring oil film thickness depending on varying load **[101]**. The capacitance method has since become the dominant electrical technique where oil film thicknesses are measured by the capacitance between to two non-contacting metal components (i.e. piston and liner/cylinder wall) separated by a dielectric medium (in this case lubricating oil). This technique has proved relatively successful **[102, 103]**. The most advanced capacitance based system has performed a series of oil film thickness measurements in a fired engine, under steady state conditions **[104]**.

Laser induced fluorescence (LIF) is the latest technique to be adopted, generally using tracer particles to detect the flow, distribution and film thickness of lubricant along and around the piston **[105, 106, 107, 108]**.

All of these test methods have been carried out on test rigs or motored engines with some degree of success, but tests on fired engines prove to be extremely difficult and challenging due to test parameters and engine operating conditions, particularly electrical interference due to the engine's injection and ignition systems. One other major disadvantage of the techniques previously used are that they are all invasive, involving considerable set-up work, but also the possibility that the addition of sensors and modifications may affect the resulting oil film thickness.

One factor that may affect the ability to take oil film thickness measurements and the quality and reliability of those measurements is the oil quality at the measurement location. Oil in the region of the piston rings is significantly more contaminated than oil in the oil sump or tank **[109, 110]**. This is purely due to its proximity to the combustion chamber where most contaminants are produced.

Previous measurements and predictions indicate oil film thicknesses in the region of the piston rings to be less than 10μm, generally with a minimum of 1μm **[93, 104,**

107]. On the piston skirt oil film thicknesses vary from approximately 1μm up to approximately 150μm **[111, 112]**.

8.3. REFLECTION OF ULTRASOUND FOR A LAYER

This section describes the theory of the ultrasonic method for measuring oil film thickness. The ultrasonic technique has the advantage that the sensors do not have to be mounted in contact with the oil film and can provide localised non-invasive measurements.

The measurement of the reflection of an ultrasonic pulse is the key principle of this measurement method. Figure 8.1 demonstrates that an incident pulse, *i*, is sent through material 1 (i.e. steel); if there is air on the opposite side of material 1, then due to the large impedance mismatch virtually all of the incident pulse is reflected, *r*. If however there is a second material (material 2) and a layer (i.e. oil) in contact with the opposite side of material 1, then depending on the relative impedance of the layer and material 2 a proportion of the incident ultrasonic pulse will be transmitted, *t*, and the remainder will be reflected, *r*.

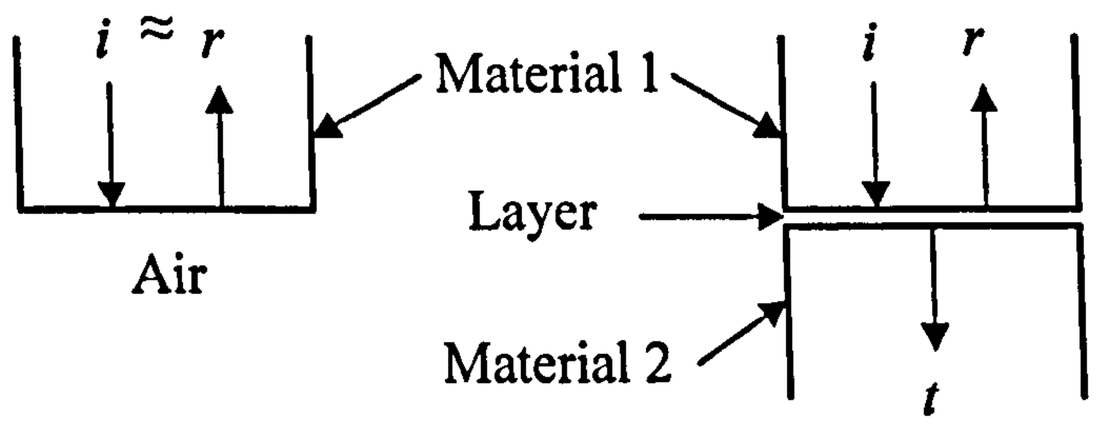

Figure 8.1. Demonstration of the reflection and transmission of an incident ultrasonic pulse.

In practice a piezoelectric sensor is coupled to the outside of a cylinder liner or wall. It is then used to generate ultrasonic pulses that propagate through the liner or wall. When the pulse strikes an oil film it is partially reflected and partially transmitted. The proportion that is reflected (known as the reflection coefficient, R) depends on, amongst other things, the thickness of the oil film. The reflection coefficient is calculated by dividing the reflected pulse amplitude (when two materials and a layer are in contact) by the reflected pulse amplitude, when material 1 is in contact with air alone (known as the reference pulse). The reflection coefficient, R can be expressed as the acoustic impedance mismatch between two materials.

$$R = \frac{z_1 - z_2}{z_1 + z_2} \tag{8.1}$$

where z_1 is the acoustic impedance of material 1 and z_2 is the acoustic impedance of material 2.

The response of a thin layer embedded between two media is governed by a quasi-static spring model **[86]**. If the embedded layer is very stiff then the ultrasound passes through, whereas if it is compliant then the wave is reflected. When the ultrasonic

wavelength is large compared with the film thickness (i.e. the low frequency regime), the analysis yields a simple relationship between the reflection coefficient and stiffness of the layer, *K*:

$$R = \frac{1}{\sqrt{1+\left(\frac{2K}{\omega z}\right)^2}} \tag{8.2}$$

Where ω is the angular frequency of the ultrasonic wave (=2 ω *f*), *f* is the frequency of the wave. The parameter *z* is the acoustic impedance of the material either side of the layer (the acoustic impedance is the product of the density and speed of sound in the medium). Equation (8.2) holds for the case when the materials either side of the layer have the same acoustic impedance. The stiffness of a liquid layer of thickness, *h* trapped between two flat surfaces and constrained laterally is given by:

$$K=\frac{B}{h} \tag{8.3}$$

where *B* is the bulk modulus of the liquid. The bulk modulus can be replaced by the speed of sound in the liquid, $c=\sqrt{(B/\rho)}$ where ρ is the density, to give:

$$K = \frac{\rho c^2}{h} \tag{8.4}$$

Combining Equations (8.2) and (8.4) leads to a simple relationship between the oil film thickness and the reflection coefficient, when the two materials either side of the layer are the same:

$$h = \frac{2\rho c^2}{\omega z}\sqrt{\frac{R^2}{1-R^2}} \tag{8.5}$$

Dwyer-Joyce et al. **[113]** have demonstrated that this relationship held for typical lubricant film thicknesses in the hydrodynamic and elastohydrodynamic regime.

The relationship between reflection coefficient and film thickness given by Equation (8.5) has been plotted in Figure 8.2, for a steel-oil-steel contact, using a calculation programme developed within the Tribology group at the University of Sheffield, based on the oil film thickness spring model relationship **[113]**. It can be seen that as the film thickness decreases, the reflection coefficient decreases as more of the wave is transmitted. The frequency axis relates to the frequency at which the ultrasonic transducer is pulsed.

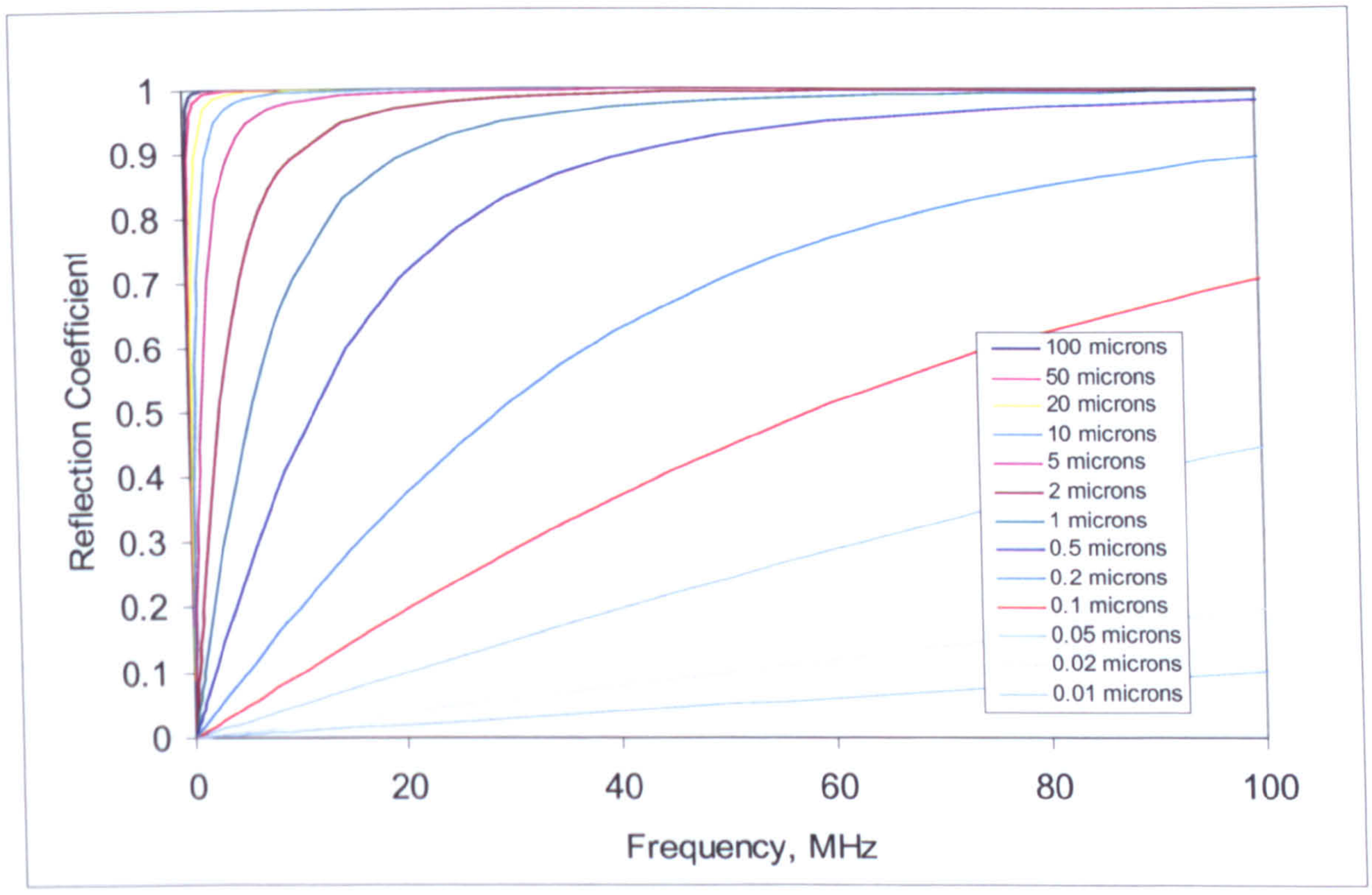

Figure 8.2 The response of a layer to an ultrasonic wave, for a steel-oil-steel system, according to Equation (8.5).

If the materials on each side of the layer are different, then Equation (8.6) must be used to calculate the oil film thickness, instead of Equation (8.5).

$$h = \frac{\rho c^2}{\omega z_1 z_2} \sqrt{\frac{|R|^2 (z_1 + z_2)^2 - (z_1 - z_2)^2}{1 - |R|^2}} \qquad (8.6)$$

The relationship between reflection coefficient and film thickness given by Equation (8.6) has been plotted in Figure 8.3, for a steel-oil-aluminium contact, using the same calculation programme as described above. It can be seen that the possible oil film thickness range has reduced because the minimum reflection coefficient value for a layer is equal to that given by Equation (8.1)

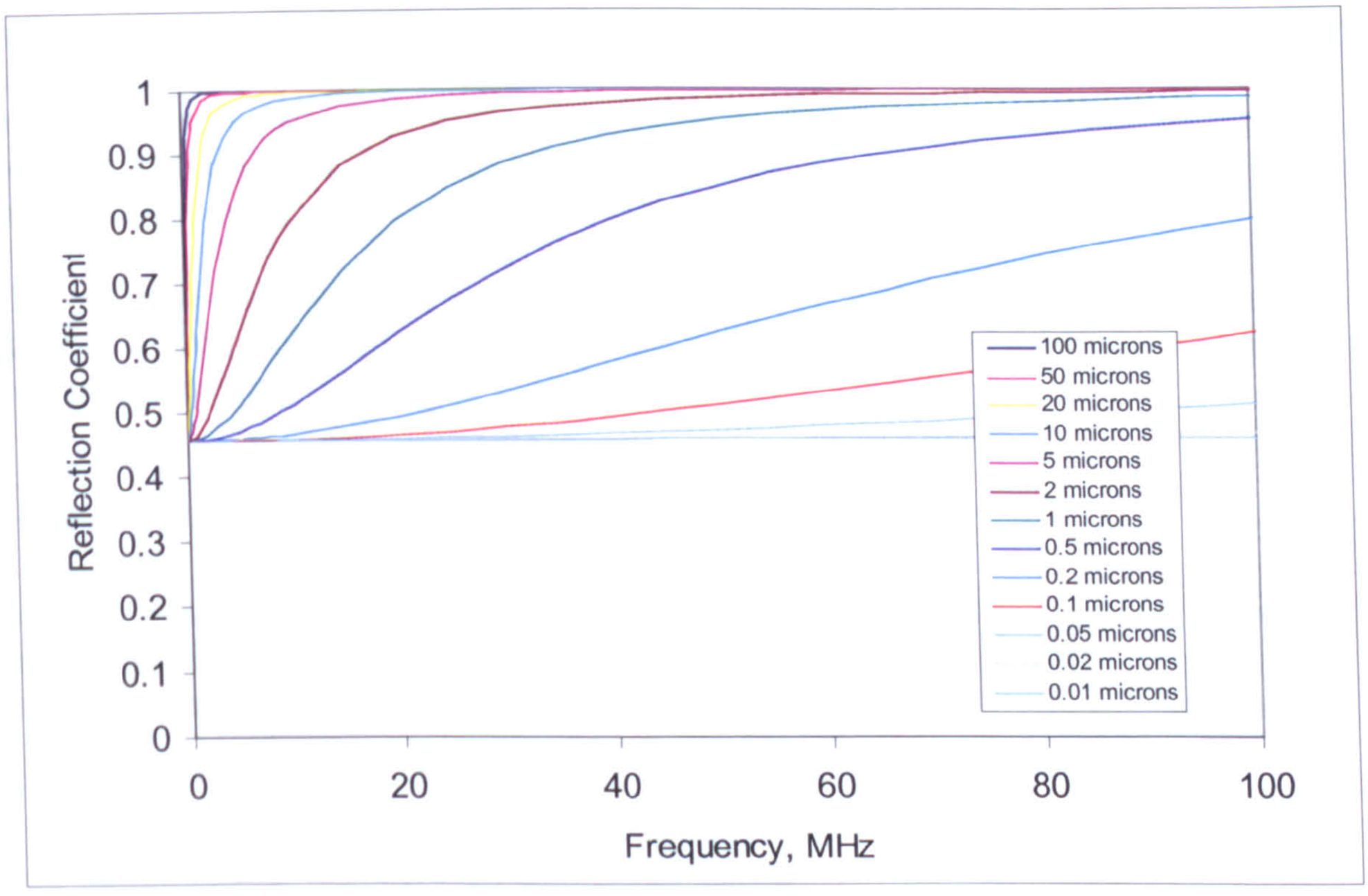

Figure 8.3. The response of a layer to an ultrasonic wave, for a steel-oil-aluminium system, according to Equation (8.6).

8.4. ULTRASONIC MEASUREMENT EQUIPMENT

A schematic of the apparatus is shown in Figure 8.4. The PC controlled ultrasonic pulser receiver (UPR) generates a series of short duration voltage pulses that excite the transducer to create an ultrasonic pulse. The pulses reflected back from the oil film, are received by the transducer, which in turn generate a voltage pulse that is received and amplified by the UPR. In this way, the transducer acts as both an emitter and receiver (i.e. pulse echo mode). The reflected signal is digitised on a storage oscilloscope and passed to a PC for processing. The PC performs the signal processing, and displays the results with software written in LabVIEW (from National Instruments).

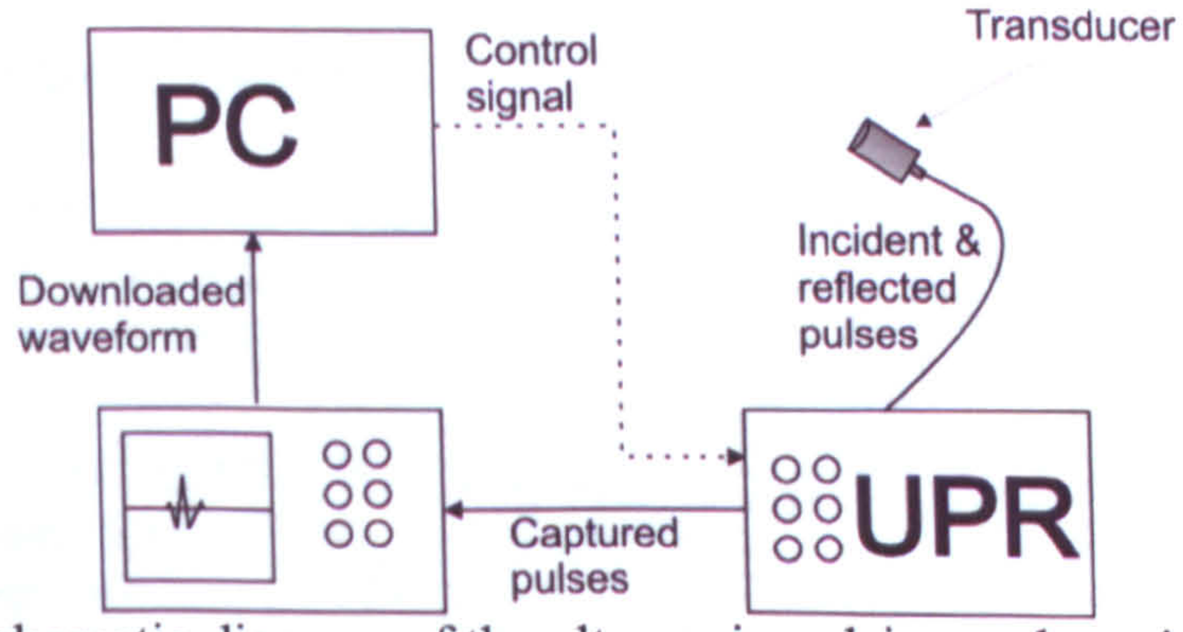

Figure 8.4. Schematic diagram of the ultrasonic pulsing and receiving apparatus.

A LeCroy LT342 oscilloscope is used to digitise and capture the received signal. In order to capture the waveforms at a high rate the onboard memory can be divided up into a number of segments. A segmentation technique on the oscilloscope allows the

user to select only the section of the waveform that is required, therefore allowing memory capacity for a series of sequential signals. At each trigger event the selected portion of the waveform is written to a segment. The trigger is provided by the UPR where a signal is sent to the oscilloscope at the same time as a pulse is sent to the sensor. Thus every signal from the pulser is written to the segmented memory.

The onboard memory of the oscilloscope was limited to 250k points. Thus the number of data points in each segment determines the number of segments that it is possible to capture.

8.5. ULTRASONIC TRANSDUCERS

Various types of piezoelectric transducer are available; the types of ultrasonic transducer that have been used in this are discussed below. Both commercially available sealed transducers and piezoelectric element transducers have been used.

8.5.1. Piezoelectric Element Transducers

Piezoelectric element transducers are bonded onto a flat surface; anode and cathode wires are soldered onto the relative points on the other face. A high frequency alternating voltage is fed the transducer, causing the piezoelectric material to vibrate, sending ultrasonic pulses through the material. Reflected pulses are received along the same wires. Figure 8.5 shows the relative size of a 10MHz element. These element transducers measure over the whole area of the surface meaning that the measurement is an average over that region.

Figure 8.5. Photograph of a 10MHz Piezoelectric Element Transducer.

8.5.2. Contact Transducers

Contact transducers are sealed commercial transducers, they operate in essentially the same way as the piezoelectric element except they are insulated and therefore the signal is not affected by external electrical fields. The 5MHz transducer used for this work is shown in Figure 8.6. The contact transducer requires the signal face to be in direct contact with the region of interest, and a couplant, typically a gel is required to make a good contact between the probe and surface. Again as with the piezoelectric element transducers, the measurement is an average of the whole contact region.

Figure 8.6. The Contact Transducer.

8.5.3. Focusing Transducers

The second commercial variety of ultrasonic transducer used for this work is the focusing transducer. The focusing transducer does not directly contact the test surface, but is positioned a specific distance away from the test surface. The test surface and transducer need to be submersed in a water bath, for focusing of the ultrasonic signal, as shown in Figure 8.7.

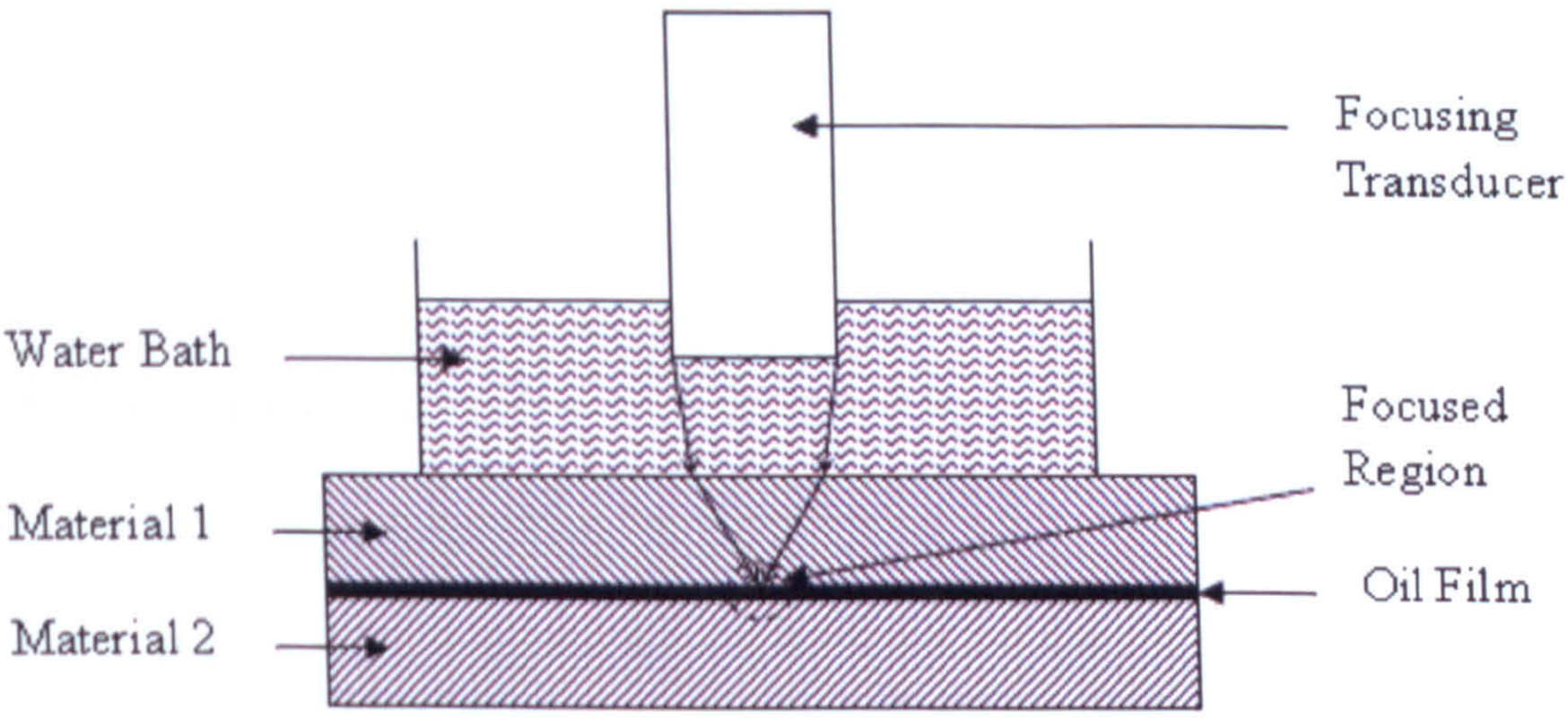

Figure 8.7. Schematic of Focusing Transducer Set-up.

Focusing transducers allow for a very small focal region, or spot size, meaning it is ideal for analysing very small contact zones. The diameter of the focal spot is determined in terms of bandwidth using the following empirical relationship **[114]**:

$$Spotdiameter(-6dB) = 1.025\frac{l_w c_w}{f d_c} \tag{8.7}$$

where the amplitude drops 6dB below the maximum, c_w and l_w are the speed of sound and the focal length of the transducer in water respectively and d_c is the diameter of the piezoelectric element of frequency f.

CHAPTER 9:
OIL FILM THICKNESS MEASUREMENT IN AN ENGINE

Using a single cylinder 4-stroke engine on a dynamometer test platform (based at Loughborough University) an initial attempt to apply the ultrasonic oil film thickness method was tried. A piezoelectric transducer was bonded to the outside of the cylinder liner and used to emit high frequency short duration ultrasonic pulses. These pulses were used to determine the oil film thickness as the piston skirt passed over the sensor location. Oil films in the range 2 to 21μm were recorded varying with engine speeds. The results have been shown to be in agreement with detailed numerical predictions.

9.1. APPARATUS

9.1.1. Engine And Dynamometer Test Bed

The test engine was a liquid-cooled, 449 cm^3 4-stroke 4-valve single overhead-camshaft single cylinder engine. It produced 41 kW at 9,000 rpm, and was resisted by a transient A/C dynamometer (see Figure 9.1). The stroke was 64 mm and the bore diameter was 96 mm. The nominal skirt clearance was 150μm. The barrel of the engine was adapted to accept wet liners as shown in Figure 9.2, on which an ultrasonic piezoelectric element transducer was bonded. The liner and piston body were manufactured from aluminium, and the piston rings from steel. A TDC pulse obtained from a digital rotary encoder was used to align the measurements from the ultrasonic transducer to the position of the engine, when processed in the data acquisition system.

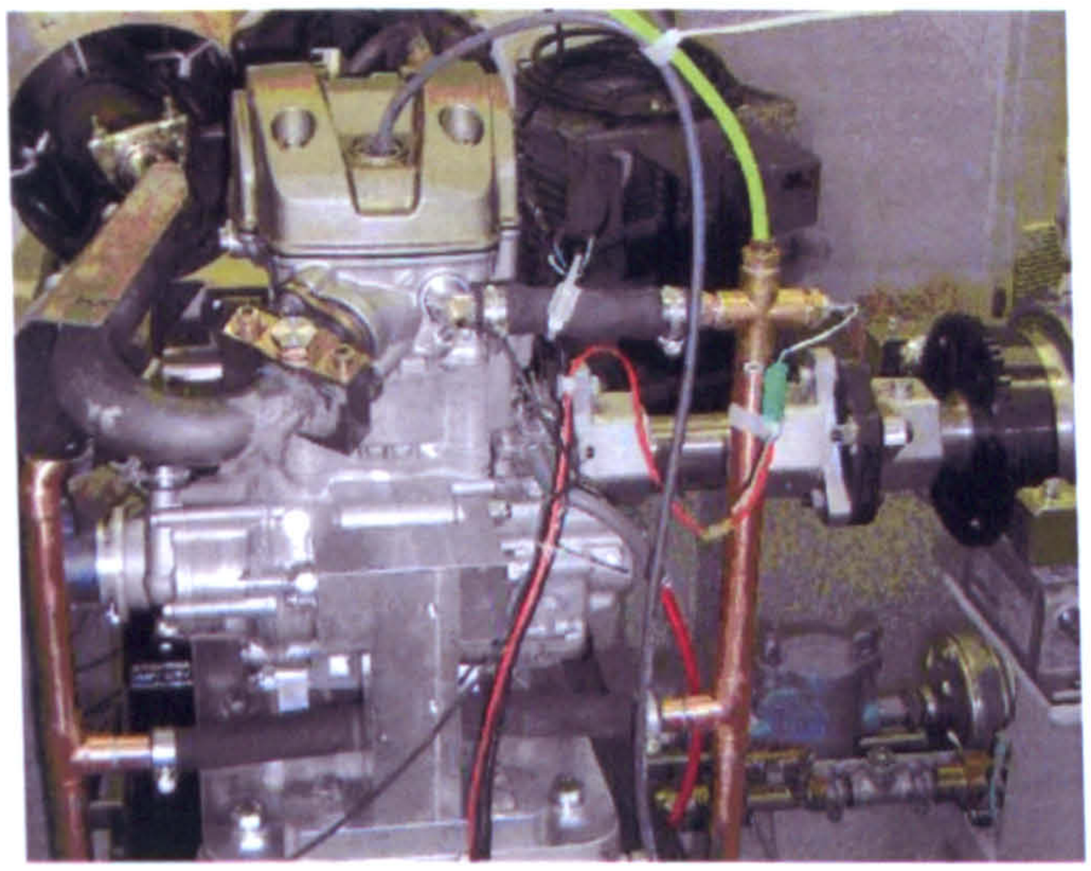

Figure 9.1: Single cylinder test engine

9.1.2. Ultrasonic Measurement Equipment

A 10 MHz piezoelectric element transducer was adhesively bonded to the outer face of the cylinder liner. The location of the transducer was such that it was coincident with the piston skirt whilst the piston was at top dead centre as shown in Figure 9.2. The transducer was a thin element of piezoelectric material of diameter 7mm and thickness 0.2mm with 'wrap-around' electrodes i.e. the top face had a bonded electrode, the bottom (contact) face electrode was wrapped over to the top face. Two wires were soldered directly to these electrodes on the top face. The wires were fed out of the liner through the water jacket to an ultrasonic pulser-receiver (UPR).

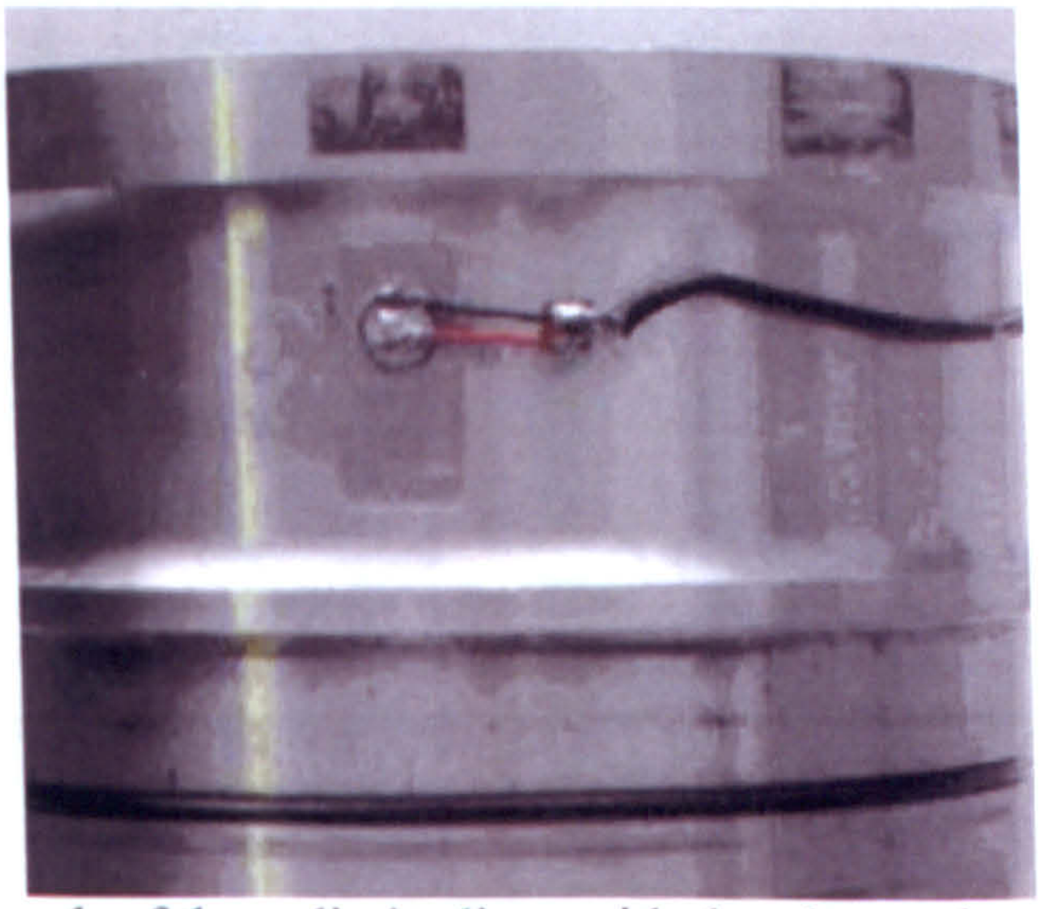

Figure 9.2: Photograph of the cylinder liner with the ultrasonic transducer bonded to the outer face.

Using the segmentation technique (described in Chapter 8) the internal memory of the oscilloscope (250kbytes) was used to capture a series of reflected signals. During testing the number of points per segment was set at 1000, resulting in 250 pulses captured per capture cycle.

The sensor was pulsed off its natural frequency (equivalent to 5.6 MHz rather than 10 MHz) to produce as short a pulse as possible. As a result the maximum pulsing rate was limited to 5 kHz. However, if a higher frequency sensor was used, a pulsing rate of up to 10 kHz could have been achieved. The oscilloscope has the capability to capture at up to 200 kHz.

9.2. METHOD

A pulse was recorded from a reflection from the internal liner face when the piston was remote from the sensor location. This pulse was reflected from a liner-air interface. This reflected pulse was then equal to the incident signal (since a wave is almost completely reflected at a solid-air interface) and was recorded as the reference signal. When the engine was operating (either motored or fired) measurements were taken in a similar fashion directly into the oscilloscope's internal memory and processed at a later time. Figure 9.3 shows a pulse reflected back from liner-air and liner-oil film-piston skirt systems. The measurement pulse is reduced in amplitude because part of the wave has been transmitted through the oil film to the piston.

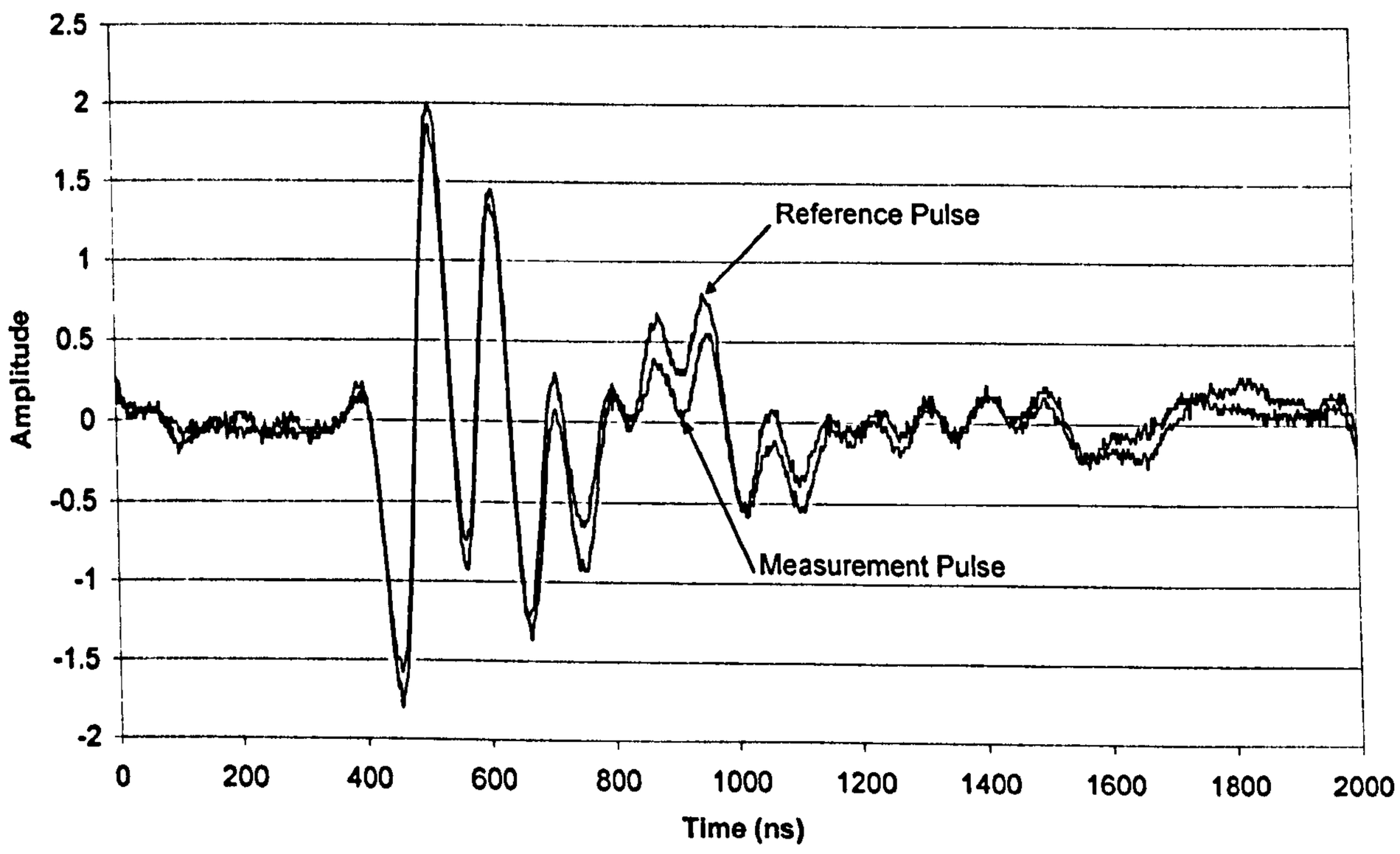

Figure 9.3. Sample pulses reflected from a liner-air interface and a liner-oil film-piston skirt interface.

The next step was to pass the reference signal and reflected pulses through a fast fourier transform (FFT) to give an amplitude spectrum. Figure 9.4 shows the data of Figure 9.3 as amplitude spectra. This data demonstrates that the centre frequency of the probe was 3 MHz. The figure also shows that the transducer has useful energy in the range 2 MHz to 4 MHz. Dividing the oil film pulse by the reference pulse gives the reflection coefficient, as shown in Figure 9.5 for a series of oil films, where the different curves represent different engine conditions and hence film thicknesses.

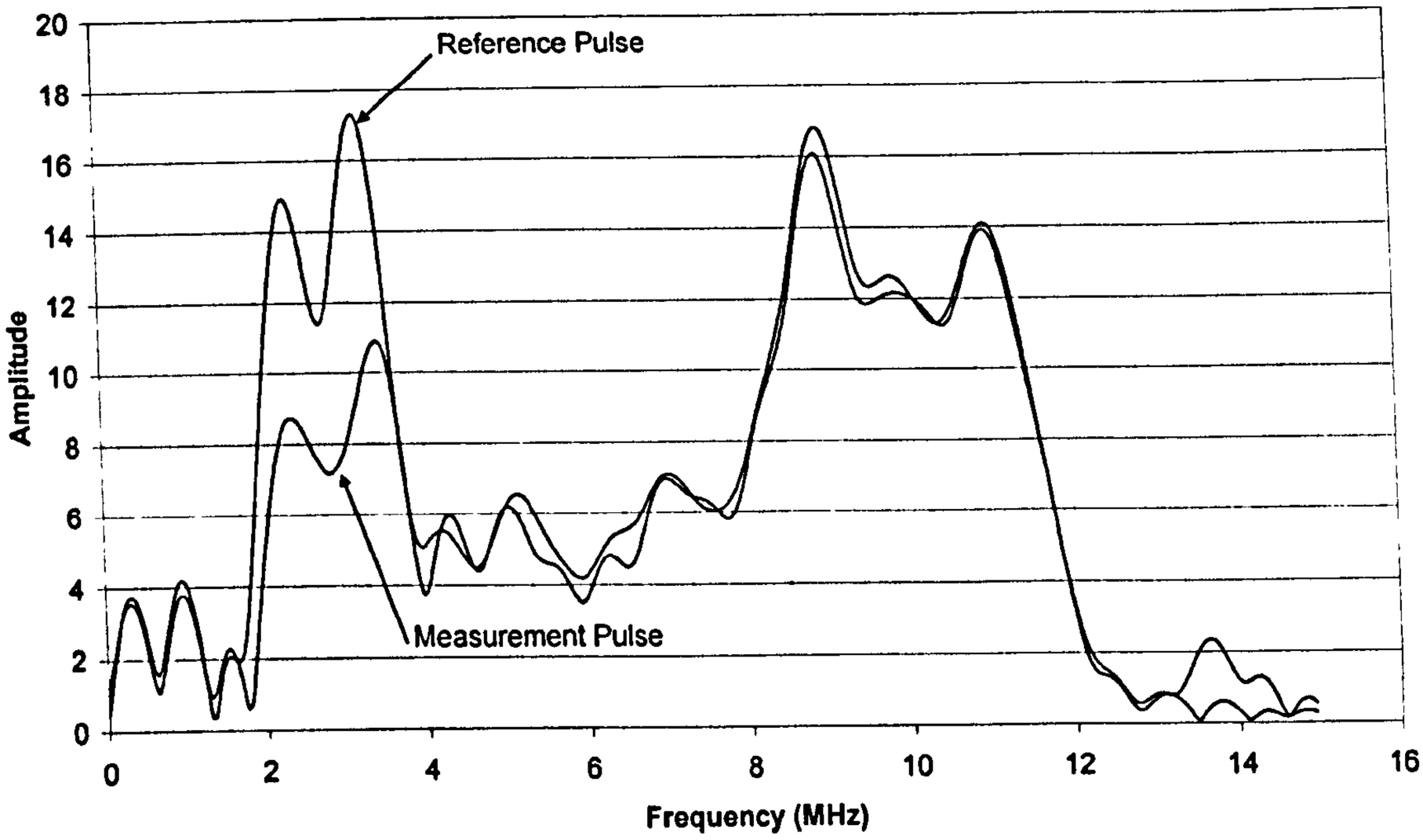

Figure 9.4. Amplitude spectra for the pulses of figure 4 obtained by performing a fast Fourier transform (FFT).

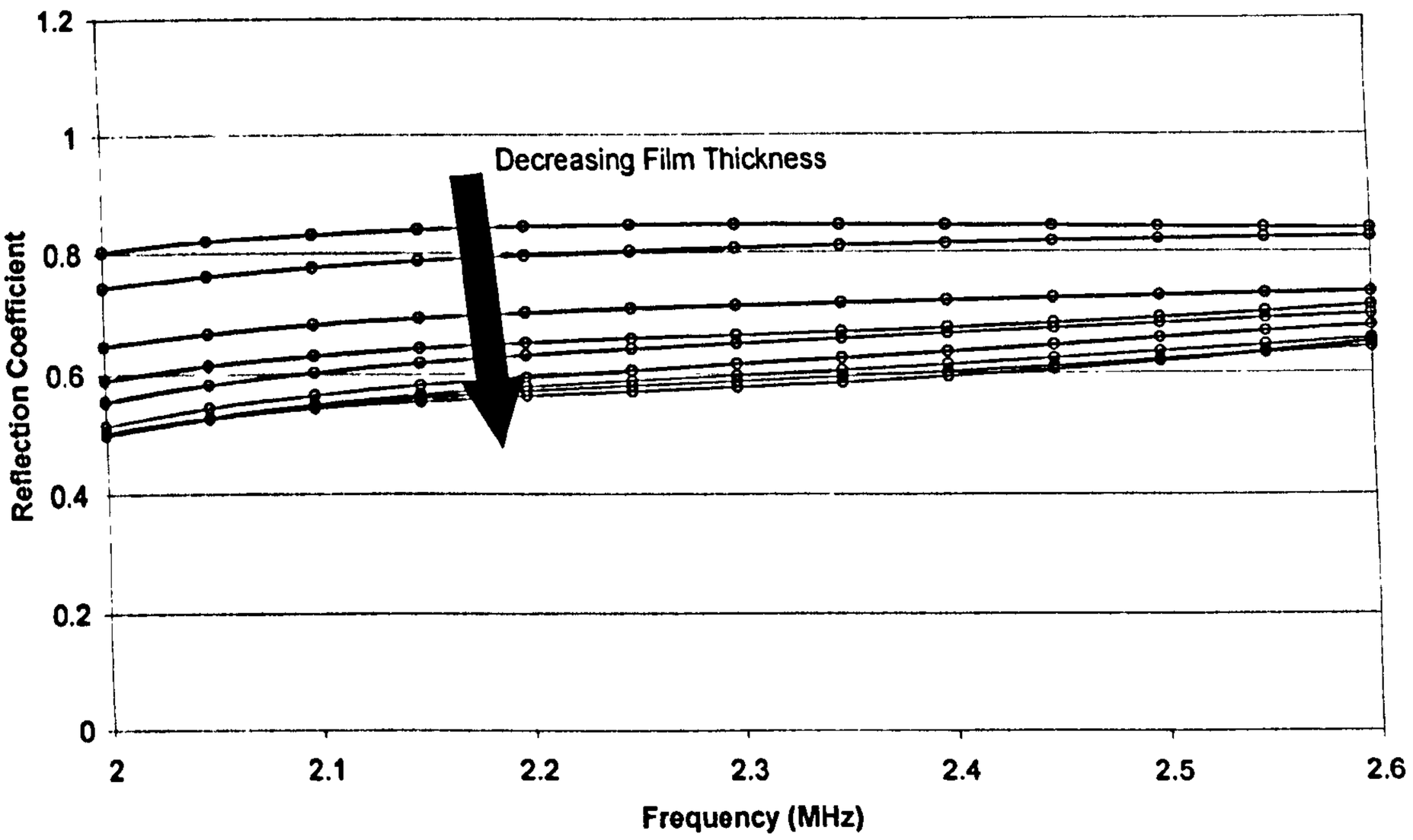

Figure 9.5. Reflection coefficient spectra (obtained by dividing the oil film FFT by the reference FFT).

In principle the reflection coefficient at any of the frequencies shown in Figure 9.5 can be used to determine the film thickness using Equation (8.5), provided it is within the bandwidth of the transducer. Typically the film thickness is determined over a range of frequencies and a mean presented.

9.3. RESULTS

9.3.1. Motored Tests

To demonstrate how the ultrasonic transducer resolves the lubricant film thickness, a series of motored tests were carried out initially. Figure 9.6 shows a typical measurement of the reflection coefficient recorded as the piston passes the sensor location (recorded at a motor speed of 850 rpm).

Zone A appears to represent the piston wall area above the ring zone, demonstrating that an oil film is produced in this region, but the reflection coefficient rapidly becomes unity as the piston ring zone approaches the measurement region. The measurement is significantly affected because the piston rings are manufactured from steel, and as discussed in Chapter 8, dissimilar materials impose limitations on the possible measurements.

Zone B therefore corresponds to the passage of the piston rings, where very little or no measurement of oil film was recorded. This is again due to the measurement limitations due to dissimilar materials, but also due to the fact that the piezoelectric element transducer averages over its whole contact zone.

Zone C represents the piston skirt passing the transducer, where a clearly progressing oil film thickness measurement is achieved as the piston passes the transducer. At approximately the mid point of zone C top dead centre appears to occur and the piston returns down the cylinder.

Minimum film thickness of 9.4 μm was recorded when at TDC. During the subsequent down-stroke the film thickness increases to 16.5 μm as the residual oil on the cylinder walls is entrained into the contact. Motored tests were performed at 850, 1800 and 6000 rpm. Figure 9.7 displays the increasing oil film thicknesses with increasing engine speed.

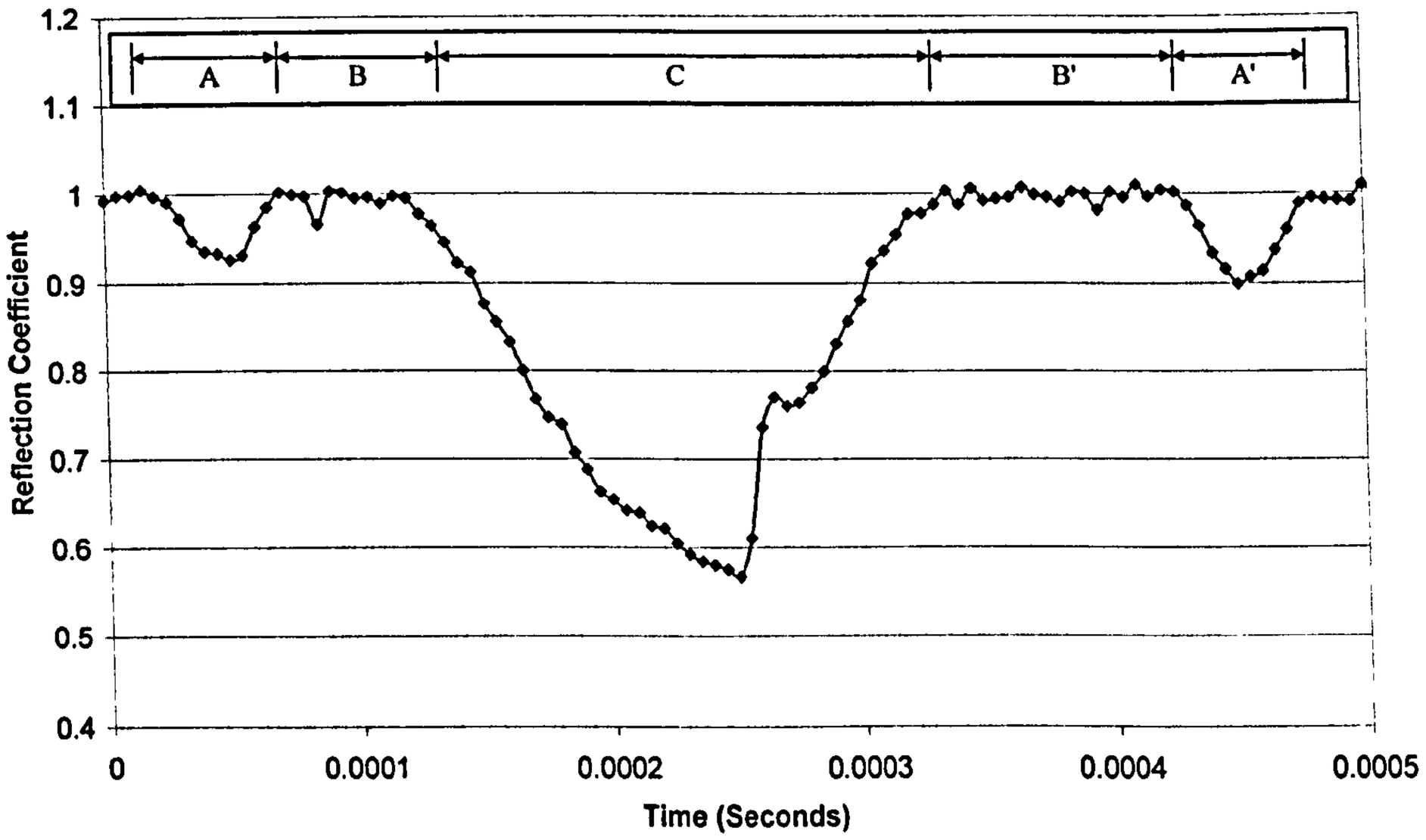

Figure 9.6. Plot of reflection coefficient recorded as the piston passes over the sensor location at an engine speed of 850 rpm.

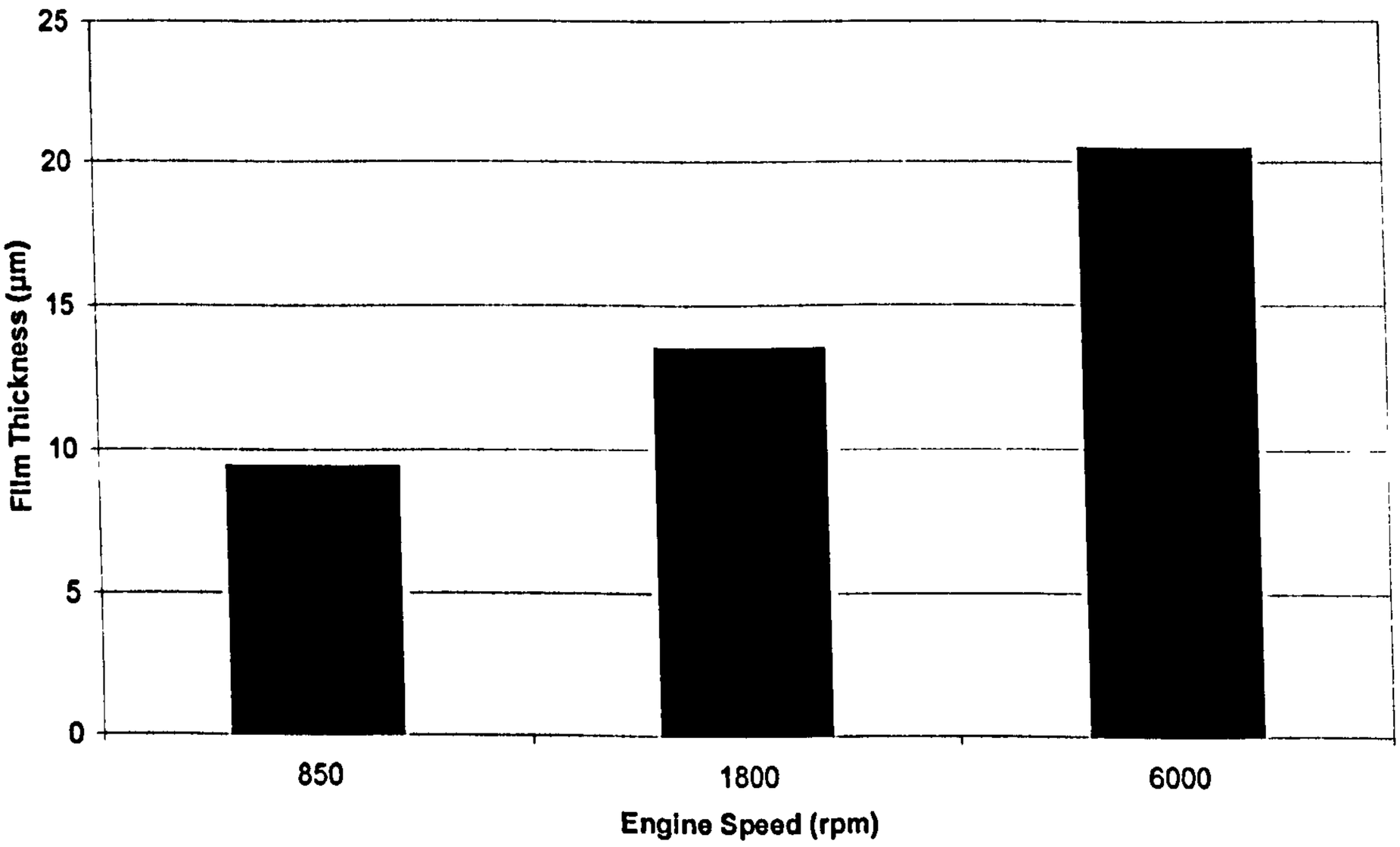

Figure 9.7. Measured liner – piston skirt oil film thickness for three motored engine tests.

9.3.2. Fired Tests

The engine was run at different speeds at wide-open throttle condition, fully resisted by the dynamometer. For each test, repeatable conditions were ensured by monitoring air-fuel ratio, test cell pressure, humidity, coolant, and bulk oil temperature. Figure

9.8 shows the approximate sensor location with respect to the piston skirt, where the TDC oil film thickness measurements occurred.

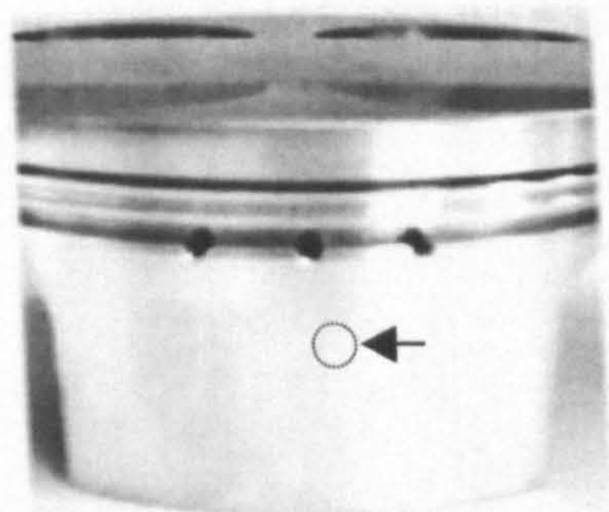

Figure 9.8. Approximate area where average film measured on the piston skirt indicated by the circle

Figure 9.9 shows the film thickness measured at the idle speed of 1800 rpm. The measurement is recorded as the piston skirt sweeps passed the sensor (from ~0.5 to 1μs) and then back again (from ~1 to 1.5μs). At this stage it is not possible to exactly match the film measurement with the piston skirt geometry, as the piston location is not exactly defined with respect to the sensor (TDC is approximately at 1μs on the plot). A minimum film of approximately 2μm is observed towards the end of the return stroke.

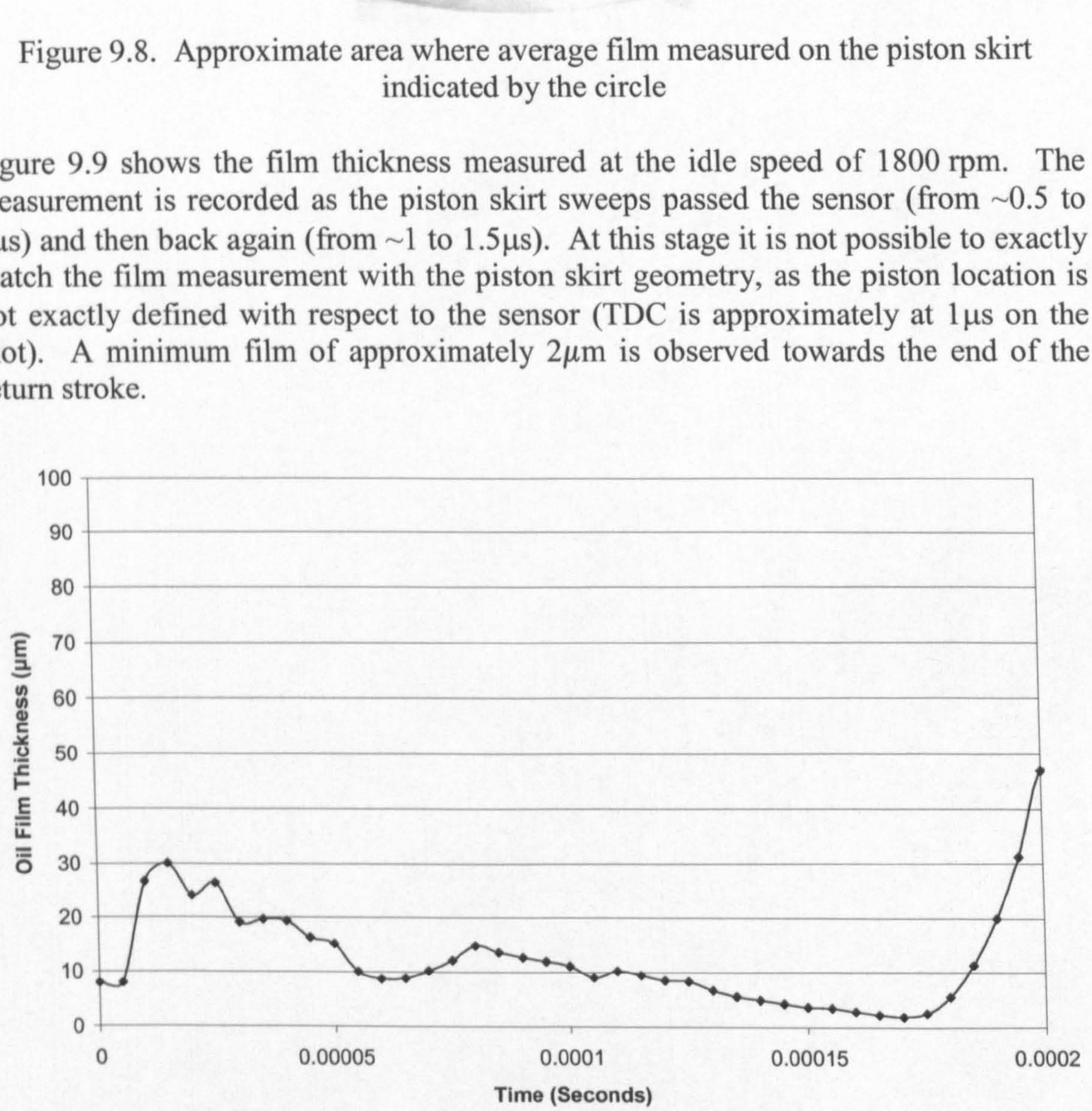

Figure 9.9. Plot of measured oil film thickness for a fired test performed at an engine speed of 1800 rpm.

Prior numerical results, based on transient analysis of piston-cylinder liner contact, reported by Balakrishnan et al **[115]** predicted a piston tilt of 0.085° with a side force of 4800N. Under these conditions the analysis indicates a minimum film thickness of 1.94μm (see Figure 9.10). Good agreement is observed between numerical prediction and measurement. Further validation could be obtained by measurements and modelling of the film at other locations on the piston stroke.

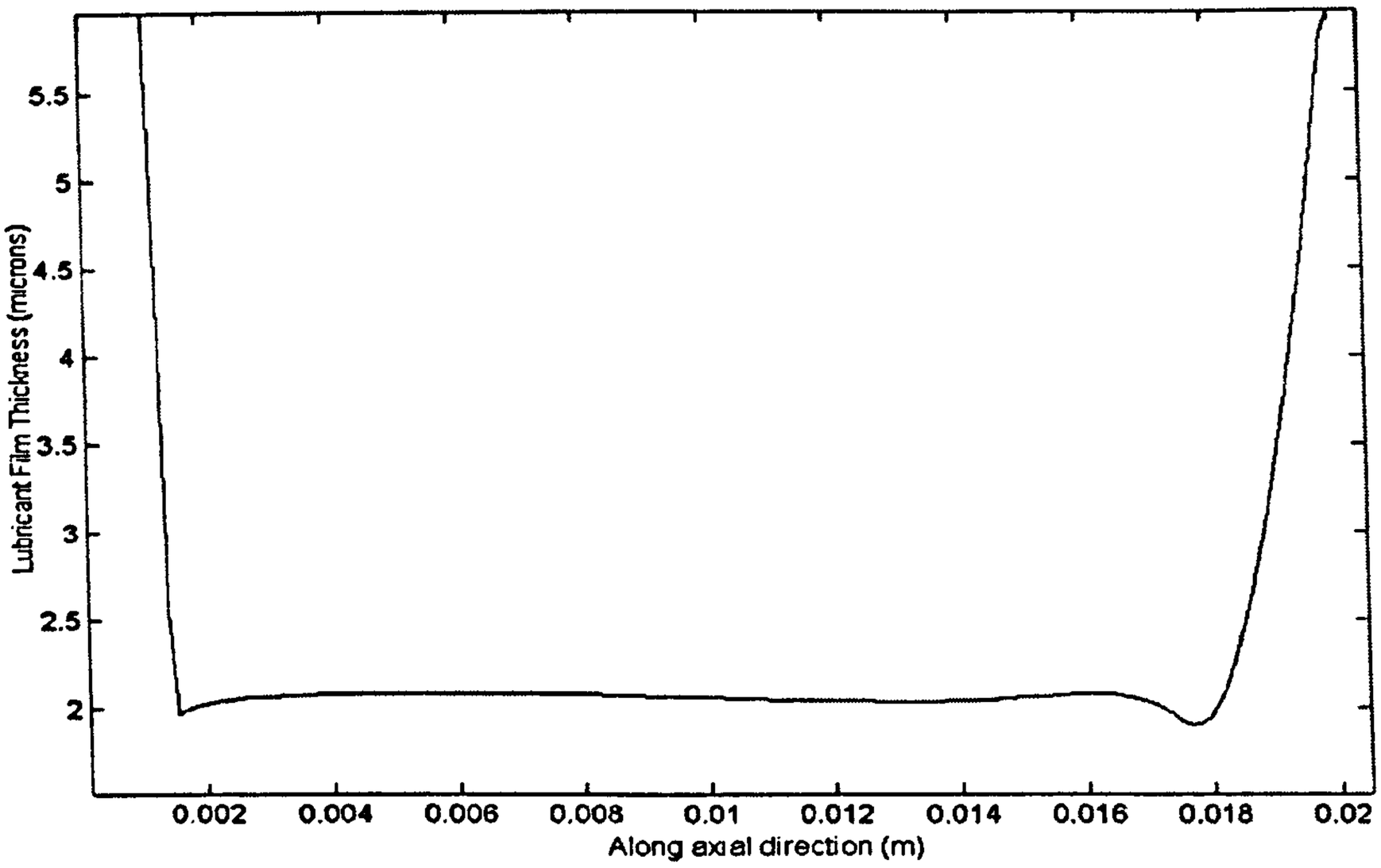

Figure 9.10. Axial lubricant film variation along the piston skirt at TDC.

9.4. CONCLUSIONS

A novel ultrasonic method for measuring oil film thickness has been evaluated for the measurement of cylinder liner - piston skirt lubrication. Reflected ultrasonic signals were recorded as the piston passed the sensor location.

The reflected signals could be interpreted using a simple spring model approach to give oil film thickness directly. Oil films in the range 2 to 21 μm were measured for the piston skirt under a range of motored and fired conditions. However, since the sensor recorded over a relatively large area it was not possible to measure the film as the piston rings passed.

The measured data agrees qualitatively with prior data from a numerical model of the piston skirt film formation.

CHAPTER 10:
DEVELOPMENT OF A MOTORED TEST ENGINE

From the success of the results of the work explained in Chapter 9, a motored test engine was built to understand and develop the ultrasonic oil film thickness technique applied to the piston to liner/cylinder wall interface. This test rig has been built so that the measurement method can be developed to create a reliable and usable platform for various oil film thickness measurements. The development of such a test engine will allow future research into the area.

10.1. APPARATUS

10.1.1. Test Engine

The test engine used for this motored test rig was a modified Perkins Engines 4 cylinder engine block. The cylinder block was donated to the tribology group after the success of the initial trial and the future plans, research opportunities potential benefits to an engine company were discussed.

The engine block was from a 4.4litre, 4 cylinder engine, with a bore of 105mm and a stroke of 127mm. The piston diameter was nominally 104.2mm in the region of the piston ring pack and the nominal piston skirt clearance was approximately 200μm (with a skirt diameter of 104.8mm). This engine did not have a cylinder liner as in many engines, but a homogeneous steel cylinder wall separating the inside of the cylinder and the water jacket.

The test rig was designed as a motored (i.e. driven by an external electrical motor) cylinder block, driving all four pistons. Many similar test rigs drive just a single cylinder engine, but this rig drives all four pistons in this block, to reduce unnecessary vibrations and to allow further development of the measurement technique.

The engine was mounted on six steel upright posts which were attached to steel cross-members, which were in turn bolted to a steel test bed. The motor to drive the engine, via its crankshaft was mounted in a similar fashion on four steel uprights. The shaft

of the motor was connected to the gearbox end of the crankshaft via a flexible tyre coupling, this was firstly to allow for any minor inaccuracies in alignment and secondly to minimise heat transfer from the engine to the motor, to prevent thermal overload of the motor during testing.

As the engine's valve train was not required for this test rig, a plate was machined to sit in the location of the cylinder head to create a top plate, which covers and seals the top of the water jacket as well as oil feeds and pushrod channels to the valve train. Holes were machined in locations relating to centres of each of the cylinders to allow the movement of air in and out of the cylinder. The area of each of the holes was the same as the cylindrical area created when an exhaust valve opens. As the valve train was not required there was no need for the valve gear either, therefore the valve gear housing was modified and a plastic cover was fitted to the outside of it to prevent air and lubricant loss – minimising oil vapour in the test cell.

The lubricant and water systems were modified to operate on this test engine, which did not have the majority of its ancillary components connected, the only major ancillary component was the oil pump located inside the oil sump. Modifications were required to the oil system to block or divert certain pathways, which would have led to various components including: the valve train, valve gear, oil cooler, oil filter and a turbocharger. Pressure relief for the oil system was provided via a control tap located on the modified valve gear cover. The tap was connected to pipe where oil vapour can condense and flow into an external oil tank. The water system was required to operate two functions in the test engine, firstly to cool and/or maintain a constant engine temperature (as ultrasound is very sensitive to variations in temperature), and secondly (and most importantly) to provide a steady flowing (non-turbulent) water bath for the focusing ultrasound technique (discussed later). This was provided by locating the water inlet as high as possible on the water jacket, a water pump connection located at the top of the cylinder block opening on the valve gear end of the engine was utilised. The exit for the water system was located on the top plate to ensure the water jacket was completely filled with water. Water was fed into the system via an electric water pump from a 25 litre holding tank. Water exited the system into the same holding tank to allow recirculation of the water.

These modifications were carried out to ensure that the engine operated as similar as possible as it would if all of the ancillary components and valve train were connected, just without the effects of combustion. A photograph of the test engine is shown in Figure 10.1.

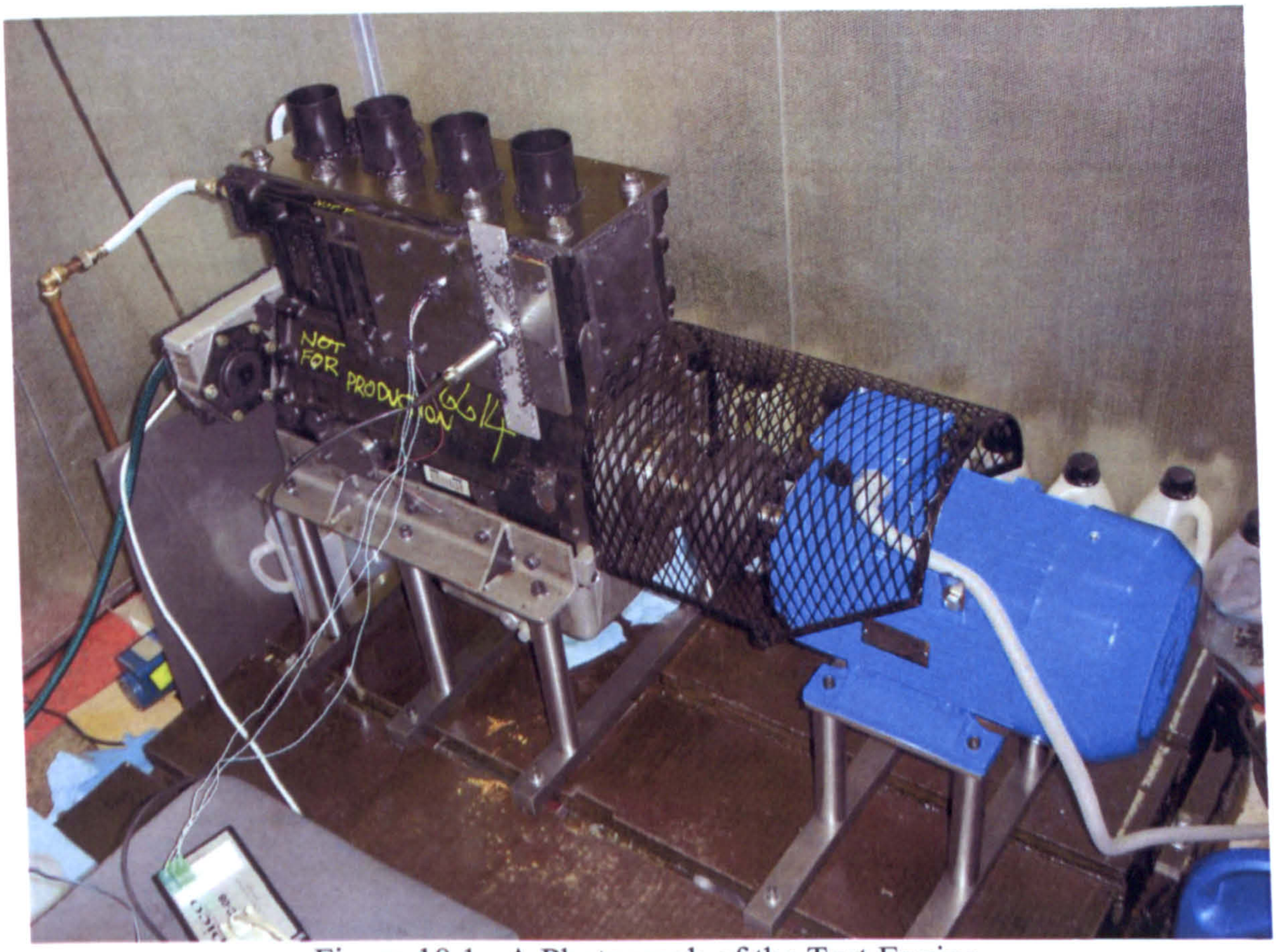

Figure 10.1. A Photograph of the Test Engine.

10.1.2. Control And Instrumentation

The 7.5kW three phase motor turning the crankshaft was controlled via an inverter which was computer controlled by a voltage input, providing a 'soft start' function and accurate speed control. Feedback of crankshaft speed and position were measured via a shaft encoder, providing two output channels, firstly a square wave voltage output for every 3000^{th} of a rotation and secondly another square wave voltage output once every rotation occurring at top dead centre (TDC) of cylinder number one in the test engine (the cylinder nearest the motor). The speed control voltage was outputted and the encoder voltage was inputted through a National Instruments USB-6009 multifunction data acquisition unit. Temperature was also monitored at various locations on the engine; these included measurement point locations on the test cylinder and the general engine water temperature, these temperatures were monitored using a Pico TC-08 thermocouple data logger. Both the National Instruments data acquisition unit and the Pico data logger were connected to the same computer and were controlled and monitored by software written in LabVIEW. The front screen for the test engine control and feedback is shown in Figure 10.2, and the front screen for temperature measurement is shown in Figure 10.3.

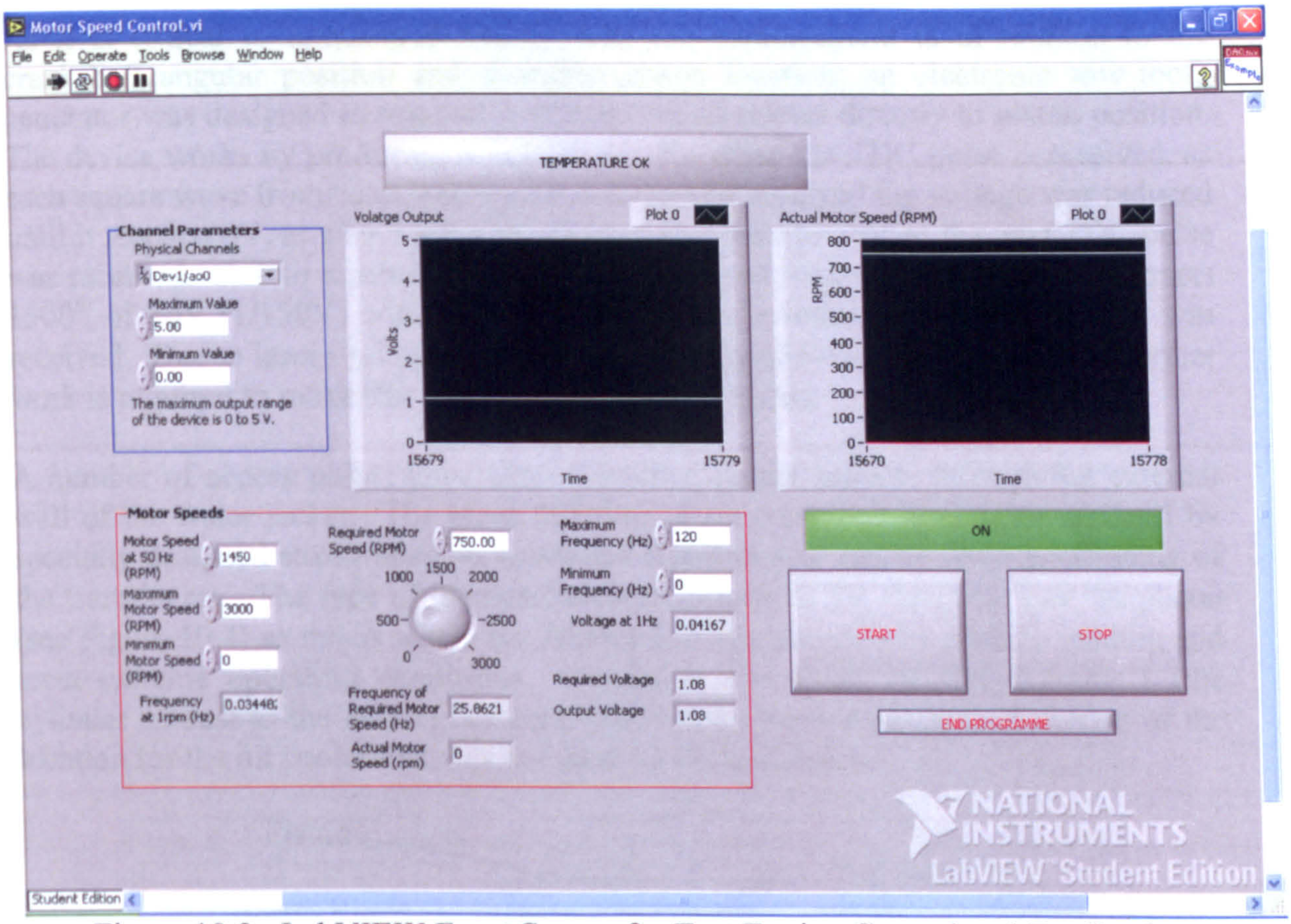

Figure 10.2. LabVIEW Front Screen for Test Engine Control and Feedback.

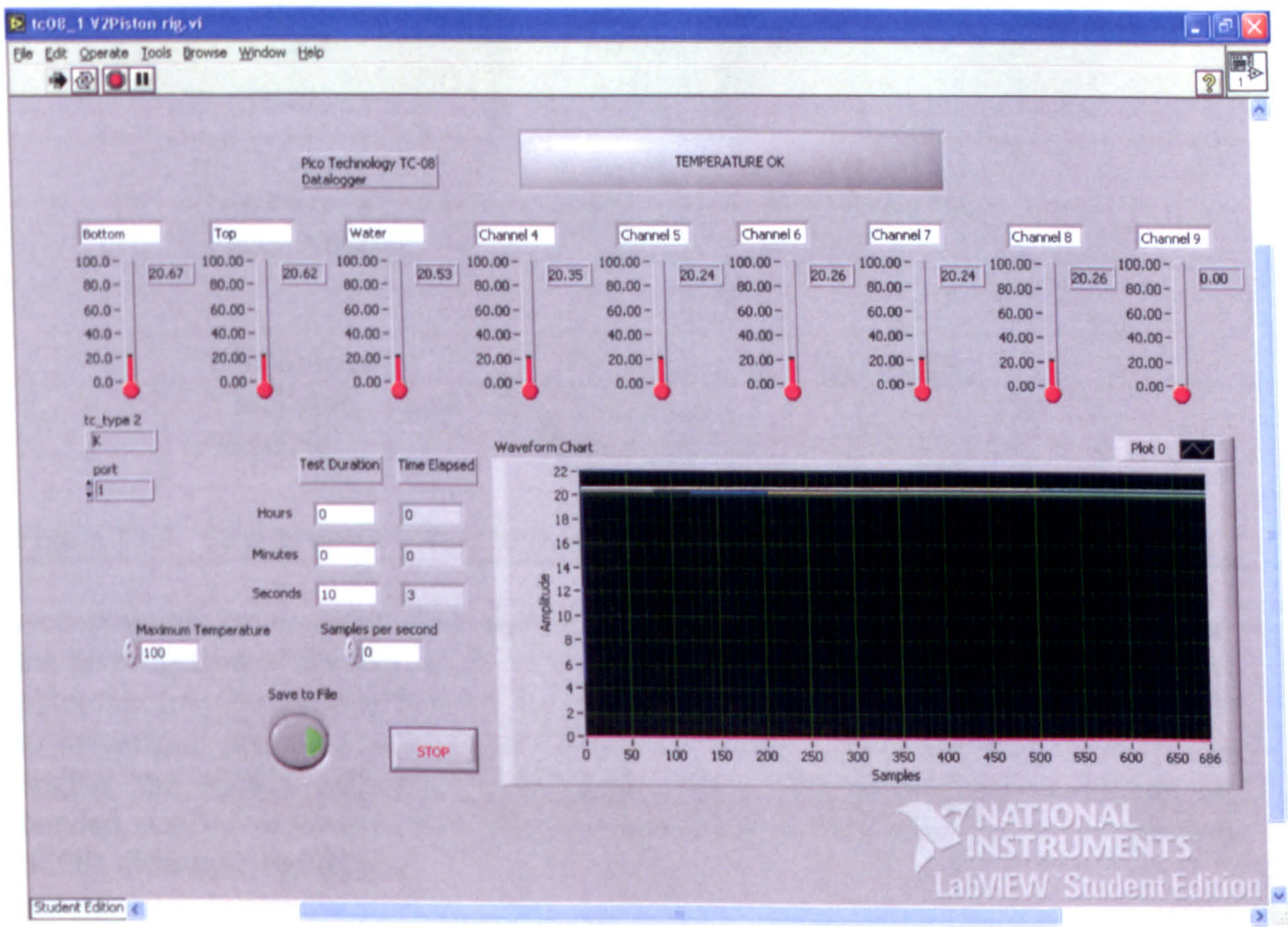

Figure 10.3. LabVIEW Front Screen for Test Engine Temperature Monitoring.

As it is critical to understand exactly where a measurement is in relation to the crankshaft angular position and therefore piston location; an electronic saw tooth generator was designed to produce a voltage which relates directly to piston position. The device works by producing a voltage of 10V when the TDC pulse is received, as each square wave from each 3000th of a rotation was received the voltage was reduced until it reached 0V, at which point the voltage was reset to 10V as the next TDC pulse was received. Due to resolution limitations and speed requirements the unit subtracts 1500th of 10V (1/150V) with every other 3000th of a rotation square wave that was received. Due to issues relating to the merging of multiple signals and timing, further work is required to make this system function as intended.

A number of access points have been machined on the engine, through the external wall of the water jacket. The areas that have been machined have been replaced by specially designed steel plates, to create the required seal and to allow positioning of the transducers. The face of greatest research interest is the thrust face of the piston (see Figure 10.4) as this is where the lubricant film undergoes its greatest loading and most extreme operating conditions. Access to the thrust face of cylinder 1 (the cylinder nearest to the motor) has been possible by machining away a section of the location for the oil cooler that was not used on the test engine.

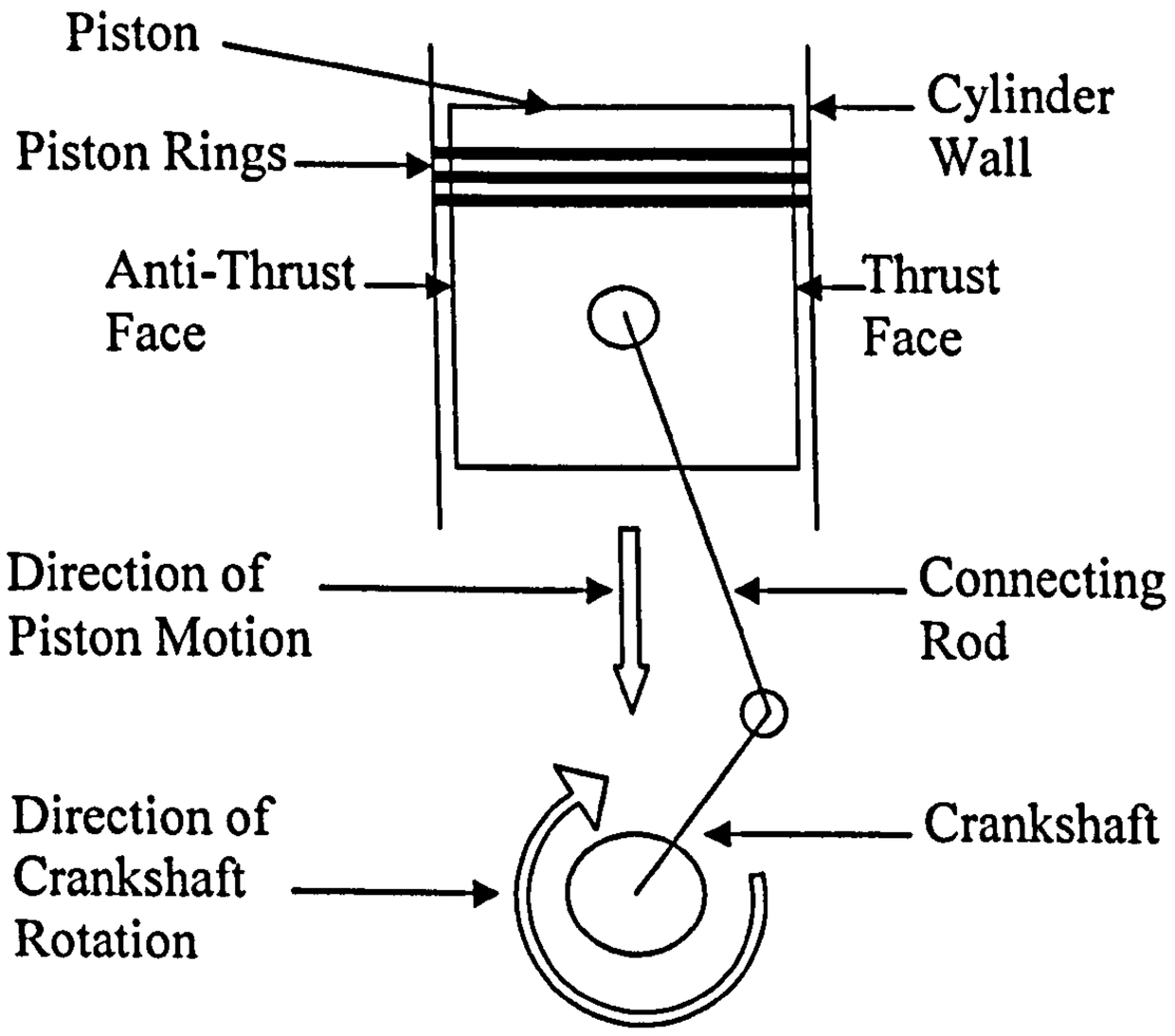

Figure 10.4. Schematic of Piston Motion, Highlighting Thrust and Anti-Thrust Faces.

Access points have also been created at the front and rear of the engine to allow for the investigation of the side walls of cylinders 1 and 4 in the future. Another access point that may be required in the future is one on the anti-thrust side of the cylinder 1 to investigate piston secondary motion and its effects. At all access points on the engine, the outside surface of the cylinder walls, onto which transducers can be bonded, applied or focused have been machined flat as is required for the application of this ultrasonic technique.

10.2. ULTRASONIC TRANSDUCERS

In this work several types of ultrasonic transducer have been used to investigate the oil film thickness between the piston and cylinder wall. Both commercially available sealed transducers and piezoelectric element transducers have been used. This section builds on the information provided in Section 8.5, demonstrating how they were applied to this application.

10.2.1. Piezoelectric Element Transducers

The piezoelectric transducer was tested to attempt to replicate the work carried out in Chapter 9. For practical reasons the piezoelectric element transducer was bonded to a Perspex delay line which was in turn bonded to the outside of the cylinder wall. This was to done to attempt to reduce electrical interference. Figure 10.5 shows a piezoelectric element on the test engine.

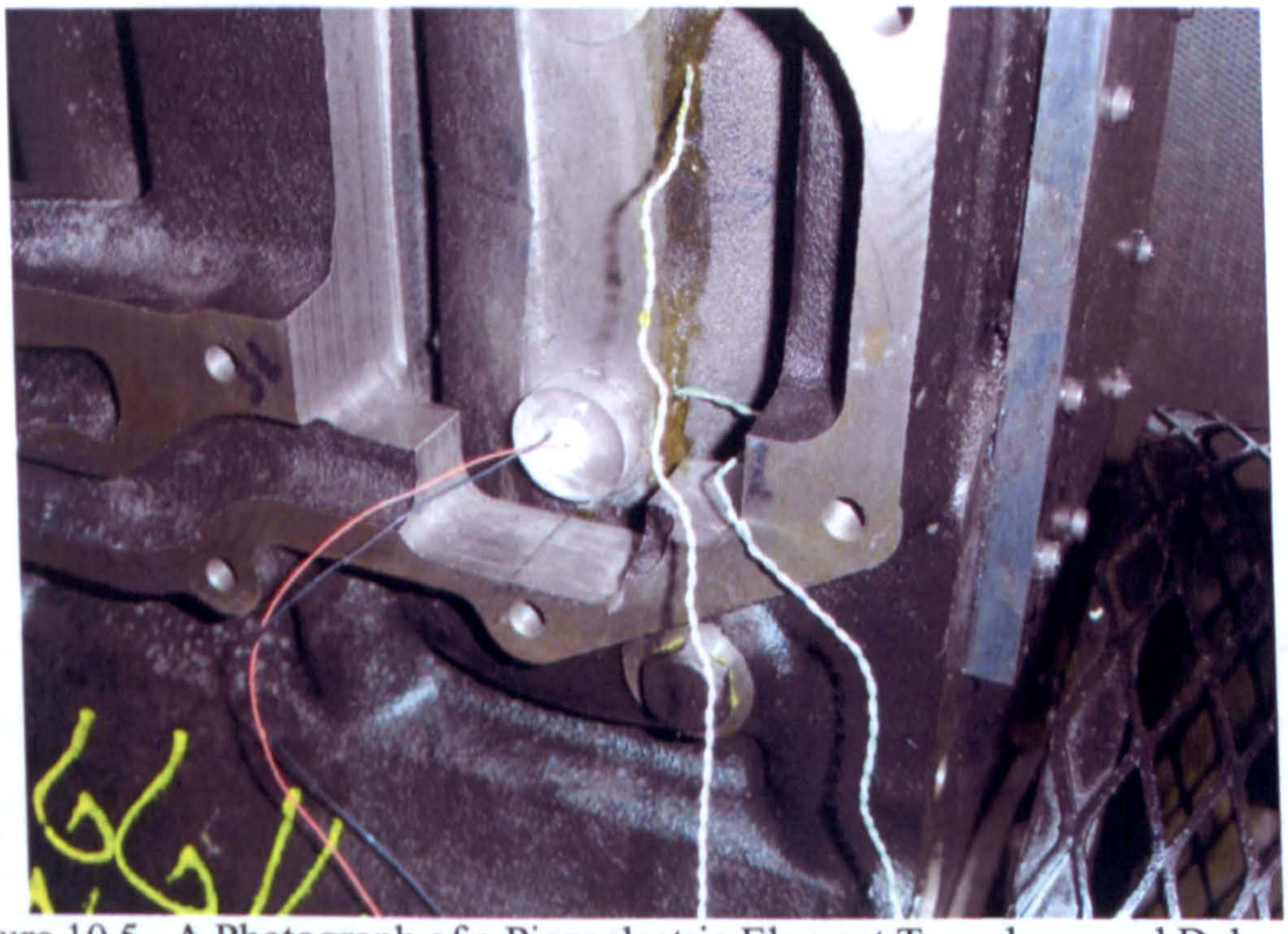

Figure 10.5. A Photograph of a Piezoelectric Element Transducer and Delay Line Bonded to the Outside of the Cylinder Wall.

This type of transducer is a broadband transducer as the spread of the ultrasonic signal is not focussed. Therefore the accuracy resolution of the transducer (i.e. the focusing spot over which it is accurate) is roughly equal to the diameter of the element itself, in this case approximately 7mm. Such accuracy was sufficient to investigate the oil film thickness of the piston skirt (Chapter 9), but not a piston ring, which has a contact patch of approximately 2mm.

Testing with this form of transducer highlighted high levels of electrical noise, predominantly from the motor and inverter. It is thought that this can be partially eliminated if the engine and motor are fully electrically insulated.

Piezoelectric elements are inside all commercial transducers, but also include incorporate various intricate components, to smooth out the resulting signal and reduce the effects of surrounding electrical noise.

10.2.2. Contact Transducers

The contact transducer used for this testing is shown in Figure 10.6. As the signal face must be in direct contact with the region of interest, the transducer was held in place via a specially designed magnetic clamp as shown in Figure 10.7. A couplant, typically a gel is required to make a good contact between the probe and surface. A contact probe is therefore not ideal for continuous use on an engine as the couplant's properties will significantly change with time and temperature.

Figure 10.6. The Contact Transducer.

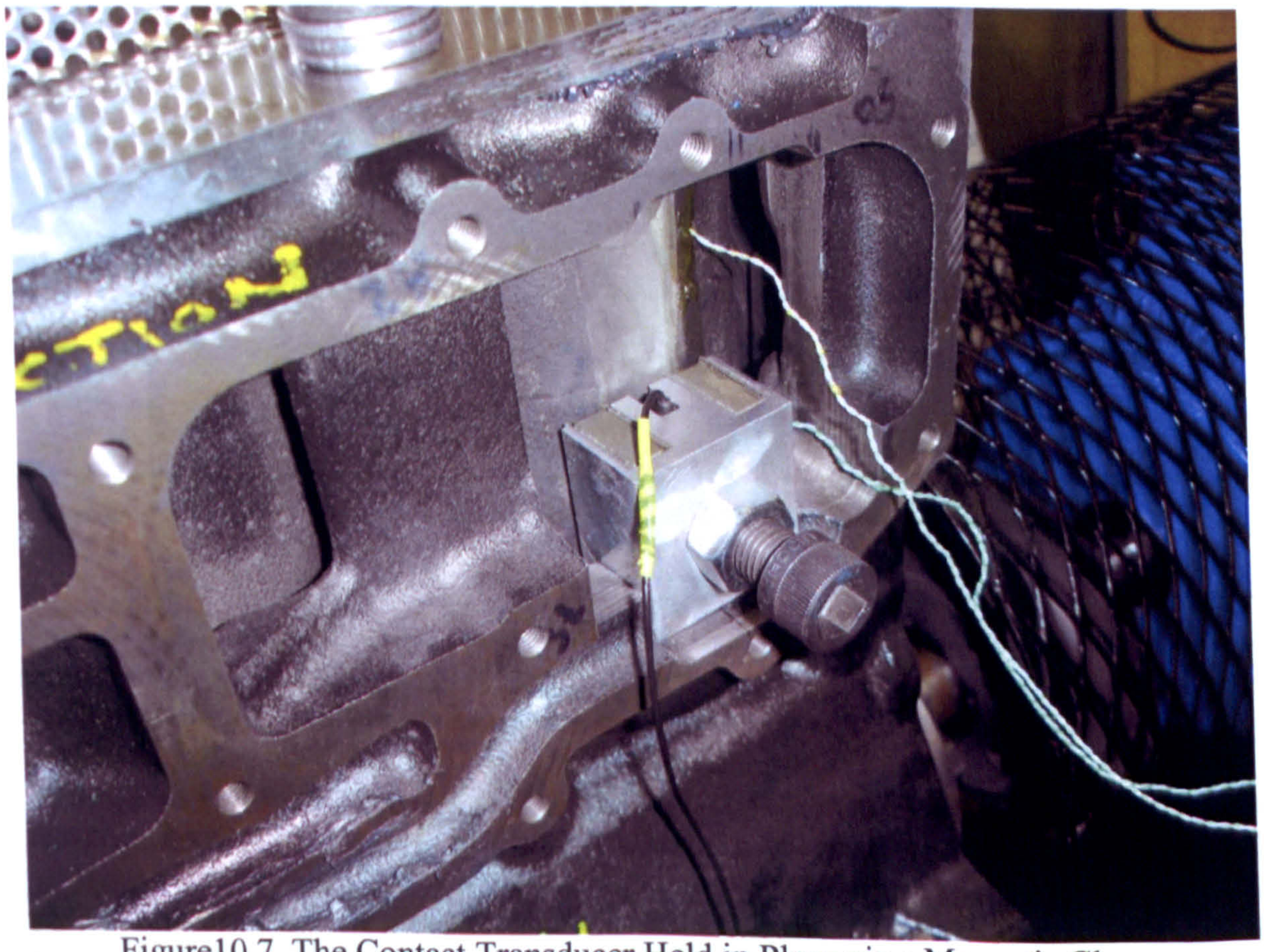

Figure10.7 The Contact Transducer Held in Place via a Magnetic Clamp.

10.2.3. Focusing Transducers

The focusing transducer (as discussed in Section 8.5) does not directly contact the test surface, but is positioned a specific distance away from the test surface. The test surface and transducer need to be submersed in a water bath, for focusing of the ultrasonic signal, as shown in Figure 10.8. For this application the modified water jacket of the engine was the water bath to focus the ultrasonic signal, for example (in Figure 10.8) material 1 would be the cylinder wall and material 2 would be the piston or piston ring. Figure 10.9 shows the focusing transducer arrangement on the test engine. The focusing transducer holding piece which located on the engine side plate (sealing the water jacket), can be located in numerous vertical locations. Vertical positioning of the holder was via a series of threaded holes.

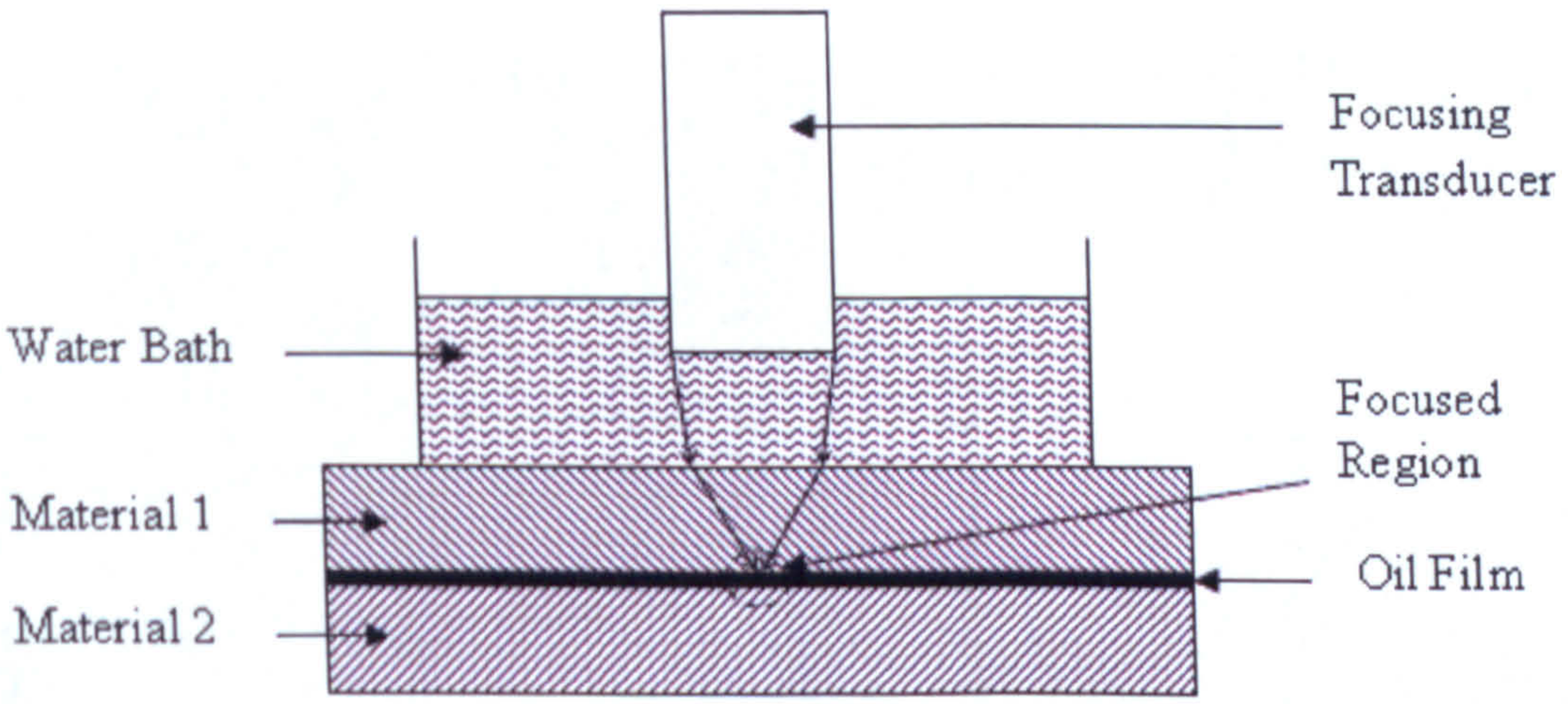

Figure 10.8. Schematic of Focusing Transducer Set-up.

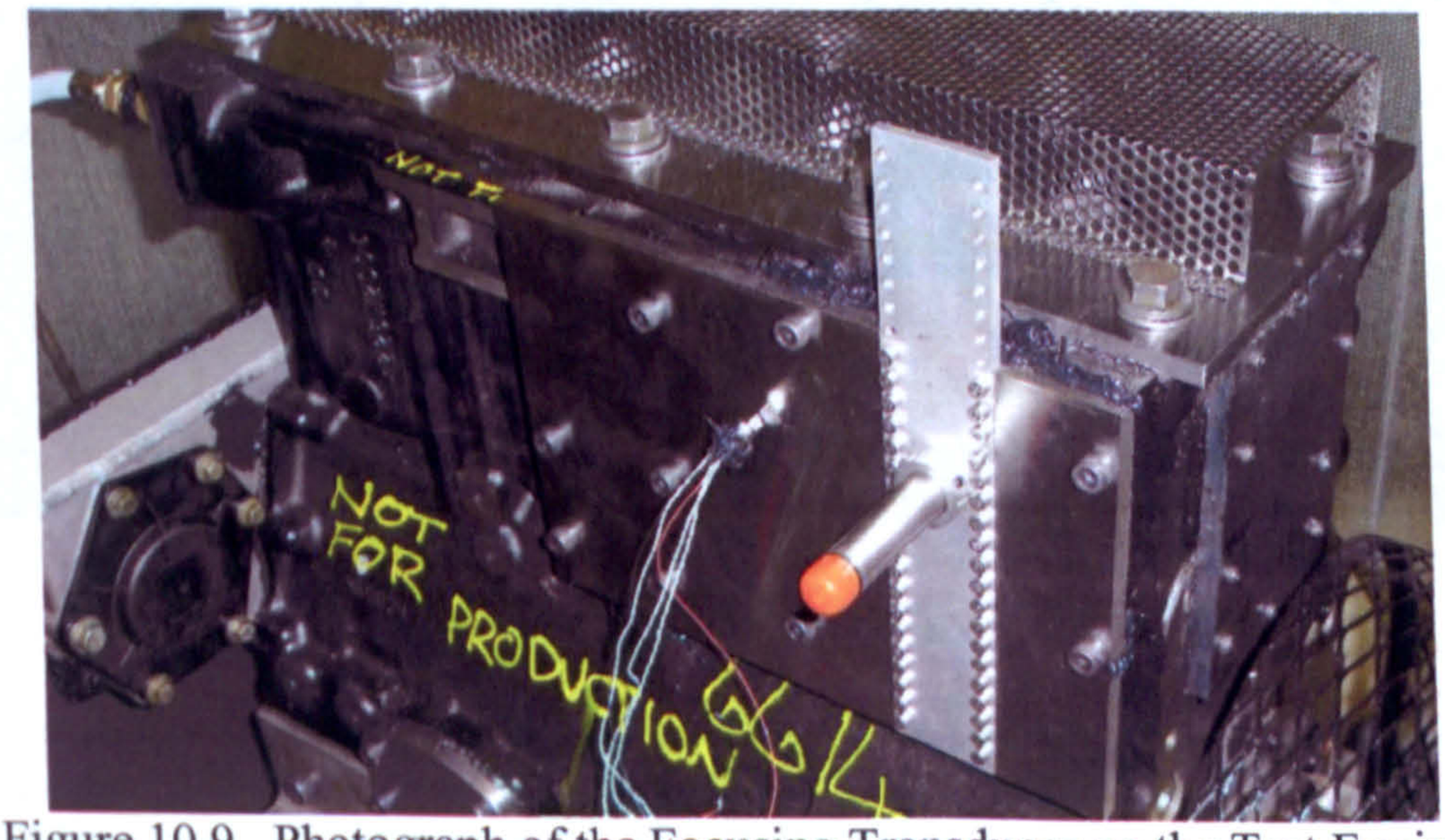

Figure 10.9. Photograph of the Focusing Transducer on the Test Engine.

The focusing properties of this type of transducer mean that a very small contact zone is achievable. The transducer used in this work had an operating frequency of 20MHz. This produced a focusing diameter of 0.65mm (see Section 8.3 and reference **[113]**). This focal spot diameter is much smaller than the contact width of a piston ring to cylinder wall of approximately 2mm and is therefore ideal for the application.

10.3. MEASUREMENT METHOD

The measurement of an oil film thickness as explained in detail in Chapter 8 requires a reference signal and the actual data signal. As ultrasonic measurements are extremely temperature sensitive, the reference and actual data signals must be taken at the same temperature. Therefore the engine was motored to warm the components to the required temperature. The engine was then stopped and the crankshaft was rotated until the piston was not at the focused point. A reference measurement was then taken via software written in LabVIEW, via the ultrasonic pulser/receiver (UPR) and a digital LeCroy oscilloscope. The PC controlled UPR sends and receives the ultrasonic signals and reflections. The resulting waveform was displayed on the oscilloscope (which was also linked to the same PC). The UPR, oscilloscope and PC set-up is shown in Figure 10.10.

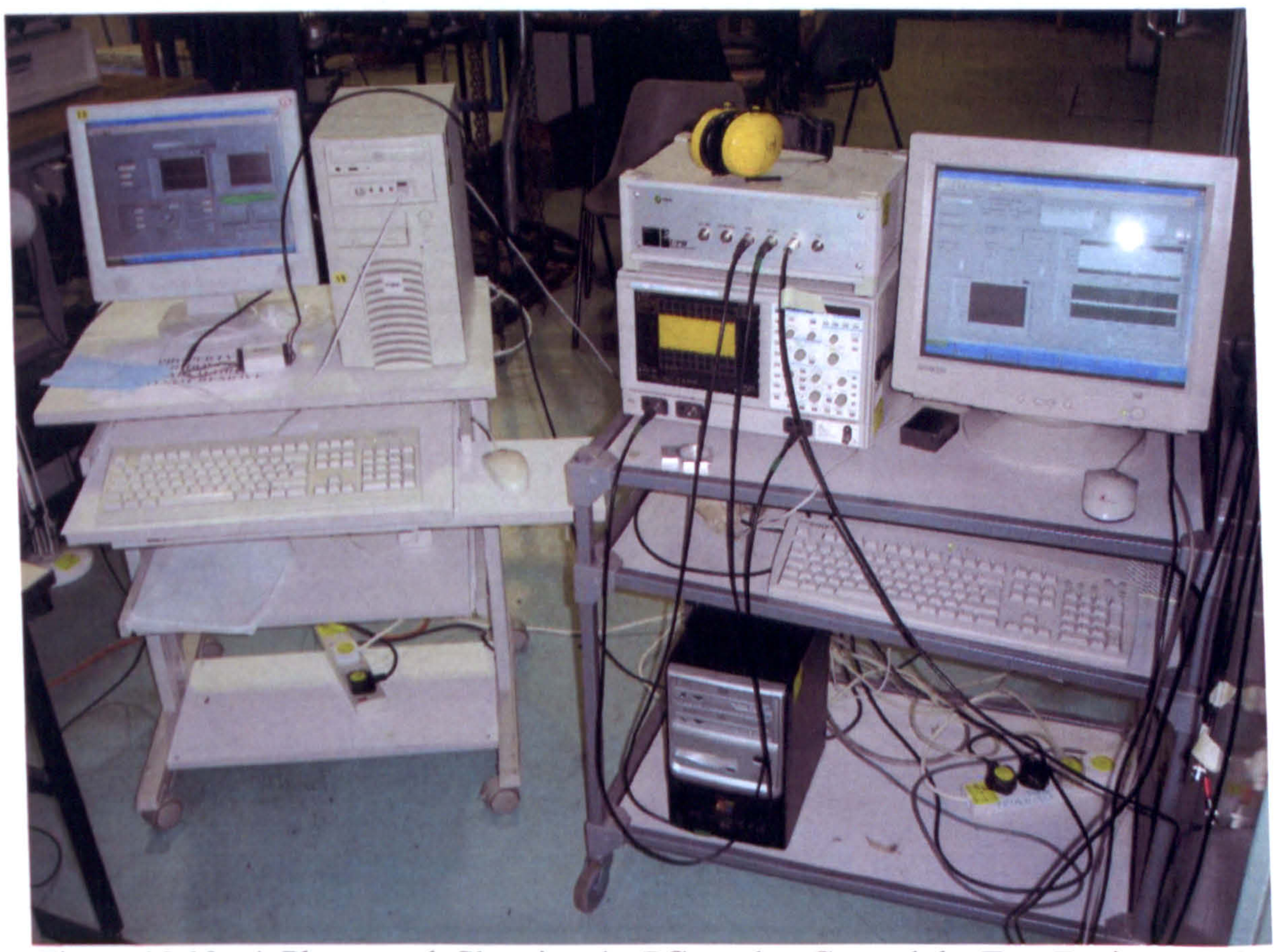

Figure 10.10. A Photograph Showing the PC used to Control the Test Engine and the UPR, Oscilloscope and PC Set-up for the Ultrasound.

Using the segmentation technique (described in Chapter 8) the internal memory of the oscilloscope (250kbytes) was used to capture a series of reflected signals. For this testing 500 segments (each with a resolution of 500 points or bytes) were captured during each data capture run.

The data capture process for both the reference and actual test data was the same, where a LabVIEW programme communicated with the oscilloscope to commence capturing (whilst using segmentation method to obtain multiple pulses), once the

oscilloscope's internal memory was full, the data was downloaded and displayed on the PC. The front screen of the data recording programme is shown in Figure 10.11.

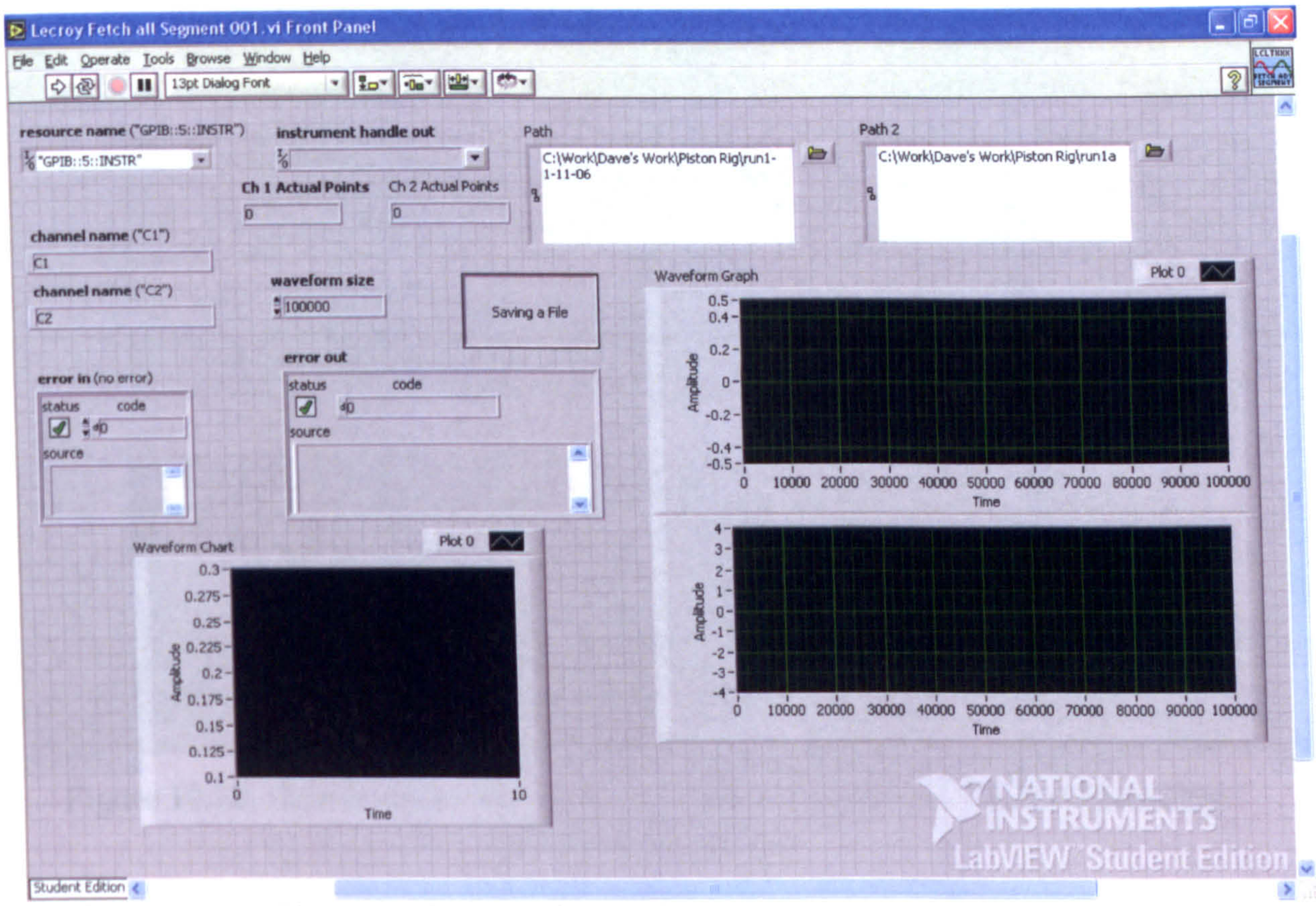

Figure 10.11. The Front Screen of the LabVIEW Programme used to Control the Capture of Data.

Full analysis of the data was carried out after the testing to produce the reflection coefficient and ultimately the oil film thickness. The reference waveform was produced in a separate LabVIEW programme where of all of the segmented pulse reflections were averaged to produce one reference waveform, the front screen of this programme is shown in Figure 10.12.

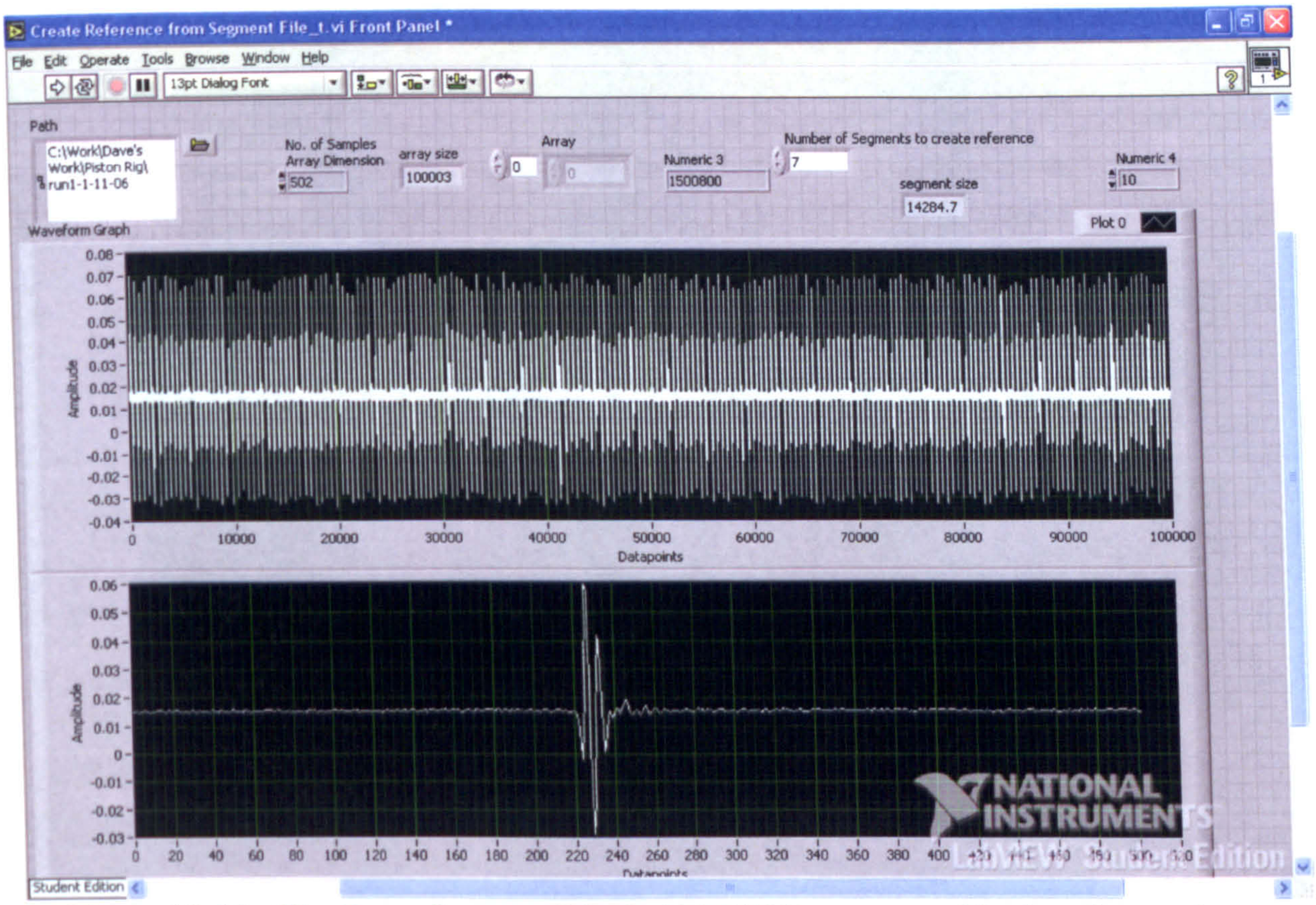

Figure 10.12. The Front Screen of the LabVIEW Programme Used to Create the Reference Waveform.

The actual test data was taken when the engine was running in steady-state conditions and at the same temperature as the reference signal was taken, using the same LabVIEW programme as was used to capture the reference signal data. This data was then post processed using another LabVIEW programme, which takes the actual test data file and breaks it down into individual segments. Each segment was transformed into the frequency domain from the time domain and then divided by the reference signal (which had also been transformed into the frequency domain). At this point the reflection coefficient was produced. Finally the oil film thickness could be calculated using Equation (8.4) in Chapter 8. The front screen of this LabVIEW programme is shown in Figure 10.13.

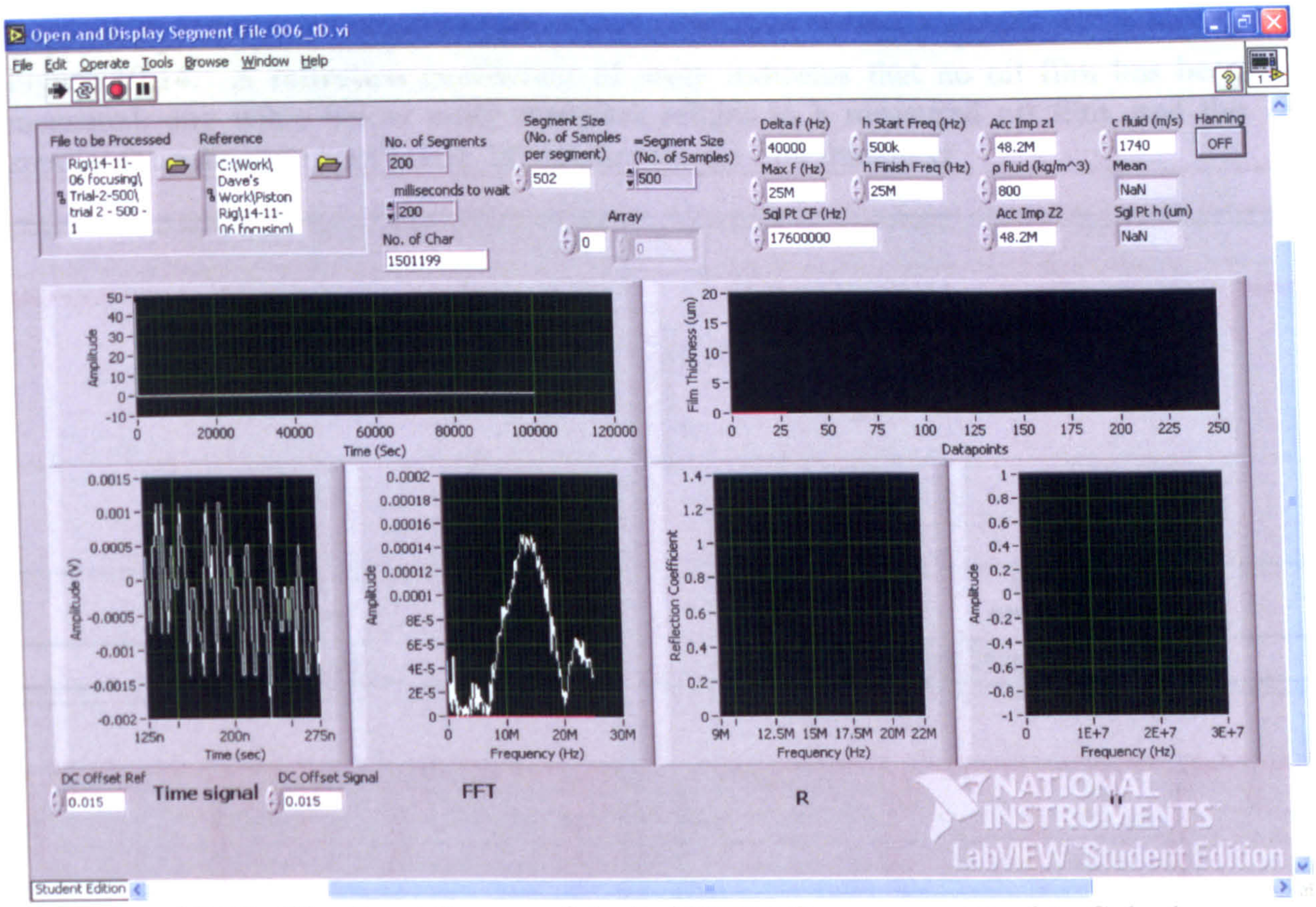

Figure 10.13. The Front Screen of the LabVIEW Programme Used to Calculate Reflection Coefficient and Oil Film Thickness.

10.4. RESULTS

From the three types of ultrasonic transducer that were tested only the contact and focusing transducers produced a measurable output. The piezoelectric element transducer suffered from too much electrical interference in the signal to produce any useful results. The obtained results are shown as reflection coefficient, as currently the measurement method is not developed enough to understand the exact location of the piston with reference to the transducer, as the occurrence of the measurements currently happens randomly, arbitrarily dictated by the operator of the control computer. This is important as the piston is a mixture of aluminium (the majority of the body) and steel for the piston rings and the region around the ring pack. Knowledge of the materials is important in the calculation of oil film thickness using this method.

10.4.1. Contact Transducer

Measurements with the contact probe were performed at a sampling rate of 250MSamples/second, for a total sample duration of 2μseconds (sampling 200 segments). Using the current method means that only a small proportion of the piston stroke can be measured at a time, this does though mean that as engine test speeds increase measurements can be taken over a greater piston displacement. Measurements were taken at engine speeds of 500, 750, 1000 and 1250rpm, equating to a piston displacement (based on maximum piston speeds) of 3.5, 5.2, 7 and 8.5mm

respectively. Typical measured reflection coefficients at these speeds are shown in Figure 10.14. A reflection coefficient of unity indicates that no oil film has been measured, any value below unity therefore relates to a measured oil film, and the smaller the reflection coefficient, the greater the oil film thickness.

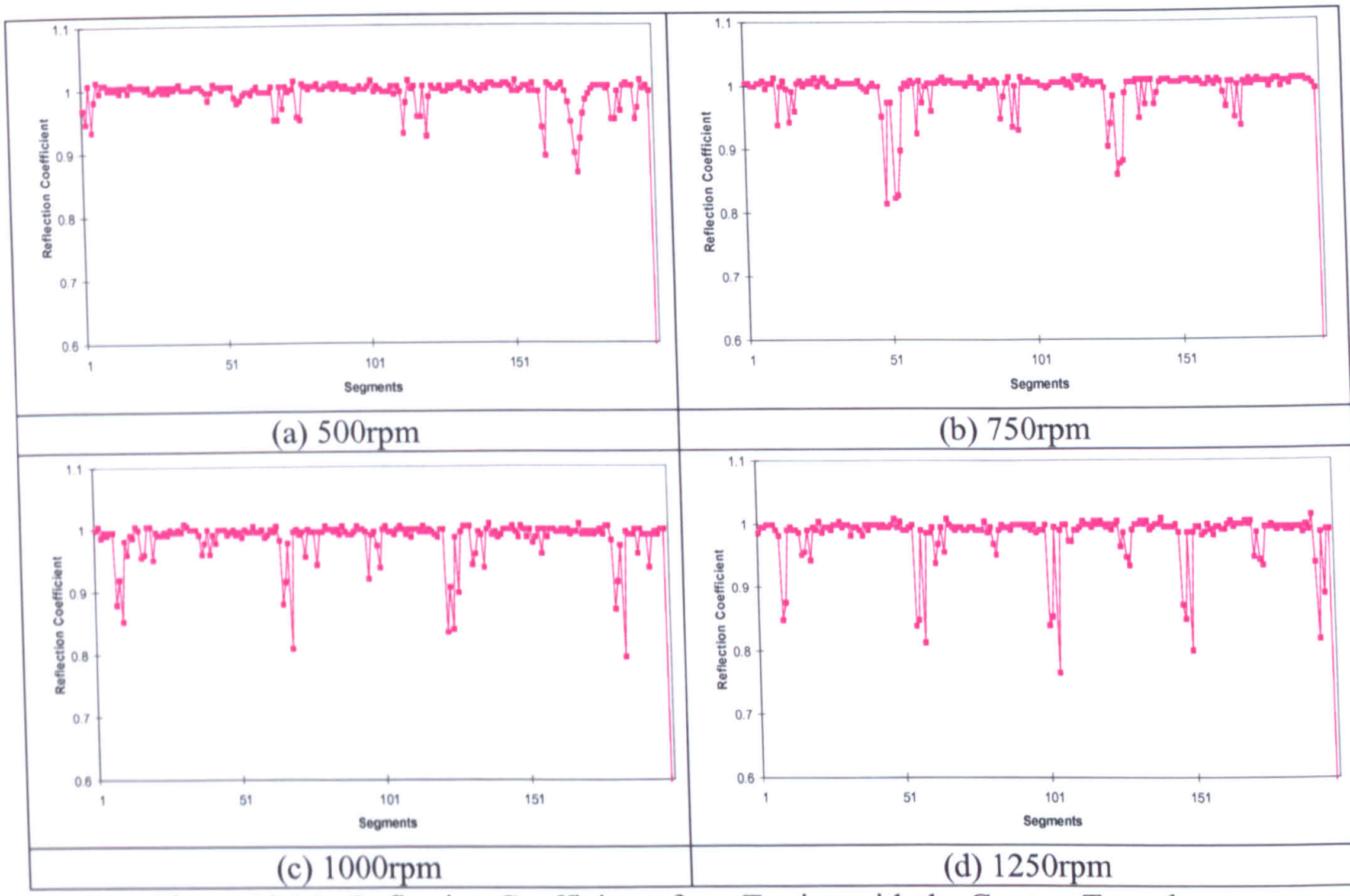

(a) 500rpm

(b) 750rpm

(c) 1000rpm

(d) 1250rpm

Figure 10.14. Reflection Coefficients from Testing with the Contact Transducer.

The results shown in Figure 10.14 demonstrate that changes in reflection coefficient were measured as the piston passed the contact transducer. Previous investigations using other techniques have shown that generally as engine speed increases the oil film thickness increases too **[111]**. This behaviour is also evident here, as reflection coefficient is inversely proportional the oil film thickness. Figure 10.14 indicates that as engine speed increases, reflection coefficient measurements tend to decrease resulting in measurements below 0.8 at 1250rpm, indicating an increasing oil film thickness.

10.4.2. Focusing Transducer

Measurement using the 20MHz focusing transducer were performed at a sampling rate of 250kSamples/second, for a total sample duration of 1msecond (sampling 500 segments). The transducer was located in a position vertically along the piston stroke so that it could potentially measure a complete stroke, plus regions at either end of the measurement (TDC and BDC) without any cylinder liner to piston contact (this is demonstrated in Figure 10.15). These non-contacting regions could potentially be used as the reference signal measured during the each cycle of a test, this will only be

possible once the method has been developed further to measure significantly more data and trace the exact location of the piston during a stroke.

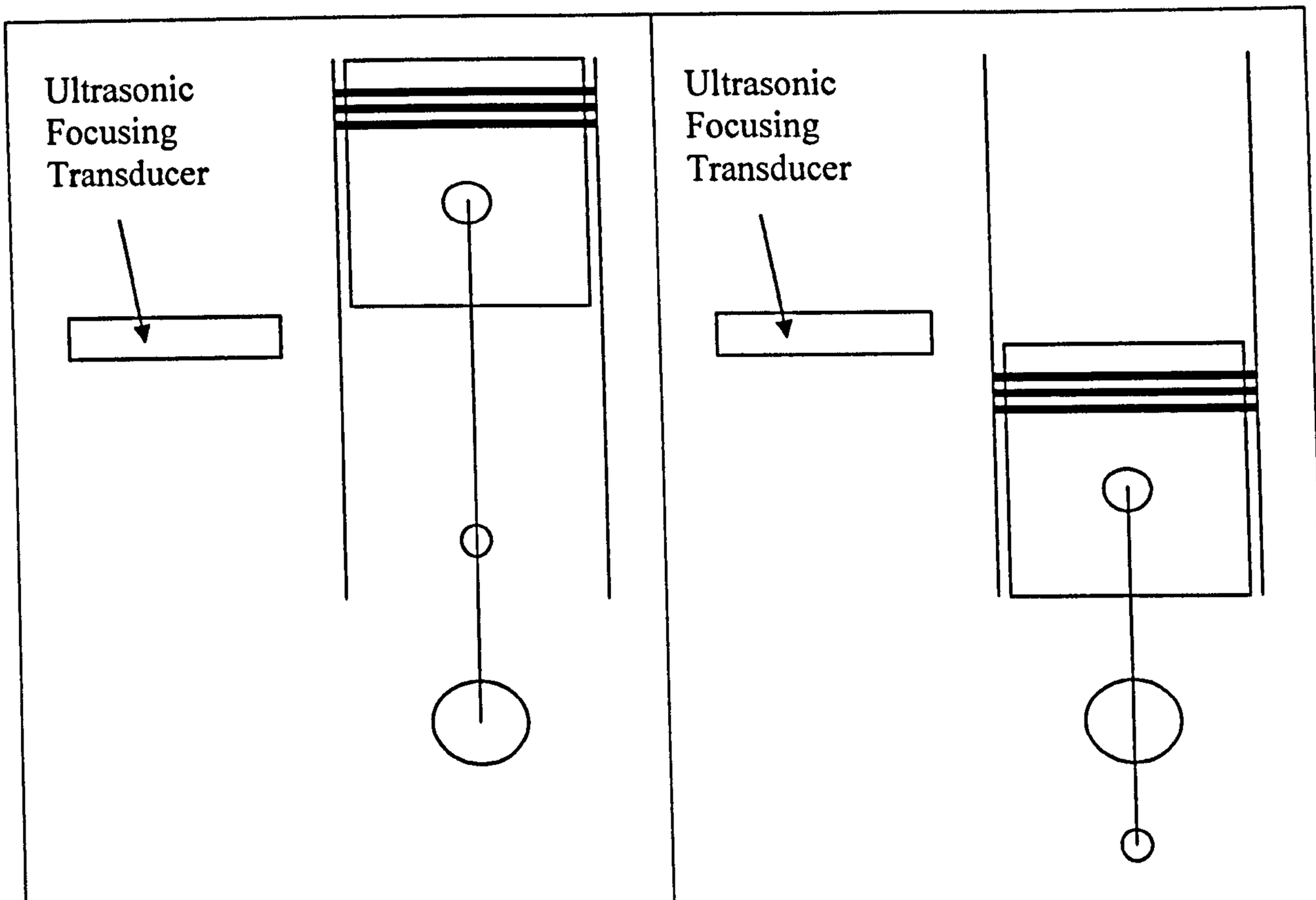

(a) Piston at TDC (b) Piston at BDC

Figure 10.15. A Schematic of the Ultrasonic Focusing Probe Positioning, with Non-Contacting Regions at TDC and BDC.

Again, using the current method means that only a small proportion of the piston stroke can be measured at a time, meaning that as engine test speeds increase measurements can be taken over a greater piston displacement. Tests were performed at engine speeds of 500, 750, 1000, 1250, 1500, 1750 and 2000 rpm, these speeds equate to a piston displacement (based on maximum piston speeds) of 3.5, 5.2, 7, 8.5, 10.4, 12.1 and 14.3mm respectively. Some typical measured reflection coefficients for 1500rpm are shown in Figure 10.16.

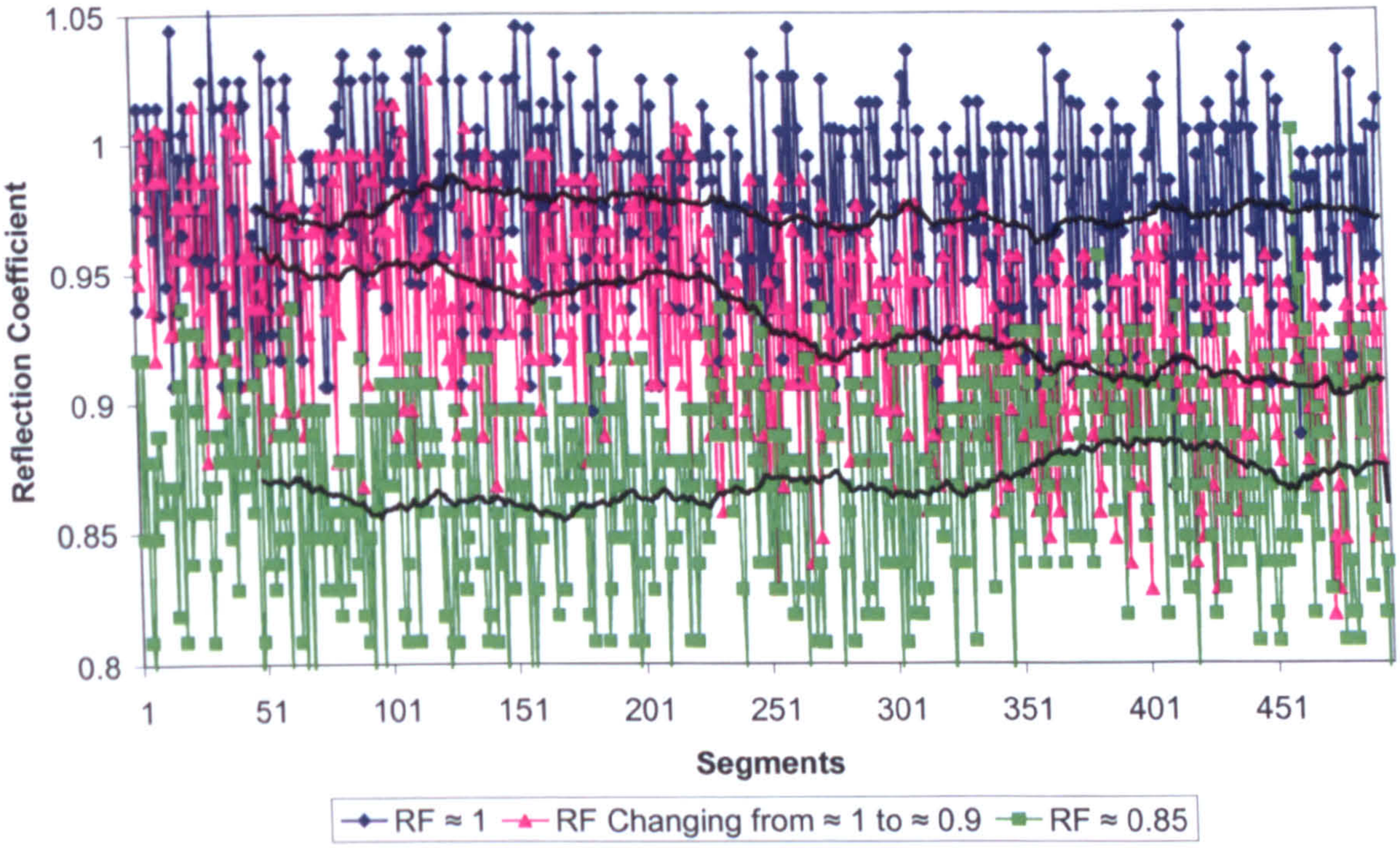

Figure 10.16. Typical Reflection Coefficient Measurements from a 1500rpm Engine Test.

Figure 10.16 clearly has significant levels of noise in the signal, but this has been averaged out, presenting three clearly defined black average lines. There are two relatively horizontal lines at reflection coefficient values of approximately 1 and 0.85 and a line sloping from approximately 1 to 0.9. These measurements clearly demonstrate that this method has the potential to evaluate differences in oil film thickness.

To understand the reasoning as to why there was so much noise in the measured signal, an analysis of the transducer, the materials it was focusing through and therefore the related oil film thickness limits was required. Using the calculation programme developed within the Tribology group at the University of Sheffield and discussed in Chapter 8, based on the oil film thickness spring model relationship **[113]**, the limits were calculated. Spectra for the transducer frequency and materials used were produced demonstrating the achievable reflection coefficients. Figure 10.17 shows the spectra for the aluminium portion of the piston and Figure 10.18 shows the spectra for the steel portion of the piston (including the piston rings).

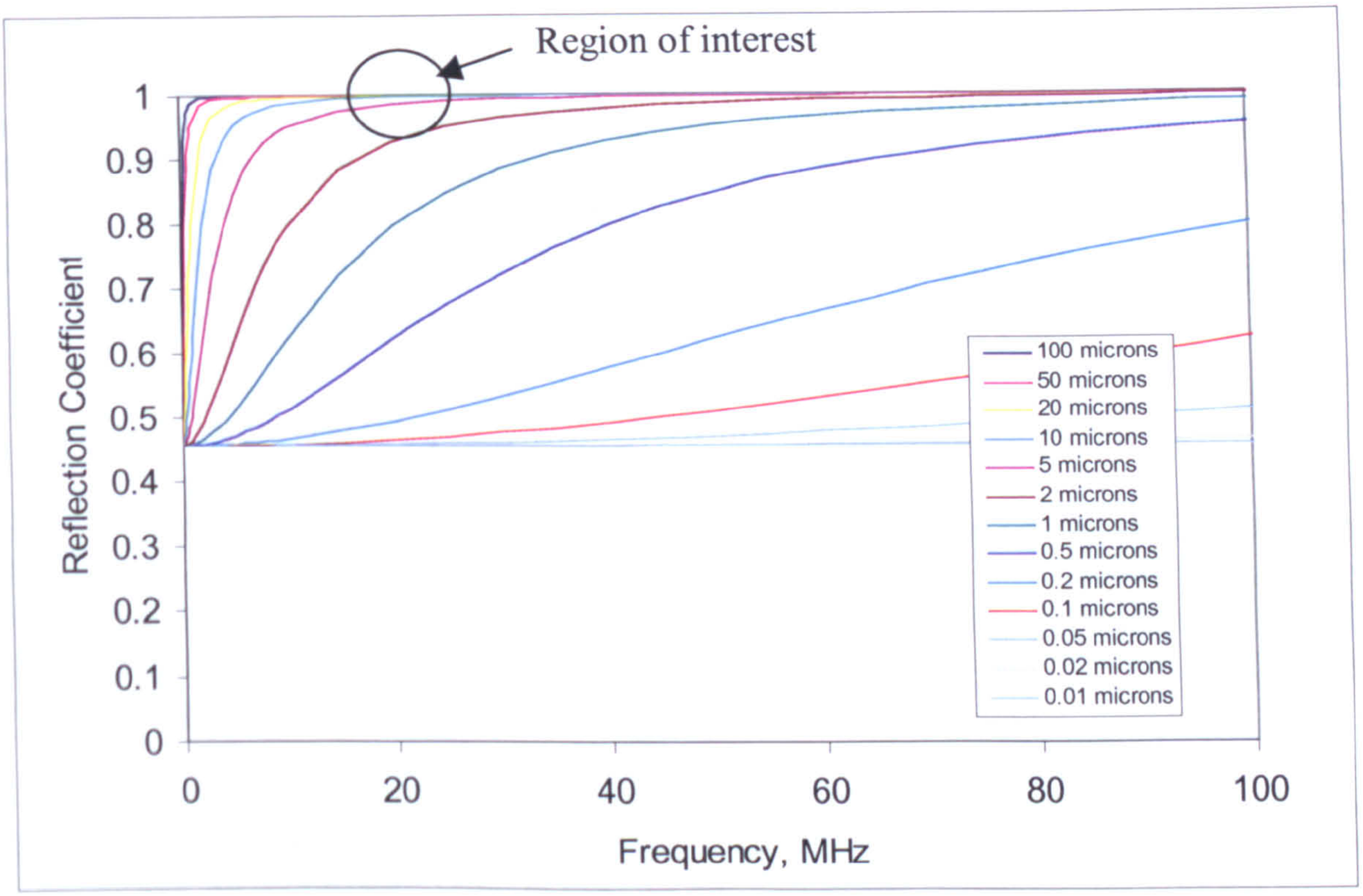

Figure 10.17. The Spectra for the Aluminium Portion of the Piston.

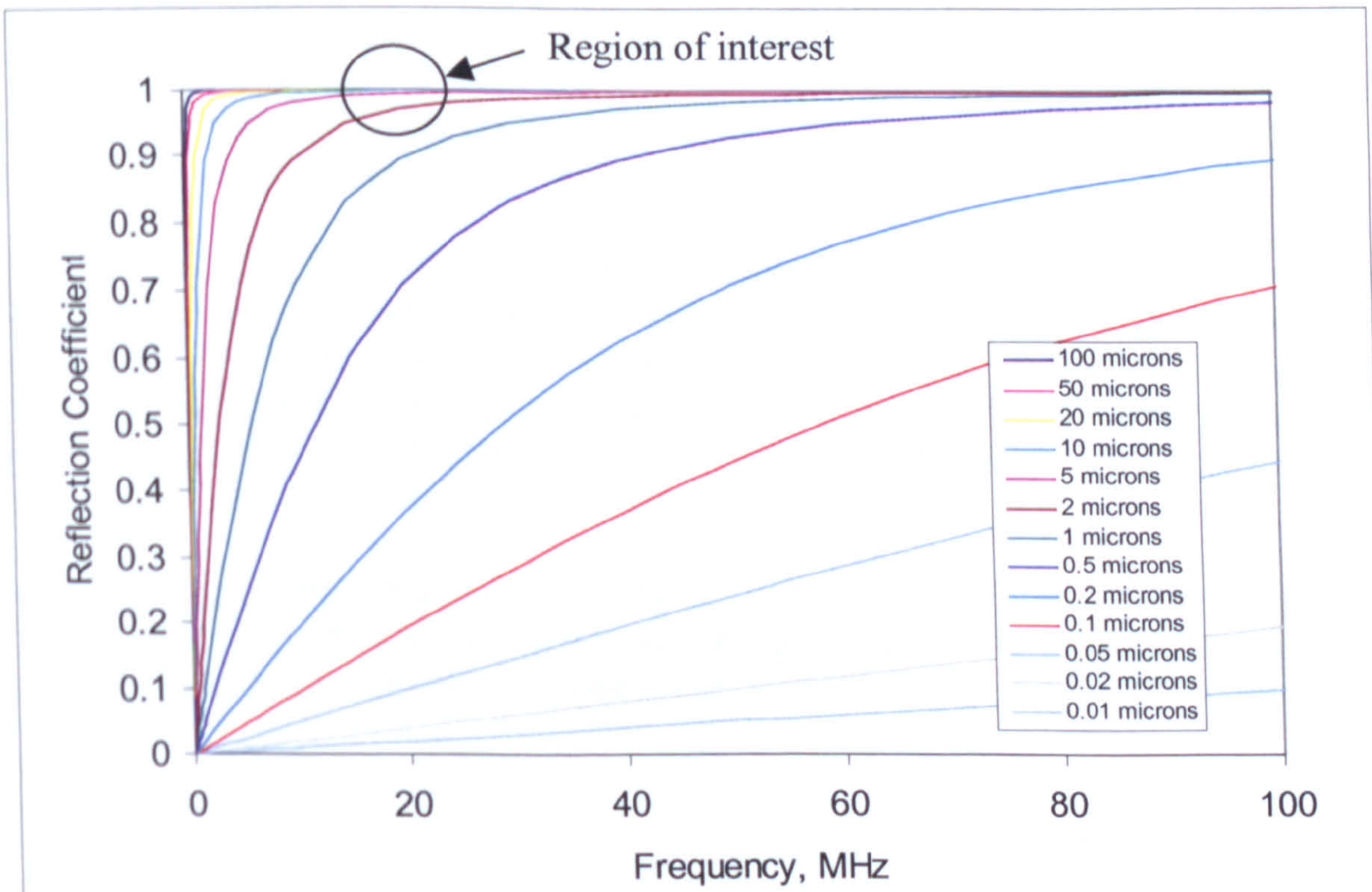

Figure 10.18. The Spectra for the Steel Portion of the Piston.

Although a 20MHz transducer produces the required focal spot diameter, Figures 10.17 and 10.18 demonstrate that this pulsing frequency is possibly too high to achieve a good level of resolution in the resultant reflection coefficient data, for the expected oil film thicknesses (as discussed in Chapter 8). The regions within which the tests discussed in this section (for the focusing transducers) are circled in Figures 10.17 and 10.18.

Therefore to produce improved data, and with less noise interference it will be necessary to use a lower frequency transducer, which is correct for the expected oil film thicknesses. This will have the effect of increasing the focal spot diameter, a 10MHz transducer will have a diameter of 1.3mm, although larger and closer to the dimensions of the piston ring to cylinder wall, an oil film thickness measurement of the contact will be possible.

10.5. CONCLUSIONS

This chapter has described the development of a motored test engine to be used as a test bed to progress the research into oil film thickness measurement using the ultrasonic technique. The test rig has been designed with the consideration of numerous ultrasonic measurement methods to ultimately produce one or two specific methodologies.

The test rig has various control and measurement instrumentation, as well as LabVIEW software interfacing. These include computer speed control and temperature measurement; there is also a shaft encoder to act as feedback to the speed control and to provide timing pulses to identify piston position. There has also been a saw tooth wave generator developed to identify the exact position of the piston, this utilises the pulses generated by the shaft encoder. To create and measure the ultrasonic signals the system utilises an ultrasonic pulser-receiver, a digital oscilloscope and a PC with specially designed LabVIEW software currently used in the Tribology group at the University of Sheffield.

Testing has highlighted that the ultrasonic technique does work, as reflected pulses have been measured and discernable differences between different test conditions have been witnessed with different techniques, including significant changes in reflection coefficient with the focusing transducer, and with the contact transducer decreasing reflection coefficient with increasing speed, which would lead to an increasing oil film thickness measurement.

From the results and practically through use of the test rig there are clearly various areas in which it can easily be improved. Improvements in the measurement method and equipment would also provide significantly clearer data. Future work is discussed in Chapter 11.

CHAPTER 11:
OIL FILM THICKNESS MEASUREMENT OF A PISTON - DISCUSSION

The work described in Chapters 8, 9 and 10 describes the initial work that has been carried out in this investigation into a non-invasive method of oil film thickness measurement, between the cylinder wall and the piston in a reciprocating engine. This area of research can potentially assist the automotive and lubricants industry in the future. The key findings so far and suggestions for future work are discussed in this chapter.

11.1. TESTING TECIINIQUES

The review of previous investigations in the measurement of the oil film thickness in the region of the piston within an internal combustion engine concluded that many methods have been tested and that the current general trend is focusing in on capacitance and laser induced fluorescence techniques. These techniques are still not perfected and both are invasive, which possess some questions regarding viability as this may inadvertently affect the lubricant flow and therefore the results.

The ultrasonic method of oil film thickness measurement has been used successfully on various engineering applications and is continuously developing, enabling it to be used under in an increasingly wide range of conditions. The technique is well proven both theoretically and practically. As the ultrasonic method is non-invasive it provides the opportunity for the technique in the future to be used on fired test engines or even engines operating in a vehicle; with the knowledge that it is not disturbing the lubrication of the components and requires significantly less specialist machining than other techniques.

The initial trial of the technique on a single cylinder engine operating under both motored and fired conditions proved very successful. The success was mainly due to the combination of component materials and the dimensions of the oil film produced.

The results obtained identified that the technique could potentially become one of the principal methods in the future once fully developed.

The application of the technique to a motored test engine provided the opportunity to assess a number of transducers and measurement positions. The testing of the transducers proved that although the contact transducer provided reasonable data, it was not particularly practical. The focusing transducer provided the opportunity to measure a very finely focused area (approximately a 0.65mm diameter), rather than a larger averaged area with approximately a 7mm diameter. With modifications to the test rig the piezoelectric element transducers would provide an extremely practical tool, though only useful for large averaged area (again approximately a 7mm diameter). If through further research an understanding between the oil film thickness of piston skirt and the piston rings can be achieved, the piezoelectric element transducers would be ideal for use on unmodified test engines or even engines in vehicles, as minimal work is required to apply it.

To advance this technique further, modifications to the test rig are required, as are developments in the electronic systems used for the ultrasonic pulsing, receiving and data storage. Finally as the research using ultrasound to measure oil film thicknesses at a fundamental level are improved, such developments can be applied to this particular application.

11.2. FUTURE WORK

The major issues that are limiting the successful measurement of oil film thicknesses on the test engine are:

- Electrical interference (noise)
- Electronics – data storage, triggering and synchronising
- Transducers and the pulsing technique

Each of these three keys areas are discussed below and potential solutions proposed.

11.2.1. Electrical Interference

The issue of electrical interference from the motor and associated inverter used to control the rotational speed of the test engine means that unshielded transducers (piezoelectric elements) produce an extremely electrically noisy signal rendering it useless. This is vastly reduced, but still visible with commercial shielded transducers. Also as the unshielded transducers are in direct contact with the engine components and therefore the motor, additional electrical interference is added to the signal too.

This can be simply solved, by firstly installing plastic insulation between the floor mountings for both the motor and test engine, and the steel floor of the engine test cell. The direct link between the motor and test engine crankshaft is already insulated, as a flexible rubber tyre coupling is used at that connection point. Secondly, further shielding of all of the wiring, both coaxial signal cables and motor power cables, will reduce electrical field interference.

11.2.2. Electronics

The current electronic measurement system has the capacity to store an extremely small amount of data (250kbytes). The total memory storage capacity is so low because the technique uses the internal memory of a LeCroy digital oscilloscope, as transmitting the data through cables to be stored in real-time on a dedicated PC is currently not possible. To store sufficiently high resolution data requires an increase in memory storage capacity of approximately 250 times the current storage capacity of the oscilloscope, for just one rotation of the crankshaft. This equates to an instantaneous storage capacity of 62.5Mbytes, but an even larger memory capacity would provide greater data resolution.

This can be solved through the use of a high capacity oscilloscope, with instantaneous storage capacity and realistically to progress the technique a memory capacity in the order of gigabytes. Such an oscilloscope would be extremely expensive; therefore a more practical approach would be to use a high capacity data logging system. It would not be possible though to use a data logging system in parallel with an oscilloscope as the same issues as are currently being experienced will occur, i.e. buffering of data and the associated delays in retransmitting data along cables. Therefore the output signal from the transducer would need to be stored directly onto the data logger, though this would mean storage of the complete pulse and not specific segments of the pulse as with the segmentation technique on the oscilloscope. The stored pulses would then require post-processing to focus on the required pulse.

Using the current measurement method the initiation of the actual recording of the pulses is determined by the push of a button on the associated the LabVIEW programme, rather than any particular occurrence in the engine's rotation i.e. TDC. Therefore an external trigger from the rotary encoder would be useful to start and stop data measurement at TDC. Due to the limitations of the UPR, when an external trigger is used, an external pulsing input is also required, i.e. a function generator. An external pulsing unit though would be extremely useful for inputting specific signals.

One final electronic modification that is required is a method to synchronise output signals, by adding artificial delays during the storage of data. The main requirement for this is in relation to the saw tooth generator that has been developed for this test engine. Obviously to create the saw tooth waveform from the two signals from the shaft encoder, signal processing is required and there is consequently an associated delay. In this case a delay of 1μsecond occurs between the input and output of the signal from the device.

11.2.3. Transducers And The Pulsing Technique

Each of the transducers used in the testing is affected to varying degrees by electrical interference; this will largely be reduced by the methods discussed in Section 11.2.1. The transducers that pose the greatest potential in the future are piezoelectric element transducers and focusing transducers. Piezoelectric element transducers will be increasingly available in smaller dimensions as the technology and demand (mainly through structural health monitoring requirements) and will therefore be applied to

this application and provide a greater resolution over a smaller area region. The focusing transducer showed significant promise and further assessment is required to match the transducer frequency to the materials of the engine and the oil film thickness dimensions.

One transducer that will most probably be successful for this type of testing, which has recently been developed at the University of Paisley, is a spluttered on type of transducer, which is capable of a very small focal spot size. Aluminium nitride is the transducer material that is deposited on the surface of the specimen via room-temperature spluttering **[115]**. When this material is spluttered onto a conductive material in a way to create a columnar structure, it acts as a piezoelectric element. To excite the transducer the aluminium nitride layer acts as one electrode and the specimen acts as the other electrode.

This method is suitable for use in the application of piston ring oil film thickness measurement, where it is spluttered onto the back face of a piston ring to measure the oil film thickness created between the front face of the piston ring and the cylinder wall, as shown in Figure 11.1. A piston ring with a spluttered on transducer is shown in Figure 11.2.

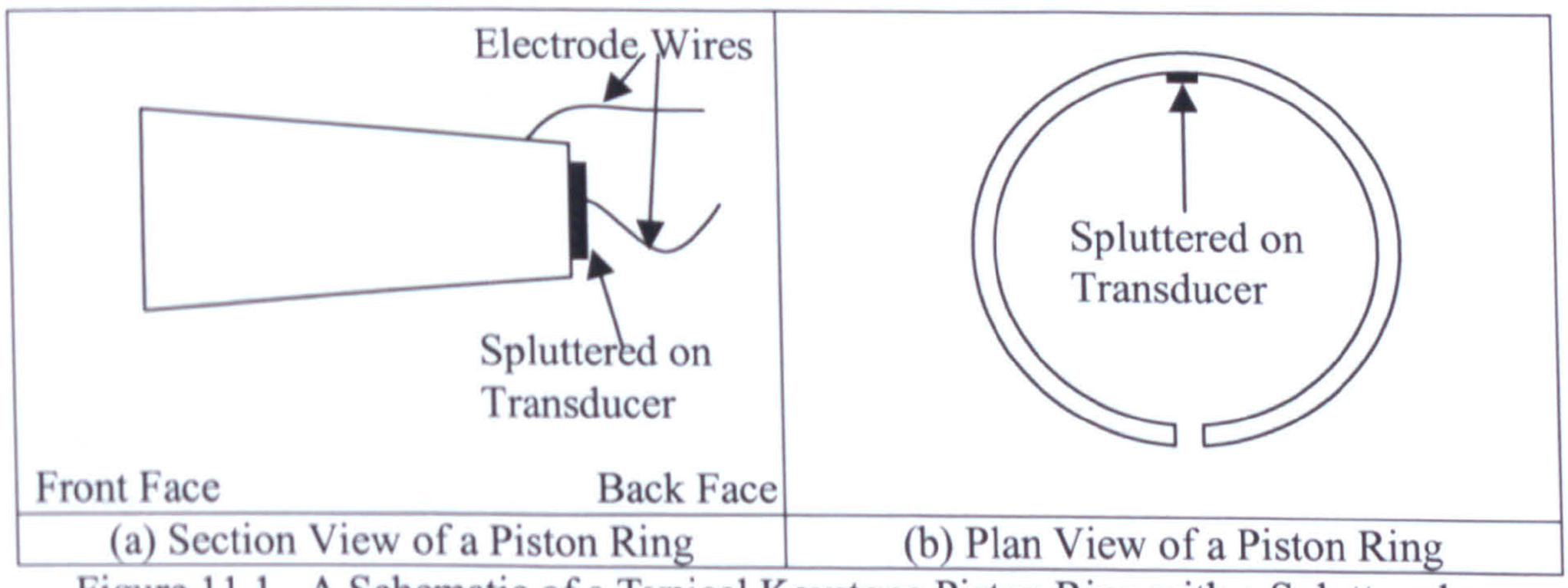

(a) Section View of a Piston Ring (b) Plan View of a Piston Ring

Figure 11.1. A Schematic of a Typical Keystone Piston Ring with a Spluttered on Transducer.

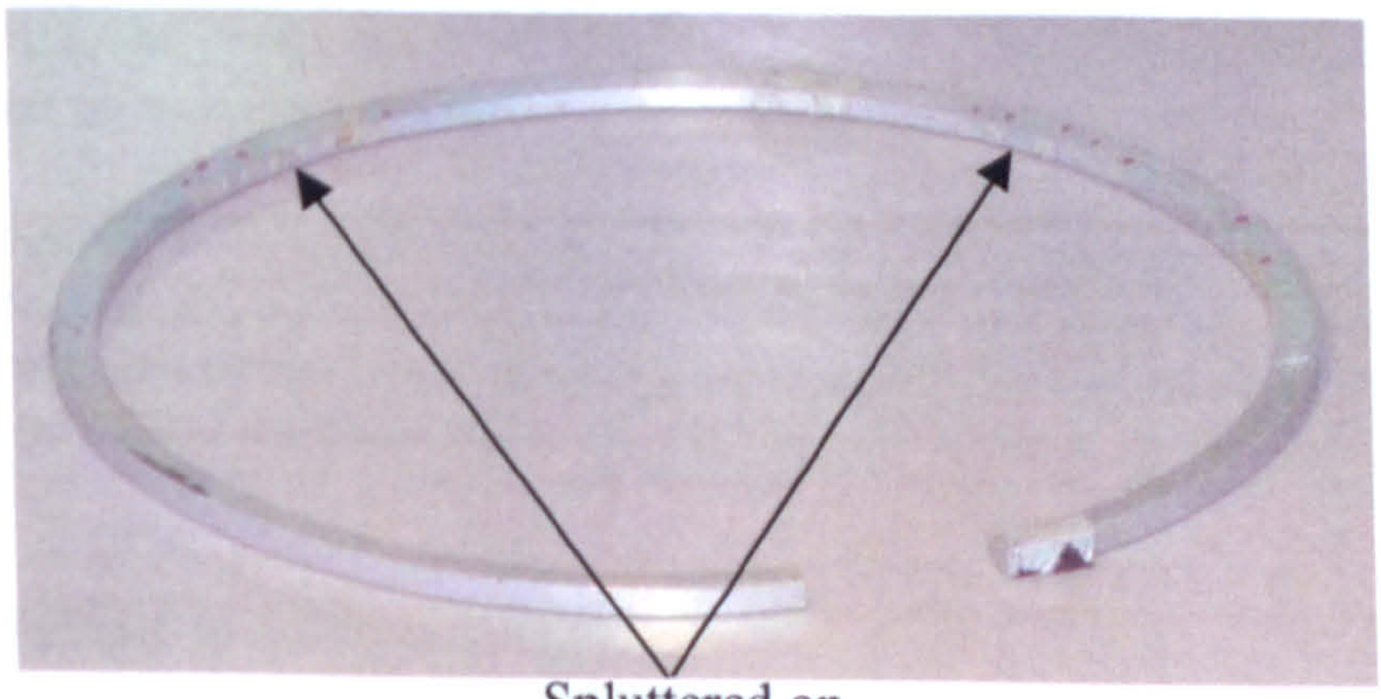

Figure 11.2. Photograph of a Piston Ring with Spluttered on Electrodes.

This technique will require specific machining of the piston on which it will locate, as a passage will need to be made in the piston body for electrical wiring to pass through. As the wires will need to be attached to the piston ring, the piston ring will need to be restrained in a way so that it cannot rotate about its groove in the piston body (as this will cause the wiring to fail), but still be able to move and flex vertically, to minimise effects on its normal operation. This spluttered on transducer technique may be seen as contradicting the key point of the ultrasonic technique of being non-invasive, but such modifications are in reality indirect modifications to the piston ring to cylinder wall contact. The rapid reciprocating motion of the piston will cause difficulty with the transmission of the signal from the piston itself to the data acquisition unit. There are three potential methods that can be applied. Firstly, the wires can be fed down the connecting rod, using a grasshopper type device **[116]** (currently used in a technique to extract sample lubricant from the ring pack zone) and feed it out the side of the engine block and to the data acquisition system. Secondly, the wiring could be fed out of the top of the piston. To do this a section from the centre of the piston crown would need to be machined away to accommodate an electrical connecting block, the wiring would then be fed out of the air holes that are machined into the top plate of the test engine. To allow for the displacement of the piston, flexible coiled wiring could link from the piston to a frame above the engine and then into the data acquisition system. One final method could be to use a wireless data transmitter located inside the piston, which would link directly to the data acquisition system. Wireless formats that could be used include FM radio signals or even Bluetooth digital data transmission. Both of the techniques involving direct wiring will be prone to fatigue of the wire, but the technique using a connection on the top of the piston and through a flexible coiled wire is the probably the more practical and most easily maintained wired solution. But the most interesting option and seemingly needing the least maintenance is the one using wireless data transmission. This spluttered on type of transducer is thought to promise the most significant research opportunities as when applied to a piston ring it will be able to measure oil film thicknesses occurring throughout the complete stroke of the piston.

Further development is also required regarding the analysis technique. The further work relates to analysis of signal data taken from pistons that contain two or more different types of material, as coefficients vary depending on the material. Once a system is developed where the exact piston location in precisely known, then software can be easily developed to apply different material coefficients during the analysis stage dependant on piston location.

Finally, very recent developments in the ultrasonic technique being developed in the Tribology group at the University of Sheffield, have found that using a specially designed pulsing waveform rather than the standard top-hat waveform will allow the measurement of thicker oil films, as lower pulsing frequencies can be achieved.

11.3. RESEARCH APPLICATIONS

Once this measurement technique and test engine has been fully developed to become reliable and repeatable, various conditions, materials and technologies can be tested.

The test rig will be able to build up an in-depth understanding of various engine operating conditions with respect to the oil film thickness that is produced. Most significantly for the various transducers applied to the engine, an understanding of the relationship between the operation of the piston rings and piston skirt can be gained. Investigations into the oil film thickness on the anti-thrust side of the piston and even other sides of the piston can be gained, to understand piston secondary motion, and how to minimise its effects and increase efficiency. If through such research direct relationships can be discovered between the different regions of the piston and from transducers located on the outside of the cylinder wall, these could be easily transferred to other test engines, including fired ones, either on engines on a dynamometer or even in a test vehicle.

This technique can be used to assess the potential and effects of incremental changes in engine design, including changes in materials used in the cylinder wall, piston body and piston rings. Another materials related area that is of interest to assess is that of surface texturing and coating, currently the main focus of this is on the piston skirt but could develop to the surface of the piston rings or surfaces within the ring pack zone. Surface texturing and coatings are generally designed (in lubricated contacts) to retain lubricant within numerous pockets on the component surface, so as it improve a surface's ability to produce the required oil film.

In combination with other test equipment developed in the Tribology Group at the University of Sheffield and standard tribological test equipment an understanding of piston to cylinder wall friction can be developed, as this is another area that is particularly difficult to measure.

Finally, the test rig engine could be used to compare the performance of different lubricants and their additive packages, in terms of oil film formation and friction reduction. It can also be used to analyse how the performance of different lubricants perform as they age and become increasing contaminated, with for example soot.

CHAPTER 12:
CONCLUSIONS AND RECOMENDATIONS

The conclusions formed from the study into the effects and wear of soot contamination of engine lubricants and the development of the ultrasonic technique to measure and understand the oil film formation around the piston are detailed in this chapter.

The recommendations for future work as discussed previously are also summarised and the details of publications that have arisen from this work are outlined.

12.1. SOOT WEAR

The background review of previous work related to soot contamination of engine lubricants demonstrated that there is a significant amount of interest in this subject from the automotive and lubricants industry. One major highlight from all of the work was that none of the investigations really tackled the issue in a methodical and practical manner, instead they either they took a highly generic route, such as 4-ball wear testing or a rather crude and unmethodical route via fully fired engine tests. Both routes demonstrated that soot contamination of engine lubricants caused component wear, but not in a way to satisfactorily compare the practical differences between various test conditions.

The main wear mechanisms proposed from previous work were:

- Chemical adsorption of the antiwear additives in the lubricant by the soot particles.
- Abrasion and polishing of the component surfaces by the soot particles in the lubricant.
- Starvation of the contact due to agglomeration of soot particles at the entrance of the contact itself.

Further findings from the background review include an understanding of the practicalities of testing with soot and the surrogate carbon black particles that can be

used for testing, and the different testing methods and test contacts that could be used for soot wear testing.

Other practical issues investigated include current and future testing standards and legislation which could be affected by soot contaminated lubricants. Future implicating trends within the automotive industry were also analysed including engine service periods, fuels and engine design.

To provide a practical basis to this work, the wear testing contact was based on an elephant's foot to valve tip engine contact. The contact is a reciprocating contact and its contact load and speed characteristics were modelled to a specimen ball-on-flat reciprocating test contact. Methodologies were devised for test specimen and lubricant preparation, the actual testing procedure and the measurement of the wear scar produced. This standardised approach ensured that minimum variation occurred during the testing.

The reciprocating wear tests were performed with base oil and a formulated lubricant, each mixed with increasing levels of carbon black contamination. After the testing, the wear scars produced were optically and physically measured and a theoretical wear groove was calculated. With all of the tests operating under boundary lubrication conditions, the results demonstrated that increasing levels of carbon black contamination causes specimen wear to increase (Chapter 4). The wear volumes measured did not tend to demonstrate a plateau in wear volume increase with increasing levels of carbon black content as maybe expected, but a continuous rise in wear, demonstrating a direct relationship between wear and carbon black content (at all contamination levels).

The different test temperatures demonstrated directly the effect of viscosity and its associated effects in reducing the oil film thickness at increased temperatures, as higher test temperatures produced significantly more wear than lower temperature tests. For all of the wear tests performed, the theoretical film thicknesses produced in the contact were less than the mean soot particle diameter of 0.2μm.

The second significant difference between wear tests depended on the type of lubricant. The base oil produced significantly greater wear volumes and increases with rising carbon black content than formulated oil. This increased protection was due to the partially the increased viscosity of formulated oil over base oil and secondly and potentially more significantly due to the additives contained within the formulated lubricant to minimise the wear effects of contamination particles. This comparative wear testing helps to demonstrate that component wear is not increased due to the soot/carbon black particles preferentially adsorbing the antiwear additives (i.e. ZDDP) in a formulated lubricant.

The wear scars produced by the specimen tests showed similarities on their surfaces, as seen via optical and SEM microscopy (Chapter 5). The characteristic wear surface features indicate the wear mechanism that dominates for various test conditions. Initially at 0% or very low carbon black concentrations the wear surfaces demonstrate purely lubricated sliding wear, with mild abrasion at approximately 2% to 3% carbon black. At the medium to high ranges of carbon black contamination, the wear surfaces appear scratched and scored, indicating an abrasive wear mechanism. At the

highest carbon black contamination levels (5% for base oil tests and 7% for formulated oil tests) there are significant signs of heavy abrasion, plus some plastic deformation, scuffing and galling, as demonstrated by a starved contact. The appearance of these wear features in relation the carbon black content depends on the type of lubricant and the test temperature. The formulated lubricant minimised the wear effects of the carbon black and the wear mechanism features appeared at a carbon black contamination level of approximately 2% higher than it would with the base oil. As oil film thickness reduced with temperature, the wear mechanism features appeared at 100°C, before they did at 25°C, with a difference in carbon black contamination level of approximately 1%.

Comparative analysis of tested and worn engine components showed similar wear mechanisms as are seen in the specimen testing. Thus demonstrating that due to the way the wear testing was designed, a practical and methodical set of tests has managed to compare as closely as possible specimen testing with system level testing.

Finally, to understand the physical properties of soot contaminated lubricants and their behaviour they were analysed (Chapter 6) via the measurement of viscosity, traction and friction, and to understand the effects of soot on the oil film itself, visualisation tests were performed. Key findings from this were that:

- increasing soot content significantly affects the viscosity of the bulk lubricant.
- increases in soot content only had a minor effect on the traction coefficient measurements operating under EHD lubrication condition.
- increasing soot content caused the measurement of reciprocating friction to increase, operating predominantly under boundary lubrication regime.

The combination of all of the results and analysis demonstrated that a key factor in understanding how soot contamination of a lubricant will affect a contact is the lubrication regime within which it is operating. This body of work has demonstrated that boundary lubricated contacts produce significant levels of wear and it is expected that contacts operating in the elastohydrodynamic regime, will suffer less wear due to the relative dimensions of the lubricant film and the soot particles, but further work is required to fully understand this. Many of the tests investigating the physical properties and effects of soot contamination showed that those operating in the boundary lubrication regime suffered considerably with an increase in contamination level, but contacts operating in the EHD lubrication regime suffered appreciably reduced effects with soot contamination.

12.2. OIL FILM THICKNESS MEASUREMENT OF A PISTON

The background review for the investigation into the measurement of the oil film thickness between a cylinder wall/liner and a piston, demonstrated that various techniques have been attempted and with varying degrees of success. Currently the most promising techniques are the capacitance and laser fluorescence methods.

The main problem with all of the current techniques is that they are invasive and require modification of the test surfaces of interest, generally requiring a window or aperture to be formed. The technique applied to this situation is this body of work was the ultrasonic technique (developed at the University of Sheffield), which is non-

invasive. Using this technique an ultrasonic pulse is transmitted through one of the contacting materials (i.e. a cylinder liner), the pulse then meets the interface between that surface and the oil film, some of the pulse is reflected back at this point (but most continues), the transmitted pulse continues through the oil film and meets the interface between the oil film and the other contacting material (i.e. a piston). At this interface due to relative difference in the acoustic properties of the test mediums, the majority of the signal is reflected back, the amplitude of this signal relates to oil film thickness.

The method required to analyse the received signal and how to convert it into an oil film thickness measurement was described.

An initial trial of the method on a single cylinder engine, to measure the oil film on the piston skirt was carried out. The results demonstrated some success and compared well with a lubricant film model for the test contact, the testing highlighted that the technique required a considerable amount to work to make it practical tool in the future.

To start the development of the technique in an engine and to provide a test platform once developed a motorised engine test rig was developed, as the platform on which to test various ultrasonic transducers and measurement methods.

The test rig demonstrated that piezoelectric element transducers and focusing transducers demonstrated the greatest potential for success in the future. Another technique using transducers spluttered on the reverse of the piston also appears to demonstrate potential for this application as it has in other applications.

A considerable amount of work is still required to develop the technique with each of the transducers and ultimately develop one which has the potential to provide the greatest success.

12.3. RECOMMENDATIONS FOR FUTURE WORK

The key recommendations for future work in both topic areas are summarised below.

12.3.1. Soot Wear

Future areas of interest to gain further understanding of soot contaminated lubricants are summarised below:

- *Types of Carbon Black and Soot.* This work has concentrated on just one type of carbon black, but others are available and may produce slightly different results, but testing with real engine soot will provide further understanding and significance to the findings

- *Lubricants and Additives.* As this body of work has only focused on baseline comparisons between base oil and formulated oils, further work would be useful to understand the real effects of different lubricant additives, particularly ZDDP.

- *Standardise Testing Method.* The method developed for this testing has proven to be reliable and provide statistically repeatable data; therefore it could be developed to become a standardised technique for understanding the effects of soot contamination under various conditions.

- *Relation to Fuels.* Diesel is the main fuel related to soot contamination, but future use of biofuels, will have also have significant effects, as some preliminary tests have already shown. The other fuel related issue include fuel dilution of the lubricant which significantly affects the combustion chamber region, where the lubricant's viscosity is reduced and therefore the oil film thickness.

- *Test Materials.* The main material used in component that current suffers greatly from soot related wear is steel, but with increasing trends to improve efficiency by reducing weight, other materials i.e. aluminium are being introduced, which may be significantly affected by soot wear. Other materials that are used for seals in particular include various plastics and PTFE; these have been shown to wear considerably due tot soot contamination in the lubricant.

- *Test Contacts.* To develop the theory that different lubrication regimes have a significant effect on the wear and performance of a contact contaminated with soot; further tests need to be carried out to measure wear and its effects in more boundary and EHD lubricated contacts.

- *Component and System Testing.* After sufficient information has been gathered from specimen level testing, then such findings need to tested and compared in system level testing either through motored engine systems or via fired engine testing.

- *In-Cylinder Testing.* As in-cylinder contacts are also susceptible to wear from soot effecting the lubrication of the contacts, then component level testing is required the flow of lubricant and soot in the contact as well as the wear levels and mechanisms that occur.

12.3.2. Oil Film Thickness Of A Piston

The major issues that are limiting the successful measurement of oil film thicknesses on the test engine are summarised below:

- *Electrical Interference.* This is mainly an issue with the test rig set-up, meaning that to reduce its effects the test rig itself needs to be insulated and the electrical and signal cables need screening too.

- *Electronics – Data Storage, Triggering and Synchronising.* The most significant issue with the current electronics set-up is that the equipment used does not have enough high speed data storage capacity, meaning that not enough data can be captured and currently the resolution of the data is compromised by attempts to increase data quantity.

With increased storage capacity, triggering techniques can be used accurately start and finish data measurement. The increased storage capacity will also allow signals relating to the positioning of the piston during a stroke to be stored. The combination of such signals will need to be synchronised though to allow to the time lost during transmission and processing of each of the input channels.

- *Transducers and the Pulsing Technique.* Many of the developments above should improve the quality of the signals received from each of the transducers, though further developments in terms of physical and focusing dimensions will assist their application to this application.

The spluttered on transducer, which is yet to be tested for this application, promises considerable potential. There are though practical issues regarding the transmission of the pulsing and receiving signal, requiring innovative wiring techniques or the use of wireless data transmission.

Further advances in the ongoing fundamental research of ultrasonic oil film thickness measurement, will allow a wider range of oil film thickness measurements increased accuracy.

12.4. PUBLICATIONS ARISING FROM THIS WORK

Details of presentations and publications that arose from this body of work are highlighted below, separated into journal papers and conference papers.

12.4.1. Journal Papers

Green, D.A., Lewis, R. and Dwyer-Joyce, R. S. *The Wear Effects and Mechanisms of Soot Contaminated Automotive Lubricants*, 2006, Proceedings of the IMech.E, Vol. 220 part J: Journal of Engineering Tribology, pp159-169.

Green, D.A., Lewis, R. and Dwyer-Joyce, R. S. *Wear of valve train components due to soot contaminated lubricant*, 2006, SAE Paper No. 2006-01-1098.

Dwyer-Joyce R.S., Green D.A., Balakrishnan S., Harper P., Lewis R., Howell-Smith S., King P.D., Rahnejat H. *The Measurement Of Liner - Piston Skirt Oil Film Thickness By An Ultrasonic Means*, 2006, SAE Paper No. 2006-01-0648.

Green, D.A., Lewis, R., Marshall, M.B. and Dwyer-Joyce, R. S. *Ultrasonic Measurement of Contact Pressures in Automotive Component Contacts*, 2006, SAE Paper No. 2006-01-1622.

Green, D.A. and Lewis, R. *Investigation of Soot Contaminated Wear Mechanisms*, 2007, JSAE, SAE Paper No. 2007-01-1964.

Green, D.A. and Lewis, R. *The Effects of Soot Contaminated Engine Oil on Wear and Friction: a Review*, 2007, Submitted to Proceedings of the IMechE, part D: Journal of Automobile Engineering.

Green, D.A. and Lewis, R. *Effect of Soot on Oil Properties and Wear of Engine Components*, 2007, Submitted to The Institute of Physics, Journal of Applied Physics: Part D.

12.4.2. Conference Papers

Green, D.A., Lewis, R. and Dwyer-Joyce, R. S. *Soot Wear of Automotive Lubricants*, 2005, extended abstract, The Mission of Tribology Research 13, IMechE Headquarters, London.

Green D.A., Dwyer-Joyce R.S., Balakrishnan S., Harper P., Lewis R., Rahnejat H. *An In-Situ Method for the Measurement of Liner - Piston Skirt Oil Film Thickness by Ultrasonic Means*, 2006, Tribology 2006: Surface Engineering and Tribology for Future Engines and Drivelines Conference, The Institution of Mechanical Engineers.

Green, D.A., Lewis, R. and Dwyer-Joyce, R. S. *The Effect of Soot Contamination on the Frictional Properties of Automotive Lubricants*, 2006, Tribology 2006: Surface Engineering and Tribology for Future Engines and Drivelines Conference, The Institution of Mechanical Engineers.

CHAPTER 13:
REFERENCES

[1] **Rounds, F.G.** *Carbon: Cause of Diesel Engine Wear?*, 1977, SAE Paper No. 770829.

[2] **Yoshida, K. and Sakurai, T.** *Some Aspects of Tribological Behaviour on Dispersed-Phase System*, 1998, Lubrication Engineering, Vol. 44, pp913-921.

[3] **Gautam, M., Durbha, M., Chitoor, K., Jaraiedi, M., Mariwalla, N. and Ripple, D.** *Contribution of Soot Contaminated Oils to Wear*, 1998, SAE Paper No. 981406.

[4] **Dennis, A.J., Garner, C.P. and Taylor, D.H.C.** *The Effect of EGR on Diesel Engine Wear*, 1999, SAE Paper No. 1999-01-0839.

[5] **Li, S., Csontos, A.A., Gable, B.M., Passut, C.A. and Jao, T.** *Wear in Cumins M-11/EGR Test Engines*, 2002, SAE Paper No. 2002-01-1672.

[6] **Clague, A.D.H., Donnet, J.B., Wang, T.K. and Peng, J.C.M.** *A Comparison of Diesel Engine Soot with Carbon Black*, 1999, Carbon, Vol. 37, pp1553-1565.

[7] **Robert Bosch GmbH** *Automotive Handbook*, 2004, Sixth Edition, Robert Bosch GmbH, Germany.

[8] **Winterbone, D.E.** *Advanced Thermodynamics for Engineers*, 1997, Arnold, UK.

[9] **Heywood, J.B.** *Internal Combustion Engine Fundamentals*, 1988, McGraw-Hill International Editions, USA.

[10] **Kennedy, I.M.** *Models of Soot Formation and Oxidation*, 1997, Progress in Energy Combustion Science, Vol. 23, pp95-132.

[11] **Taylor, C.F.** *The Internal- Combustion Engine in Theory and Practice Volume 2: Combustion, Fuels, Materials, Design*, 1985, Revised Edition, The M.I.T. Press, USA.

[12] **Stone, R.** *Introduction to Internal Combustion Engines*, 1999, Third Edition, Palgrave, New York, USA.

[13] **Lapuerta, M., Hernandez, J.J. Ballesteros, R. and Duran, A.** *Composition and size of diesel particulate emissions from a commercial European engine tested with present and future fuels*, 2003, Proceedings of the IMechE, Vol. 217, Part D: Journal of Automobile Engineering, pp907-919.

[14] **Daido, S., Kodama, Y., Inohara, T., Ohyama, N. and Sugiyama, T.** *Analysis of Soot Accumulation inside Diesel Engines*, 2000, JSAE Review, Vol. 21, pp303-308.

[15] **Querlioz, E., Ville, F., Lubrecht, A.A., Lenon, H.** *Theoretical and Experimental Investigations on the Reduction of Contact Fatigue Life under*

Starved Conditions, 2006, presented at the Leeds-Lyon Symposium on Tribology, Sept. 12-15, 2006, Leeds, UK.

[16] **Chinas-Castillo, F. and Spikes, H.A.** *The Behaviour of Diluted Sooted Oils in Lubricated Contacts*, 2004, Transient Processes in Tribology, pp37-43.

[17] **Nagai, I., Endo, H., Nakamura, H. and Yano, H.** *Soot and Valve Train Wear in Passenger Car Diesel Engines*, 1983, SAE Paper No. 831757.

[18] **Ramkumar, P., Wang, L., Harvey, T.J., Wood, R.J.K., Nelson, K., Yamaguchi, E.S., Harrison, J.J. and Powrie, H.E.G.** *The Effect of Diesel Engine Oil Contamination on Friction and Wear,* 2005, Proceedings of WTC2005, WTC2005-63854.

[19] **Yamaguchi, E.S., Untermann, M., Roby, S.H., Ryason, P.R. and Yeh, S.W.** *Soot Wear in Diesel Engines*, 2006, Proceedings of the IMech.E, Vol. 220 part J: Journal of Engineering Tribology, pp463-469.

[20] **Bell, J.C.** *Reproducing the Kinematic Conditions for Automotive Valve Train Wear in a Laboratory Test Machine*", 1996, Proceedings of the IMechE, Vol. 210, Part J: Journal of Tribology, pp135-44.

[21] **Kuo, C.C., Passut, C.A., Jao, T., Csontos, A.A. and Howe, J.M.** *Wear Mechanism in Cummins M-11 High Soot Diesel Test Engines*, 1998, SAE Paper No. 981372.

[22] **Japan Automobile Manufacturers Association** *Global Performance Specification for Diesel Engine Oil (Global DHD-1) – Recommended Guideline*, 2001, Japan Automobile Manufacturers Association, Inc.

[23] **Groff, W.P.** *Evaluation and Qualification of Gasoline and Diesel Engine Lubricants*, 1997, Southwest Research Institute USA.

[24] **ASTM** *G133-05 Standard Test Method for Linearly Reciprocating Ball-on-Flat Sliding Wear*, 1995, ASTM Book of Standards Volume: 03.02.

[25] **Truhan, J.J., Qu, J. and Blau, P.J.** *The Effect of Lubricating Oil Condition on The Friction and Wear of Piston Ring and Cylinder Liner Materials in a Reciprocating Bench Test*, 2005, Wear, Vol. 259, pp1048-1055.

[26] **Mascolo, G., Rausa, R., Bagnuolo, G., Mininni, G., Tinucci, L.** *Thermal Degradation of Synthetic Lubricants under Oxidative Pyrolytic Conditions*, 2006, Journal of Analytical and Applied Pyrolysis, Vol. 75, No. 2, pp 167-173.

[27] **Rounds, F.G.** *The Generation of Synthetic Diesel Engine Oil Soots for Wear Studies*, 1984, Lubrication Engineering, Vol. 40, 7, pp394-401.

[28] **Wedlock, D.J., Shuff, P., Dare-Edwards, M., Jia, X. and Williams, R.A.** *Experimental and Simulation Approaches to Understanding Soot Aggregation*, 1999, SAE Paper No. 1999-01-1516.

[29] **Hosonuma, K., Yoshida, K. and Matsunaga, A.** *The Decomposition Products of Zinc Dialkyldithiophosphate in an Engine and their Interaction with Diesel Soot*, 1985, Wear, Vol. 103, pp297-309.

[30] **Torrance, M.** Wear *of Lubricated Steel in the Presence of Dispersed Carbon*, 2004, IMechE Mission of Tribology Conference, The Institution of Mechanical Engineers.

[31] **Kawamutra, M., Ishiguro, T., Fujita, K. and Morimoto, H.** *Deterioration of Antiwear Properties of Diesel Engine Oils During Use*, 1988, Wear, Vol. 123, pp269-280

[32] **Berbezier, I., Martin, J.M. and Kapsa, P.** *The Role of Carbon In Lubricated Mild Wear*, 1986, Tribology International, Vol. 19, No. 3, pp115-122.

[33] **Ryason, P.R., Chan, I.Y. and Gilmore, J.T.** *Polishing Wear by Soot*, 1990, Wear, Vol. 137, pp15-24.

[34] **Gautam, M., Chitoor, K., Durbha, M. and Summers, J.C.** *Effect of Diesel Soot Contaminated Oil on Engine Wear – Investigation of Novel Oil Formulations*, 1999, Tribology International, Vol. 32, pp687-699.

[35] **Gautam, M., Chitoor, K., Balla, S. and Keane, M.** *Contribution of Soot Contaminated Oils to Wear - Part II*, 1999, SAE Paper No. 1999-01-1519.

[36] **Sato, H., Tokuoka, N., Yamamoto, H. and Sasaki, M.** *Study Of Wear Mechanism by Soot Contaminated in Engine Oil*, 1999, SAE Paper No. 1999-01-3573.

[37] **Mainwaring, R.** *Soot and Wear in Heavy Duty Diesel Engines*, 1997, SAE Paper No. 971631.

[38] **Soejima, M., Ejima, Y., Uemori, K. and Kawasaki, M.** *Studies on Friction and Wear Characteristics of Cam and Follower: Influences of Soot Contamination in Engine Oil*, 2002, JSAE review, Vol. 23, pp113-119.

[39] **Kim, C., Passut, C.A., and Zang, D.M.** *Relationships among Oil Composition Combustion-Generated Soot, and Diesel Engine Valve Train Wear*, 1992, SAE paper No. 922199.

[40] **Devlin, M.T., Baren, R.E., Sheets, R.M., McIntosh, K., Turner, T.L. and Jao, T.** *Characterization of Deposits Formed on Sequence IIIG Pistons*, 2005, SAE Paper No. 2005-01-3820.

[41] **Ishiki, K., Oshida, S., Takiguchi, M. and Urabe, M.** *A Study of Abnormal Wear in Power Cylinder of Diesel Engine With EGR – Wear Mechanism Of Soot Contaminated In Lubricating Oil*, 2000, SAE paper No. 2000-01-0925.

[42] **Yahagi, Y.** *Corrosive Wear of Diesel Engine Cylinder Bore*, 1987, Tribology International, Vol. 20, No 6, pp365-373

[43] **Masuko, M., Suzuki, A. and Ureno, T.** *Influence of Chemical and Physical Contaminants on the Antiwear Performance of Model Automotive Engine Oil*, 2006, Proceedings of the IMech.E, Vol. 220 part J: Journal of Engineering Tribology, pp455-462.

[44] **Liu, C., Nemoto, S. and Ogano, S.** *Effect of Soot Properties in Diesel Engine Oils on Frictional Characteristics*, 2003, Tribology Transactions, Vol. 46, 1, pp12-18.

[45] **Devlin, M.T., Greene, S.V. and Wooton, D.L.** *Molecular Changes to Polymeric Additives Occurring During Fuel Economy Aging Tests*, 1998, SAE Paper No. 982507.

[46] **Devlin, M.T., Lam, W.Y. and McDonnell, T.F.** *Comparison of the Physical and Chemical Changes Occurring in Oils During Aging in Vehicle and Engine Economy Tests*, 1998, SAE Paper No. 982504.

[47] **Ryason, P.R. and Hansen, T.P.** *Voluminosity Of Soot Aggregates: A Means of Characterizing Soot-Laden Oils*, 1991, SAE Paper No. 912343.

[48] **Batko, M.A., Florkowski, D.W., Devlin, M.T., Li, S., Eggerding, D.W., Lam, W.Y., McDonnell, T.F. and Jao, T.** *Low Temperature Rheological Properties of Aged Crankcase Oils*, 2000, SAE Paper No. 2000-01-2943.

[49] **Zeidan, M., Jia, X.,.Williams, R.A and Wedlock, D.J.** *Simulation of Aggregation with Applications of Soot Laden Lubricating Fluids*, 2004, Particle and Particle Systems Characterization, Vol. 21, pp473-482.

[50] **Taylor, R.I.** *Future Challenges for engine lubricants*, 2006, Tribology 2006: Surface Engineering and Tribology for Future Engines and Drivelines Conference, The Institution of Mechanical Engineers.

[51] **Taylor, R.I., Mainwaring, R. and Mortier, R.M.** *Engine Lubricant Trends Since 1990*, 2005, Proceedings of the IMech.E, Vol. 219 part J: Journal of Engineering Tribology, pp331-346.

[52] **United States Environmental Protection Agency** *Federal and California Exhaust and Evaporative Emission Standards for Light-Duty Vehicles and Light-Duty Trucks*, 2000, EPA, USA.

[53] **Kliesh, J. and Langer, T.** *Deliberating Diesel: Environmental ,Technical, and Social Factors Affecting Diesel Passenger Vehicle Prospects in the United States*, 2003, American Council for an Energy-Efficient Economy, Washington D.C., USA.

[54] **Gotze, H.J., Schneider, J.** and **Herzog, H.G.** *Determination of Polycyclic Aromatic Hydrocarbons in Diesel Soot by High Performance Liquid Chromatography*, 1991, Fresenius Journal of Analytical Chemistry, Vol. 340(1), pp27–30.

[55] **Munson, J. W.** and **Hertz, P. B.** *Seasonal Diesel Fuel And Fuel Additive Lubricity Survey Using the Munson ROCLE Bench Test*, 1999, SAE paper No. 1999-01-3588.

[56] **Beatrice, C., Bertoli, C., Del Giacomo, N.** and **Migliaccio, M.N.A.** *Potential of Oxygenated Synthetic Fuel and Reformulated Fuel on Emissions From a Modern DI Diesel Engine*, 1999, SAE paper No. 1999-01-3595.

[57] **Cheng, A.S.** and **Dibble, R.W.** *Emissions Performance of Oxygenate-In-Diesel Blends and Fischer–Tropsch Diesel in a Compression Ignition Engine*, 1999, SAE paper No. 1999-01-3606.

[58] **Staat, F. and Gateau, P.** *The Effects of Rapeseed Oil Methyl Ester on Diesel Engine Performance, Exhaust Emissions and Long-Term Behaviour — A Summary of Three Years of Experimentation*, 1995, SAE paper No. 950053.

[59] **Hansen, K.L. and Jensen, M.G.** *Chemical and Biological Characteristics of Exhaust Emissions from a DI Diesel Engine Fuelled with Rapeseed Oil Methyl Ester (RME)*, 1997, SAE paper No. 971689.

[60] **Sapuan, S.M., Masjuki, H.H. and Azlan, A.** *The Use of Palm Oil as Diesel Fuel Substitute*, 1995, Proceedings of the IMechE Vol. 210, Part D: Journal of Automobile Engineering, pp47–53.

[61] **Raadnui, S., Meenak, A.** *Effects of Refined Palm Oil (RPO) Fuel on Wear of Diesel Engine Components,* 2003, Wear, Vol. 254, pp1281-1288.

[62] **Chang, D.Y. and Van Gerpen, J.H.** *Fuel Properties and Engine Performance for Biodiesel Prepared from Modified Feedstocks*, 1997, SAE paper No. 971684.

[63] **Tritthart, P. and Zelenka, P.** *Vegetable Oils and Alcohols Additive Fuels for Diesel Engines*, 1990, SAE paper No. 905112.

[64] **Watson, J.H.P.** *Magnetic Filtration*, 1973, American Institute of Physics, Journal of Applied Physics, Vol.44, No. 9, pp4209-4213.

[65] **Papp, G. and Peeters, F.M.** *Spin Filtering in a Magnetic-Electric Barrier Structure*, 2001, American Institute of Physics, Applied Physics Letters, Vol.78, No. 15, pp2184-2186.

[66] **Hawkes, J.J., Cefai, J.J., Barrow, D.A., Coakley, W.T. and Briarty, L.G.** *Ultrasonic Manipulation of Particles in Microgravity*, 1998, Journal of Physics, Part D: Applied Physics Vol. 31, pp1673-1680.

[67] **Tarleton, E.S. and Wakeman, R.J.** *Microfiltration Enhancement by Electrical and Ultrasonic Force Fields*, 1989, Proceedings of the Filtration

Society, presented at Filtration Society at Filtech 89, Karlsruhe, West Germany, September, 1989.

[68] Gupta, S., Feke, D.L. and Manas-Zloczower, I. *Fractionation of Mixed Particulate Solids According to Compressibility Using Ultrasonic Standing Wave Fields*, 1995, Chemical Engineering Science, Vol. 50, No. 20, pp.3275-3284.

[69] Petersson, F., Nilsson, A., Holm, C., Jonsson, H. and Laurell, T. *Separation of Lipids From Blood Utilizing Ultrasonic Standing Waves in Microfluidic Channels*, 2004, The Analyst, The Royal Society of Chemistry 2004, Vol. 129, pp938-943.

[70] Booth, J.E., Nelson, K.D., Harvey, T.J., Wood, R.J.K., Wang, L., Powrie, H.E.G. and Martinez, J.G. *The Feasibility of Using Electrostatic Monitoring to Identify Diesel Lubricant Additives and Soot Contamination Interactions by Factorial Analysis*, 2006, Tribology International, Vol. 39, pp1564-1575.

[71] Park, B.Y., Paradiso, A., Kawabe, M. and Madou, M.J. *A Novel Dielectrophoretic Oil Filter*, 2006, Proceedings of the IMechE Vol. 220, Part D: Journal of Automobile Engineering, pp481-496.

[72] Wadenpohl, C. and Loffler, F. *Electrostatic Agglomeration and Centrifugal Separation of Diesel Soot Particles*, 1994, Chemical Engineering and Processing, Vol. 33, pp371-377.

[73] Needle, D.J. *Lubricants Recycling*, 1994, Industrial Lubrication and Tribology, Vol. 46 No.4, pp5-7.

[74] Bergmann, H., Rittel, A., Iourtchouk, T., Schoeps, K. and Bouzek, K. *Electrochemical Treatment of Cooling Lubricants*, 2003, Chemical Engineering and Processing, Vol. 42, pp105-119.

[75] Williams, J.A. *Engineering Tribology*, 1994, Oxford University Press.

[76] Hamrock, B.J., Schmid, S.R. and Jacobson, B.O. *Fundamentals of Fluid Film Lubrication, 2nd Edition*, 2004, Marcel Dekker, Inc.

[77] Chatfield, C. *Statistics for Technology, 3rd Edition*, 1983, Chapman and Hall, London.

[78] ASTM D341-93 *Standard Viscosity-Temperature Charts for Liquid Petroleum Products*, 1998, ASTM Book of Standards Volume: 05.01.

[79] Kaneta, M., Irie, T., Nishikawa, H. and Matsuda, K. *Effects of Soot on Wear in Elastohydrodynamic Lubrication Contacts*, 2006, Proceedings of the IMechE, Part J: Journal of Engineering Tribology, Vol.220, pp307-317.

[80] Archard, J.F. *Contact and Rubbing of Flat Surfaces*, 1953, Journal of Applied Physics, Vol. 24, No. 8, pp981-988.

[81] Rabinowicz, E. *The Wear Coefficient – Magnitude, Scatter, Uses*, 1981, Transactions of the ASME, Vol. 103, pp188-194.

[82] Andersson, B.S. *Company's Perspective in Vehicle Tribology*, 1991, Leeds-Lyon Symposium on Tribology Elsevier, pp. 503-506.

[83] Balakrishnan, S. & Rahnejat, H. *Isothermal Transient Analysis of Piston Skirt-to-Cylinder Wall Contacts |Under Combined Axial, Lateral and Tilting Motion*, 2005, J. Phys. D: Appl. Phys. 38 pp. 787–79.

[84] Brown M.A., McCann, H. and Thompson, D.M. *Characterization of The Oil Film Behaviour Between the Liner and Piston of a Heavy Duty Diesel Engine*, 1993, Tribological Insights and Performance Characteristics of Modern Engine Lubricants, SAE/SP-93/996/932784.

[85] Graddage, M.J., Czysz, F.J. and Killinger, A. *Field Testing to Validate Models Used in Explaining a Piston Problem in a Large Diesel Engine*, 1993, Transactions of the ASME J. Eng. Gas Turb. Power, Vol. 115, pp. 721-727.

[86] **Dwyer-Joyce, R.S., Harper, P. and Drinkwater, B.** *Investigation into Film Formation in a Hydro-Electric Power Station Thrust Bearing*, 2006, Proc IMechE part A, Journal of Power & Energy, Vol. 220, pp.619 – 628.

[87] **Dwyer-Joyce, R.S., Harper, P., and Drinkwater, B.** *A Method for the Measurement of Hydrodynamic Oil Films Using Ultrasonic Reflection*, 2004, Tribology Letters, Vol. 17, pp. 337-348.

[88] **Dwyer-Joyce, R.S., Reddyhoff, T., and Drinkwater, B.** *Operating Limits for Acoustic Measurement of Rolling Bearing Oil Film Thickness*, 2004, STLE Tribology Transactions, pp. 366-375, Vol. 47.

[89] **Harper, P., Dwyer-Joyce, R.S., Sjödin, U., and Olofsson, O.** Evaluation of an Ultrasonic Method for Measurement of Oil Film Thickness in a Hydraulic Motor Piston Ring, 2005, Proceedings of the 31th Leeds-Lyon Symposium on Tribology, "Life Cycle Tribology", eds. D.Dowson, M.Priest, G.Dalmaz, A.A.Lubrecht, Elsevier Tribology Series No. 48, pp. 305-312

[90] **Priest, M. and Taylor, C.M.** Automobile Engine Tribology – Approaching the Surface, 2000, Wear 241, pp193-203.

[91] **Truhan, J.J., Qu, J. and Blau, P.J.** *A Test Rig to Measure Friction and Wear of Heavy Duty Diesel Engine Piston Rings an Cylinder Liners using Realistic Lubricants*, 2005, Tribology International, Vol. 38, pp211-218.

[92] **Bolander, N.W., Steenwyk, B.D., Sadeghi, F. and Gerber, G.R.** *Lubrication Regime Transitions at the Piston Ring – Cylinder Liner Interface*, 2005, Proceedings of the IMech.E, Vol. 219 Part J: Journal of Engineering Tribology, pp19-31.

[93] **Taylor, R.I. and Evans, P.G.** *In-Situ Piston Measurements*, 2004, Proceedings of the IMech.E, Vol. 218 Part J: Journal of Engineering Tribology, pp185-200.

[94] **Truhan, J.J., Qu, J. and Blau, P.J.** *The Effect of Lubricating Oil Condition on the Friction and Wear of Piston Ring and Cylinder Liner Materials in a Reciprocating Bench Test*, 2005, Wear, Vol. 259, pp1048-1055.

[95] **Andersson, P., Tamminen, J. & Sandstrom, C.** *Piston Ring Tribology – A Literature Survey*, 2002, VTT Industrial Systems, Finland, Research Notes 2178, ESPOO 2002.

[96] **Richardson, D. E. and Borman, G. L.** *Theoretical and Experimental Investigation of Oil Films for Application to Piston Ring Lubrication*, 1992, SAE Paper 922341 (SAE SP-936).

[97] **Dearlove, J. and Cheng, W. K.** *Simultaneous Piston Ring Friction and Oil Film Thickness Measurements in a Reciprocating Test Rig. In: Recent Snapshots and Insights into Lubricant Tribology*, 1995, SAE paper No. 952470 (SAE SP-1116).

[98] **Shenghua, L., Jijun, L., Lonbao, Z. and Rong, W.** *An Experimental Investigation of the Oil Film Lubricating Piston Rings*, 1996, SAE paper No. 961912.

[99] **Harigaya, Y., Akagi, J. and Suzuki, M.** *Prediction of Temperature, Viscosity and Thickness in Oil Film Between Ring and Liner of an Internal Combustion Engine*, 2000, SAE paper No. 2000-01-1790, 9 p.

[100] **Wing, R. D. ands Saunders, O.** *Oil Film Temperature and Thickness Measurements on the Piston-Rings of a Diesel Engine*, 1972, Proceedings of the IMechE, Vol. 186, pp 1-9.

[101] **Tamminen, J., Sandstrom, C and Andersson, P.** *Influence of Load on the Tribological Conditions in Piston Ring and Cylinder Liner Contacts in a Medium-Speed Diesel Engine*, 2006, Tribology International 39 pp1643-1652.

[102] Grice, N., Sherrington, I. *An experimental investigation into the lubrication of piston-rings in an internal combustion engine - oil film thickness trends, film stability and cavitation*, 1993, SAE Paper No. 920651.

[103] Mattsson, C. *Measurement of the oil film thickness between the cylinder liner and the piston rings in a heavy duty directly injected diesel engine*, 1995, SAE paper No. 952469.

[104] Sherrington, I. and Sochting, S. *An Experimental Study of Variability in the Thickness of the Hydrodynamic Lubricant Film Between the Piston-Rings And Cylinder Bore of an Internal Combustion Engine Under Steady Operating Conditions*, 2006, Tribology 2006: Surface Engineering and Tribology for Future Engines and Drivelines Conference, The Institution of Mechanical Engineers.

[105] Richardson, D.E. and Borman, G.L. *Using Fibre Optics and Laser Fluorescence for Measuring Thin Oil Films with Applications to Engines*, 1991, SAE Paper No. 912388.

[106] Shaw, B.T., Hoult, D.P., Wong. V. *Development of Engine Lubricant Film Thickness Diagnostics Using Fibre Optics and Laser Fluorescence*, 1992, SAE paper No. 920651.

[107] Seki, T., Nakayama, K., Yamada, T., Yoshida, A. and Takiguchi, M. *A Study on Varitaion in Oil Film Thickness of a Piston Ring Package: Variation of Oil Film Thickness in Piston Sliding Direction*, 2000, JSAE Review 21 pp315-320.

[108] Frølund, K. and Schramm, J. *An Investigation of the Cylinder Wall Oil Film Development During Warm-Up of an SI-Engine Using Laser Induced Fluorescence*, 1997, SAE paper No. 971699.

[109] Datoo, A. & Fox, M. F. *The Lubricant Condition in the Ring Zone under Cold Start Conditions*, 2002, Synopses, The 29th Leeds-Lyon Symposium on Tribology, Tribological Research and Design for Engineering Systems, 3-6 September 2002.

[110] Fox, M. F., Picken, D. J., Symons, M.C.R & Thompson, A.L. *Paramagnetic species in I/C Engine Top Ring Zone Lubricant Samples*, 1996, Tribology International, 30 (1996) 6, pp.417-422.

[111] Taylor, R.I. *Transient Effects in Engine Operating at Steady Speeds and Loads*, 2003, The 30th Leeds-Lyon Symposium on Tribology, Transient Processes in Tribology, pp123-131.

[112] Balakrishnan, S., Howell-Smith, S. and Rahnejat, H. *Investigation of Reciprocating Conformal Contact of Piston Skirt-to-Surface Modified Cylinder Liner in High Performance Engines*, 2005, Proceedings of the IMechE Part C: Journal of Mechanical Engineering Science, Vol. 219, pp1235-1246.

[113] Dwyer-Joyce, R.S., Drinkwater, B.W., and Donohoe, C.J. *The Measurement of Lubricant Film Thickness using Ultrasound*, 2002, Proc. Roy. Soc., Vol. 459A, pp 957-976.

[114] Panametrics NDT Ltd, *Panametrics transducer catalogue*, 1999, Panametrics Inc.

[115] Balakrishnan, S. & Rahnejat, H. *Combined Secondary Piston Dynamics and Transient Elastohydrodynamic Analysis of Piston Skirt to Cylinder Contact Conjunctions*, 2002, AIMETA Symp., Salerno, Italy.

[116] Lee, C.K., Cochran, S., Abrar, A., Kirk, K.J. and Placido, F. *Thick Aluminium Nitride Films Deposited by Room-Temperature Spluttering for Ultrasonic Applications*, 2004, Ultrasonics, Vol. 42, pp 485-490.

[117] Saville S.B., Gainey F.D., Cupples S.D., Fox M.F. and Picken D.J. *A study of lubricant condition in the piston ring zone of single-cylinder diesel engines under typical operating conditions*, 1988, SAE paper No. 881586.

APPENDIX 1:

Carbon Black Datasheet

Material Safety Data Sheet
According to 91/155/EC

Printing date 03.06.2004 Reviewed on 28.05.2004

1 Identification of substance

Product details
Trade name: Carbon black, acetylene, (100% compressed)
Stock number: 39723
Manufacturer/Supplier: Alfa Aesar. Johnson Matthey GmbH & Co.KG
Zeppelinstrasse 7
D-76185 Karlsruhe
Tel. +49(0)721/84007-0
www.alfa-chemcat.com
Informing department: Product safety department.
Emergency information: Giftnotruf Universiat Mainz / Poison Information Center Mainz
www.giftinfo.uni-mainz.de Telefon:+49(0)6131/19240

2 Composition/Data on components:

Chemical characterization:
Designation: (CAS#) Carbon black (CAS# 1333-86-4). 100%
Identification number(s):
EINECS Number: 231-153-3

3 Hazards identification

Hazard designation: Xi Irritant
F Highly flammable

Information pertaining to particular dangers for man and environment
R 11 Highly flammable
R 36/37/38 Irritating to eyes, respiratory system and skin

4 First aid measures

After inhalation Supply fresh air. If required, provide artificial respiration. Keep patient warm. Consult doctor if symptoms persist
Seek immediate medical advice
After skin contact Instantly wash with water and soap and rinse thoroughly.
Seek immediate medical advice
After eye contact Rinse opened eye for several minutes under running water. Then consult doctor.
After swallowing Seek immediate medical advice.

5 Fire fighting measures

Suitable extinguishing agents Extinguishing powder. Do not use water.
For safety reasons unsuitable extinguishing agents Water
Special hazards caused by the material, its products of combustion or flue gases: Can be released in case of fire:
Carbon monoxide (CO)
Protective equipment: Wear self-contained breathing apparatus.
Wear full protective suit.

6 Accidental release measures

Person-related safety precautions: Wear protective equipment. Keep unprotected persons away
Ensure adequate ventilation
Keep away from ignition sources
Measures for environmental protection: Do not allow material to be released to the environment without proper governmental permits
Measures for cleaning/collecting: Ensure adequate ventilation
Keep away from ignition sources.
Additional information: See Section 7 for information on safe handling
See section 8 for information on personal protection equipment.
See Section 13 for information on disposal.

7 Handling and storage

Handling
Information for safe handling: Keep containers tightly sealed.
Store in cool, dry place in tightly closed containers
Ensure good ventilation/exhaustion at the workplace.

Information about protection against explosions and fires: Keep ignition sources away - Do not smoke.
Protect against electrostatic charges.
Fumes can combine with air to form an explosive mixture.

Storage
Requirements to be met by storerooms and containers: Store in cool location
Information about storage in one common storage facility: Store away from oxidizing agents.
Store away from halogens.
Do not store together with acids.
Further information about storage conditions: Keep container tightly sealed.
Store in cool, dry conditions in well sealed containers.

8 Exposure controls and personal protection

Additional information about design of technical systems: Properly operating chemical fume hood designed for hazardous chemicals and having an average face velocity of at least 100 feet per minute.

(Contd on page 2)

Material Safety Data Sheet
According to 91/155/EC

Printing date 03.06.2004 Reviewed on 28.05.2004

Trade name *Carbon black, acetylene, (100% compressed)*

(Contd. of page 1)

Components with critical values that require monitoring at the workplace:

Carbon black

	mg/m3
ACGIH TLV	3.5; Not classified as a human carcinogen
Belgium TWA	3.5
Denmark TWA	3.5
Finland TWA	3.5; ?-STEL
France VME	3.5
Korea TLV	3.5; Not classified as a human carcinogen
Netherlands MAC-TGG	3.5
Norway TWA	3.5
Russia	4-STEL
Sweden NGV	3 (dust)
United Kingdom TWA	3.5; 7 STEL
USA PEL	3.5

Additional Occupational Exposure Limit Values for possible hazards during processing: Not applicable
Additional information: No data

Personal protective equipment
General protective and hygienic measures: The usual precautionary measures should be adhered to in handling the chemicals.
Keep away from foodstuffs, beverages and food.
Instantly remove any soiled and impregnated garments.
Wash hands during breaks and at the end of the work
Avoid contact with the eyes and skin.
Breathing equipment: Use breathing protection with high concentrations
Protection of hands: Impervious gloves
Eye protection: Safety glasses
Face protection
Body protection: Protective work clothing.

9 Physical and chemical properties:

General Information

Form:	Powder
Colour:	Black
Smell:	Odourless
Change in condition	
Melting point/Melting range:	3652-3697 °C
Boiling point/Boiling range:	4200°C
Sublimation temperature / start:	Not determined
Flash point:	Not applicable
Inflammability (solid, gaseous)	Highly flammable.
Ignition temperature:	900°C
Decomposition temperature:	Not determined
Critical values for explosion:	
Lower:	Not determined
Upper:	Not determined
Steam pressure:	Not determined
Density at 20°C	1.8-2.1 g/cm³
Solubility in / Miscibility with	
Water:	Insoluble

10 Stability and reactivity

Thermal decomposition / conditions to be avoided: No decomposition if used and stored according to specifications.
Materials to be avoided: Oxidizing agents
Acids
Halogens
Dangerous reactions: No dangerous reactions known
Dangerous products of decomposition: Carbon monoxide and carbon dioxide

11 Toxicological Information

Acute toxicity:
Primary irritant effect:
on the skin: Irritant for skin and mucous membranes.
on the eye: Irritant effect.
Sensitization: No sensitizing effect known.
Additional toxicological information: To the best of our knowledge the acute and chronic toxicity of this substance is not fully known.
IARC-2B: Possibly carcinogenic to humans: limited evidence in humans in the absence of sufficient evidence in experimental animals.
ACGIH A4: Not classifiable as a human carcinogen: Inadequate data on which to classify the agent in terms of it's carcinogenicity in humans and/or animals

12 Ecological information:

General notes: Generally not hazardous for water.
Do not allow material to be released to the environment without proper governmental permits.

GB

(Contd. on page 3)

Material Safety Data Sheet
According to 91/155/EC

Printing date 03.06.2004 Reviewed on 28.05.2004

Trade name **Carbon black, acetylene, (100% compressed)**

(Contd. of page 2)

13 Disposal considerations

Product:
Recommendation Consult state, local or national regulations for proper disposal.
Hand over to disposers of hazardous waste.
Must be specially treated under adherence to official regulations.

Uncleaned packagings:
Recommendation: Disposal must be made according to official regulations.

14 Transport Information

Land transport ADR/RID and GGVS/GGVE (cross-border/domestic)

ADR/RID-GGVS/E Class: 4.1 (F1)
Kemler Number: 40
UN-Number: 1325
Packaging group: III
Label 4.1
Designation of goods: 1325 FLAMMABLE SOLID, ORGANIC, N.O.S. (carbon black)

Maritime transport IMDG/GGVSea:

IMDG/GGVSea Class: 4.1
UN Number: 1325
Label 4.1
Packaging group: III
Correct technical name: FLAMMABLE SOLID, ORGANIC, N.O.S. (carbon black)

Air transport ICAO-TI and IATA-DGR:

ICAO/IATA Class: 4.1
UN/ID Number: 1325
Label 4.1
Packaging group: III
Correct technical name: FLAMMABLE SOLID, ORGANIC, N.O.S. (carbon black)

15 Regulatory Information

Designation according to EC guidelines:

Code letter and hazard designation of product:

Xi Irritant
F Highly flammable

Risk phrases: 11 Highly flammable.
36/37/38 Irritating to eyes, respiratory system and skin.

Safety phrases: 26 In case of contact with eyes, rinse immediately with plenty of water and seek medical advice.

National regulations

Information about limitation of use: Employment restrictions concerning young persons must be observed
For use only by technically qualified individuals.

Water hazard class: Generally not hazardous for water.

16 Other Information:

Employers should use this information only as a supplement to other information gathered by them, and should make independent judgement of suitability of this information to ensure proper use and protect the health and safety of employees. This information is furnished without warranty, and any use of the product not in conformance with this Material Safety Data Sheet, or in combination with any other product or process, is the responsibility of the user.

Department issuing data specification sheet: Health, Safety and Environmental Department.
Contact: Darrell R. Sanders

GB

APPENDIX 2:
Base Oil Test Data

All Base Oil Test Data

	A	B	C	D	E	F	G	H
1	CB Content	Temp	Ra	Rq	Rt	Wear Depth (mm)	Wear Depth (microns)	Percentage Inc in wear depth
2								
3								
4								
5	0%	25	0.275333	0.364	1.902	0.001141667	1.141666667	0
6	1%	25	0.3562	0.4774	2.2632	0.0011594	1.1594	0.015532847
7	2%	25	0.416	0.519333333	2.392666667	0.001248333	1.248333333	0.093430657
8	3%	25	0.500667	0.626666667	2.942666667	0.001540333	1.540333333	0.34919708
9	4%	25	0.623333	0.779	3.325	0.001662667	1.662666667	0.456350365
10	5%	25	0.514333	0.631	2.736	0.001765333	1.765333333	0.546277372
11								
12	0%	25-100	0.486333	0.605	2.688333333	0.001159	1.159	0
13	1%	25-100	0.448667	0.581666667	2.945	0.001718667	1.718666667	0.482887547
14	2%	25-100	0.661333	0.864666667	4.097666667	0.002405667	2.405666667	1.075639919
15	3%	25-100	0.917333	1.113	4.346	0.002624	2.624	1.264020708
16	4%	25-100	1.017	1.315333333	5.063666667	0.003191667	3.191666667	1.753810756
17	5%	25-100	1.379333	1.67	6.097666667	0.003711	3.711	2.201898188
18								
19	0%	100	0.214667	0.266	1.417333333	0.000831667	0.831666667	0
20	1%	100	0.307	0.407333333	2.287666667	0.001455333	1.455333333	0.7498998
21	2%	100	0.7645	0.9415	4.009	0.002151	2.151	1.586372745
22	3%	100	0.50275	0.6535	5.4475	0.00242875	2.42875	1.920340681
23	4%	100	0.907333	1.201	5.008	0.003212	3.212	2.862124248
24	5%	100	1.229333	1.484333333	5.482333333	0.003402333	3.402333333	3.090981964

All Base Oil Test Data Continued

	I	J	K	L	M	N	O	P
1	Max Value (microns)	Max Diff	Min Value (microns)	Min Diff	Width (mm)	Width (microns)	Length (mm)	Length (microns)
2								
3								
4								
5	1.366	0.224333333	0.753	0.388666667	0.267233333	267.2333333	1.7586	1758.6
6	2.257	1.0976	0.633	0.5264	0.38278	382.78	1.95	1950
7	1.791	0.542666667	0.744	0.504333333	0.396533333	396.5333333	2.0086	2008.6
8	2.307	0.766666667	1.007	0.533333333	0.5517	551.7	1.827566667	1827.566667
9	1.874	0.211333333	1.28	0.382666667	0.465533333	465.5333333	1.870666667	1870.666667
10	1.778	0.012666667	1.747	0.018333333	0.4569	456.9	1.767233333	1767.233333
11								
12	2.289	1.13	0.576	0.583	0.422433333	422.4333333	1.5948	1594.8
13	2.688	0.969333333	1.019	0.699666667	0.508633333	508.6333333	1.931033333	1931.033333
14	2.668	0.262333333	2.273	0.132666667	0.439666667	439.6666667	1.939666667	1939.666667
15	3.33	0.706	1.968	0.656	0.508633333	508.6333333	1.896533333	1896.533333
16	3.656	0.464333333	2.615	0.576666667	0.439633333	439.6333333	2.181033333	2181.033333
17	4.668	0.957	3.142	0.569	0.517233333	517.2333333	2.051733333	2051.733333
18								
19	0.962	0.130333333	0.694	0.137666667	0.4655	465.5	1.931033333	1931.033333
20	1.945	0.489666667	0.878	0.577333333	0.491366667	491.3666667	1.836233333	1836.233333
21	2.35	0.199	1.952	0.199	0.46555	465.55	2.00435	2004.35
22	3.057	0.62825	1.997	0.43175	0.45905	321.775	1.829725	1885.775
23	4.4	1.188	1.204	2.008	0.491366667	491.3666667	1.870666667	1870.666667
24	3.698	0.295666667	3.126	0.276333333	0.5	500	2.086233333	2086.233333

All Base Oil Test Data Continued

	Q	R	S	T	U
1	V of both curved ends (mm^3)	V of both curved ends (microns^3)	Cap radius, a (mm)	Cap radius, a (microns)	Modified Length (sub 2a) (mm)
2					
3					
4					
5	1.0833E-05	10833.01575	0.074928454	74.92845351	1.608743093
6	1.39368E-05	13936.76048	0.07329665	73.29664954	1.803406701
7	1.36771E-05	13677.0804	0.07779117	77.79117014	1.85301766
8	2.10552E-05	21055.15302	0.086385235	86.38523519	1.654796196
9	2.2284E-05	22283.97741	0.090837644	90.83764361	1.688991379
10	2.44718E-05	24471.78425	0.093933089	93.93308881	1.579367156
11					
12	1.55618E-05	15561.84218	0.071977746	71.9777458	1.450844508
13	2.71229E-05	27122.86089	0.090792358	90.79235788	1.749448618
14	4.57082E-05	45708.23317	0.109567806	109.5678061	1.720531054
15	5.64942E-05	56494.17784	0.11386199	113.8619904	1.668809353
16	8.14386E-05	81438.63732	0.12598595	125.9859501	1.929061433
17	0.000111742	111741.5459	0.135619836	135.6198359	1.780493661
18					
19	5.52595E-06	5525.954097	0.064337831	64.33783144	1.80235767
20	1.81511E-05	18151.06696	0.084223003	84.22300275	1.667787328
21	3.66391E-05	36639.14603	0.103572683	103.5726833	1.797204633
22	4.75434E-05	47543.4264	0.109819418	109.8194175	1.610086165
23	9.6987E-05	96987.01185	0.122588888	122.588888	1.625488891
24	9.13046E-05	91304.60727	0.13030741	130.30741	1.825618513

All Base Oil Test Data Continued

	V	W	X	Y	Z	AA	AB
1	Modified Length (sub 2a) (microns)	Volume (mm^3)	Percentage Inc in wear vol	Standard Deviation	Test range/sqrt(n)	test/SD	SD/Mean Vol(mm^3) Coeff of Variation
2							
3		0.068537896					
4							
5	1608.743093	0.000213821	0	8.06021E-05	8.08769E-05	1.00340926	0.376960017
6	1803.406701	0.000269508	0.260433371	0.000248771	0.000327685	1.317212685	0.92305886
7	1853.01766	0.00028464	0.331205724	0.000135007	0.000182917	1.354874804	0.474306816
8	1654.796196	0.000384842	0.799827788	0.000304769	0.000325145	1.06685781	0.791933976
9	1688.991379	0.000407772	0.907067238	0.000134757	0.000141891	1.052939656	0.330471737
10	1579.367156	0.000415184	0.941735161	7.32837E-05	1.14252E-05	0.155903929	0.176508821
11							
12	1450.844508	0.000185273	0	0.000258737	0.000261937	1.01236735	1.396519969
13	1749.448618	0.000481952	1.601305743	0.000401383	0.000436779	1.088186048	0.832828179
14	1720.531054	0.000723427	2.904657429	7.92757E-05	4.279E-05	0.539761645	0.109583572
15	1668.809353	0.000842724	3.548556248	0.000334594	0.000430116	1.285484568	0.397038672
16	1929.061433	0.001232721	5.653541544	0.000178314	0.000195827	1.098218683	0.144650485
17	1780.493661	0.001499059	7.091083015	0.000468621	0.000482083	1.028728123	0.312610083
18							
19	1802.35767	0.000145067	0	4.04071E-05	4.58992E-05	1.135919078	0.278540817
20	1667.787328	0.000322875	1.225693133	0.000148874	0.000168847	1.134157915	0.461089301
21	1797.204633	0.000628761	3.334271496	0.000321727	5.42289E-05	0.16855534	0.511685058
22	1666.136165	0.000705938	3.866282197	0.000289636	0.000260903	0.900796017	0.41028497
23	1625.488891	0.001200908	7.278289093	0.000839742	0.000897343	1.068593096	0.699255795
24	1825.618513	0.001326391	8.143283424	0.000157596	0.000180514	1.145425257	0.118815364

Base Oil Tests Results

	A	B	C	D	E	F	G	H	I
1	Test No.	Ra	Rq	Rt	Wear Depth (microns)	Width (mm)	Length (mm)	Volume (mm^3)	Volume (microns^3)
2									
3	BO + 4% Disp + 1% CB		25 degC						
4	Test 6	0.478	0.65	2.828	0.687	0.4138	2.3017	0.00012727	127269.8421
5	Test 4	0.427	0.599	2.532	1.581	0.4914	1.9914	0.000392825	392824.9703
6	Test 5	0.181	0.227	1.27	0.633	0.3621	1.8621	9.15597E-05	91559.67359
7	Average	0.362	0.492	2.21	0.967	0.422433333	2.051733333	0.000203885	203884.8287
8								0.000248771	
9	BO + 4% Disp + 1% CB		25-100 degC						
10	Test 6	0.39	0.595	3.872	2.688	0.4914	2.1207	0.000937729	937729.2225
11	Test 3	0.344	0.446	2.286	1.019	0.4914	1.7845	0.000181206	181205.5185
12	Test 4	0.612	0.704	2.677	1.449	0.5431	1.8879	0.00032692	326919.799
13	Average	0.448666667	0.581666667	2.945	1.718666667	0.508633333	1.931033333	0.000481952	481951.5133
14								0.000401383	
15	BO + 4% Disp + 1% CB		100 degC						
16	Test 7	0.258	0.328	1.871	0.878	0.569	1.9914	0.000160509	160508.5026
17	Test 8	0.315	0.402	2.375	1.543	0.5172	1.8621	0.000355157	355156.8284
18	Test 9	0.348	0.492	2.617	1.945	0.3879	1.6552	0.00045296	452959.9214
19	Average	0.307	0.407333333	2.287666667	1.455333333	0.491366667	1.836233333	0.000322875	322875.0841
20									
21									
22	BO + 4% Disp + 2% CB		25 degC						
23	Test 6	0.687	0.849	3.729	1.791	0.4138	1.8362	0.000440084	440084.177
24	Test 1	0.25	0.308	1.477	0.744	0.3879	1.9655	0.000123262	123262.0747
25	Test 2	0.374	0.443	1.771	0.97	0.3879	2.2241	0.000207702	207702.4263
26	Test 2a	0.311	0.401	1.972	1.21	0.3879	2.2241	0.000290574	290574.4975
27	Average	0.416	0.519333333	2.392666667	1.248333333	0.396533333	2.0086	0.00028464	284640.2497
28								0.000135007	
29	BO + 4% Disp + 2% CB		25-100 degC						
30	Test 7	0.604	0.855	3.907	2.948	0.3879	1.7328	0.000895003	895003.3305
31	Test 3	0.868	1.065	5.266	2.317	0.4397	2.069	0.000730031	730031.3251
32	Test 6	0.843	0.993	3.972	2.576	0.4914	2.0172	0.000838284	838283.6326
33	Test 7a	0.702	0.919	4.185	2.668	0.3879	1.7328	0.000767725	767724.863
34	Test 3a	0.59	0.74	3.273	2.273	0.4397	2.069	0.000708947	708946.6021
35	Test 6a	0.692	0.935	4.835	2.276	0.4914	2.0172	0.00069361	693610.3962

Base Oil Tests Results Continued

	A	B	C	D	E	F	G	H	I
36	Average	0.661333333	0.864666667	4.097666667	2.405666667	0.439666667	1.939666667	0.000723427	723427.2871
37								7.92757E-05	
38	BO + 4% Disp + 2% CB		100 degC						
39	Test 8	1.444	1.749	8 11	4.016	0.4914	1.7586	0.001460667	1460667.271
40	Test 4	1.154	1.375	5 222	2.984	0.4914	2.1466	0.001112932	1112932 486
41	Test 5	0.929	1.166	4.761	2.957	0.4397	1 8621	0.000961185	961184 836
42	Test 8a	1.023	1.222	5 092	2.727	0.4914	1.7586	0.000804915	804915.4309
43	Test 4a	0.668	0 821	3.731	1.952	0.4914	2.1466	0.000581797	581797.0707
44	Test 5a	0.861	1.062	4.287	2.35	0.4397	1.8621	0.000675724	675724.2407
45	Average	0.7645	0.9415	4.009	2.151	0.46555	2.00435	0.000628761	628760.6557
46									
47									
48	BO + 4% Disp + 3% CB		25 degC						
49	Test 1	0.971	1.202	4.901	2.307	0 931	2.0948	0.000733743	733742.5415
50	Test 2	0.304	0.374	2.485	1.307	0.3362	1.681	0.000250208	250208.2615
51	Test 3	0.227	0.304	1 442	1.007	0.3879	1.7069	0.000170574	170574.2007
52	Average	0.500666667	0.626666667	2.942666667	1.540333333	0.5517	1.827566667	0.000384842	384841.6679
53								0.000304769	
54	BO + 4% Disp + 3% CB		25-100 degC						
55	Test 4	0.506	0.637	2.824	1.185	0.3621	1.681	0.000215454	215453.9403
56	Test 1	0.667	0.794	3.621	1.426	0.5948	2.0431	0.000343954	343953.9846
57	Test 2	1.305	1.561	6.932	2.736	0.569	1.9655	0.000897264	897264.4161
58	Test 4a	0.504	0.611	2.879	1.968	0.3621	1.681	0.00046791	467910.4235
59	Test 1a	0.859	1.006	3.165	1.7791	0.5948	2.0431	0.000481908	481907.5253
60	Test 2a	1.499	1.845	7.116	3.33	0 569	1.9655	0.001212892	1212892.497
61	Test 1b	0.749	0.883	3.043	2.574	0.5948	2.0431	0.00084737	847369.9863
62	E2A	0.228	0.288	8.876	1.846	0.4655	1.8879	0.000473135	452351.7316
63	Average	0.917333333	1.113	4.346	2.624	0.508633333	1.896533333	0.000842724	842724.3021
64								0.000334594	
65	BO + 4% Disp + 3% CB		100 degC						
66	Test 5	0.835	1.135	5.041	2.871	0.4397	1.8103	0.000894849	894848.7794
67	Test 6	0.404	0.493	2.53	1.164	0.4914	1.7069	0.000212723	212723.2229
68	Test 7	0.485	0.613	2.608	1.574	0.4655	1.7328	0.000342035	342034.5717
69	Test 5a	0.909	1.172	4.414	3.057	0.4397	1.8103	0.000985458	985457.6647
70	Test 6a	0.404	0.493	2.53	1.288	0.4914	1.7069	0.000248246	248245.8871

Base Oil Tests Results Continued

	A	B	C	D	E	F	G	H	I
71	Test 7a	0.453	0.584	2.624	2.216	0.4655	1.7328	0.000577408	577408.2615
72	E3	0.391	0.525	6.876	2.445	0.4655	1.8879	0.000727325	695646.3287
73	E3A	0.258	0.333	7.876	1.997	0.4655	1.8879	0.000533561	616590.43
74	Average	0.50275	0.6535	5.4475	2.42875	0.45905	1.829725	0.000705938	718775.6712
75								0.000289636	
76									
77	BO + 4% D	25 degC							
78	Test 1	0.673	0.83	3.701	1.834	0.4914	2.0172	0.000498717	498717.3224
79	Test 7	0.745	0.957	4.179	1.874	0.4914	1.8362	0.000471643	471643.0978
80	Test 8	0.452	0.55	2.095	1.28	0.4138	1.7586	0.000252955	252954.8463
81	Average	0.623333333	0.779	3.325	1.662666667	0.465533333	1.870666667	0.000407772	407771.7555
82								0.000134757	
83	BO + 4% D	25-100 degC							
84	Test 2	1.161	1.53	5.742	3.656	0.4655	2.0172	0.001434117	1434116.633
85	Test 9	0.968	1.284	5.555	3.304	0.3879	1.9138	0.001169113	1169113.038
86	Test 1	0.922	1.132	3.894	2.615	0.4655	2.6121	0.001094934	1094933.559
87	Average	1.017	1.315333333	5.063666667	3.191666667	0.439633333	2.181033333	0.001232721	1232721.076
88								0.000178314	
89	BO + 4% D	100 degC							
90	Test 3	1.217	1.621	7.035	4.4	0.4655	1.8879	0.001794319	1794318.941
91	Test 10	1.079	1.452	5.796	4.032	0.4914	1.8879	0.00156833	1568329.854
92	Test 11	0.426	0.53	2.193	1.204	0.5172	1.8362	0.000240076	240076.011
93	Average	0.907333333	1.201	5.008	3.212	0.491366667	1.870666667	0.001200908	1200908.269
94								0.000839742	
95									
96	BO + 4% Disp + 5% CB		25 degC						
97	Test 1	0.449	0.545	2.614	1.778	0.3879	1.7845	0.000423656	423656.244
98	Test 2	0.499	0.598	2.826	1.747	0.569	1.8103	0.00041803	418030.0716
99	Test 3	0.595	0.75	2.768	1.771	0.4138	1.7069	0.000403867	403867.1809
100	Test 1	0.338	0.436	2.46	1.413	0.4138	1.6034	0.000269566	269565.9821
101	Average	0.514333333	0.631	2.736	1.765333333	0.4569	1.767233333	0.000415184	415184.4988
102								7.32837E-05	
103	BO + 4% Disp + 5% CB		25-100 degC						
104	Test 4	1.485	1.902	6.973	4.668	0.5172	1.9655	0.00203944	2039440.062
105	Test 2	1.172	1.423	5.505	3.142	0.4655	2.1466	0.001204447	1204447.077

Base Oil Tests Results Continued

	A	B	C	D	E	F	G	H	I
106	Test 4	1.481	1.685	5.815	3.323	0.569	2.0431	0.001253289	1253288.613
107	Average	1.379333333	1.67	6.097666667	3.711	0.517233333	2.051733333	0.001499059	1499058.584
108								0.000468621	
109	BO + 4% Disp + 5% CB		100 degC						
110	Test 5	1.183	1.378	5.438	3.126	0.4397	2.1207	0.00118157	1181570.325
111	Test 3	1.375	1.627	5.667	3.383	0.5172	2.069	0.001303372	1303371.743
112	Test 5	1.13	1.448	5.342	3.698	0.5431	2.069	0.00149423	1494229.671
113	Average	1.229333333	1.484333333	5.482333333	3.402333333	0.5	2.086233333	0.001326391	1326390.579

Graph of Base Oil Wear Volumes (25 and 100°C)

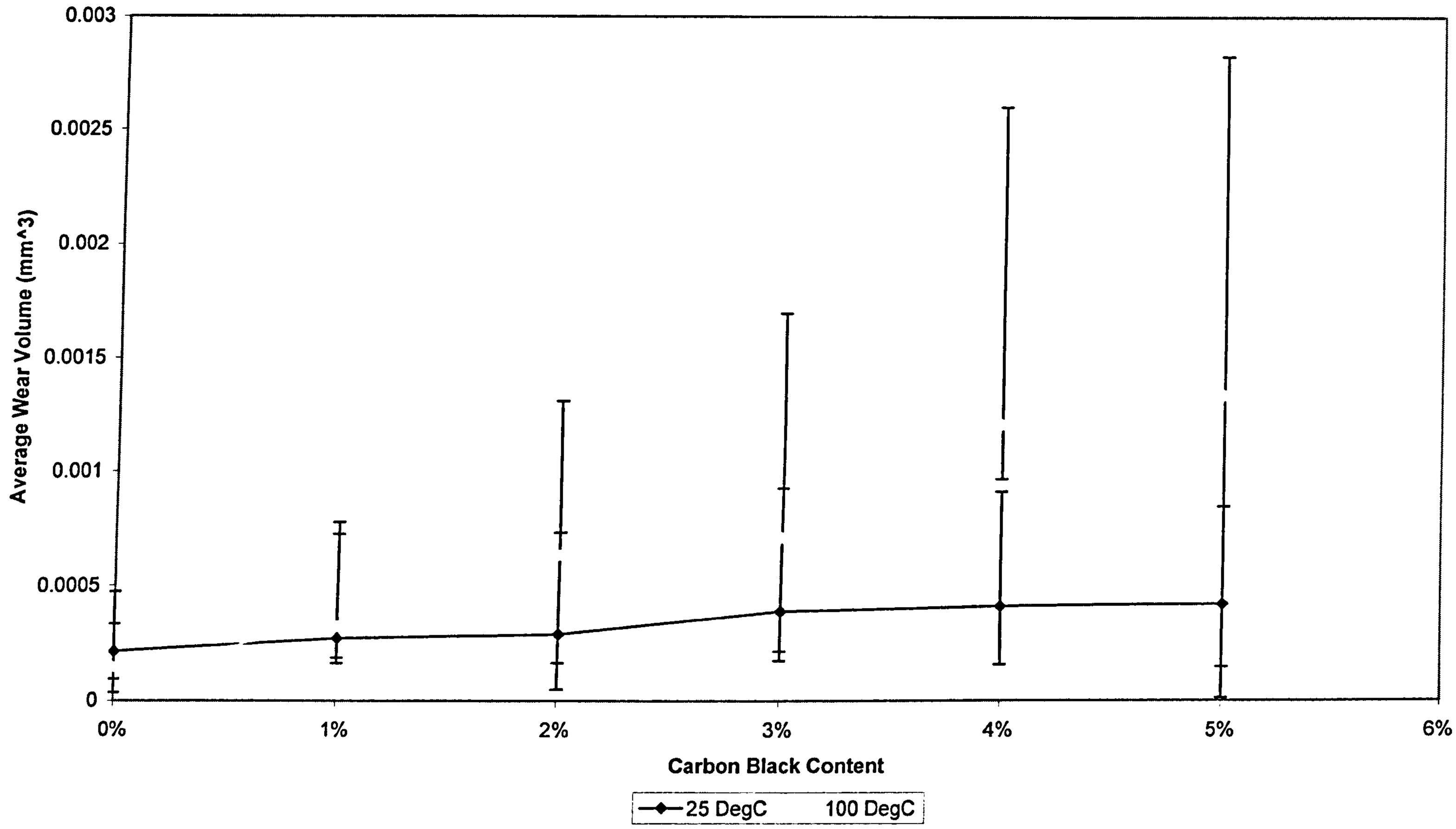

APPENDIX 3:

Formulated Oil Test Data

All Formulated Wear Volume Data

	A	B	C	D	E	F	G
3	Test	Temperature °C	Percentage	Depth (mm)	Length (mm)	Width (mm)	Wear volume (mm^3)
4	1	25	0%	0.001081	0.8638	0.2402	0.000075252
5	2	25	0%	0.001101	0.8468	0.1804	0.000082098
6	3	25	0%	0.002643	0.9213	0.3235	0.000296979
7	4	25	0%	0.000846	0.7958	0.1218	0.000055065
8	5	25	0%	0.000751	0.9209	0.1697	0.000050521
9	6	25	0%	0.001225	0.9827	0.3284	0.000095416
10	1	25	1%	0.001951	0.9077	0.2546	0.000197667
11	2	25	1%	0.000626	0.9322	0.2865	0.000033228
12	3	25	1%	0.000578	0.9561	0.2717	0.000030977
13	4	25	1%	0.000871	0.9781	0.2330	0.000063059
14	5	25	1%	0.000384	1.2443	0.3057	0.000022215
15	6	25	1%	0.000549	1.2396	0.3161	0.000037783
16	1	25	3%	0.000439	0.9187	0.3416	0.000017339
17	2	25	3%	0.001028	0.7538	0.2406	0.000058727
18	3	25	3%	0.001914	0.8682	0.2550	0.000181834
19	4	25	3%	0.000871	0.7846	0.2149	0.000049617
20	1	25	5%	0.000863	1.1855	0.3035	0.000072538
21	2	25	5%	0.002061	0.8723	0.2363	0.000210748
22	3	25	5%	0.000636	0.7703	0.1642	0.000032159
23	4	25	5%	0.002478	0.9022	0.2772	0.000278033
24	1	25	7%	0.002255	0.8880	0.2837	0.000232828
25	2	25	7%	0.002034	0.8923	0.2758	0.000201074
26	3	25	7%	0.001363	0.8551	0.2885	0.000099586
27	4	25	7%	0.001949	0.8637	0.2771	0.000180290
28	1	100	0%	0.005428	1.0894	0.4267	0.001021112
29	2	100	0%	0.009477	1.1107	0.4920	0.002405341
30	3	100	0%	0.007546	1.0341	0.4550	0.001578015
31	4	100	0%	0.000956	0.8065	0.1909	0.000061425
32	5	100	0%	0.008517	1.0287	0.4647	0.001890099
33	6	100	0%	0.010335	1.2264	0.5772	0.002870095
34	7	100	0%	0.00227325	0.8079	0.2237	0.000229329
35	1	100	1%	0.003284	0.9618	0.3052	0.000453001
36	2	100	1%	0.006365	1.0277	0.4439	0.001201446
37	3	100	1%	0.004612	1.0213	0.3977	0.000749117
38	4	100	1%	0.004301	0.9638	0.3417	0.000668234
39	5	100	1%	0.003175	1.0879	0.4490	0.000419853
40	6	100	1%	0.003114	1.0088	0.4145	0.000383969
41	1	100	3%	0.005137	1.0528	0.4657	0.000851383
42	2	100	3%	0.004889	0.9363	0.3830	0.000751357
43	3	100	3%	0.006715	0.9802	0.3935	0.001315959
44	4	100	3%	0.005046	0.9736	0.4073	0.000804850
45	1	100	5%	0.007379	1.1275	0.5405	0.001536058
46	2	100	5%	0.009059	1.1231	0.5408	0.002139842
47	3	100	5%	0.008652	1.0703	0.4817	0.001998788
48	4	100	5%	0.007116	1.0550	0.4333	0.001509503
49	1	100	7%	0.007905	1.1014	0.4582	0.001837422
50	2	100	7%	0.006578	1.1034	0.4831	0.001325812
51	3	100	7%	0.006502	1.0528	0.4427	0.001285039
52	4	100	7%	0.011215	1.1891	0.5419	0.003276542

Formulated Oil Test Results

	A	B	C	D	E	F	G	H	I
1				25 deg C		Test	test/SD	SD/Mean Vol(mm^3)	Volume (m^3)
2	Soot	Wear Volume (mm^3)	%age inc	%age inc	Standard Deviation	range/sqrt(n)		Coeff of Variation	
3	0%	0.000071670	1	0	9.35004E-05	0.000142293	1.521839116	1.30	7.16704E-14
4	1%	0.000074914	1.045258597	4.525859697	6.68405E-05	0.000101297	1.515507652	0.89	7.49141E-14
5	3%	0.000096726	1.349596544	34.95965436	7.21881E-05	9.49714E-05	1.315610226	0.75	9.67261E-14
6	5%	0.000148370	2.070167287	107.0167287	0.000115411	0.000141955	1.22999893	0.78	1.4837E-13
7	7%	0.000204731	2.856560331	185.6560331	5.6838E-05	7.69272E-05	1.353445614	0.28	2.04731E-13
8									
9									
10				100 deg C		Test	test/SD	SD/Mean Vol(mm^3)	Volume (m^3)
11	Soot	Wear Volume (mm^3)	%age inc	%age inc	Standard Deviation	range/sqrt(n)		Coeff of Variation	
12	0%	0.00072247	1	0	0.000835696	0.001621586	1.940401057	1.16	7.2247E-13
13	1%	0.00075966	1.051479517	5.147951654	0.000308772	0.000471971	1.528543262	0.41	7.59663E-13
14	3%	0.00108367	1.499951899	49.99518992	0.000259947	0.000325973	1.253997824	0.24	1.08367E-12
15	5%	0.00179605	2.485981569	148.5981569	0.000320937	0.000363926	1.133951115	0.18	1.79605E-12
16	7%	0.002146592	2.971184222	197.1184222	0.000931443	0.001149795	1.234423336	0.43	2.14659E-12

Graph of Formulated Oil Wear Volumes